# Curvature Mode Shape Analyses of Damage in Structures

## RMIT University

A thesis submitted in total fulfilment of the requirements for the degree of

**Master of Engineering**

by

**Mohammad Mehdizadeh**
**B Eng.**

School of Aerospace, Mechanical & Manufacturing Engineering
College of Science, Engineering and Technology

RMIT University
March 2009

# Dedicated to …

**My Parents**, **Ahmad and Marzyeh**, who continue to learn, grow and develop and who have been a source of encouragement and inspiration to me throughout my life, a very special thank you for providing me this wonderful opportunity. Also for the myriad ways in which, throughout my life, you have actively supported me in my determination to find and realise my potential, and make this contribution to our world.

**The Great Soul of My Grandmother** who taught me the power of generosity.

**My Brother and Sister, Ali and Melika** for all their supports and kindnesses through out this journey.

# Declaration

I certify that except where due acknowledgement has been made, the work is that of the author alone; the work has not been submitted previously, in whole or in part, to qualify for any other academic award; the content of the thesis is the result of work which has been carried out since the official commencement date of the approved research program; and, any editorial work, paid or unpaid, carried out by a third party is acknowledged.

Mohammad Mehdizadeh

26 March 2009

# Acknowledgement

First I wish to dedicate my deep down appreciation to my first supervisor, Professor Sabu John of the Royal Melbourne Institute of Technology (RMIT), for his invaluable help and support from the first day of this project as well as his technical guidance, endless forbearance, and constant encouragement.

I wish to thank the CRC-ACS for helping me with a postgraduate scholarship

I also wish to thank the following:

- Dr. Mehdi Mahdavian for his kind help and support.
- Krishna Oruganti for his assistance in the progress of the project and for supporting the manufacture and testing of the carbon-epoxy beams.
- Terry Rosewarne of RMIT for his assistance in the manufacture of carbon/epoxy beams at RMIT's composite laboratory.
- Peter Tkatchyk for his technical support and assistance in the testing of the composite beams using the Laser Vibrometer and C-SCAN as well as Fatigue Propagation test.

# Abstract

In recent years, the use of composite structures in engineering application has increased. This is mainly due to their special advantages such as high structural performance, high corrosion resistance, tolerance of temperature; extreme fatigue resistance and high strength/weight ratio. However, some disorders like fibre breakage, matrix cracking and delaminations could be caused by operational loading, aging, chemical attack, mechanical vibration, changing of ambient conditions and shock etc. during the service. Although these disorders are hardly visible, they can severely reduce the mechanical properties and the load carrying capability of the composite structure. The aim of this research project is to develop a Vibration-based Structural Health Monitoring (SHM) method for carbon/epoxy composite beam specimens with the embedded artificial delaminations.

The Laser Vibrometer Machine was used to excite the beams and gather the responses of the structure to the excitations. The physical properties such as frequency, velocity, mode shapes, and damping of the defective beams were measured. By using a C-SCAN machine, the accuracy of the positions of the delaminations were verified to be about 95% is accurate. Curvature mode shapes as a scalable damage detection parameter is calculated using an analytical model based on the Heaviside step function and the Central Difference Approximation (CDA) technique.

The vibration-based damage detection method is then obtained using the difference between curvature mode shapes of the intact and damaged carbon/epoxy beams. An accurate prediction of 90% was attained. These results are proposed and discussed in detail in this study.

Finally, the Fatigue Crack Propagation Test was applied on Samples with embedded delamination to extend the crack. The ASTM E399-90 standard is used for the experiment and a careful fatigue crack growth routine was designed and implemented to advance the delamination in a controlled manner. The total extension of 17 mm was observed with Microscope. The total propagation as determined by the curvature mode plots was 17.84 mm.

# Table of Contents

# List of Tables

# List of Figures

# Abbreviations and Acronyms

| | |
|---|---|
| ANN | Artificial Neural Network |
| CAD | Computer Aided Design |
| CAE | Computer Aided Engineering |
| CDA | Central Difference Approximation |
| CMCs | Ceramic Matrix Composites |
| CMSECR | Compression Modal Strain Energy Change Ratio |
| DOF | Degree of Freedom |
| FEA | Finite Element Analysis |
| FMSECR | Flexural Modal Strain Energy Change Ratio |
| FRF | Frequency Response Function |
| GAs | Genetic Algorithms |
| ICA | Independent Component Analysis |
| IRR | Implicit Redundant Representation |
| LHS | Latin hypercube sampling |
| MB | Model-Based |
| MMCs | Metal Matrix Composites |
| MP | Mega Pascal |
| NDT | Non-Destructive Test |
| ODS | Operational Defection Shape |
| PMC | Polymer Matrix Composite |
| RMS | Route Mean Square |
| RTM | Resin Transfer Molding |
| SEA | Statistical Energy Analysis |
| SHM | Structural Health Monitoring |
| SHMS | Structural Health Monitoring System |
| SLDV | Scanning Laser Doppler vibrometer |
| TTDD | Traditional Type Damage Detection |
| WPT | Wavelet packet transforms |

# List of Symbols

| | | |
|---|---|---|
| $\Delta\phi$ | | Correlation Phase |
| $d$ | *m* | Out of plane displacement of the object due to the applied stress |
| $\delta d/\delta x$ | | Rate of displacement |
| S | | Magnitude of image shear |
| $\lambda$ | *m* | Wavelength of laser beams |
| $\pi$ | | PI |
| *B* | | Translation parameter |
| $a$ | | Scale parameter |
| $f(t)$ | | Function (signal) to be transformed |
| $\psi(t)$ | | Transforming function |
| $W_f$ | | Wavelet coefficients |
| *EI(x)* | *GPa* | Bending stiffness distribution of the beam |
| $m(x)$ | *Kg/m* | Mass distribution of the beam per unit length along the x-axis |
| $W(x,t)$ | *m* | Displacement of the beam as a function of the location *(x)* and time *(t)* |
| H | | Heaviside step function |
| $EI_0$ | *GPa* | Bending stiffness of the undamaged structure |
| Z | *Ω* | Impedance |
| F | *N* | Applied force input to the structure |
| $v$ | *m/s* | Resultant velocity of the structure at the same point |
| $\lambda_B$ | *m* | Bragg wavelength |
| $n$ | *m* | Effective wavelength of the fibre |
| $\Lambda$ | | Period of the grating 20 |
| $\Delta\lambda_{Bs}$ | *m* | Wavelength shift |
| $\Delta\epsilon$ | | Applied longitudinal strain |
| $\rho_e$ | | Photo elastic co-efficient of fibre material |
| *RG* | *Ω* | Resistance of the undeformed gauge |
| $\Delta R$ | *Ω* | Change in resistance caused by strain |
| $\varepsilon$ | | Strain |
| *GF* | | Gauge factor |

# CHAPTER 1

# Introduction

## 1.1 Background and Rationale

In recent years, the use of composite structures in engineering application has increased. This is mainly due to their special advantages such as high structural performance, high corrosion resistance, tolerance of temperature; extreme fatigue resistance and high strength/weight ratio. In addition, Composite structures can be designed to suit the objectives of the user. However, some disorders like fibre breakage, matrix cracking and delaminations are inevitable. Although these disorders are hardly visible, they can severely reduce the mechanical properties and the load carrying capability of the composite structure. Damage occurred during service because of the operational loading, aging, chemical attack, mechanical vibration, changing of ambient conditions and shocks. Hence, early detection of damage and its severity and location is a key point. The initial way of damage detection is to remove the structure from a service and check for its damage zones, however this is time consuming and expensive. Therefore online detection of damage which means checking the structure while it is in-service is preferred. Thus the online damage detection of a structure called "Structural Health Monitoring (SHM)" has become a major issue in various fields and industries. It has contributed to the maintenance and repair of structures and is used by companies in high technological sectors. Generally, structural health monitoring has 3 steps: exciting the structure, gathering responses of the structure to excitation and establishing the relationship between these responses and damage status (location and severity).Once damage is detected in the structure, the mechanical and dynamic properties of the structure change. Therefore responses of the intact and damaged structures to the excitations are different. These differences can be used to extract the damage status according to the method used for structural health monitoring such as vibration-based method, stress wave method, static strain response-based method, stress memory alloy method and acoustic emission etc. Using each of these methods provides characteristic responses which the structure responded to because of the excitations. The most important step of the SHM is analysing the responses to determine the damage status. This relationship could be established

by using an artificial system like “Artificial Neural Network (ANN), or Genetic Algorithms (GA`s) to collect the responses (signals), process them and ascertain the damage status. As it mentioned above, one of the effective methods of damage detection in composite structures is dynamic-based method which is based on the responses of the composite structure to the dynamic excitations. The dynamic response-based damage detection method is an interesting method due to its simplicity of implementation. On the other hand, using the structural response directly without the appropriate analysis is not useful. Hence, finding an analyzed factor which contain enough information about damage status i.e. curvature mode shape is a major issue in current research.

## 1.2 Objectives

In this study, dynamic response-based damage detection techniques using smart materials are explored for carbon/epoxy composites. The dynamic response of structures can offer unique information on defects that may be contained within these structures. Changes in the physical properties of the structure due to damage will alter the dynamic responses such as natural frequencies, damping and mode shapes. These parameter changes can be extracted to predict damage information, such as the presence, location and severity of damage in a structure. One method, in which the dynamic response is utilized, is to use the curvature mode shapes to detect damage. The curvature mode shape change due to damage has a local effect in nature; hence, it can be used to locate damage properly, provided that the changes of curvature are closely related to the changes of physical properties in the structures. The curvature mode shape methods have the potential to identify damage types that are hardly visible or lay beneath the surface, such as delamination. The challenge is to develop the ability to identify the changes of response parameters (e.g., deformations and dynamic characteristics) and interpret them in relation to the changes in physical properties of the structures. Moreover, the ability to differentiate the type of damage in a structure is also very important, since two different types of damage may result in the same changes in the parameters tested. For example, a beam with large delamination and a beam with two small delaminations may cause the same frequency changes. Moreover, damage detection in composite structures is more difficult compared to the metallic structures due to the anisotropy of the material, the conductivity of the carbon fibre, and the fact that much of the damage often occurs beneath the surface and is hence hardly detectable or visible.

The major effort in this research project is to obtain scalability factors and analysis method which could extract the damage type and status (severity and location) of the composite structure by using the dynamic responses of the structure to the excitations. In other words, it

is possible to measure different factors i.e. displacement mode shape, natural frequency, damping, velocity etc. from the structure. But appropriate factors with enough information about the damage status are needed for damage detection. Furthermore we need an optimized analysis method to analyze the initial factors and obtain the new factors which clearly show the damage type and status by comparing intact and damaged structure results.

## 1.3. Methodology

First, an appropriate literature review was obtained by gathering related resources to SHM and Vibration-based damage detection from different databases and reading them to realize the background of this work and investigate the future possibilities. The aim is to find two kinds of databases; firstly, the articles related to the background of the proposed topic. In other words, useful ideas and research in the field of SHM and vibration-based damage detection which had done in the past few years were gathered. The second kind of article was new work including research, studies, methods, experiments, and techniques etc. carried out in this field. As a matter of fact, all new databases are not reliable in terms of methodology, equations and results, but extracting the correct and related information from these databases and comparing them with the information which was collected from past articles would be helpful to find a new reliable method for damage detection. The main goal in this literature review was to realizing the scalability factors for experiments, optimized methods for various structural configurations, appropriate analytical modelling. After this comprehensive search thorough different databases, curvature mode shapes were obtained as a reliable factor which contains enough information about the damage. Also the severity and location of the damage is possible by comparing the curvature mode shapes of intact and damaged structure.

Then, different excitation modes and method of gathering its corresponding structural response will be investigated. All of these methods are vibration-based methods. Generally speaking, there are three steps to complete an experimental result; Making the appropriate samples according to desired specifications, scanning the samples to ensure the correctness of them, and conducting the experiments on these samples to get obtain the results. In the first step, experiments were conducted in this study; nine carbon/epoxy laminated composite beam specimens were tested. The specimens were made of carbon fiber and epoxy resins and had a [0/90/±45] lay-up of a total of six layers, with each layer thickness of 1.25 mm and a total thickness of 7.5 mm. Each beam specimen has a width of 50 mm and a length of 600 mm. During the manufacturing, seven Teflon layers were put as a delamination in the sample in different levels and locations and two remaining beams were considered as a healthy sample. As a result of manufacturing process, some errors i.e. misalignments, shifts, gaps etc. occurred

in the samples. Therefore all samples should be scanned by a C-SCAN machine. In this process, the c-scan machine scanned all the samples through soft and rough surface to distinguish whether or not any shifts or manufacturing errors exist in the samples. Fortunately after gathering the results, it was shown that errors were not remarkable and all samples were reliable for testing. The last step was testing the samples to get the dynamic responses and analyse them to find the damage status (severity and location) in each sample. Polytec Laser Vibrometer Machine, which is one of the most remarkable Non Destructive testing machines in SHM and damage detection, was used to get the responses. After the laser vibrometer finished scanning the sample, the measured factors i.e. frequency, velocity, displacement mode shapes, damping etc was shown on the monitor. As a matter of fact, this step was done before the second step to distinguish if it is possible to guess the damage status by comparing the magnitude of healthy and defect samples.. As a result of this process some shifts and peaks was categorized in the graph of defect samples in different locations. However further analysis is required to find suitable scalability factors.

The next step of the project is to find the appropriate analytical modelling to validate the experimental results with. As a matter of fact, natural frequency, velocity and displacement mode shape could directly measure from the laser vibrometer. But some analytical equations and relations are required to get the curvature mode shapes from this information. Therefore an analytical modelling was obtained based on the Euler-Bernoulli beam theory and the governing equation for a beam in vibration was achieved. The governing equation for a beam in vibration can expressed as equation (2-1):

$$\partial^2/\partial x^2 \left(EI(X)\,\partial^2/\partial x^2 [W(x,t) + m(x)\,\partial^2/\partial x^2 W(x,t)]\right) = 0 \qquad (2\text{-}1)$$

Where EI(x) is the bending stiffness distribution of the beam, m(x) is the mass distribution of the beam per unit length along the x-axis, and W(x, t) is the displacement of the beam as a function of the location (x) and time (t).

Some assumptions should be defined to make a relationship between curvature mode shape and physical properties which was gathered from the laser vibrometer. By assuming ″ε″ is the stiffness loss parameter at the location of damage, the effect of damage on the stiffness distribution of the beam can be expressed as equation (2-2)

$$EI_d(x) = EI_0\{1 - \varepsilon[H(x - x_1) - H(x - x_2)]\} \qquad (2\text{-}2)$$

Where H is a Heaviside step function; EI0 is the bending stiffness of the undamaged structures; $x_1$ and $x_2$ are the beginning and the end of damage area, respectively. Finally the governing equation for defective beam can be written as equation (2-3)

$$\frac{d^2}{dx^2}(EI_d(x)\frac{d^2}{dx^2}[\phi_i''(x)]) - \lambda_i' m[\phi_i''(x)] = 0 \qquad (2\text{-}3)$$

Where E $I_d$(x) is defined in Equation (2-2), $\phi_i''(x)$ and $\lambda_i$ is the Eigen functions and Eigen value of the damaged.

After the experimental and analytical result is calculated, these results will be compared. This comparison and discussion will help in determining the optimized method of damage detection. Also this comparison will validate the method used for experiments.

Finally, the best structural damage detection system based on analytical and experimental design will be analysed. Also, computational and other signal processing results obtained from other sources will be analysed.

## 1.4. Thesis Outline

### Chapter 1: Introduction

This chapter consists of a brief background of composite structures, Rationale for this project, Methodology and Thesis outline.

### Chapter 2: Literature Review

A Wide-range Literature Review of Composite structures and their applications is proposed. Also different types of Structural Health Monitoring/Non-Destructive Techniques and their backgrounds are briefly introduced. As an illustration, the basis of Vibration-based damage detection techniques based on physical properties of the structure is explained.

### Chapter 3: Experimental Modelling

In this chapter, the experiments and the modelling procedure performed in this research is explained. At first the process of manufacturing the appropriate samples for testing is described. Then the designed tests and the structural responses for each type of sample are mentioned. Finally, the gathered results and how to distinguish the damage presence and status from these results are discussed.

## Chapter 4: Manufacture of Composite Samples for Experiments

In this chapter, the process of manufacture carbon/epoxy samples is outlined. The process consists of putting the carbon/epoxy layers in different directions according to manufacture plot, curing the final laminate, and cutting the laminate into nine beams with embedded delaminations in different locations and levels.

## Chapter 5: Curvature mode shapes of Carbon/Epoxy Composite Beams

Chapter 5 introduces the Curvature Mode Shape as a preferred factor for damage detection. In this chapter the different methods of calculation is described. In the next step, curvature mode shapes of Carbon/Epoxy samples are calculated for each healthy and defect sample from displacement mode shapes by using the central difference approximation method and comparison is made between the curvature mode shapes of healthy and defect samples to detect the presence, location and severity of damage.

## Chapter 6: Sample Preparation and Curing for Fatigue Crack Propagation Test

This chapter looks at how Sample 1 with embedded delamination is prepared and cured with bonded insert for Fatigue Crack Propagation Test. All the manufacture steps as well as Curing Process is described.

## Chapter 7: Fatigue Propagation Test on Carbon/Epoxy Beams

Following the preparation and installation in last Chapter, the sample is now ready for experiment. The setup for the test as well as INSTRON Fatigue Test Machine is illustrated. Furthermore, the gathered results and propagation status are described.

## Chapter 8: Curvature Mode Shapes of Propagated Samples

As previously outlined, the preferred technique for damage detection in this research project is Curvature Mode Shape-based technique. Therefore, the curvature mode shapes of the sample before and after propagation are calculated using gathered displacement mode shapes from Laser Vibrometer. Finally, the experimental results are verified by checking the resultant curvature plots between sample 1 before and after propagation.

## Chapter 9: Conclusion

Upon gathering all experimental and analytical results from this research project and comparing those with some FEM and computational results derived from other relevant research projects, a summary of the research findings is described.

## Chapter 10: References

In this Chapter, all the databases consist of catalogues, journals, e-resources, referenced.

## 1.5. List of Publications

### Journals

1. M Mehdizadeh, K Oruganti, M Bannister, I Herszberg & S John (2009), 'Vibration-based Analysis of an Increasing Delamination in a Polymeric Composite Structure', Submitted to the Journal of Int. Mat, Systems & Structures', (Under Review).

### Conferences

2. K Oruganti, M Mehdizadeh, S John, I Herszberg (2008), *Damage Detection in Composites Using Vibration Signatures*, Proceedings of the 2008 International Conference on Scientific Computing, (CSC 2008), ISBN 1-60132-059-0, pp. 16-22.

3. K Oruganti, M Mehdizadeh, S John, I Herszberg (2008), *Damage Detection in Composites using Vibration signatures and Mode Shapes*, Proceedings of SMASIS08 ASME Conference on Smart Materials, Adaptive Structures and Intelligent Systems October 28-30, 2008, Ellicott City, Maryland, USA, Paper SMASIS2008-404, ISBN 978-0-7918-3839-6.

4. K Oruganti, M Mehdizadeh, S John, I Herszberg (2008), *Vibration-based Analysis of Damage in Composites* Proceedings of the Asia-Pacific Workshop on Structural Health Monitoring (2APWSHM), Published as Materials Forum, Vol.33, pp 496 * 504, ISBN 978 1 876 855 33 9.

# CHAPTER 2

# Literature Review

## 2.1. Introduction

Composite Material is a substance that is made up of a combination of two or more different materials. A composite material can provide superior and unique mechanical and physical properties as it combines the most desirable properties of its constituents while suppressing their least desirable properties. (Keith Kedward, 2007).For example, a glass-fiber reinforced plastic combines the high strength of thin glass fibers with the ductility and chemical resistance of plastic; the brittleness that the glass fibers have when isolated is not a characteristic of the composite. The opportunity to develop superior products for aerospace, automotive, and recreational applications has sustained the interest in advanced composites (Figure 2.1).

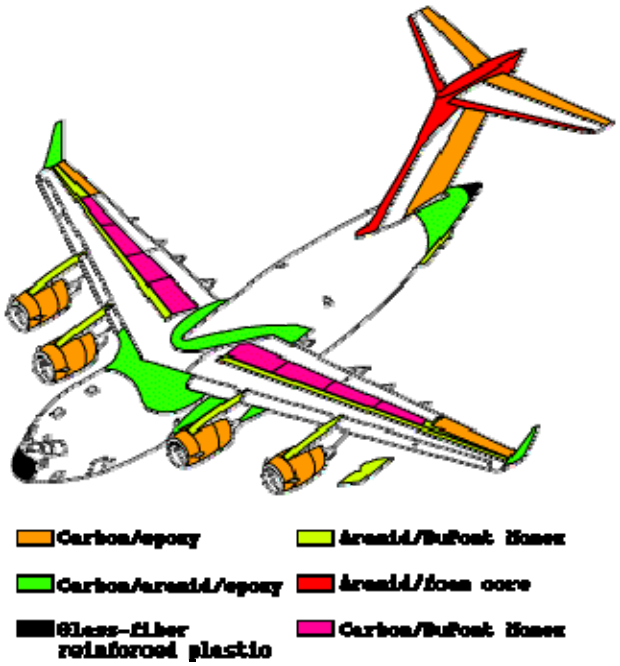


**Figure 2-1: Application of different types of composite materials in aircraft (Courtesy: Boeing)**

Currently composites are being considered on a broader basis for applications that include civil engineering structures such as bridges and freeway pillar reinforcement; and for biomedical products, such as prosthetic devices (Figure 2.2). Composite materials usually consist of synthetic fibers embedded within a matrix, a material that surrounds and is tightly bound to the fibers. The most widely used type of composite material is polymer matrix composites (PMCs). PMCs consist of fibers made of a ceramic material such as carbon or glass embedded in a plastic matrix. (Keith Kedward, 2007).

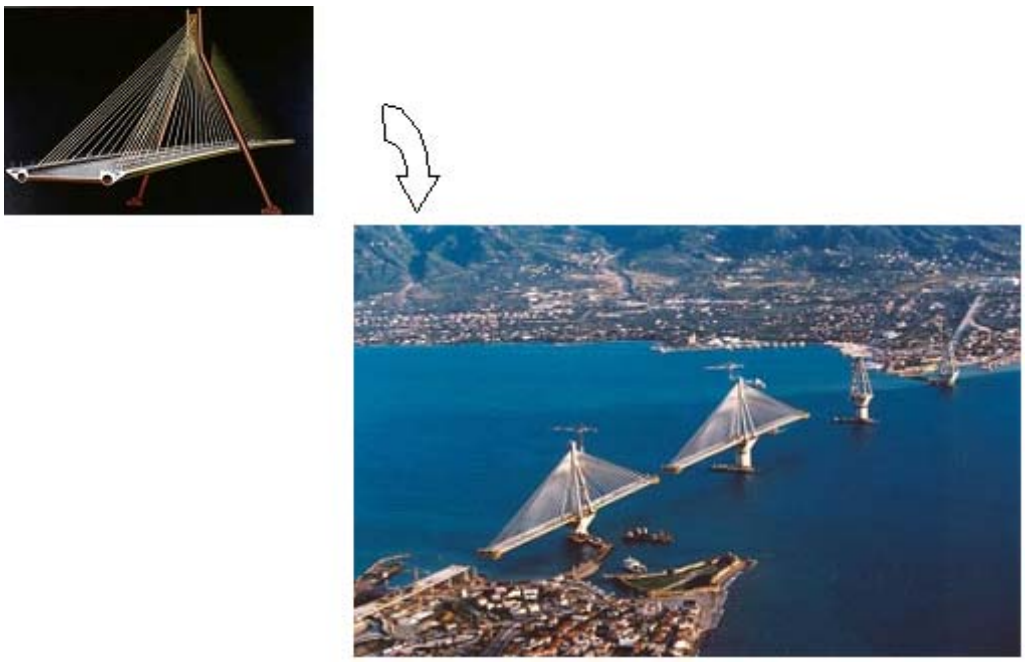

**Figure 2-2: Fibre Reinforced Polymer (FRP) Composite Bridge Technology (Courtesy: FHWA)**

Typically, the fibers make up about 60 percent of a polymer matrix composite by volume (Hull, 1996; Mallick, 1988; Schwartz, 1996). Metal matrices or ceramic matrices can be substituted for the plastic matrix to provide more specialized composite systems called metal matrix composites (MMCs) and ceramic matrix composites (CMCs), respectively. Some important applications of MMCs and CMCs are displayed in Figures 2.3 and 2.4.

**Figure 2-3: Structures and Applications of CMC`s (Courtesy: www.cmc-concrete.com)**

**Figure 2-4: Structures and Applications of MMC`s (Courtesy: www.Ceramtec.com)**

The fibrous reinforcing constituent of composites may consist of thin continuous fibers or relatively short fiber segments. When using short fiber segments, however, fibers with a high aspect ratio (length-to-diameter ratio) are used (Keith Kedward, 2007).Continuous-fiber composites are generally required for high performance structural applications. The specific strength (strength-to-density ratio) and specific stiffness (elastic modulus-to-density ratio) of continuous carbon fiber PMCs (Figure 2.5), for example, can be vastly superior to conventional metal alloys (see Elasticity). Composites can also have other attractive properties, such as high thermal or electrical conductivity, and a low coefficient of thermal expansion. Also, depending on how the fibers are oriented or interwoven within the matrix, composites can be fabricated to have structural properties specifically tailored for a particular structural use.

**Figure 2-5: Structures and Applications of PMC`s (Courtesy: en.Wikipedia.org)**

Although composite materials have certain advantages over conventional materials, composites also have some disadvantages. For example, PMCs and other composite materials tend to be highly anisotropic—that is, their strength, stiffness, and other engineering properties are different depending on the orientation of the composite material. For example, if a PMC is fabricated so that all the fibers are lined up parallel to one another, then the PMC will be very stiff in the direction parallel to the fibers, but not stiff in the perpendicular direction. These anisotropic properties pose a significant challenge for the designer who uses composite materials in structures that place multidirectional forces on the structural members. Also, forming strong connections between separate composite material components is difficult. The broader use of advanced composites is inhibited by high manufacturing costs. Currently, fabricating composite materials is a labor-intensive process. However, as improved manufacturing techniques are developed, it will become possible to produce composite materials at higher volumes and at a lower cost than is now possible, accelerating the wider use of these materials (Hull, 1996; Mallick, 1988; Schwartz, 1996).

Advanced composite materials have been extensively used in structural applications, due to their advantageous characteristics, such as high stiffness and strength to weight ratio, improved fatigue resistance, and superior damage tolerance capability compared to metallic structure. Carbon/epoxy composites (Figure 2.6) have higher stiffness and strength properties than other composites, in particular, the commonly used E-glass/epoxy composites. These advantageous properties have led to the use of carbon/epoxy composites in structures that undergo higher stresses, such as aircraft and aerospace structures. (Keith Kedward, 2007).

However, carbon/epoxy composites laminates, like any composite material and structures are susceptible to defects like fibre breakage, matrix cracking, deboning between the fibres and matrix, and delaminations or interlayer cracks. The defect can significantly reduce the strength of structures and may produce failure of the structure. When failure occurs, it is often

catastrophic not only in human life or monetary losses; it can also have devastating effects on the psychological state of the public as well.

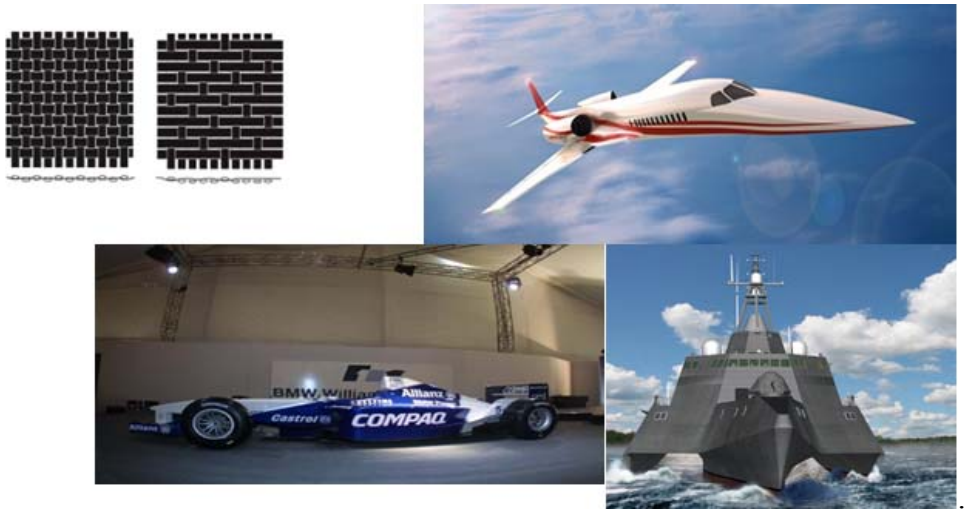


**Figure 2-6: Structures and Applications of Carbon/Epoxy Composites (www.CompociteWorld.com)**

## 2.2. Composites and their application

The most primitive composite materials were comprised of straw and mud in the form of bricks for building construction; the Biblical book of Exodus speaks of the Israelites being oppressed by Pharaoh, by being forced to make bricks without straw. The ancient brick-making process can still be seen on Egyptian tomb paintings in the Metropolitan Museum of Art. The most advanced examples are performed routinely on spacecraft in demanding environments. The most visible applications pave our roadways in the form of either steel and aggregate reinforced Portland cement or asphalt concrete. Those composites closest to our personal hygiene form our shower stalls and bath tubs made of fiberglass. Solid surface, imitation granite and cultured marble sinks and counter tops are widely used to enhance our living experiences.

### 2.2.1. Molding Methods

In general, the reinforcing and matrix materials are combined, compacted and processed to undergo a melding event. After the melding event, the part shape is essentially set, although it can deform under certain process conditions. For a thermoset polymeric matrix material, the melding event is a curing reaction that is initiated by the application of additional heat or chemical reactivity such as organic peroxide (Keller & Tirelli, 2004).. For a thermoplastic polymeric matrix material, the melding event is solidification from the melted state. For a metal matrix material such as titanium foil, the melding event is fusing at high pressure and a

temperature near the melt point. For many molding methods, it is convenient to refer to one mold piece as a "lower" mold and another mold piece as an "upper" mold. Lower and upper refer to the different faces of the molded panel, not the mold's configuration in space. In this convention, there is always a lower mold, and sometimes an upper mold. Part construction begins by applying materials to the lower mold. Lower mold and upper mold are more generalized descriptors than more common and specific terms such as male side, female side, a-side, b-side, tool side, bowl, hat, mandrel, etc. Continuous manufacturing processes use a different nomenclature. The molded product is often referred to as a panel. For certain geometries and material combinations, it can be referred to as a casting. For certain continuous processes, it can be referred to as a profile.

## 2.2.1.1. Open Molding

Molding is a process using a rigid, one sided mold which shapes only one surface of the panel. The opposite surface is determined by the amount of material placed upon the lower mold. Reinforcement materials can be placed manually or robotically. They include continuous fiber forms fashioned into textile constructions and chopped fiber. The matrix is generally resin, and can be applied with a pressure roller, a spray device or manually. This process is generally done at ambient temperature and atmospheric pressure. Two variations of open molding are Hand Layup and Spray-up. The process is shown in Figure 2.7. (Wikipedia®, November 2007)

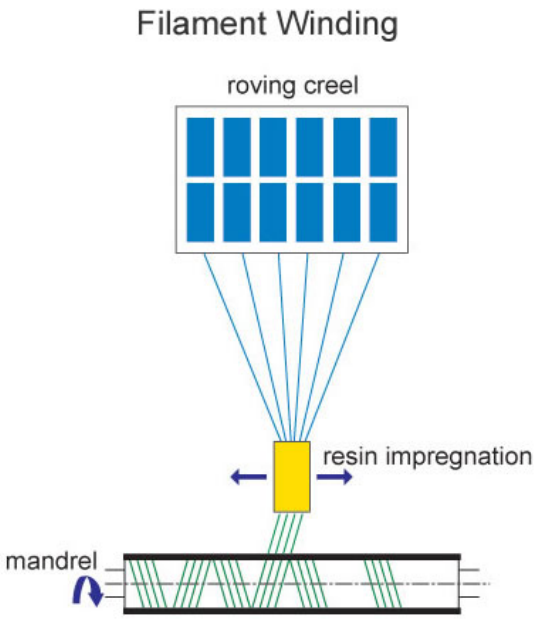


**Figure 2-7: Open Molding Process (OCV Reinforcements)**

## 2.2.1.2. Vacuum bag Molding

Vacuum bag Molding is a process using a two-sided mold set that shapes both surfaces of the panel. On the lower side there is a rigid mold and on the upper side there is a flexible membrane or vacuum bag. The flexible membrane can be a reusable silicone material or an extruded polymer film such as nylon. Reinforcement materials can be placed on the lower mold manually or robotically, generally as continuous fiber forms fashioned into textile constructions. The matrix is generally a resin. The fiber form may be pre-impregnated with the resin in the form of prepreg fabrics or unidirectional tapes. Otherwise, liquid matrix material is introduced to dry fiber forms prior to applying the flexible film. Then, vacuum is applied to the mold cavity (Justin Furness, November 2007).This process can be performed at either ambient or elevated temperature with ambient atmospheric pressure acting upon the vacuum bag. The most economical way is using a venturi vacuum and air compressor or a vacuum pump. The process can be seen from Figure 2.8.

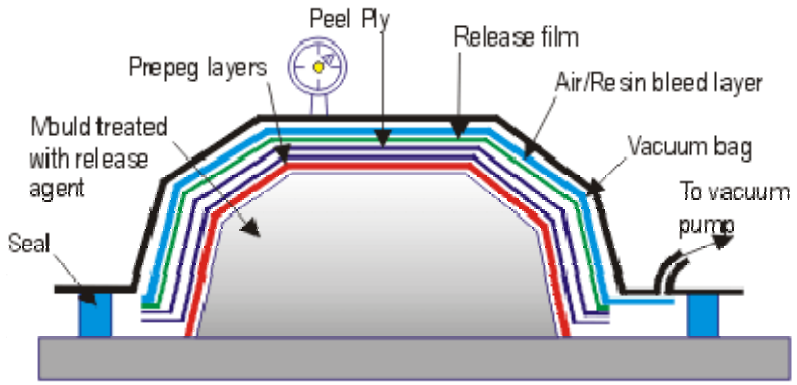


**Figure 2-8: Vacuum Bag Molding Process (Justin Furness, 1998)**

## 2.2.1.3. Pressure bag Molding

This process is related to vacuum bag molding in exactly the same way as it sounds (Figure 2.9). A solid female mold is used along with a flexible male mold. The reinforcement is placed inside the female mold with just enough resin to allow the fabric to bond in place. A measured amount of resin is then liberally brushed indiscriminately into the mold and the mold is then clamped to a machine that contains the male flexible mold. The flexible male membrane is then inflated with heated compressed air or possibly steam. The female mold can also be heated. Excess resin is forced out along with trapped air. This process is extensively used in the production of composite helmets due to the lower cost of unskilled labor. Cycle times for a helmet bag molding machine vary from 20 to 45 minutes, but the finished shells require no further curing if the molds are heated. (Waterman, Pamela J. 2007)

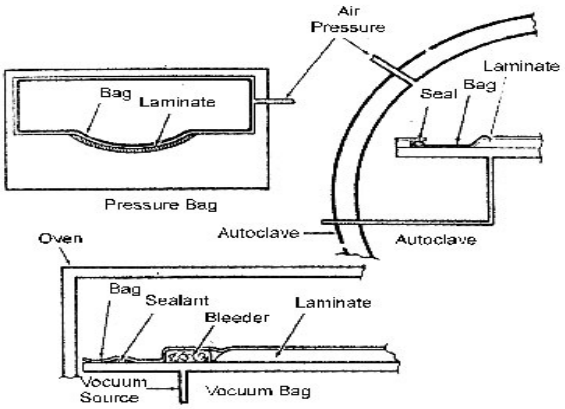


**Figure 2-9: Pressure Bag Molding Process (Kamala Nagar, 2001)**

## 2.2.1.4. Autoclave Molding

A process using a two-sided mold set that forms both surfaces of the panel. On the lower side is a rigid mold and on the upper side there is a flexible membrane made from silicone or an extruded polymer film such as nylon. Reinforcement materials can be placed manually or robotically (Waterman, Pamela J. 2007). They include continuous fiber forms fashioned into textile constructions. Most often, they are pre-impregnated with the resin in the form of prepreg fabrics or unidirectional tapes. In some instances, a resin film is placed upon the lower mold and dry reinforcement is placed above. The upper mold is installed and vacuum is applied to the mold cavity. The assembly is placed into an autoclave pressure vessel. This process is generally performed at both elevated pressure and elevated temperature. The use of elevated pressure facilitates a high fiber volume fraction and low void content for maximum structural efficiency. The Schematic figure of Autoclave process is displayed in Figure 2.10.

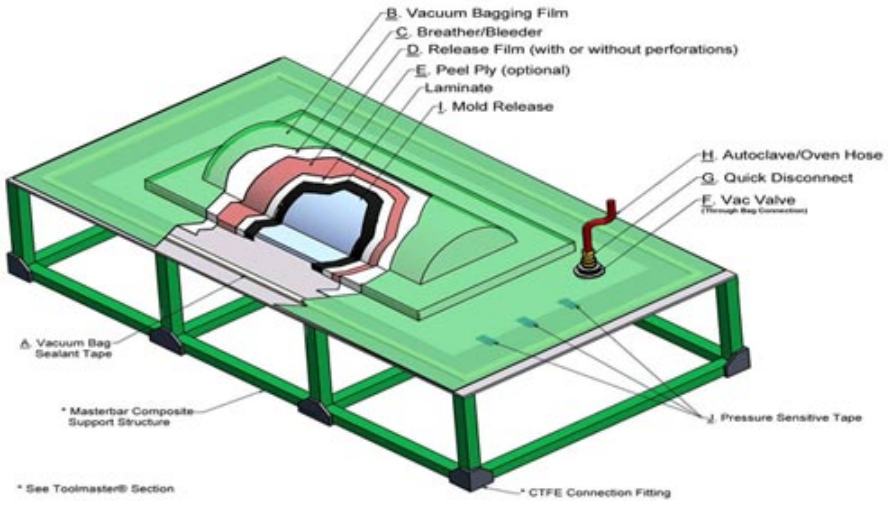


**Figure 2-10: Autoclave Molding Process (Courtesy: Kingsway West Business)**

## 2.2.1.5. Resin Transfer Molding (RTM)

A process using a two-sided mold set that forms both surfaces of the panel. The lower side is a rigid mold; the upper side can be a rigid or flexible mold. Flexible molds can be made from composite materials, silicone or extruded polymer films such as nylon. The two sides fit together to produce a mold cavity (Osborne Industries, Inc. November 2007). The distinguishing feature of resin transfer molding is that the reinforcement materials are placed into this cavity and the mold set is closed prior to the introduction of matrix material. Resin transfer molding includes numerous varieties which differ in the mechanics of how the resin is introduced to the reinforcement in the mold cavity. These variations include everything from vacuum infusion (see also resin infusion) to vacuum assisted resin transfer molding. This process can be performed at either ambient or elevated temperatures (Figure 2.11).

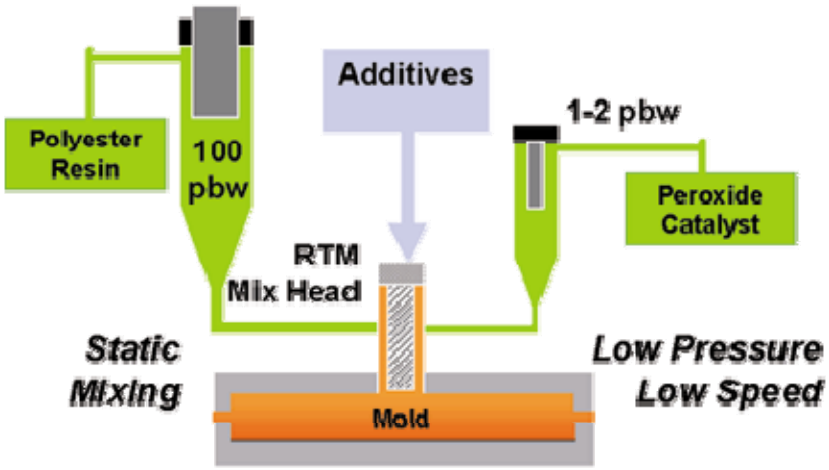


**Figure 2-11: Free Transfer Molding Process (RTM) (Courtesy: Osborne Industries, Inc.)**

## 2.2.1.6. Other

Other types of molding include press molding, transfer molding, pultrusion molding, filament winding, casting, centrifugal casting and continuous casting. (Keller & Tirelli, 2004).

## 2.2. FE Dynamic Analysis

Finite element analysis (FEA) is a computer simulation technique used in engineering analysis. It uses a numerical technique called the finite element method (FEM). There are many finite element software packages, both free and proprietary. Development of the finite

element method in structural mechanics is usually based on an energy principle such as the virtual work principle or the minimum total potential energy principle. In its application, the object or system is represented by a geometrically similar model consisting of multiple, linked, simplified representations of discrete regions—i.e., finite elements on an unstructured grid (S.Rajendran *et al.* 1998). Equations of equilibrium, in conjunction with applicable physical considerations such as compatibility and constitutive relations, are applied to each element, and a system of simultaneous equations is constructed. The system of equations is solved for unknown values using the techniques of linear algebra or non-linear numerical schemes, as appropriate. While being an approximate method, the accuracy of the FEA method can be improved by refining the mesh in the model using more elements and nodes. A common use of FEA is for the determination of stresses and displacements in mechanical objects and systems. However, it is also routinely used in the analysis of many other types of problems, including those in heat transfer, solid state diffusion and reactions with moving boundaries, fluid dynamics, and electromagnetism. FEA is able to handle complex systems that defy closed-form analytical solutions. (S.Rajendran *et al.* 1998)

## 2.2.1. Finite Element Method

Computer-aided engineering (CAE) is the application of computer software in engineering to evaluate components and assemblies. It encompasses simulation, validation, and optimization of products and manufacturing tools. The primary application of CAE, used in civil, mechanical, aerospace, and electronic engineering, takes the form of FEA alongside computer-aided design. In general, there are three phases in any computer-aided engineering task:

- Pre-processing

- Analysis solver

- Post-processing

## 2.2.1.1. Pre-Processing

The first step in using FEA, pre-processing, is constructing a finite element model of the structure to be analysed. The input of a topological description of the structure's geometric features is required in most FEA packages. This can be in either 1D, 2D or 3D form, modelled by line, shape, or surface representation, respectively, although nowadays 3D models are predominantly used (S.Rajendran *et al.* 1998). The primary objective of the model is to

realistically replicate the important parameters and features of the real model. The simplest mechanism to achieve modelling similarity in structural analysis is to utilize pre-existing digital blueprints, design files, CAD models, and/or data by importing that into an FEA environment. Once the finite element geometric model has been created, a meshing procedure is used to define and break up the model into small elements. In general, a finite element model is defined by a mesh network, which is made up of the geometric arrangement of elements and nodes. Nodes represent points at which features such as displacements are calculated. (Keller & Tirelli, 2004). FEA packages use node numbers to serve as an identification tool in viewing solutions in structures such as deflections. Elements are bound by sets of nodes, and define localized mass and stiffness properties of the model. Elements are also defined by mesh numbers, which allow references to be made to corresponding deflections or stresses at specific model locations.

### 2.2.1.2. Analysis Solver

The next stage of the FEA process is analysis. The FEM conducts a series of computational procedures involving applied forces, and the properties of the elements which produce a model solution. Such a structural analysis allows the determination of effects such as deformations, strains, and stresses which are caused by applied structural loads such as force, pressure and gravity. (S.Rajendran *et al.* 1998)

### 2.2.1.3. Post-processing

These results can then be studied using visualization tools within the FEA environment to view and to fully identify implications of the analysis. Numerical and graphical tools allow the precise location of data such as stresses and deflections to be identified (Figure 2.12).

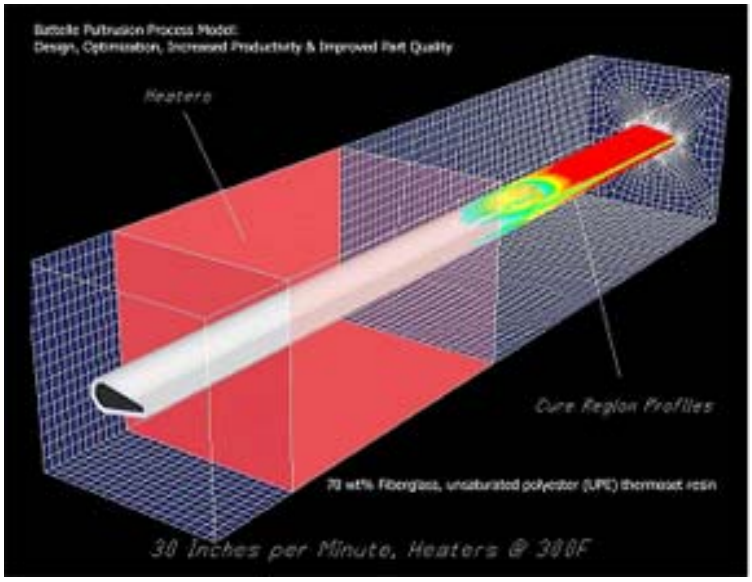


**Figure 2-12: An example of FEM Analysis (J. M. Trewhella *et al.* 1999)**

## 2.2.2. Dynamic FEA Modelling

There is increasing demand for dynamic FEA modelling in the heavy vehicle industry. Many heavy vehicle companies are moving away from traditional static analysis and are employing dynamic simulation software. Dynamic simulation involves applying FEA in a more realistic sense to take into account the complicated effects of analysing multiple components and assemblies with real properties. (Baker *et al.*, 2004;Greene, 1998).

Dynamic simulation, used in conjunction with assembly modelling, introduces the need to fasten together components of different materials and geometries. Therefore, CAE tools should have comprehensive capabilities to easily and reliably model connectors, including joints that allow relative motion between components, rivets, and welds. Typical MSS models are composed of rigid bodies (wheels, axles, frame, engine, cab, and trailer) connected by idealized joints and force elements. Joints and links may be modelled as rigid links, springs, or dampers in order to simulate the dynamic characteristics of real truck components. Force transfer across assembly components through connectors makes them susceptible to high stresses. It is simpler and easier to idealize connectors as rigid links in these systems. This idealization provides a basic study of assembly behaviour in terms of understanding system characteristics; engineers must model joining parameters like fasteners accurately when performing stress analysis to determine how failures might take place. "Representing connectors as rigid links assumes that connectors transfer loads across components without deforming and undergoing stress

themselves (S.Rajendran *et al.* 1998). This unrealistic idealization yields incorrect predicted stresses in the regions local to the connectors, the exact locations where part failures will most likely initiate." Understandably, the detailed inclusion of every connection point and/or mechanism in an assembly is impractical to model. Therefore, improved representations of fasteners that are simple to use yet reliable should be investigated for use on a case-by-case basis. Dynamic FEA simulation enables a variety of manoeuvres to be accurately tested. Tests such as steady-state cornering, roll-over testing, lane changing, J-turns, vibration analysis, collisions, and straight-line braking can all be conducted accurately using dynamic FEA. Non-linear and time-varying loads allow engineers to perform advanced realistic FEA, enabling them to locate critical operating conditions and determine performance characteristics. As a result of the improved dynamic testing capabilities, engineers are able to determine the ultimate performance characteristics of the vehicle's design without having to take physical risks. As a result of dynamic FEA, the need for expensive destructive testing has been lessened substantially.

Nowadays there are numerous finite element modelling and analysis tools available i.e. ALGOR, ANSYS, COSMOS/M, STARDYNE / FEMAP,
MSC.PATRAN™, MSC. NASTRAN, SAP90/2000, ADINA, NISA, ABACUS etc. However, in this research study all the finite element models were created using ANSYS and analysed using MSC.NASTRAN.

## 2.3. Structural Health Monitoring/NDT

At present, using non-destructive examination (NDE) method to detect damage status of engineering structures has become a hotspot and difficult issue. Recently, NDE technique is widely applied in industries, such as astronautics aviation, space vehicle, power plant equipment, architecture, metallurgy and mechanical manufacture, etc. Generally, structural damage detection can be classified as local-damage detection and global-damage detection. Local-damage detection techniques refer to non-destructive testing (NDT) as CT scanning and ultrasonic (Figure 2.13), etc., because it is mainly used to detect local damage in structures, and it can determine damage existence and its location.

(a)


(b)

**Figure 2-13: Local damage detection facilities: (a) C-SCAN, (b) Ultrasonic (Courtesy: en.Wikipedia.org)**

Local damage detection methods utilise only data obtained from the damaged structure. Baseline data and theoretical models of the undamaged structure are not used. These are the main advantages of local damage detection (Wikipedia November 2007). For small and regular structures, such as pressure vessels, local damage detection is very effective. However, for the large and complicated structures in invisible or closed environments, it is very difficult to detect damage using local damage detection method. The engineers have to make on-site structural damage detection. Therefore, local damage detection methodology can only be used to detect some special components of a structure. In order to detect damage throughout the whole structure, especially some large complicated structures, a methodology called global vibration-based structural damage detection has been proposed. Its basic principle can be explained as follows.

## 2.4. Optical NDT Techniques

### 2.4.1. Holographic Interferometry

An advanced form of photography that allows pictures to be recorded in three dimensions is Holography (Gryzagoridis, 1996). This particular science has the ability of recording both the amplitude and phase of light. On reconstruction, the resultant light field is identical to that which emanated from the original scene. To create a recording, holography uses a reference

beam which is combined with light from the object. Optical interference between the two beams produces a series of intensity fringes which are recorded on a standard photographic film. These fringes form a diffraction grating on the film, which is called a hologram. Once the film is processed and illuminated for a second time by the reference beam, diffraction from the fringe occurs and the film forms the object beam in both intensity and phase. Examination of the fringe patterns created when the wave fronts are reconstructed gives substantial quantity of information on the type and enormity of surface movements. The presence of damage in the structure causes a deviation in the surface displacement; this disturbs the fringe pattern which occurs as a consequence of image interference. Ambu *et al*. (2006) have documented the use of this procedure for impact damage detection in composite laminates. Gryzagoridis (1989) made use of both the techniques discussed for non-destructive testing of composites. He found the real-time holographic interferometry technique to be far more time consuming than the former. A typical optical arrangement for holographic interferometry is shown in Figure 2.14. High cost as compared to other non-destructive testing techniques is a disadvantage.

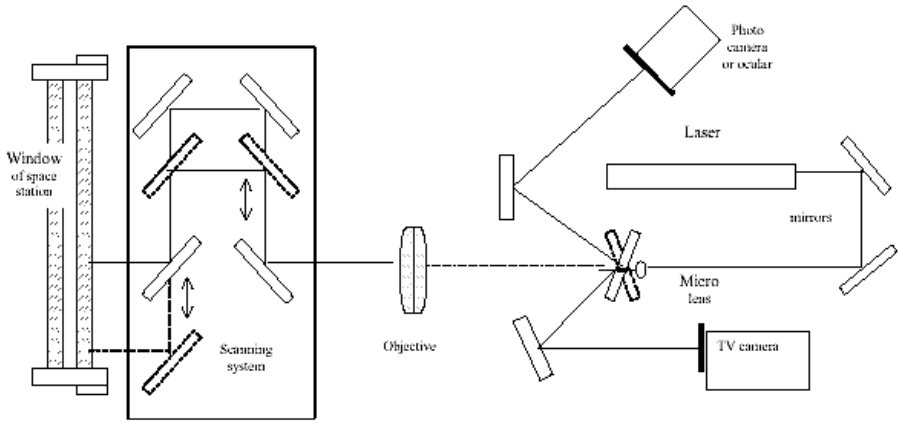


**Figure 2-14: The optical scheme of holographic TV interferometer for non destructive testing (Veronika Babenko *et al.*, 2001)**

## 2.4.2 Laser Shearography

Shearography technique involves qualitative judgment of fringe patterns created by video imaging of surface displacements illuminated by a coherent laser beam. Shearography provides full-field and non destructive testing for an express wide-field assessment of composites structures. Shearography (Hung and Taylor, 1997) as a full-field strain analysis method is based on the principle where coherent waves of light having dissimilar path lengths generate a fringe pattern whilst interference occurs. This fringe pattern represents changes in the out-of plane displacement derivative of the surface under test. This is mathematically expressed below:

$$\Delta\phi = \frac{4\pi}{\lambda}\left(\frac{\delta d}{\delta x}\right)S \qquad (2\text{-}1)$$

Where:

$\Delta\phi$ : Correlation Phase,

d: Out of plane displacement of the object due to the applied stress,

$\frac{\delta d}{\delta x}$: Rate of displacement

S: Magnitude of image shear,

$\lambda$ : Wavelength of laser beam

The out of plane displacement is a representative of strain. The occurrence of defects in a structure leads to strain concentration when the structure is loaded, either during pressure or thermal excitation. Li *et al*., 2004 validated this along with other researchers. These strain concentrations shape fringe patterns which are then used to detect and analyze the defects. The correctness of the outcome depends on two factors. The technique used for stimulating the specimens and the image examination technique. During Shearographic analysis, the test specimen is energized while it is illuminated by a laser beam. An image shearing Charge-Coupled Device (CCD) camera is then used to acquire the displacements on the surface of the structure. The image which represents the strain signature is then stored in digital format for further processing. A typical representation of the laser Shearography setup is shown in Figure 2.15.

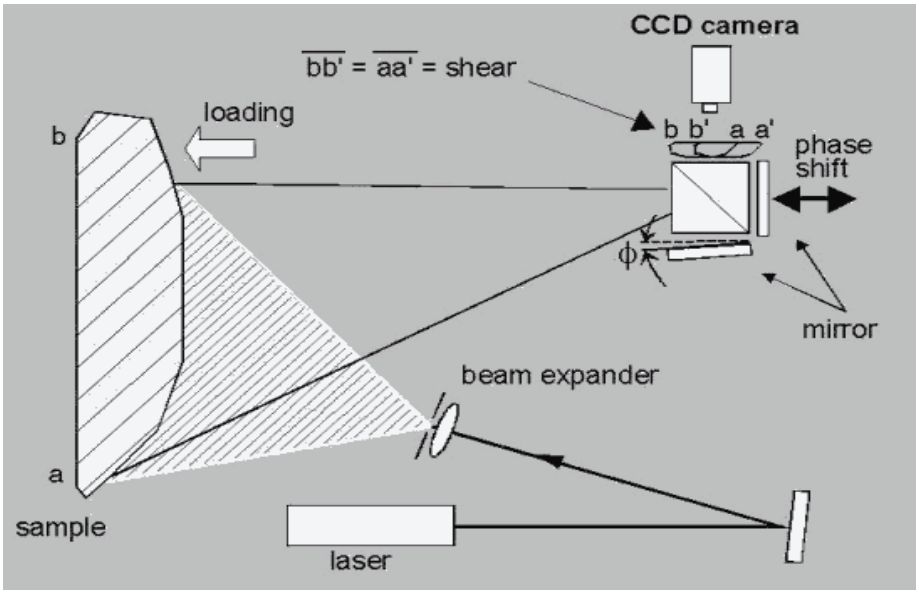


**Figure 2-15: Typical representation of laser Shearography setup (R. Pezzoni *et al.*, 2000)**

## 2.5 Ultrasonic NDT Techniques

Ultrasonic Testing (UT) uses high frequency sound energy to conduct examinations and take measurements. Ultrasonic inspection can be used for flaw detection/evaluation, dimensional measurements, material characterization, and more. To illustrate the general inspection principle, a typical pulse/echo inspection configuration as illustrated in Figure 4-16 will be used.

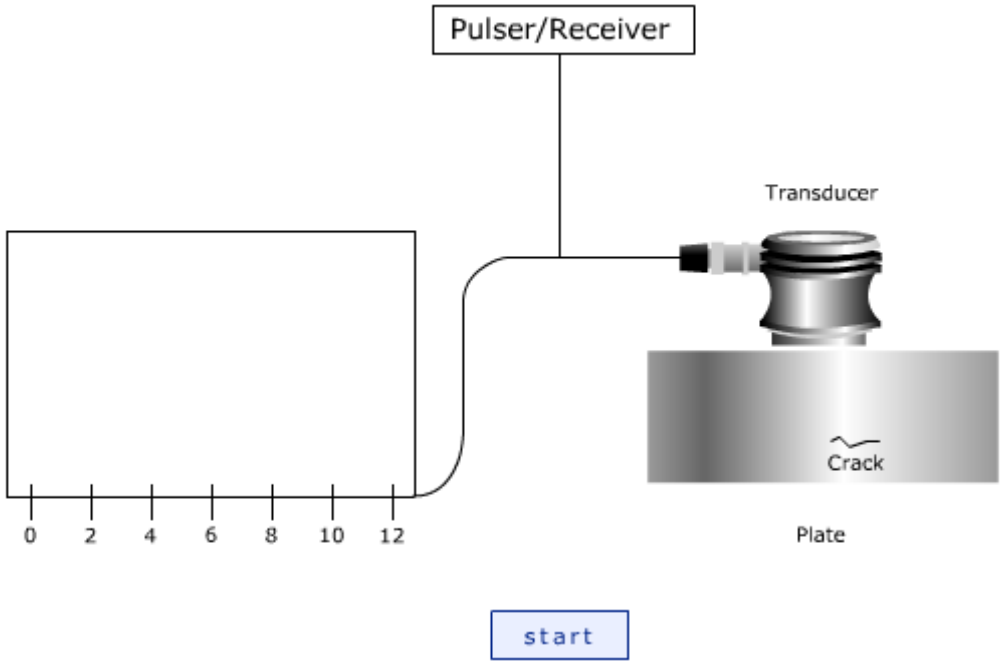


**Figure 2-16: a typical pulse/echo inspection configuration (Courtesy: www.ndt-ed.org)**

## 2.5.1 Conventional Ultrasonic Methods

Ultrasonic A, B or C (Mallick, 1988) scan involves the generation of an ultrasonic plot of the structure under study. The plot is generated by scanning the complete structure at regular intervals with a piezoelectric transducer. In the A-Scan procedure, output signal amplitudes are displayed against a time scale and the depths of various defect locations are judged from the position of the signal peaks on the time sweep. The B-Scan procedure scans the top and the bottom surfaces of a flaw, while the C-Scan procedure displays the plan view of the defect boundaries in the material. To scan, two sensor configurations namely the Through Transmission Method (Mallick, 1988) or a Pulse Echo Method (Mourtiz *et al.*, 2000) can be used. Mourtiz *et al*. (2000) used the pulse echo ultrasonic technique for detecting fatigue cracks in thick composites. The ultrasonic scan technique is capable of detecting delaminations, large voids, clusters of micro voids, and alien material. Conversely, this technique is time intense, as it involves line scanning of the entire structure, and also needs access to the complete structure under study, which is hard to achieve in a majority of cases (Bray &McBride, 1992; Shull, 2002). Thus it is not an ideal online health monitoring system.

## 2.5.2 Acoustic Emissions

Acoustic Emission, according to ASTM, refers to the generation of transient elastic waves during the rapid release of energy from localized sources within a material. The source of these emissions in metals is closely associated with the dislocation movement accompanying plastic deformation and the initiation and extension of cracks in a structure under stress. Other sources of Acoustic Emission are: melting, phase transformation, thermal stresses, cools down cracking and stress builds up. The Acoustic Emission NDT technique is based on the detection and conversion of these high frequency elastic waves to electrical signals. This is accomplished by directly coupling piezoelectric transducers on the surface of the structure under test and loading the structure. Sensors are coupled to the structure by means of a fluid couplant and are secured with tape, adhesive bonds or magnetic hold downs. The output of each piezoelectric sensor (during structure loading) is amplified through a low-noise preamplifier, filtered to remove any extraneous noise and furthered processed by suitable electronic equipment. The instrumentation of Acoustic Emission must provide some measure of the total quantity of detected emission for correlation with time and/or load. The Schematic process is shown in Figure 4.17. (ASTM Standard 2005)

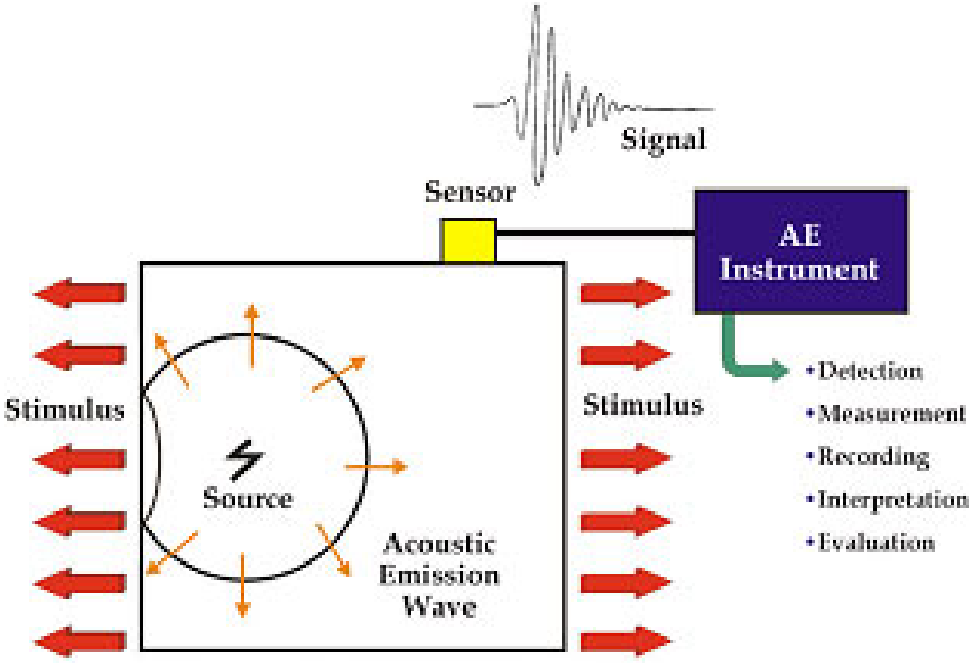


**Figure 2-17: Acoustic Emission Process (ASME E610-52)**

Compared to conventional inspection methods the advantages of the Acoustic Emission technique are:

- High sensitivity.
- Early and rapid detection of defects, flaws, cracks etc.
- Real time monitoring
- Cost Reduction
- Defective area location: only critical defects provide sustainable Acoustic Emission sources.
- Minimization of plant downtime for inspection, no need for scanning the whole structural surface.
- Minor disturbance of insulation.
- Application of Artificial Intelligence (AI) and Technological Packages: Expert systems for evaluating the condition of metallic pressure systems and tank bottoms based on the acquired experience of a huge number of tests are used worldwide.

The applications of Acoustic Emission in different fields are explained below:

## 2.5.2.1. Acoustic Emission for Laboratory Testing

Acoustic Emission inspection is a powerful aid to materials testing and the study of deformation, fracture and corrosion (ASTM Standard 2005). It gives an immediate indication of the response and behaviour of a material under stress, intimately connected with strength,

damage and failure. Acoustic Emission is also is also for monitoring chemical reactions including corrosion process, liquid solid transformations, and phase transformations. (Lee & Tsuda, 2005).

### 2.5.2.2. Acoustic Emission IN FIELD TESTING

Many codes and standards exist for Acoustic Emission testing of vessels, from transportation gas cylinders and railroad tanks to thousands tons storage tanks. Since only active defects and deterioration produce Acoustic Emission no time is wasted on inactive defects which are not threatening structural integrity. (ASTM Standard 2005)

### 2.5.2.3. Global monitoring- 100% Inspection of the structure

A major advantage of Acoustic Emission inspection is that does not require access to the whole examination area. E.g. for covering a total area of a 16 m-diameter sphere 30-40 sensors are needed. Thus, the cost of the test is significantly less than inspection with conventional NDT methods (for 100% inspection and scanning of the whole area). Identified problem areas can be inspected using conventional NDT methods. (ASTM Standard 2005)

### 2.5.2.4. Testing with insulation /high temperature processes

In cases of insulation, only small holes in insulation are required for sensors mounting, resulting in more cost savings. In cases of high temperature processes, wave-guides are used to guide the Acoustic Emission waves from the hot surface to the edge where the sensor is mounted. Finally, in large cryogenic vessels, permanent sensors are mounted under insulation for periodic inspection control. (ASTM Standard 2005)

### 2.5.2.5. On-line testing

As the method records defects in real time, it offers the possibility of on-line inspection, e.g. during hydrostatic testing. Other types of on-line stress application are introduction of gas into the upper vapour space, temperature control etc. (ASTM Standard 2005)

### 2.5.2.6. Rapid inspection

The actual Acoustic Emission test takes a matter of hours, and, in some cases, even less. There is no comparable technique which can provide 100% volumetric inspection. (ASTM Standard 2005)

### 2.5.2.7. Cost Reduction

The use of Acoustic Emission results in considerable reduction in plant maintenance costs, while increasing the available information about plant integrity (ASTM Standard 2005). Plant downtime for inspection is also minimized.

### 2.5.2.8. Permanent recording of test

Acoustic Emission data are digitized and stored on a PC, providing permanent recording of the test to be used at any time for re-evaluation and post processing analysis. (ASTM Standard 2005)

### 2.5.2.9. Defect Location

When more than one sensor are used, Acoustic Emission source can be located and, thus, the defective area. Location is based on the wave propagation principles within the materials and is effectuated by measuring the signal's arrival time to each sensor (ASTM Standard 2005). By comparing the signal's arrival time at different sensors, the flaw`s location can be defined through triangulation.
Linear location is used on long gas cylinders; planar (2-dimensional) location for thick walled and gas filled vessels, while 3-dimensional location is used for power transformers and concrete structures.

## 2.8 Radiographic Technique

This technique involves the use of penetrating gamma or X-radiation to examine parts and products for imperfections. An X-ray machine or radioactive isotope is used as a source of radiation. Radiation is directed through a part and onto film or other media. The resulting shadowgraph shows the internal soundness of the part. Possible imperfections are indicated as density changes in the film in the same manner as X-ray shows broken bones. Radiographic applications fall into two distinct categories evaluation of material properties and evaluation of manufacturing and assembly properties (Bray & McBride, 1992; Shull, 2002; Summer scales,

1987; US Department of Defense, 1989). Material property evaluation includes the determination of composition, density, uniformity, and cell or particle size. Manufacturing and assembly property evaluation is normally concerned with dimensions, flaws (voids, inclusions, and cracks), bond integrity (welds, brazes, etc.), and verification of proper assembly of component pieces (Figure 4-18).

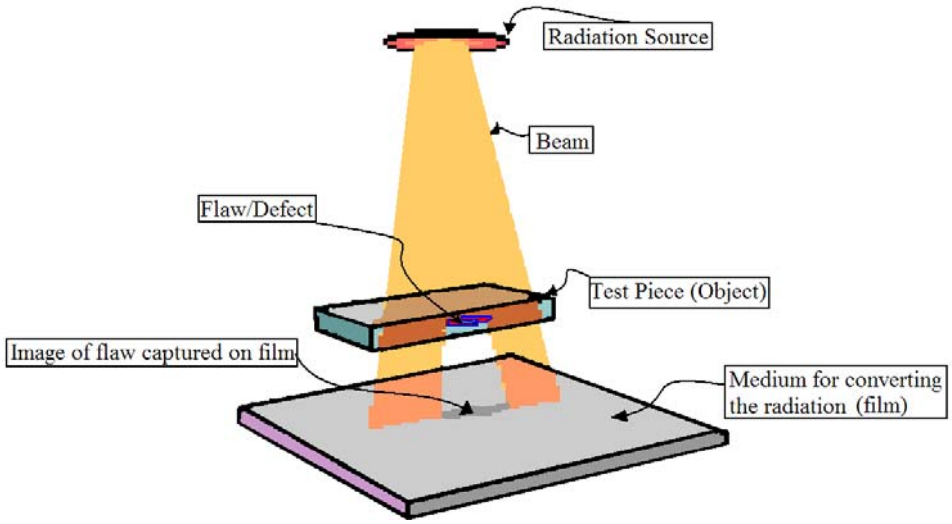


**Figure 2-18: Radiography Testing (Engineers` Handbook 2004)**

## 2.4. Vibration-based damage detection technique

Structural health monitoring (SHM) is one of the important tools to maintain the safety and integrity of structures, such as aerospace, automotive, machinery, and civil structures. A reliable non destructive damage identification and assessment is essential for the development of such monitoring systems, since undetected or untreated damage may grow and lead to structural failure. The challenge is to interpret the changes of the response parameters due to damage and correlate them with the corresponding measured parameters. Specifying the relationship between the damage and characteristic parameters provides the foundation of identification and assessment algorithm required for the SHM system. Furthermore, the anisotropy of material and the fact that much of the damage in composites occurs beneath the surface of laminates increase the complexity of damage assessment in composite structures. The present research focuses on developing the relationship between the dynamic response and the damage as a basis of the damage identification method for composite structures. Structural dynamic response-based damage detection technique offers an identification method with basic assumptions that the dynamic parameters such as natural frequencies, mode shapes, transfer functions, or frequency response functions (FRFs) are functions of the physical properties of the structures. Therefore, the changes in these dynamic characteristics can be used to locate and

assess damages. The experimentally measured data from the surface-bonded sensors provide useful information about the structural health without costly dismantling procedures of the structures. By comparing the identified structural dynamic characteristics of the structure at a later date in service with the intact or healthy structure, damage locations and corresponding magnitudes can be identified. The steps of Vibrational-based damage detection technique are shown in Figure 4.19

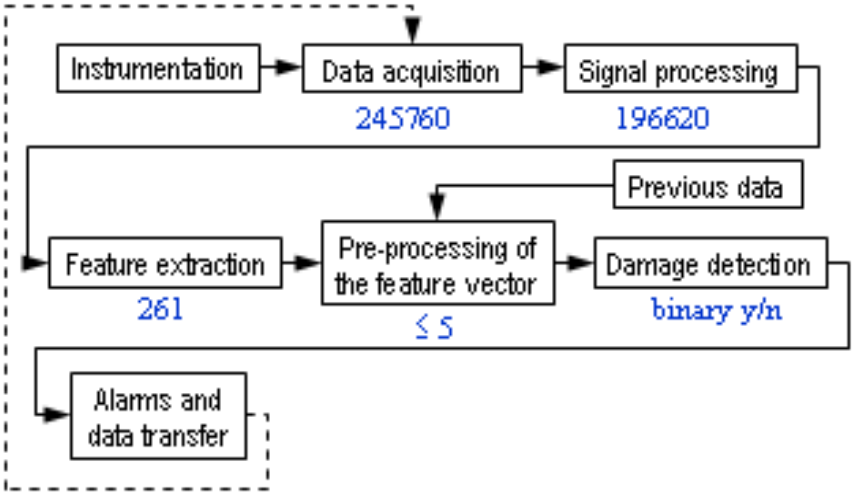


**Figure 2-19: Vibration-based damage detection technique (Jari Savolainen *et al.*, 2001)**

## 2.4.1. Traditional type Damage Detection Method

The traditional-type vibration-based structural damage detection method is mainly based on the natural vibration characteristics of the structures. For example, the natural frequency or mode shapes. The damage location and severity can be determined through finding difference of structural dynamic characteristics between the intact and damaged structures. The traditional-type damage detection (TTDD) method is equivalent to the determination of structural character in given structural locations (Y.J. Yan et al. 2007) Hence, it is the practical application and development of structural dynamic modification method, which is an inverse problem in structural vibration. Since any change of structural mass or stiffness matrix caused by structural mass or stiffness loss in the given part of the structure will be reflected in the measured natural frequency and mode shape, when the measured data of the natural frequency or mode shape are different from those of the intact system, it indicates the damage emergence in the structural system. Some typical TTDD methods can be briefly summarized as follows:

### 2.4.1.1. Natural Frequency

Examples of existing sensitivity analysis method for damage detection of practical structures based on natural frequency and mode shape show that the sensitivity of the stiffness losing at different natural frequency. It is necessary to measure structural vibration modes for most of the TTDD methods. Generally speaking, structural damage existence can be detected through the natural frequency change, while ascertaining the location of structural damage needs information of vibration modes. Yang *et al*. present a method of damage detection using the invariance property of element modal strain energy. This method is to assign element modal strain energy to two parts, and defines two damage detection indicators. One is compression modal strain energy change ratio (CMSECR); the other is flexural modal strain energy change ratio (FMSECR). The present modal strain energy is obtained by incomplete mode shape and structural stiffness matrix. Structural health monitoring is thus accomplished via monitoring the elemental CMSECR and FMSECR. Khoo *et al*. present modal analysis techniques for locating damage in a wooden wall structure by evaluating damage-sensitive parameters such as resonant pole shifts and mode shapes, and the damaged region is identified by visual comparison of the deformation mode shapes before and after damage. The modal residue and stiffness changes are also quantified for a better representation of the damage location. (Y.J. Yan et al. 2007)
However, the measurement error of vibration mode is distinctly larger than that of the natural frequency. Besides, the measured vibration modes are often not complete, so that vibration mode expansion becomes necessary; as a result, it is quite possible that the measurement errors mix with the errors caused by the vibration mode expansion. Although the measurement accuracy of structural vibration mode is lower than that of the natural frequency, the vibration mode contains more damage information. For example, using the mode shape curvature method can ascertain structural damage location according to the change of mode shape curvature. Similarly, using the graphic change of mode shape can confirm the structural damage location.

### 2.4.1.2. Stiffness

The principle of structural damage detection based on the change of flexibility matrix can be explained as follows. When the structural vibration modes satisfy the normalization condition, the flexibility matrix is a function of the mode shape and the reciprocal of natural frequency. Thus, the effect of high-frequency components in flexibility matrix will rapidly decrease with the increase of natural frequency (Y.J. Yan et al. 2007). Therefore, one can get the flexibility matrix with enough accuracy by only measuring several low-order modes and frequencies. According to the difference matrix of the flexibility matrixes before and after structural

damage, the largest element value in each column can be found, and then the structural damage location can be ascertained by examining the largest element value in each column. Aoki and Byon pay attention to deducing localized flexibility properties from the experimentally determined global flexibility matrix, and present the underlying theory that can be viewed as a generalized flexibility formulation in three different generalized coordinates, namely, localized or sub structural displacement-basis, elemental deformation-basis and element strain-basis. Yan and Golinval also present a damage diagnosis technique based on changes in dynamically measured flexibility and stiffness of structures. The covariance-driven subspace identification technique is applied to identify structural modal parameters, and these are then used to assemble the flexibility matrix of dimensions corresponding to the measured degrees of freedom (Y.J. Yan et al. 2007). The corresponding stiffness matrix is obtained by a pseudo-inversion of the flexibility matrix. Damage localization is achieved by a combined assessment of changes in these two measured matrices in moving from the reference state to the damaged state. Since the location of damage is given directly by the position of sensors, no geometrical measurements and

Finite-element models are needed. Generally, when some damage appears in a structure, stiffness matrix can offer more information than the mass matrix. Using the change of stiffness matrix to detect damage is because the stiffness changes remarkably when big damage appears in a structure. However, if the damage is very small, this method cannot work well.

## 2.4.1.3. Statistics Information

In system analysis, damage can be regarded as an additive excitation on the system. It can cause the change of output signal from the system. When one tries to search the additive excitation using the measured output signals, the noise problem in output signal must be taken into account, especially that the signal change caused by small damage may be covered by noise. Hence, detection method for initial damage based on statistic information is proposed. In using statistic mode, the detection for structural damage is based on the probability of damage emergence. Iwasaki *et al.* present a methodology of damage detection by judging the statistical difference between data of the intact state and the damaged state. The method requires data of the undamaged state, but does not require complicated modeling or data for training. Damage is detected from the change of strain data using statistical tools such as the response surface and F-statistics (Y.J. Yan et al. 2007). As a result, the method successfully diagnoses the damage without the need to use modeling or data of the damaged state. Fugate et al focuses on applying statistical process control methods referred to as ‘control charts’ to vibration-based damage detection. First, an autoregressive (AR) model is fit to the measured acceleration-time histories

from an undamaged structure. Residual errors, which quantify the difference between the prediction from the AR model and the actual measured time history at each time interval, are used as the damage-sensitive features. Next, the X-bar and S control charts are employed to monitor the mean and variance of the selected features. Control limits for the control charts are constructed based on the features obtained from the initial intact structure. The residual errors computed from the previous AR model and subsequent new data are then monitored relative to the control limits (Y.J. Yan et al. 2007). A statistically significant number of error terms outside the control limits indicate a system transit from a healthy state to a damaged state. Lopez-Diez *et al.* analyze the applicability of the statistical energy analysis (SEA) for detecting incipient damage in a typical spacecraft structure, and point out that, because incipient damage affects mainly on the highest modes, rather than on the lowest ones, the coupling loss factor between sub-elements can be used to detect and localize the damage.

## 2.4.2. Applications of Sensors in Structural Health Monitoring

## 2.4.2.1 Introduction

This chapter discusses the sensors used in structural health monitoring systems. The frequently used sensors comprise: optic fibre sensors (Bragg grating or Fabry- Perot system) piezoelectric sensors, strain gauges, shape memory alloys Scanning Laser Vibrometer (SLV) systems. A brief review of few is discussed below. (M. H. H. SHEN and J. E. GRADY 1992)

## 2.4.2.2 Piezoelectric Sensors

Piezoelectricity (Baker *et al*., 2004) was discovered by Pierre and Jacques Curie in 1880. Ever since, the use of piezoelectricity has been of impressive use to a number of fields. There are fundamentally two types of piezoelectricity observed, direct and the indirect piezoelectricity (Baker *et al*., 2004). Under direct piezoelectricity, a piezoelectric material when stressed mechanically produces an electric discharge on the surface of the material. In comparison, under in-direct piezoelectricity, the piezoelectric material produces mechanical deformation when subjected to an electric field (Fig 2.20). The materials exhibiting above behavior are called piezoelectric materials.

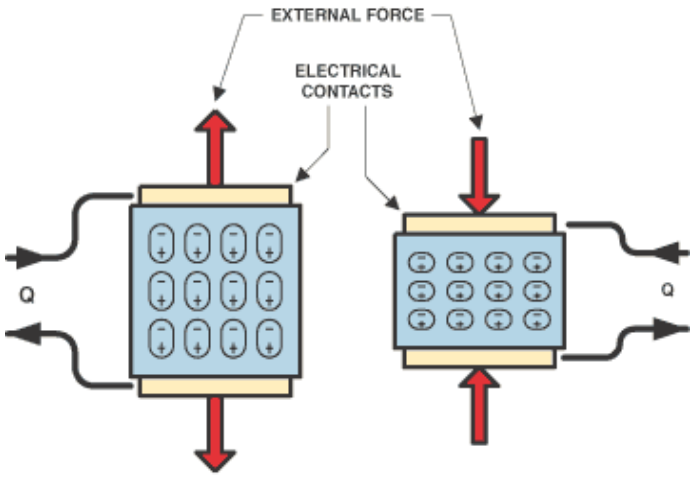


**Figure 2-20: Piezoelectric material(Ed Ramsden, 2006)**

When a high electrical field is applied to the material at high temperatures, in a particular direction, the ferroelectric domains within the material align in the direction of the electric field. This action is called poling. The common types of piezoelectric materials (Encyclopedia of Smart Structures 2002, P.149-155) used are: quartz, barium titanate, cadmium sulphide, and lead zirconium titanate (PZT). Majority of these piezoelectric materials are ceramic and hence brittle in nature, this makes it unsuitable to embed within composite structures. To overcome these difficulties piezoelectric polymers (Encyclopedia of Smart Structures 2002, P.149-155) such as: Polyvinyl Chloride (PVC), Polyvinylidene Fluoride (PVDF) and polymer films, and are being increasingly used as sensors. Piezoelectric materials can be manufactured in thin plates, strips, or films. The widespread use of piezoelectric materials is largely because they provide a coupling between electrical and mechanical energy. Direct piezoelectric phenomenon is used in spark ignition devices such as gas stoves and even cigarette lighters. Piezoelectric-based pressure and vibration sensors such as accelerometers, automobile airbag sensors, and vibration sensors also use the direct piezoelectric principle. A typical example of an in-direct piezoelectric material used in everyday life is within automatic dispensing of goods and services such as vending machines. These machines rely on payment beforehand with coins and due allowance for many possible combinations. The system recognizes the coins by validating the vibration response after the coin strikes the piezoelectric sensor after it is inserted into the machine (Figure: 2-21).

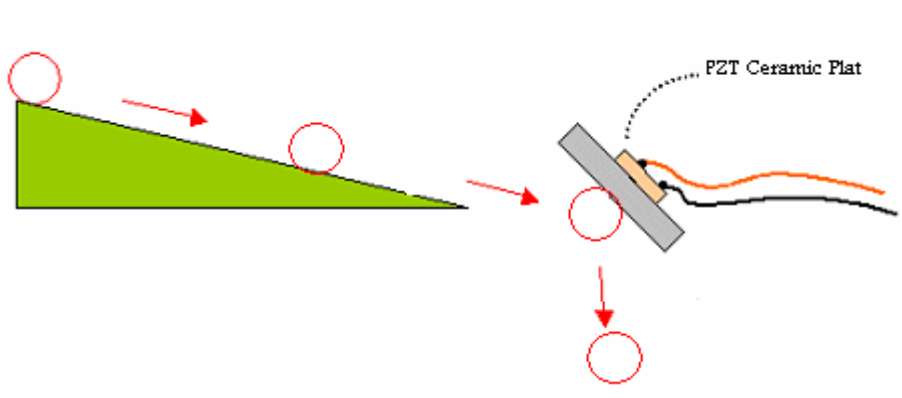


**Figure 2-21: Schematic representation of coin validation in vending machines (Courtesy: transducer-sensor.com)**

## 2.4.2.3 Optical Fibers

Optical fibers (Baker *et al*., 2004) consist of three main parts; the core through which light travels, surrounded by a cladding and an outermost protective jacket also known as buffer coating (Courtesy: www.howstuffworks.com), as shown in Figure 2.22. The core and the cladding are made out of silica, where the refractive index of the core is higher than that of the cladding.

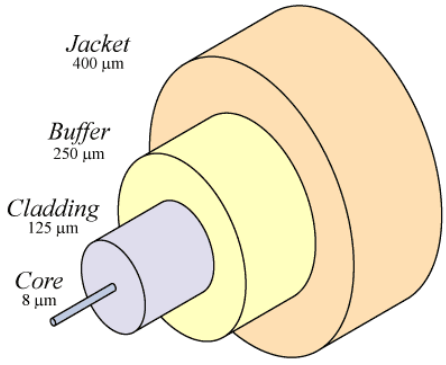


**Figure 2-22: Optical Fibre (Courtesy: www.howstuffworks.com)**

This change in refractive index facilitates the required mechanics (total internal reflection) for light propagation within the core. The primary function of the optical fibre is to conduct light from one point to another. There are three main ways of classifying (Encyclopedia of Smart Structures 2002, P.715-736) optical fibers based on: the bandwidth (Multimode or Single mode), the variation of refractive index of the core (Stepped or graded), and the location of the sensing region of the optical fibre (Intrinsic or Extrinsic). Multimode optical fibers permit the propagation of several modes of light, whereas single mode permits the transmission of the only the zero-order mode (Figure 2-23).

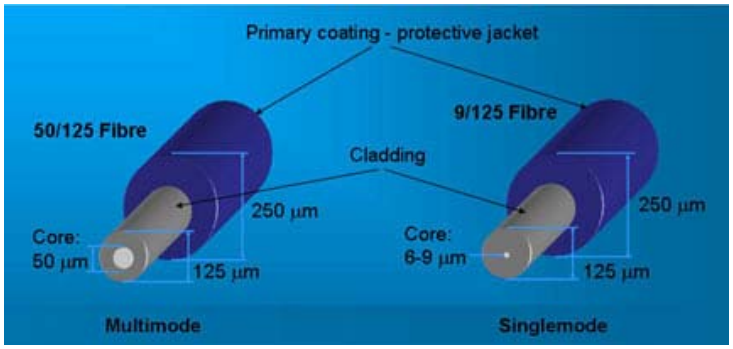


**Figure 2-23: Comparison of Multi mode and Single mode optical fibres (Encyclopaedia of Smart Structures, 2002)**

If the sensing region of the fibre sensor is located outside the optic fibre then it is classified as extrinsic type (e.g. Fabry-Perot Interferometer), whereas if it were within the optic fibre then it is classified as intrinsic type (e.g. Bragg Grating). Different kinds (Encyclopedia of Smart Structures 2002, P.715-736) of fibre-optic sensors used for in-situ health monitoring namely: interferometry based sensors, intensity-based sensors, polar metric sensors, and extrinsic Fabry-Perot interferometers, Fibre Bragg grating sensors (FBG), Raman scattering sensors, and Brillion scattering sensors. Among these the ones used most frequently for structural health monitoring are: the Fibre Bragg grating sensors and the extrinsic Fabry- Perot interferometers. Optical fibers have been used to detect a wide range of parameters including: strain, temperature, displacement, acceleration, angular velocity, acoustic emission and vibration. Takeda *et al*. (2005) have acknowledged the use of fibre Bragg Grating sensors for sensing lamb waves, which in succession are used for quantitative evaluation of damage in CFRP laminates. FBG sensors were used by Lee *et al*. (2005) to sense acoustic emissions for mechanical testing of materials. The Fabry-Perot interferometry sensor was used by Oliveira *et al*. (2004) to sense acoustic emission resulting due to damage.

## 2.4.2.4. Bragg Grating Optical Fibre Sensor

A Fibre Bragg grating sensor (Baker *et al*., 2004) consists of periodic modulation of the core refractive index of an optical fibre. These gratings are created on the optical fibre by exposure of intense ultraviolet light. Due to the presence of the grating, a narrow band of wavelength is reflected back down the fibre, as shown in Figure 2.24

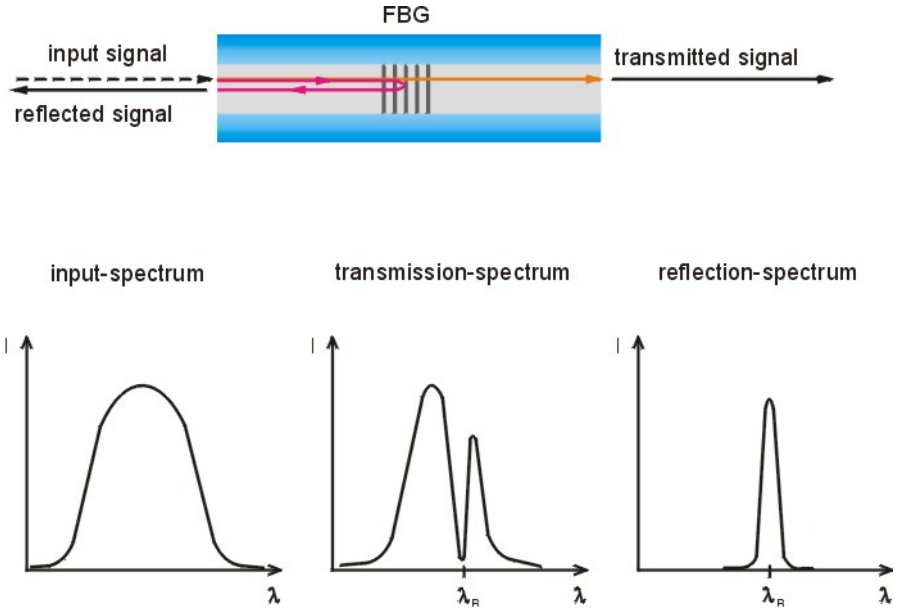


**Figure 2-24: Schematic of a Bragg grating sensor (Schmit, 2000)**

## 2.4.2.5. Fabry-Perot Optical Fibre Sensor

The Fabry Perot Interferometry (Encyclopedia of Smart Structures 2002, P.727-728) sensor works with the principle of coherent interference between reflected and transmitted light waves. A schematic of an extrinsic Fabry-Perot sensor is shown in Figure 2.25

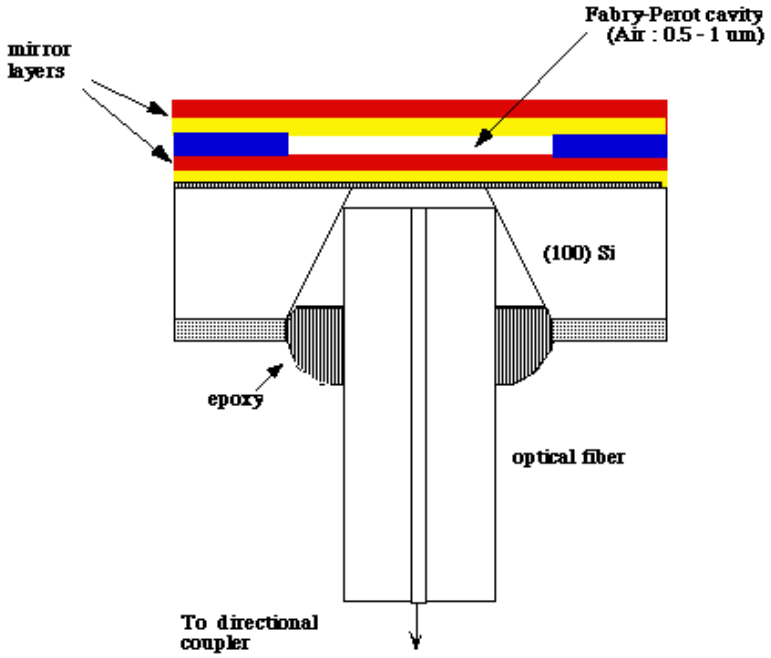


**Figure 2-25: Schematic of an Extrinsic-Fabry-Perot grating sensor (Youngmin Kim *et al.*. 2002 )**

A Fabry-Perot sensor consists of a single-mode fibre which is used as the input/output lead. The function of the multimode fibre is to act as a reflector, reflecting the transmitted light. The single-mode fibre and the multimode fibre are coupled in an alignment tube with an air gap between them. The transmitted light that travels through the single-mode fibre passes through

the air gap and is reflected at the face of the multimode fibre. A percentage of this reflected light re-enters the single-mode fibre. This results in interference between the transmitted light and the reflected light and a fringe pattern is obtained. Any change in the air gap causes a change in the interference pattern, from which information on strain levels can be measured. The use of these sensors is limited although they are sensitive to strain and temperature variations as they are difficult to manufacture and also have very limited multiplexing capabilities.

## 2.4.2.6. Strain Gauges

Strain gauge is the most commonly used device for the measurement of strain. The frequently used strain gauge, i.e. the bonded metallic strain gauge, consists of a flexible backing which supports a metallic foil pattern etched on to the backing. The strain gauge is bonded on to a structure by means of an adhesive. The working principle of the strain gauge is based on the piezo-resistive effect, i.e. when the foil is deformed (because of structural deformation) the resistance of the foil changes (Wikipedia: The free encyclopedia, 2004). Visualization of the working concept behind the strain gauge on a beam under exaggerated bending is shown in Figure 2.26. A Wheatstone bridge circuit is then used to calculate the strain, from the resistance change. Different types of Wheatstone bridge circuits can be used for this purpose including: Full bridge circuit, half bridge circuit and the quarter bridge circuit.

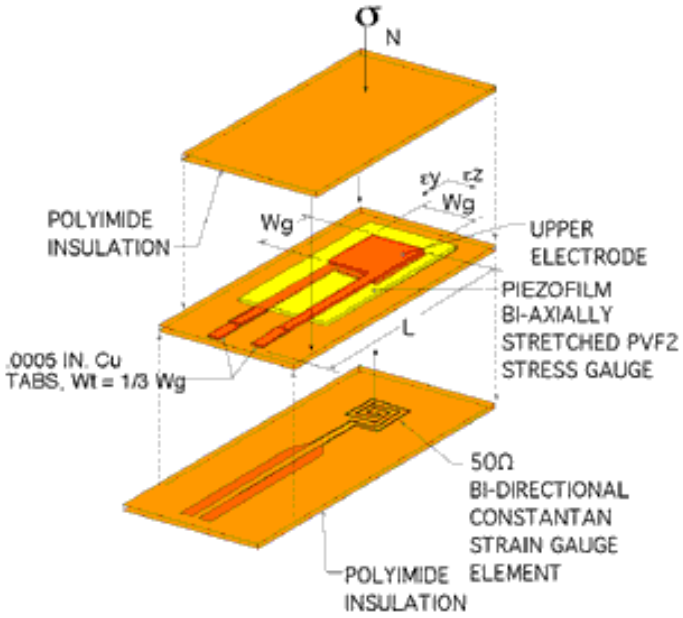


**Figure 2-26: Visualization of the working concept behind the strain gauge under exaggerated bending**

**(Courtesy: Dynasen Inc.)**

The sensitivity of a strain gauge to strain is determined by the gauge factor (Wikipedia: The free encyclopedia, 2004), which is:

$$GF = \frac{\frac{\Delta R}{R_G}}{\varepsilon} \qquad (2\text{-}2)$$

Where:

GF: is the gauge factor

R G: is the resistance of the unreformed gauge

ΔR: is the change in resistance caused by strain

$\varepsilon$ : is strain

## 2.4.2.7. Shape Memory Alloys

Shape memory alloys (SMA's) are metals, which exhibit two very unique properties, pseudo elasticity, and the shape memory effect.. The most effective and widely used alloys include NiTi (Nickel - Titanium), CuZnAl, and CuAlNi (Baker *et al*., 2004, SMA/MEMS Research Group, 2001). In the one way effect a SMA (Baker *et al*., Oishi *et al*., 2005, SMA/MEMS Research Group, 2001) in its martens tic form, is plastically deformed from its original shape. This SMA then regains its original shape when it is heated to a temperature above the austenitic finish temperature as shown in Figure 2.27 below.

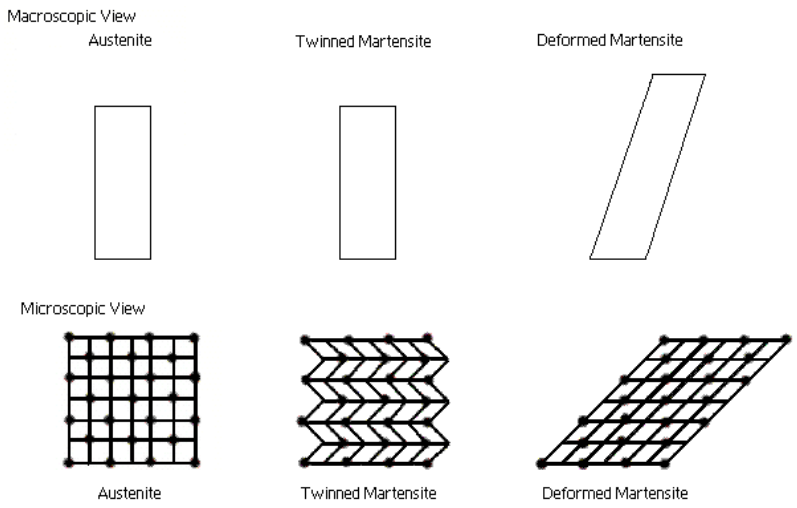


**Figure 2-27: Shape Memory Alloys (Courtesy: Oulo University)**

## 2.5.2. Modern type Damage Detection Methods

Modern-type vibration-based structural damage detection, also called intelligent damage diagnosis (Y.J. Yan et al), is a method using online measured structural vibration responses to detect damage. These methods mainly take modern signal-processing technique and artificial intelligence as analysis tools. With well universality and less dependence on structural shape, they are also called intelligent damage diagnosis methods. The structural dynamic response measured by online and non-destructive technology may indicate the change of structural dynamic parameters at the structural damaged status. Vibration-based structural damage detection is a vital field both in theoretical research and engineering application. Many scholars have carried out a great deal of research to perform damage detection for large and complex structures. The representative methods among them are wavelet analysis, NN, GAs, etc.

### 2.5.2.1. Wavelet Analysis Method

Wavelet analysis is very suitable to analyze non-stationary signal, so it can be used as a feasible method for processing signal in damage detection to construct the needed feature index of structural damage. Wavelet analysis has various applications in structural damage detection, for example, singular signal detection, signal-to-noise separation, frequency-band analysis and so on. The spectrum graph obtained using wavelet transform can indicate the damage existence directly (Y.J. Yan et al). Rajasekaran and Varghese proposed a wavelet based approach for structural damage detection in beams, plate and delamination detection of composite plates. The main concept used is the breaking down of the dynamic signal of a structural response into a series of local basis function called wavelets, so as to detect the special characteristics of the structure using scaling and transformation property of wavelets. Lu and Hsu present a study based on the wavelet transform for structural damage detection. Through comparing the discrete wavelet transforms of two sets of vibration signals from the undamaged and damaged structures in the space domain, not only the presence of defects can be detected, but also their number and location as well. To simulate the defects of the structure, they attached several point masses and springs on the string. Numerical results show that even a minor localized defect can induce significant changes in the wavelet coefficients of the vibration signals. Law *et al.* have derived analytically the sensitivity of wavelet packet transform (WPT) component energy with respect to local change in the system parameters based on the dynamic response sensitivity. The proposed method shows both analytically and numerically to be not sensitive to measurement noise. The method can differentiate damages at close proximity to each other with good resolution using a very short duration of measured data from only two sensors. Yan and

Yam [36] present the method for online detection of initial damage in a composite laminated plate based on energy variation of structural dynamic responses decomposed using wavelet analysis (Figure 4.20). (Y.J. Yan et al. 2007)

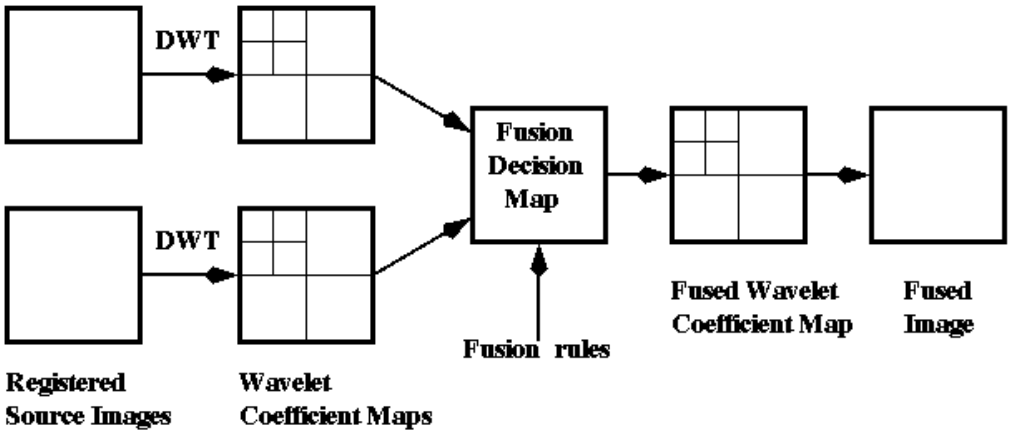


**Figure 2-28: The principle of wavelet Transform Method (elensar, 2008)**

This study shows that the constructed structural damage index is basically monotonously changeable with the severity of crack damage in the plates, and is also very sensitive to small damage. (Y.J. Yan et al)

## 2.5.2.2. Neural Network Method

The BP NN has been widely used in structural analysis because of its strong non-linear mapping ability. It is usually constructed by three layers, an input layer, a hidden layer and an output layer. Structural damage detection based on NN includes the following steps: to determine the network structure; to select the network parameters; to normalize the learning samples; to give initial weight value and to detect structural damage. Based on this idea, the constructed NN will be first trained according to the following step. The known feature information (NN input) and the corresponding status (NN output) of structural damage are taken as train samples to train the constructed NN (Y.J. Yan et al). This damage information as train sample can be obtained by experiments or numerical simulations for a structure to be detected. When the NN has been well trained, one can input the experimentally measured real structural damage feature index into the trained NN, and the output of the trained NN will be able to give the location and severity of the structural damage. Kao and Hung present a NN-based approach for detecting structural damage. The proposed approach involves two steps. The first step, system identification, the neural system identification networks (NSINs) is used to identify the undamaged and damaged status of a structural system. The second step,

structural damage detection, the aforementioned trained NSINs is used to generate free vibration responses with the same initial condition or impulsive force. Comparing the periods and amplitudes of the free vibration responses of the damaged and undamaged status allows the extent of changes to be assessed. Chen *et al.* studied the diagnose of faults in engineering structures in the situations where the excitation signals are unavailable or inaccessible, and response-only data are utilized to train NNs. The NN classifiers clearly deliver the diagnostic indications of the faults introduced into the structural systems, which suggests that the transmissibility function is a sensible response-only data source for structural fault diagnosis. Qu et al deals with structural damage detection by using BPNN. Features extracted from FRFs by applying independent component analysis (ICA) are used as input data to NN. The Latin hypercube sampling (LHS) is adopted for efficient generation of the patterns for training the NN. The principle of Neural Network Method is shown in Figure 4.21. (Y.J. Yan et al)

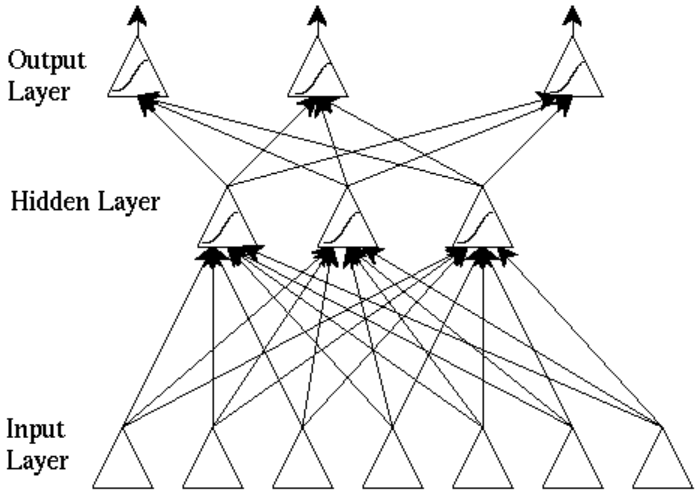


**Figure 2-29: Basic Principle of Neural Network Method (Leslie Smith *et al.*, 2002)**

## 2.5.2.3. GA Method

GA is a powerful universal tool to solve optimization problem, and it is independent of the details of the research object. In structural damage detection, it is suitable to use GA to ascertain the damage locations. The encoding operation of GA ensures that it can fully use the information in every set of solutions in iteration. Meanwhile, GA has high calculation efficiency in parallel data processing, and it can search for accurate solutions simultaneously. Thus, it is possible to obtain the global optimum solution. Moslem and Nafaspour present a two-stage procedure; they utilize incomplete measurements to detect the location and extent of structural damage. In the first stage, candidate damaged elements are identified using the residual force method. Based on prior knowledge from the first stage, the damage extent is

determined from candidate elements using a proposed optimization scheme based on the method of simulated evolution. Chou and Ghaboussi have proposed a method of structural damage detection by using GA. Static measurements of displacements at few degrees of freedom (DOFs) are used to identify the changes of characteristic properties of structural members, such as Young's modulus and cross-sectional area, which are indicated by the difference of measured and computed structural responses. In order to avoid structural analyses in fitness evaluation, the displacements at unmeasured DOFs are also determined by GA. Unlike the traditional mathematical methods, which guide the direction of hill climbing by the derivatives of objective functions, GA searches the problem domain by the objective function itself at multiple points. The proposed method is able to detect the approximate location of the damage, even when practical considerations limit the number of on-site measurements to only a few. Raich and Liszkai have discussed robust structural damage detection method that can handle noisy frequency-response function information. The inherent unstructured nature of damage detection problems is exploited by applying an implicit redundant representation (IRR) GA. The General method is shown in figure 4.22. (Y.J. Yan et al)

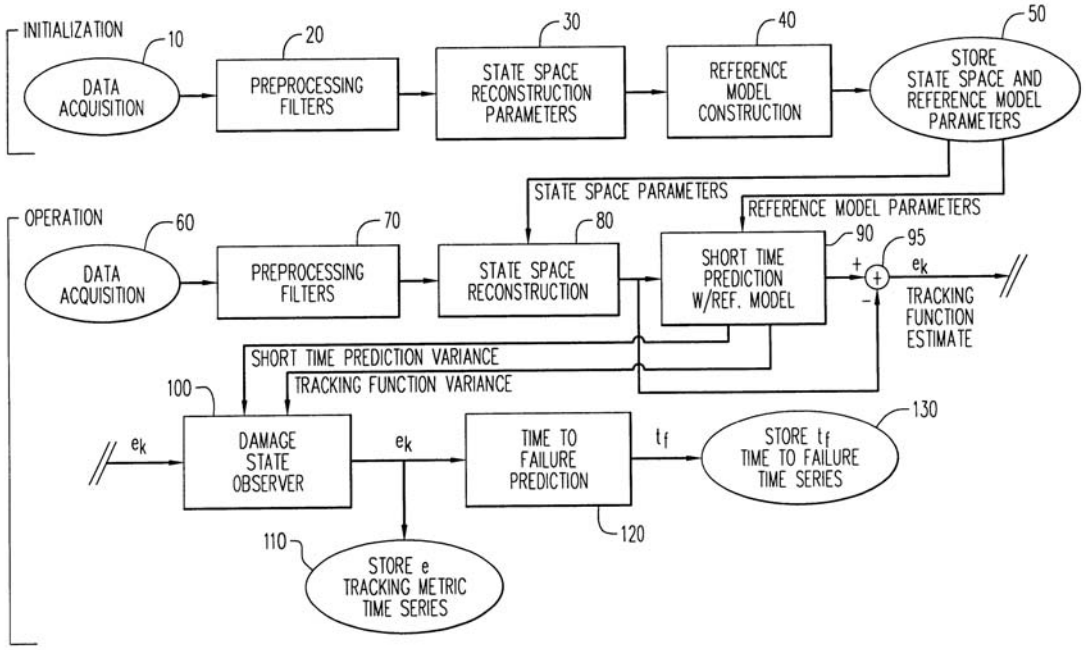


**Figure 2-30: GA`s Method for damage detection (Cusumano Joseph, 2002)**

## 2.5.3. Model-based Damage Detection Methods

The model-based (MB) methods undertake analysis of structural models and are usually implemented by Finite element analysis. Damage is simulated by modifying the models. Experimental data can then be compared with the analytical data to determine damage location

and extent. The electiveness of the whole group of MB techniques, however, is dependent on the accuracy of the structural model and these methods may have difficulties when applied to complex structures. With the model, various response characteristics of the structure such as modal analysis, time response, frequency response and impedance response can be extracted and analyzed.

### 2.5.3.1. Modal Analysis Method

This group of methods utilizes the information from all modal parameters (modal frequencies, mode shapes and modal damping ratio) or combinations of some of them to detect damage. The basic idea of these methods is that modal parameters are functions of the physical properties of the structure (mass, damping and stiffness). Therefore, changes in the physical properties, e.g., damage, will cause changes in the modal properties (C. P. Ratcliffe *et al*. 1998). Usually, damage will decrease mass and stiffness of the structure and increase damping ratio locally. Among the three structural property parameters, mass is less sensitive to damage while damping is most sensitive to damage. Because of its complex physical nature, proportional damping is often adapted in damage detection methods. According to their different detection techniques, the modal analysis methods can be divided into the following major categories: modal shape changes methods, modal shape curve methods, sensitivity-based update methods, eigenstructure assignment methods, and optimal matrix update methods, changes in measured stiffness matrix methods, frequency response function method, and combined modal parameters method.( A. K. Pandey *et al*. 1991)

The majority of this group of methods uses the lower frequencies of the modal and can best describe the global behavior of the structure (Y. Zou *et al*. 1999).. Therefore, they hold promise for global non-destructive inspection of a variety of structures, because surface measurements of a vibrating structure can provide information about the health of the internal members without costly (or impossible) dismantling of the structure. Also, because of their global nature, these techniques allow the customization of measurement points. Another major advantage is that the modal information is cheap to obtain and easy to extract.

However, there are many limitations to this group of methods. Firstly, some of the modal-based methods can only detect particular forms of damage in their diagnostic schemes. Secondly, the methods usually use the undamaged structural modal parameters as the baseline compared with the damage information. This will result in the need for a large data storage capacity for complex structures, but, a newly developed method, which tries to quantify damage without using a base line, may be a solution to this difficulty. Thirdly, they fail to detect small defects in global features.

### 2.5.3.2. Frequency Domain

Damage may be detected only using frequency response of the structure. The foundation of this group of methods is that damage produces a decrease in structural stiffness, which, in turn, produces decreases in natural frequencies (Y. Zou *et al*. 1998). The location of the defect can be estimated from the degree of change in natural frequency, which in turn, depends on the position of the defect for a particular mode of vibration. In other words, local or distributed changes in stiffness produce changes in natural frequencies, which affect each mode differently depending on the damage location. This is because the damage event is a local phenomenon in most cases. Therefore, it was suggested that monitoring local high-frequency modes of local area provide (A. Rytter *et al*. 1994) a better indication of damage for small damage. It was also pointed out that locating damage from changes in frequencies alone is impractical. It was suggested that resonant frequency is a better indicator of defects than frequencies because it can change more significantly than frequencies do when properties change. There are several other methods available in this frequency domain category such as the damage index method, the sensitivity analysis method, etc.. As only frequency information is required, these approaches can provide cost effective structural assessment techniques. However, natural frequency changes alone may not be sufficient for a unique identification of the location of structural damage. The current frequency domain methods are either using lower frequencies for providing global information of structures or using higher frequencies for providing local information of structures. None of these can provide sufficient information for the detection of both small and large defects. (Y. Zou *et al*. 1998)

### 2.5.3.3. Time Domain

Basically, all methods in this category are related because they use time history. These methods could be independent of modal information although they are usually combined with frequency domain methods (Y. Zou *et al*. 1998). Damage is estimated using time histories of the input and vibration responses of the structure. Using time response over a long period while at the same time taking into account the information in several modes so that the damage evaluation is not dependent on any particular one, could be sensitive to any modes. The big advantage of the methods in this group is that they can detect damage situations both globally and locally by changing the input frequencies.

### 2.5.3.4. Impedance Domain

Damage is detected through measuring the changes of impedance in the structure. The basis of this technique is that each part of the structure contributes to the impedance of structure to some

extent. Any variation in the structure integrity will generally result in changes in the impedance, i.e., the impedance will change with changes of the stiffness. This group of techniques models the defect as a spring and assumes that it is clamped around the edges of the defect. The spring stiffness is given by the stiffness of the layers above the defect. In the absence of a defect, the spring stiffness is infinite (Y. Zou *et al*. 1998). The damage detection process, therefore, becomes that of inspecting the change of stiffness and location of the spring within the structure. There are two groups of techniques in this domain. One is mechanical impedance, and the other is electrical impedance. Mechanical impedance techniques are based on the measurement of the impedance, $Z$, at a point of a structure. The impedance is defined as $Z'F/v$, where $F$ is the applied force input to the structure, and $v$ is the resultant velocity of the structure at the same point. Similar to the mechanical impedance, electrical impedance techniques measure changes of electrical impedance which is defined as the ratio of the applied voltage to the resulting current of the structure. The elastic admittance of the collocated sensor/actuator is assumed to be functionally equivalent to its mechanical impedance (Y. Zou *et al*. 1998). This group of methods is capable of multi-location and real-time health monitoring. Impedance domain methods are particularly suitable for detecting planar defects such as delamination. The inspection is reliable except when the system impedance becomes spring-controlled and then the impedance only decreases with spring stiffness, i.e., the layer above the defect are thin and the base structure is relatively stiff.

## 2.5.4. Preferred Technique

The curvature mode shapes are utilized as a base parameter for damage identification and assessment technique in the present study. The changes of the curvature mode shapes are localized in the region of the damage and consequently may be used effectively to identify damage location in structures. Pandey *et al.* (1991) was among the first who demonstrated the possibility of curvature mode shape application in health monitoring. The curvature mode shape information in combination with data of frequency changes was used to identify cracks by Pabst and Hagedorn (1993). Salawu and Williams (1994) compared the performance of both curvature and displacement mode shapes for locating damage, which confirmed the advantage of curvature mode in locating damage as compared to the displacement mode.

## 2.5.5. Conclusion

A damage in a structure alters its dynamic characteristics. The change is characterized by changes in the eigenparameters, i.e., natural frequency, damping values and the mode shapes associated with each natural frequency. Considerable effort was spent in obtaining a relationship between the changes in the eigenparameters, the damage location and the damage size. Most of the emphasis has been on using the changes in the natural frequencies and the damping values to determine the location and the size of the damage.

In this project a new parameter called curvature mode shape is investigated as a possible candidate for identifying and locating damage in a structure. By using a cantilever and a simply supported analytical beam model, it is shown here that the absolute changes in the curvature mode shapes are localized in the region of damage and hence can be used to detect damage in a structure. The changes in the curvature mode shape increase with increasing size of damage. This information can be used to obtain the amount of damage in the structure.

# CHAPTER 3

# Manufacture of Composite Samples

## 3.1. Introduction

Composite beams with artificial delaminations were manufactured for testing at the RMIT University's Composites laboratory. Various beams were manufactured by the vacuum bag resin infusion technique (Mallick, 1988; Schwartz, 1996; Barbero, 1998) and hand lay-up technique (Mallick, 1988; Schwartz, 1996; Barbero, 1998). Plywood was also chosen as an additional composite material for testing and evaluation purposes. Both types of composites were introduced with artificial defects and tested using a Laser Vibrometer to acquire the dynamic responses.

## 3.2. Plywood Panels

Plywood composites (Figure 3-1) with simulated defects were used as shown in Figure 3-2 to recognise the system setup parameters. Plywood is manufactured by slicing or rotary peeling thin sheets less than 2.5 mm of material veneer from a flitch or log and then laminating three or more veneers into rectangular sheets. Generally 1200 mm × 1200 mm used for very thin sheets and 1200 mm × 2400 mm for other thickness (Brandon, 1995). Plywood is a type of engineered wood made from thin sheets of wood veneer, called plies or veneers. The layers are glued together, each with its grain at right angles to adjacent layers for greater strength. There are usually an odd number of plies, as the symmetry makes the board less prone to warping, and the grain on the outside surfaces runs in the same direction (J. R. Watson). The plies are bonded under heat and pressure with strong adhesives, usually phenol formaldehyde resin, making plywood a type of composite material (J. R. Watson). Plywood is sometimes called the original engineered wood

**Figure 3-1: Plywood Composites**

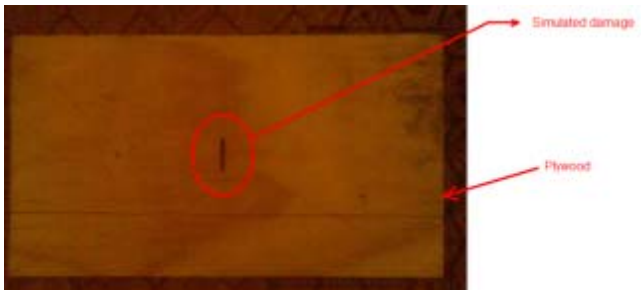


**Figure 3-2: Plywood sheets used in experiments**

Also because of their easy accessibility and cost efficiency compare with Carbon/Epoxy composites the experiment began with plywood samples to find the optimal method of experimental modelling. As it is shown in Figure 3- 4 two plywood samples were acquired from the unique sheet to minimize the natural differences within the samples. One of the samples has a notch in the centre as a defect. Another one considered as a healthy sample. The comparison of defect and healthy Plywood samples is shown in Figure 3-3.

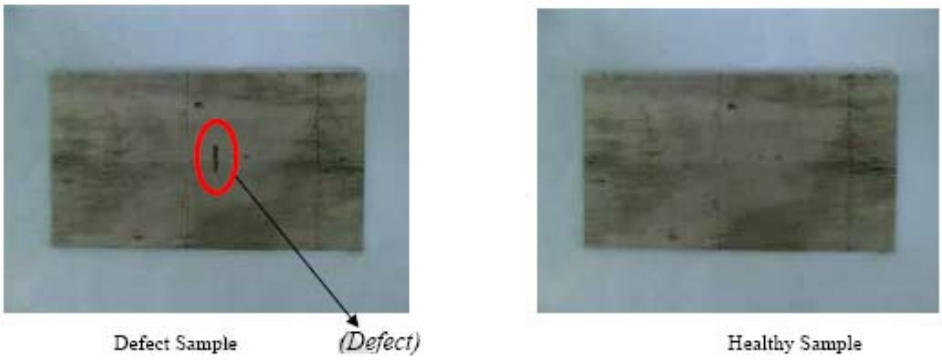


**Figure 3-3: Comparison of Plywood Defect and Healthy Sample**

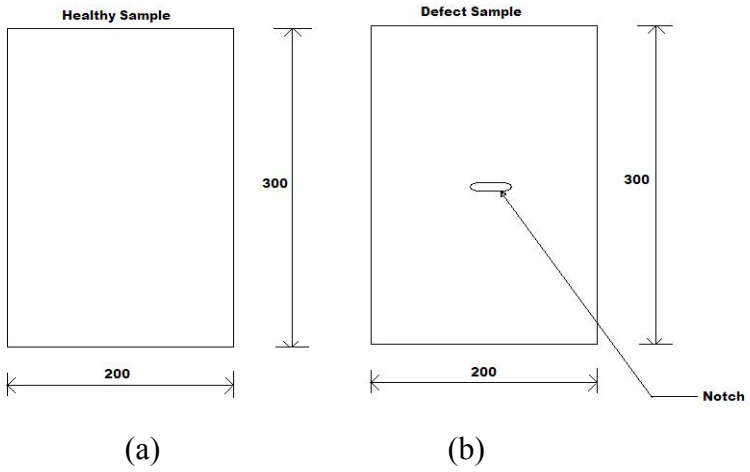


**Figure 3-4: Plywood Panels (a) Healthy Sample, (b) Damaged Sample**

## 3.3. Manufacture of Carbon/Epoxy Composite Beams

Carbon fibre reinforced epoxy unidirectional (UD) prepreg each 1.25mm thick were used to make the composite beams along with Teflon impregnated glass film (~60 μm) inserted as artificial delaminations.

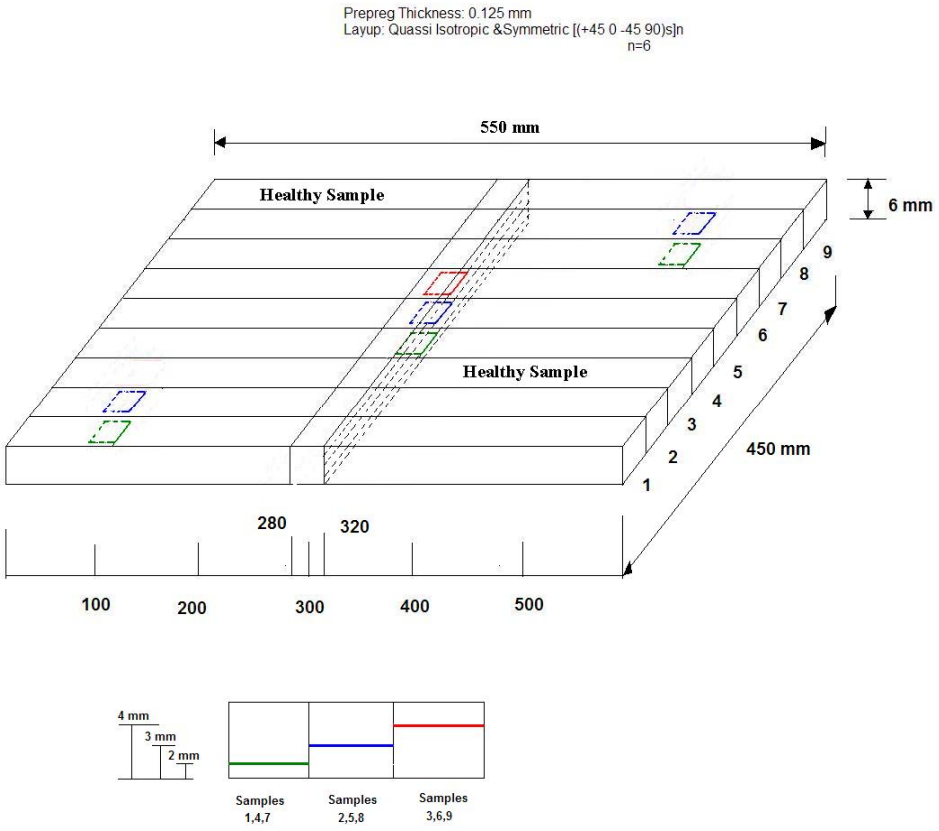


**Figure 3-5: The model used as manufacturing guideline**

After the appropriate set up of the system by using Plywood samples, the process of manufacturing Carbon/Epoxy beams started. The specimens were made of carbon fiber and epoxy resins and had a [0/90/±45] lay-up of a total of six layers, with each layer thickness of 1.25mm and a total thickness of 7.5 mm. Each beam specimen has a width of 50 mm and a length of 550 mm (Figure 3-5)

During the manufacturing, seven Teflon layers were put as a delamination in the sample in different levels and different locations and two remaining beams considered as a healthy sample.

A total of thirty-two plies were cut and arranged into a 550 mm × 450 mm rectangle and stacked using the hand layup technique (Mallick, 1988; Schwartz, 1996; Barbero, 1998) using a hand roller onto a steel plate in a Quasi Isotropic & Symmetric layup [(+45 0 -45 90)s]n ; n=6 (Figure 3.6). During stacking, each ply was rolled to ensure no air is trapped in between the layers.

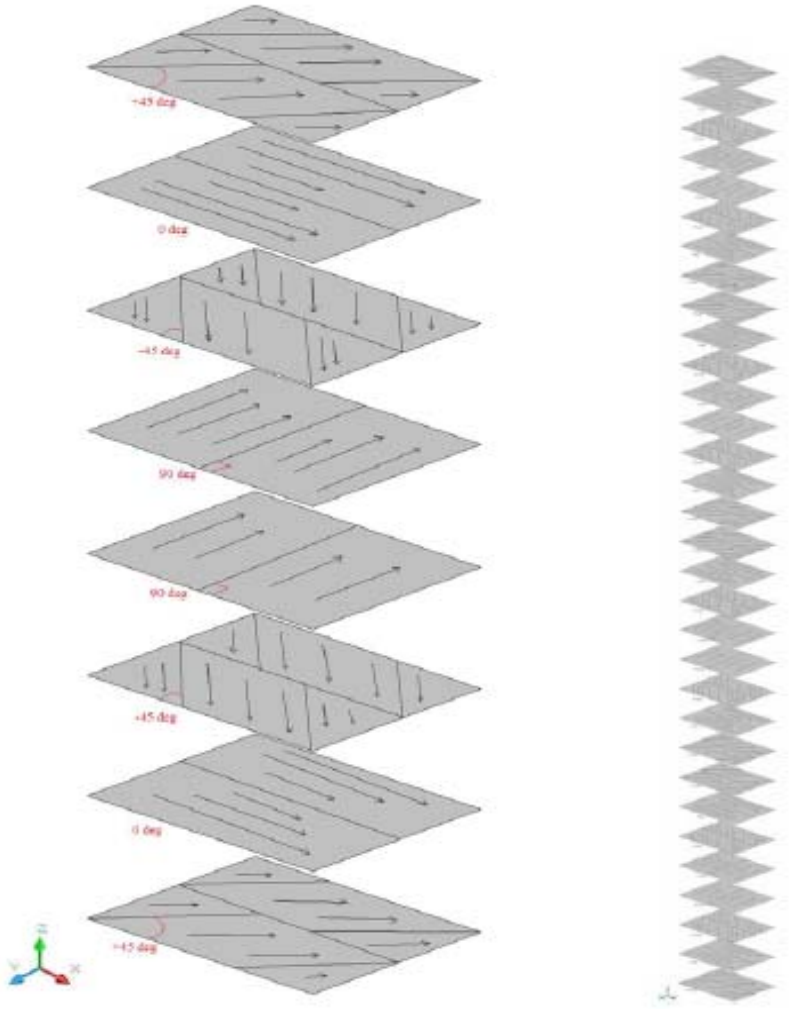

**Figure 3-6: Quasi Isotropic & Symmetric layup using 32 plies**

Also the Teflon impregnated glass film was introduced in between layers to simulate delamination. During the manufacturing, the aim is to make the samples as accurate as possible although the manufacturing errors i.e. bubbles, gaps, shifts are inevitable. A total of nine beams was manufactured, most of which were embedded with artificial delaminations. As it can be seen from Figure 3-7, after putting all layers together the carbon/epoxy laminate is ready for the next step which will be curing. The laminate was vacuumed and placed inside the chamber.

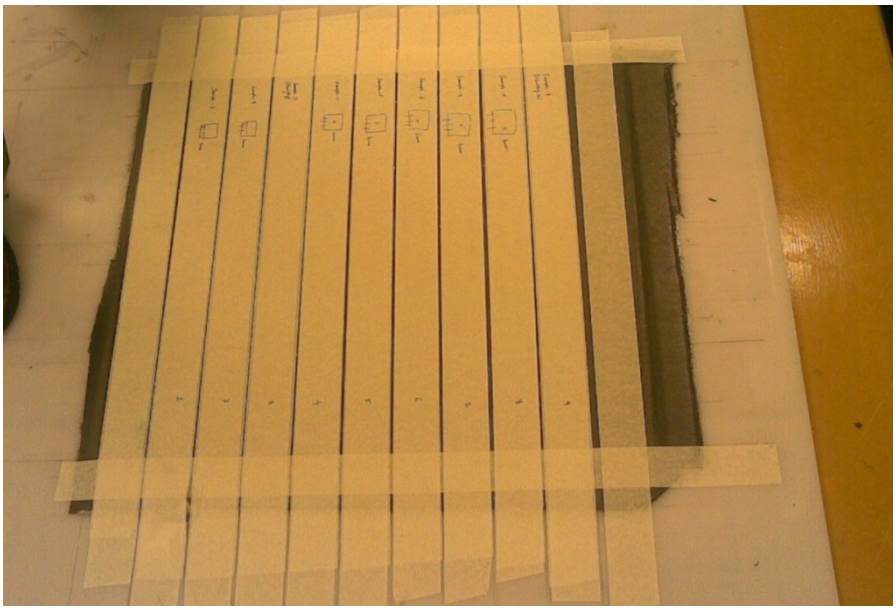

**Figure 3-7: Carbon/Epoxy Laminate**

There is an overlap in each side of the laminate to make sure that the final edges are completely straight and accurate. The steel plate was polished several times and a sheet of release paper was placed onto it before the laminates were stacked onto it. A release film was also placed on the surface of the uppermost laminate. A layer of breather-bleeder combination was placed over this surface. The laminate was then covered with a flexible bag, all ends of which were sealed to the plate. The release film prevents the cured laminate from sticking to the plate. The breather enables the uniform distribution of the applied vacuum and permits the uniform flow of the resin during the curing process. The uniform pressure applied also helps in removing excess trapped air. Autoclave curing is the most extensively used method of producing high-quality laminates within the Marin/Aerospace industry. Autoclaves are extremely resourceful pieces of equipment (Mallick, 1988; Schwartz, 1996; Barbero, 1998). Since the gas pressure is applied isostatically to the part, almost any shape can be cured in an autoclave. The only limitation is the size of the autoclave and the large initial capital investment to purchase and install an autoclave. The resin is held at this cure temperature for normally 4 to 6 hours, allowing time for the cross linking process to be completed. Figure 4.6 explains the preparation

of the laminate for curing in an Autoclave. After the over-laminate was fully cured, the composite was ready to be machined to make the required beam specimens for testing. A typical Vacuum bag system is shown in Fig 3-8.

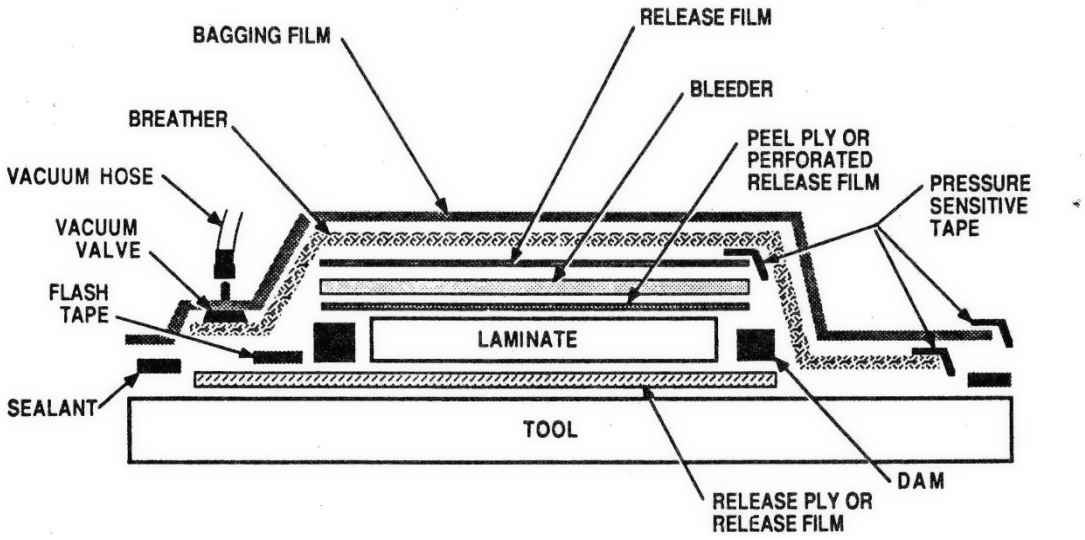


**Figure 3-8: The schematic of Vacuum bag Molding Process (Courtesy: Max Band Low Viscosity)**

When a composite is made by wet lay-up (hand lamination) or spray techniques, it is generally resin rich and hence of low fibre volume fraction. The fibre volume fraction, and hence mechanical properties, can be improved by bleeding off excess resin. To achieve this, laminate is enclosed by a polymeric film sealed to the mould edges. A breach unit penetrates the bag and permit a vacuum to be drawn in the bag. This imposes a consolidation pressure of up to ~1000 mbar on the materials in the bag. The principal disadvantage of this technique is the disposable materials that are included in the bag (Table 3-1).

**Table 3-1: Consumable materials and equipment required for vacuum bagging**

| | |
|---|---|
| Peel-ply | A sacrificial open weave fibreglass or perforated heat-set nylon ply placed between the laminate and the bleeder/breather to provide the textured and clean surface necessary for further lamination or secondary bonding. |
| Bleeder cloth | A non-structural fabric designed to absorb excess resin and reactants from the laminate. This may also act as the breather cloth. |
| Breather cloth | A loose weave or non-woven porous material use to provide a gas flow path over the laminate both to permit the escape of air, reactants, moisture and volatiles and to ensure uniform vacuum pressure across the component. This may also act as the bleeder cloth. |
| Release film | A (perforated) sheet of material placed between the laminate and the mould surfaces to prevent adhesion. |
| Edge dams | Profile used to define the edge of the component |
| Caul plate | A mould or tool placed on top of the laminate inside the bag to define the second surface. |
| Intensifiers | Generally hard rubber profiles incorporated in the bag to consolidate the laminate at sharp radii. |
| Bagging film | The membrane which permits a vacuum to be drawn within the bag. |
| Tacky tape | Adhesive strip used to bond the bag to the tool and provide a vacuum seal. |
| Breach unit | A connector through the bagging film to permit a vacuum to be drawn. |
| Vacuum pipes | The link between the breach unit and the vacuum pump. |
| Resin trap | A container in the vacuum line to collect any excess resin before it can damage the vacuum pump. |
| Vacuum pump | Generally a high-volume pump (absolute vacuum is rarely required) suitable for continuous running. For some slow-curing epoxy resins twenty-four operation may be needed. |
| Pressure gauges | Generally clock-type gauges attached via a breach unit connection. |

Stringer considered the wet lay-up/vacuum bag process and concluded that the viscosity at the start of the vacuum bag consolidation was the critical parameter in the achievement of high fibre volume fraction and low void content carbon fibre/epoxy resin composites. It was concluded that a dwell time window "exists between the same viscosity limits regardless of the resin system and temperature being used". For carbon fibre composites, up to 58% fibre by volume and less than 2% void content by volume were obtained with the dwell time window corresponding to 7500-16500 MP.

The process was started by vacuuming the composite laminate and placing it into a curing chamber (Figure 3-9).

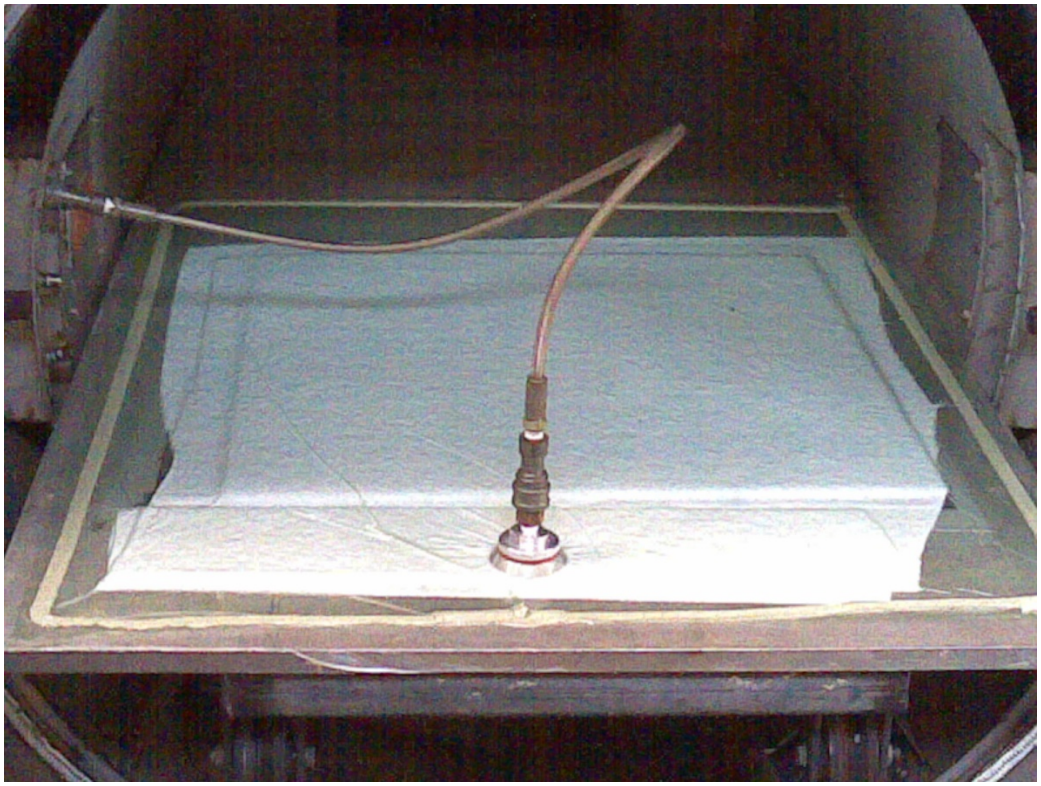

**Figure 3-9: Vacuuming the carbon/epoxy composite laminate**

As it can seen from Figure 3-10, it is very important to completely isolate the vacuum and then remove the air from inside the vacuum by air suction.

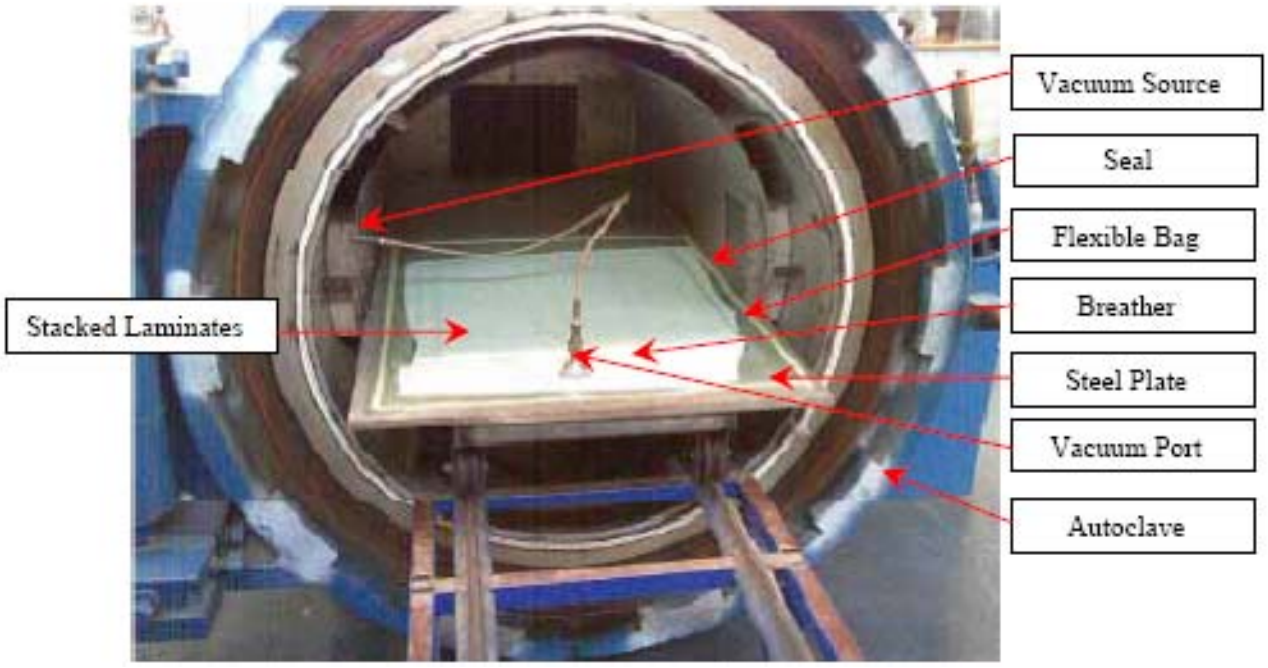


**Figure 3-10: Placing the laminate inside the curing chamber**

For more, the behavior of carbon/epoxy composite material during the curing process is shown in Figure 3- 11.

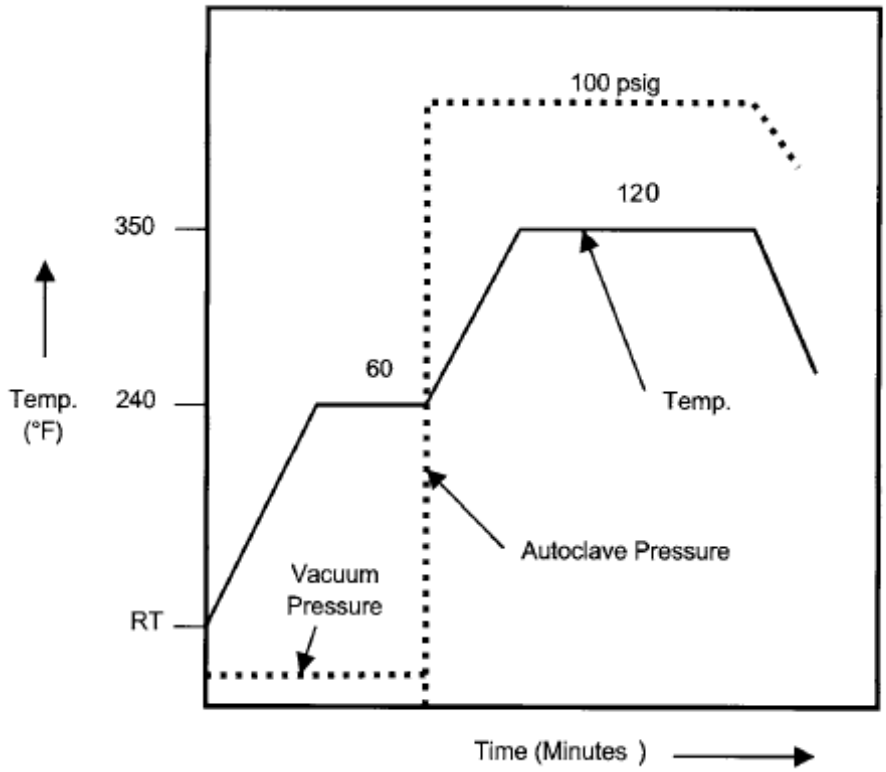


**Figure 3-11: Classical Carbon Epoxy Cure Cycle**

## 3.4. Cutting and Machining

After the over laminate is fully cured, the composite laminate is cut into nine beams. Each beam has a length of 550 mm, width of 50 mm and the thickness of 6 mm. As it is mentioned before, seven of the beams have delaminations in different locations and levels and two remaining beams are kept as healthy samples.

## 3.5. Conclusion

Firstly, the plywood composites with simulated defects were used to establish the system setup parameters. The experiment started with plywood samples to find the optimal experimental modelling because of their relative low cost and similar planar characteristics as carbon fibre composites.

By using the optimal experimental modelling which was obtained by evaluating plywood composites, the process of testing Carbon/Epoxy samples commenced. A 550 mm ×450 mm Carbon/Epoxy laminate was made and Teflon was attached at the designated positions as an artificial delamination. After curing and cutting processes, nine Carbon/Epoxy beams were

prepared including 2 healthy and 7 defective samples with delaminations at various locations and levels for further experiments.

# CHAPTER 4

# Experimental Modelling

## 4.1. Introduction

An experimental investigation to detect embedded delamination and other forms of damage in composite structure using laser vibrometer is presented.. The use of Vibration Deflection Shapes (VDSs), which are the actual vibration patterns of a structure undergoing steady-state vibration, is selected as an appropriate method to gather the structural responses to the excitations made by a hanger. Experiments are conducted on plywood and composite beams, using the VDS method and a Scanning Laser Doppler Vibrometer. A series of experiments is performed on composite plate-beams with various placements of delaminations to comprehensively evaluate the performance of the laser technique. The VDSs are shown to be sensitive to structural parameter variations, and hence can be used to detect and locate damage in large composite structures. The successful experimental demonstration of the procedure using different test articles shows that the VDS method can become an effective and time saving tool for structural health monitoring, particularly for detection of damage in composites.
The PSV-400 is easy and intuitive to operate, especially when compared with traditional multipoint vibration measurement methods requiring time-consuming preparation of the test object and sensors. It takes just a few minutes to set up the system, define the geometry and scan grid, and measure. The vibrometer automatically moves to each point on the scan grid, measures the response and validates the measurement by checking signal to- noise. When the scan is complete, choose the appropriate frequencies and then display and animate the deflection shape in several convenient 2-D and 3-D presentation modes. These on-screen displays are extremely effective tools for understanding the details of the structural vibration.

## 4.2. Specification of Sensor – PSV Laser Vibrometer

Polytec Laser Doppler Vibrometer (Figure 4.1) are used to precisely measure mechanical vibrations, quickly, easily and free from mass-loading or feedback problems.
POLYTEC Vibrometer operates on the Doppler principle, measuring the frequency shift of backscattered laser light from a vibrating structure to determine its instantaneous velocity and

displacement. Users get a quick, easily understood and accurate visualization of a structure's global and local vibrational characteristics. The PSV-400 avoids the necessity of attaching a transducer array to the test sample and then individually collecting and processing each transducer's output. The PSV-400 Scanning Vibrometer comprises both state-of-the-art hardware and software. It includes a compact sensor head with an integrated scanning unit, a vibrometer controller and a data acquisition and management system. These components are complimented by a powerful software package that controls the scanners, data processing, and visualization of the measurement results.

**Figure 4-1: PSV-400 Laser Vibrometer System (Courtesy: www.Polytec.com)**

The PSV-400 series is built upon the combined strength of a proven OFV-5000 Controller and a high-performance OFV-505 Sensor Head featuring auto-focus and focus memory functionality. The PSV-400 is designed to scan both small ($mm^2$) and large ($m^2$) structures. Depending on the chosen configuration, the PSV-400 covers vibration frequencies up to 20 MHz and vibration velocities up to 20 m/s. As it can seen from Figure 4.2 The sample hanged in front of the laser vibrometer and attached to the impulse hammer for excitations. The antinodes of the structure would be a suitable place to attach the exciter (impulse hammer).

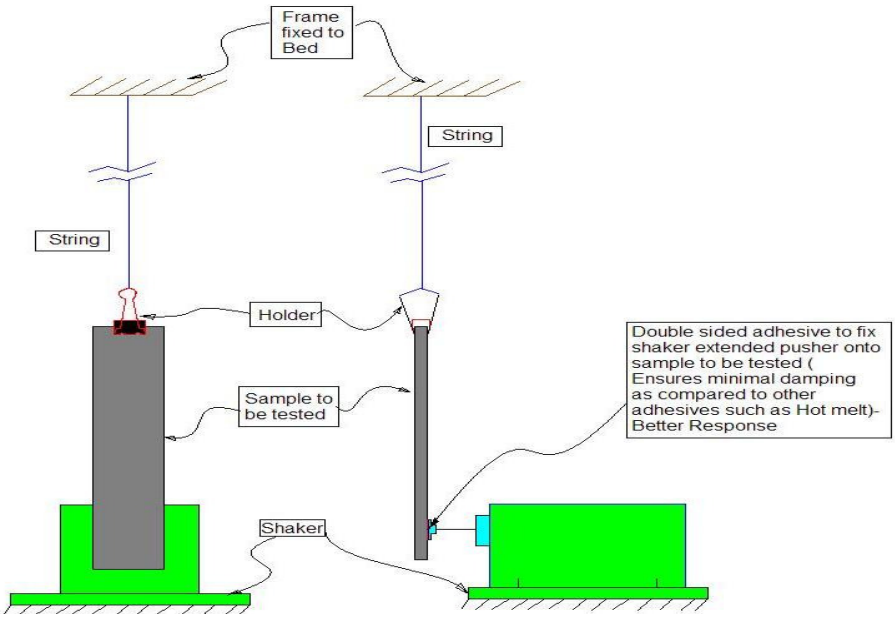


**Figure 4-2: The experimental setup**

The whole process of gathering structural response with laser vibrometer is shown in Figure 4.3.

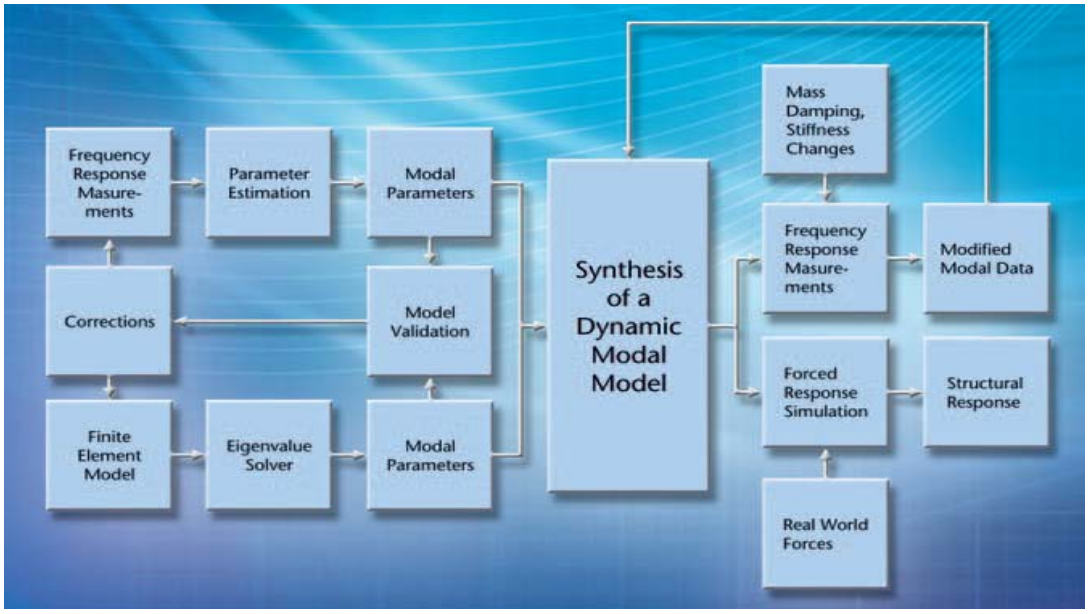


**Figure 4-3: The Process of Gathering Structural Responses**

## 4.2.1. Installation and Setup

### 4.2.1.1 Specimen Surface Preparation

No specific surface preparation is required for scanning with the aid of a Laser Vibrometer. However both the plywood as well as the carbon/epoxy beams were cleaned with a neutralizer to clean the surface of grease and dust particles with a cotton stick prior to them being adhered to the actuator system.

### 4.2.1.2. Actuator setup

Once the surface has been cleaned using a neutralizer, the actuator head (impulse head from the mechanical shaker) is bonded to both the plywood and carbon/epoxy surfaces (Figure 4.4) using an AVERY double sided tape patch.

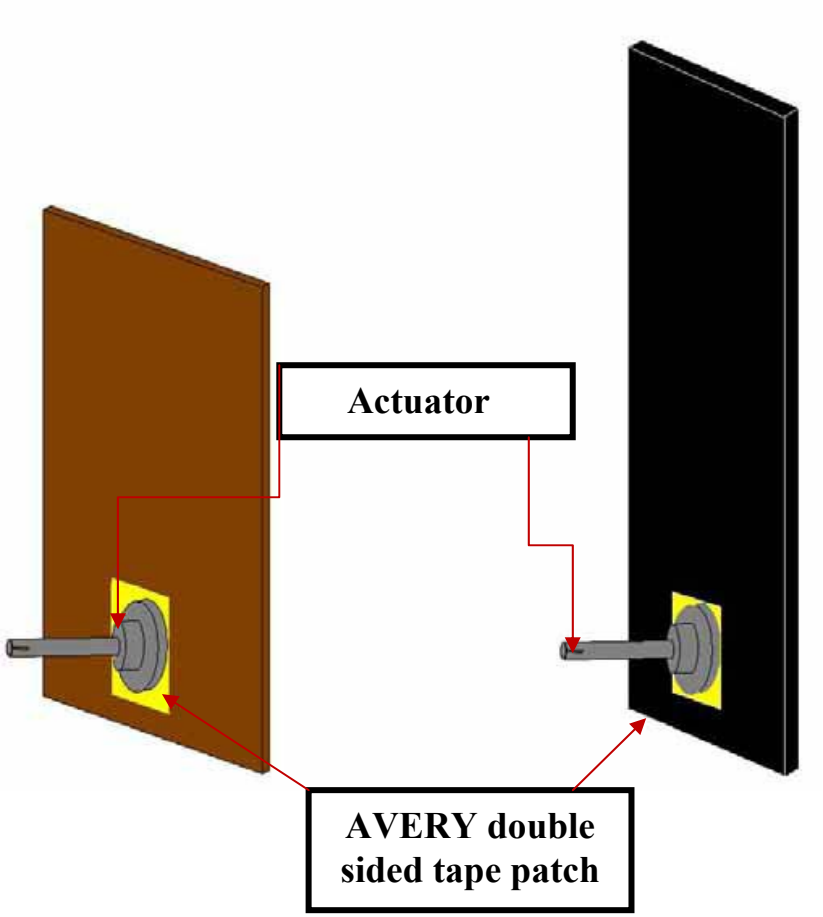


**Figure 4-4: Actuator bonding onto plywood and carbon/epoxy specimen surfaces**

### 4.2.1.3. Sensor- Actuator system preparation

A data acquisition system along with the Scanning Head provided with the PSV-400 SLV system was used to acquire data from the samples during the test. For impulse excitation, a mechanical shaker was connected to an actuator head. The frequency range of 1 to 1000 Hz was chosen for the excitation using an impulse hammer; the impulse location remained stationary and was located behind the surface being scanned. 3200 FFT lines were defined in the range from 1 to 2000 Hz for each measurement point. The FRFs for each data set at each point were averaged 3 times over the scan points to minimize noise interference.

### 4.2.1.4. Data Acquisition System

The POLYTEC analyzer, PSV-400 Scanning Head and the POLYTEC PSV-400 signal generator were used as the Data Acquisition System for testing the specimen prepared.

### 4.2.1.5. Testing the Samples

Experiments are conducted on plywood and composite beams, using the Vibration Deflection Shapes (VDS) method and a Scanning Laser Doppler Vibrometer. A series of experiments were performed on plywood specimen initially to comprehensively evaluate the performance of the laser technique and evaluate the various setup parameters. The VDS's are sensitive to structural parameter variations, and hence can be used to detect and locate damage in large composite structures. The laser vibrometer has proven to be an effective and time saving tool for structural health monitoring, particularly for detection of damage in composites (Sriram *et al*,. 1992; Stanbridge *et al*., 1999; Arruda *et al*., 1996). The PSV-400 is easy and intuitive to operate, especially when compared with traditional multipoint vibration measurement methods requiring time consuming preparation of the test object and sensors. The samples were supported on a frame using a string and clip arrangement while bonded to the actuator head. This assembly was then connected to the impulse hammer or the mechanical shaker. The hammer was connected to the PSV-400 signal generator through the signal amplifier as shown in Figure 4.9. The Scanning Head of the PSV-400 Laser Vibrator system was positioned in front of the specimen. The sample was ready once it was aligned. Alignment is defining the boundary conditions on the sample/specimen for the Scanning Head to reference against.

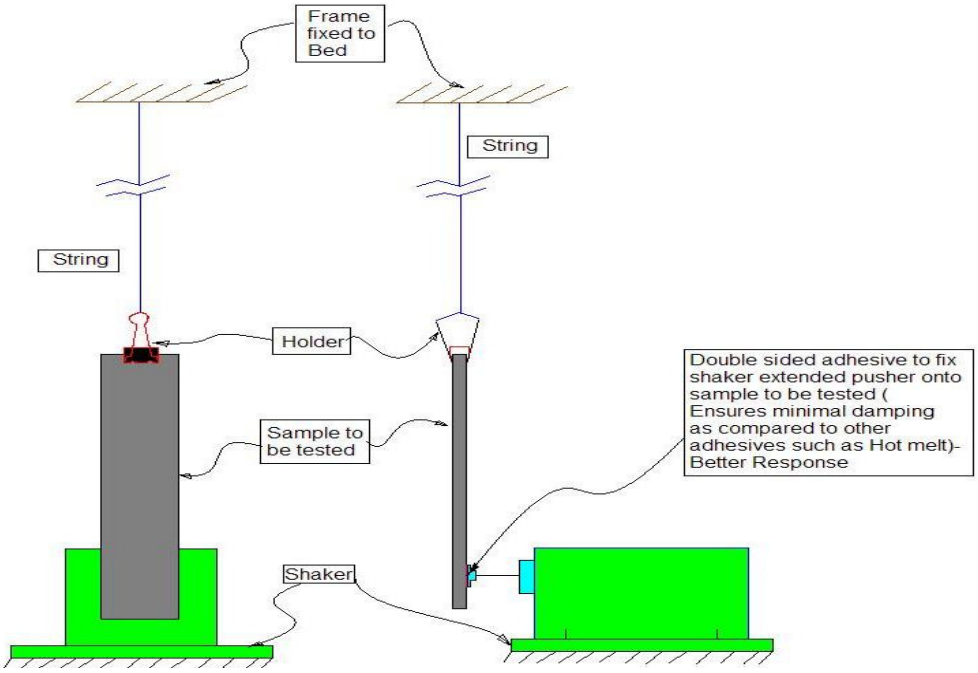


**Figure 4-5: Experimental Setup**

The various acquisition settings considered for testing both the plywood and carbon/epoxy specimen are published as under. An FFT measurement mode with a three time averaging at each scan point was chosen. The three time averaging mode relates to the Scanning head measuring the dynamic response at each of the scan points thrice and averaging it to finalize the value at that particular point. A bandwidth of 1.25 kHz starting from 0 kHz with 3200 FFT lines was considered with 0% overlap. This resulted with a Sample Frequency of 3.2 kHz while Sample Time and Resolution of being 2.56 s and 390.6 MHz OFV-5000, provided with the PSV-400 SLV system was used as the controller for the Vibrometer. A Low Pass Filter and a Fast tracking filter with a frequency of 1.5 MHz were also used to filter noise. VD-03 1000 mm/s/V was chosen as the velocity mode with a maximum frequency of 1.5 MHz based on the Low Pass Filter. Finally a Periodic Chirp type of a waveform with amplitude of 1V was passed to the signal amplifier and through to the mechanical shaker to excite the specimen connected to it. Table 4.1 summarizes the various acquisition settings below.

**Table 4-1: Acquisition settings using the PSV-400 Laser Vibrometer System (Courtesy: www.Polytec.com)**

| | |
|---|---|
| Measurement Mode | *FFT* |
| Averaging (Peak Hold) | *3* |
| Filter | *Low Pass Filter (1.5 MHz)*<br>*Fast Tracking* |
| Vibrometer Controller | *OFV-5000* |
| Controller set Velocity | *VD-03 1000 mm/s/V* |
| Bandwidth | *0-1.25kHz* |
| Sample Frequency | *3.2 kHz* |
| Sample Time | *2.56 s* |
| Resolution | *390.6 MHz* |
| FFT lines used | *3200* |
| Overlap | *0%* |
| Waveform | *Periodic Chirp* |
| Waveform Amplitude | *1 V* |

## 4.3. Plywood Composites

As it demonstrated in chapter 3, two plywood samples are selected and prepared from the same sheet to scan with laser vibrometer during excitation with a hammer. One of the samples has a defect on the surface and other one is a healthy sample. The results for healthy and defect samples collected in the PC which is connected to the laser vibrometer and compared to figure out the damage status (location and severity). Of course the main goal of this step is to find an appropriate set up configuration for the experiment to get the best results from laser vibrometer and make sense of the databases which are given by the POLYTEC software after the experiments.

### 4.3.1. Healthy Sample results

The experiment was started by defining the scanning points on the surface of the sample and gathering the structural responses to the dynamic excitations. The final result for healthy sample is shown below. It is possible to get the velocity, AP velocity $^2$, Displacement, AP Displacement $^2$ from the POLYTEC software. As it mentioned before, the aim of this step is to find the optimized set up of the experiment to get the best results.

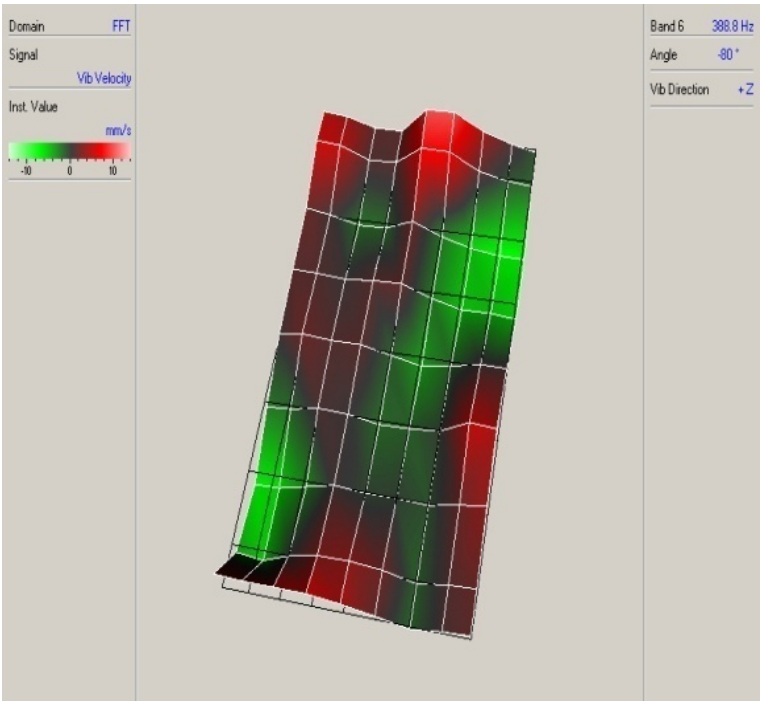


**Figure 4-6: Velocity of the scanning points for Healthy Sample**

As a matter of fact, the results for defect sample needed to distinguish the damage location by comparing them with current results.

## 4.3.2. Defect Sample results

The defect sample has a simulated damage at the centre (Figure 4.7), so it would be predictable to see some differences on that point in the scanning results. The shaker attached at the same point as healthy sample to make the comparison more accurate.

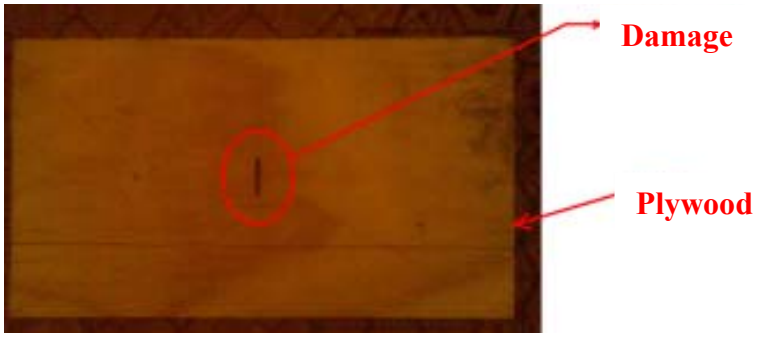


**Figure 4-7: Plywood defect sample**

The result is shown in Figure 4.8 and 4.9.

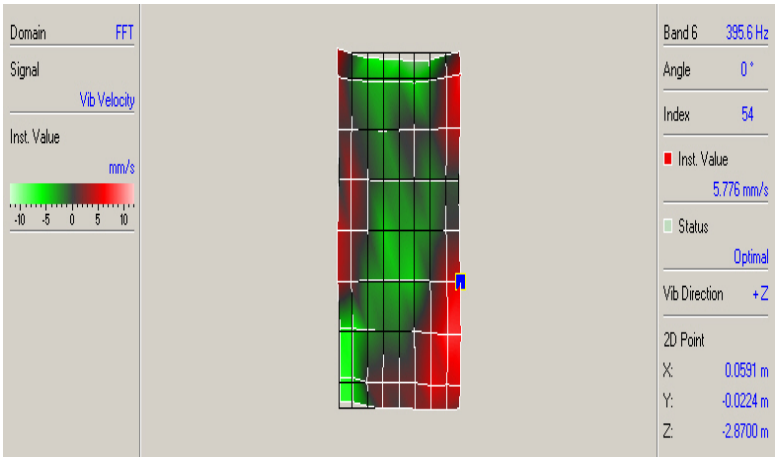


**Figure 4-8: Velocity of the scanning points for Defect Sample**

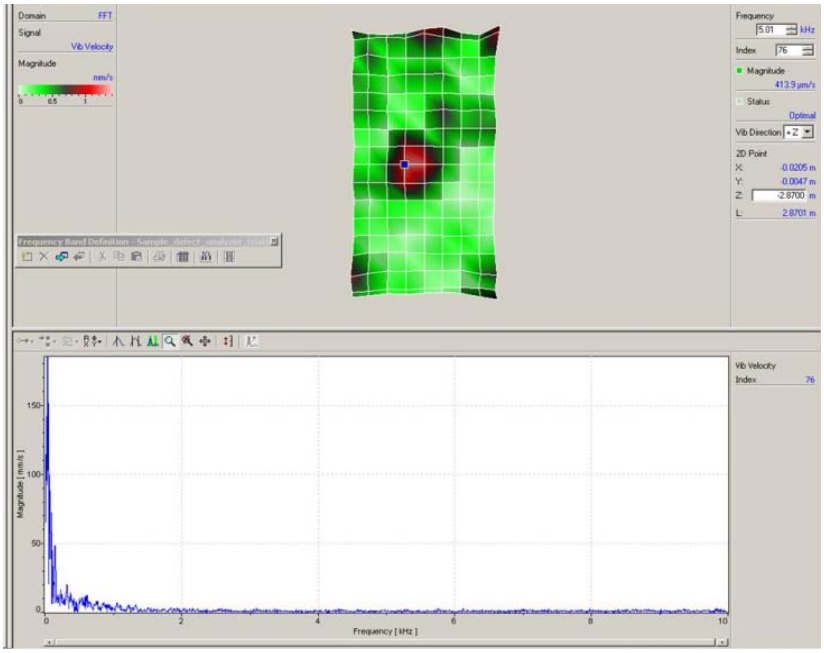


**Figure 4-9: Frequency trend of the defect sample**

By comparing the structural responses of the healthy and defect samples, the damage located at the centre of the panel which is acceptable according to the defect sample information. However, the damage detection of the carbon/epoxy structures with multi-damages are more complicated and further analyses needed to obtain the damage severity on those structures.

## 4.4. Carbon/Epoxy Composite Beams

After finding an appropriate set up for experiment in the previous step, the nine carbon/epoxy composite beams are tested with laser vibrometer to gather the structural responses to the

excitations. Seven out of nine beams have embedded artificial delaminations in different locations and levels the other two beams kept as healthy samples for comparison.

A data acquisition system of the POLYTEC soft was used to acquire data from the samples during the test. For impulse excitation, an impulse hammer was connected to the sample. The experimental setup configuration is presented in Figure 4.10. The frequency range of 1 to 1000 Hz over a time of 140 s, with a magnitude of 140 V was selected. For the excitation using an impulse hammer, the impulse location remained stationary and was located at the free-end of the beams. In the impulse hammer testing, 3200 FFT lines defined on a range from 1 to 2000 Hz for each measurement point. The density of measurement points are 70×80 with zero rotation. Then, the FRFs of each data set at each point were averaged 3 times over measurement points to minimize noise interference recorded by the impulse hammer. In the next step, the laser point on the sample fixed by autofocus to make a focused laser point on the sample to get the better scanning results. (Figure 4.11)

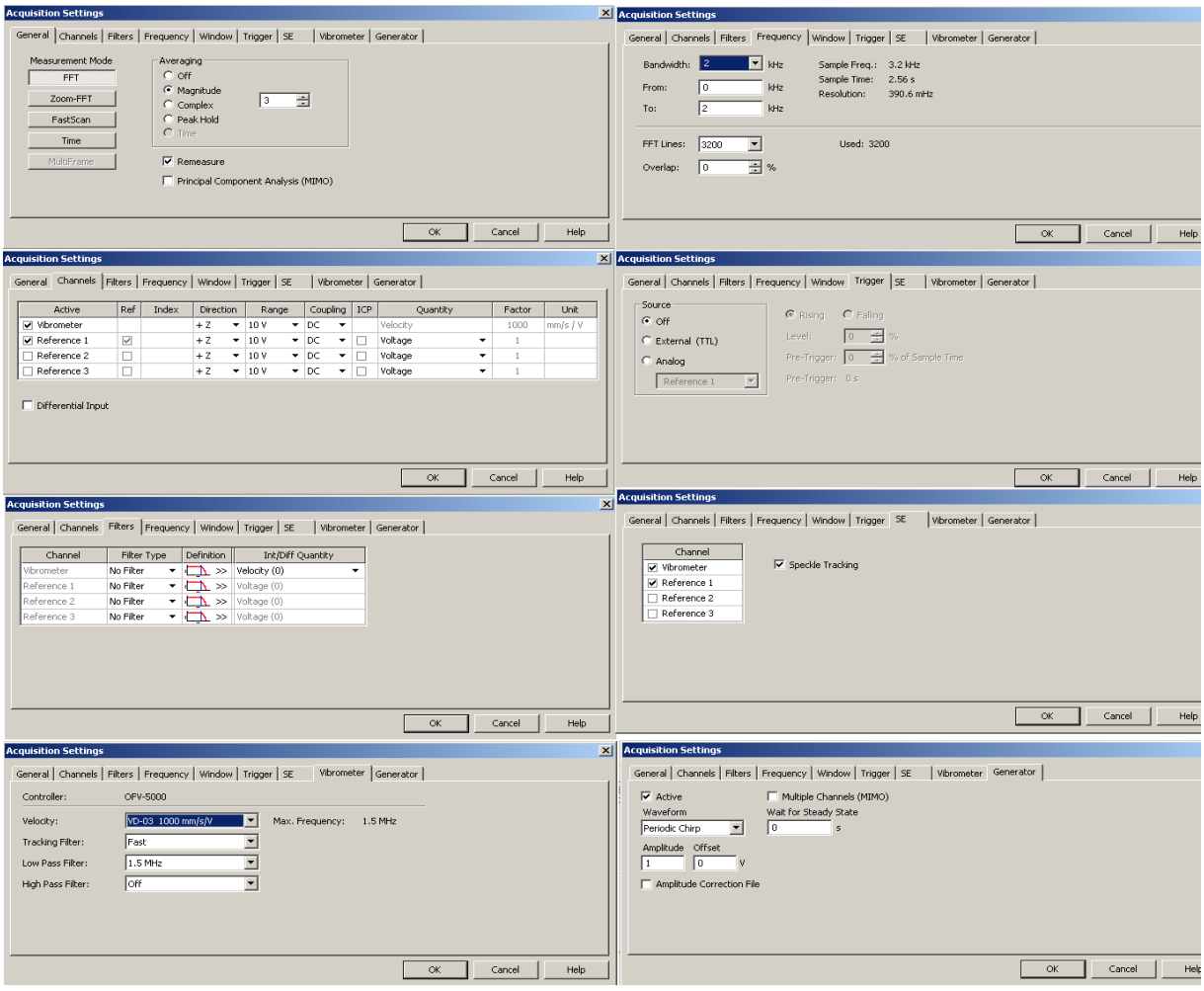


**Figure 4-10: The experimental setup configuration for carbon/epoxy sample**

**Figure 4-11: Focusing the laser point**

Then, the samples were aligned by defining fourteen laser points on the edges of each sample after hanging in front of the laser vibrometer, as it shown in Figure 4.12.

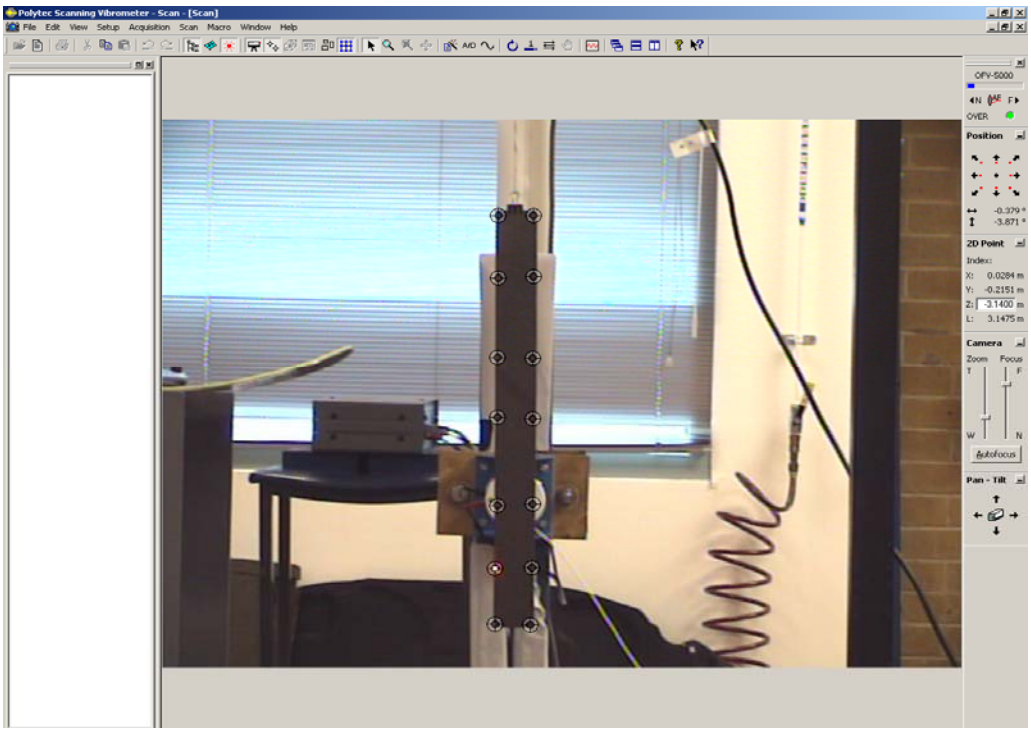


**Figure 4-12: The alignment of the samples**

The more scanning points defined, the higher the accuracy obtained from the laser vibrometer test. It is possible to make an appropriate meshing all over the surface of the structure by defining the x and y density according to the dimensions of the beams and the accuracy which needed for the experiment. In this test, 70×80 density magnitude was considered (Figure 4-13). As a matter of fact, all the processes explained previously were the pre-processing steps to prepare the testing devices for desire experiments. The experiments started by scanning the beams with laser vibrometer and gathering the results with the POLYTEC software connected to the vibrometer. The procedure of scanning is shown in Figure 4.14. During this process, the machine recognises the scanned points in four states: Not measured, Valid, Optimal, Over ranged, Invalidated. The valid and optimal states are acceptable by the software but for other states, the scanner tries to change them to acceptable states by the further scanning after all the points scanned once. As it mentioned above, each point was scanned three times and the average amount was considered in the results.

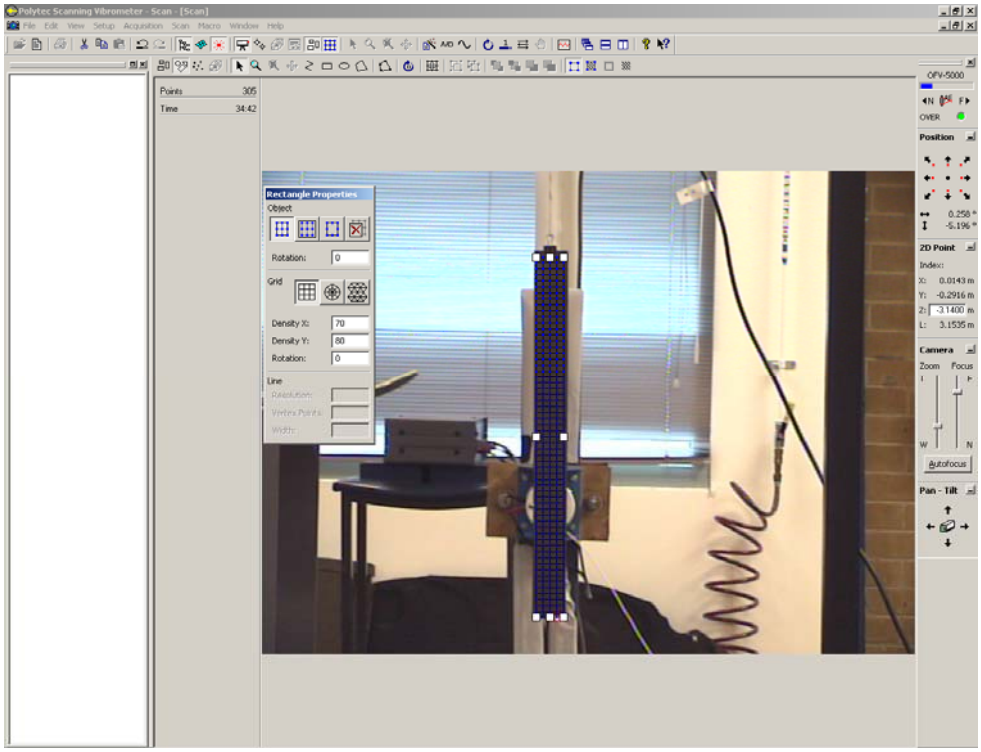


**Figure 4-13: Density of the scanning points**

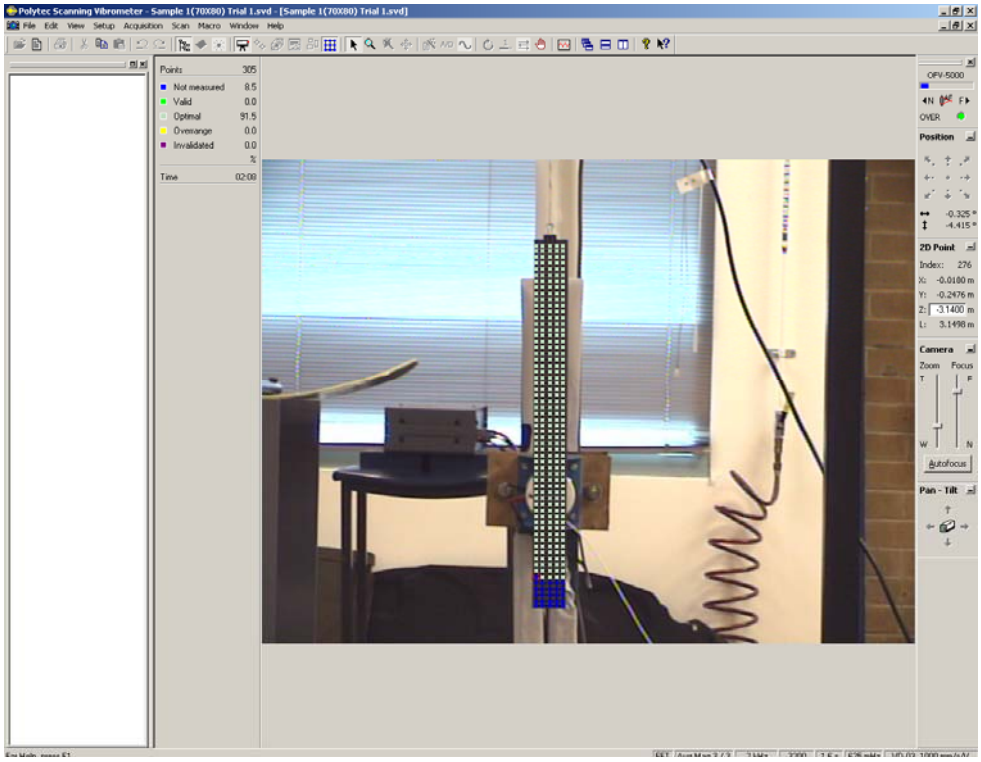


**Figure 4-14: Scanning process**

## 4.4.1. Laser Vibrometer testing results and Discussions

In previous steps of the experiment, all nine beams were scanned and the initial results were gathered by the software. When damage occurred in the composite structure it affected all the physical properties of that structure i.e. stiffness, natural frequency etc., so it would be part of this project to establish the relationship between these properties and different types of damage. The POLYTEC software has the advantage of showing the results in different graphs such as frequency, displacement, velocity, mode shape. In the following sections, the results were obtained in various types to find a significant change in the trends of damaged beams compare with healthy ones. Of course it would be predictable that further analyses are needed to get clearer changes between the healthy and damaged beams. To start two different domains could be selected for data acquisition: FRF (Frequency Response Function) or RMS (Rout Mean Square).

### 4.4.1.1. FRF Domain

Although there are many advantages to using the frequency response as detection techniques, the effect of damage on frequency response primarily provides global information about the condition of structures. In addition, the natural frequency measurements are very sensitive to interference, especially at the low order modes. Examples of interferences include fiber

misalignment during manufacturing, introduction of non-negligible mass by sensors, and simulated approximate boundary conditions that prompt the largest error in the frequency measurement (Kessler *et al.*, 2002). Nevertheless, the natural frequency can be used as an early warning system of global structural condition.

The location of the defect can be estimated with the percentage of change in the natural frequencies of intact and damaged structures which depend on the position of the defect for a particular mode of vibration. So, using natural frequency without other factors is not a reliable method to detect the damage status (severity and location). The magnitude of displacement through the range of frequencies for each sample was displayed in Figures 4.15 to 4.22. In fact, sample 3 and 9 which are the healthy samples were used as references to compare the results for other samples with but a healthy sample needed for possible material properties tests so sample 9 kept for the material test which is destructive and further tests were done on remaining samples. For better comparison, the changes in different graphs were highlighted for further discussions. As it can be seen from the figures, there are four highlighted areas in each graph which are the selected peaks to calculate 4 mode shapes of each samples.

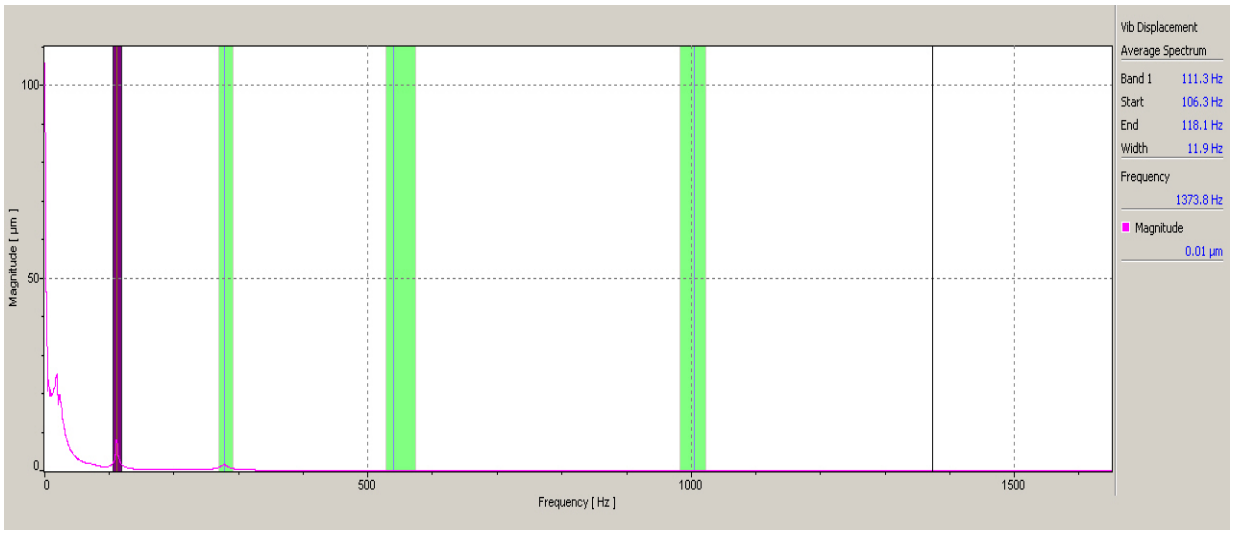


**Figure 4-15: FFT of Sample 1**

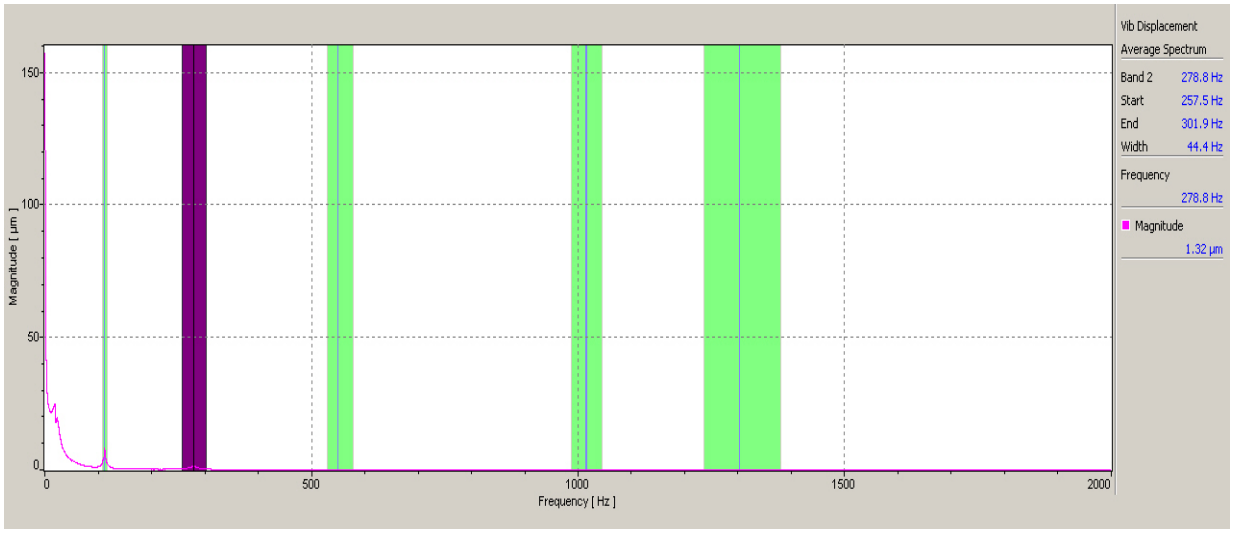


**Figure 4-16: FFT of Sample 2**

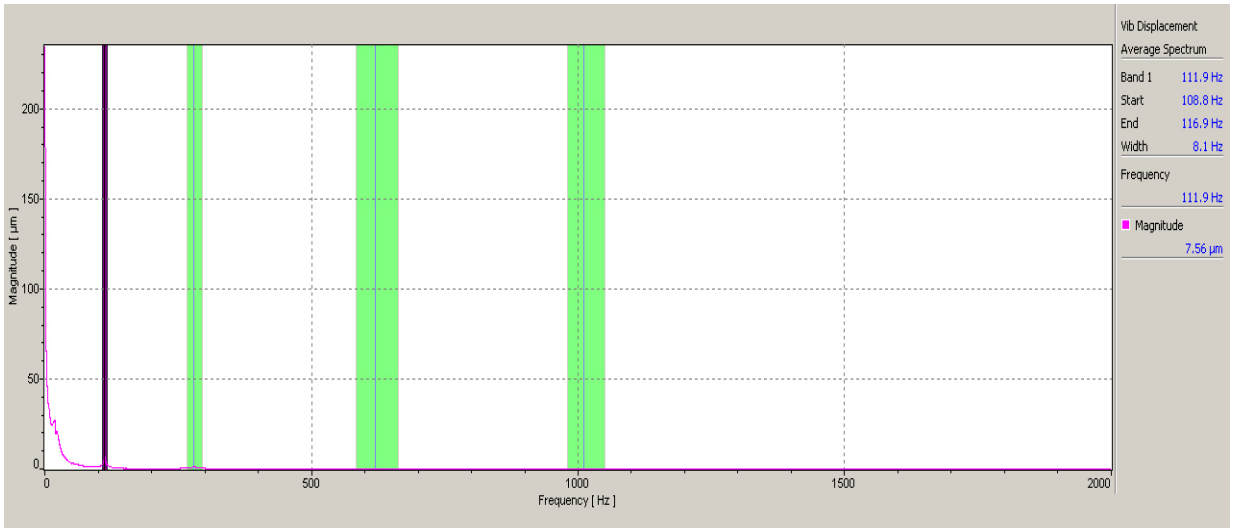


**Figure 4-17: FFT of Sample 3(Healthy)**

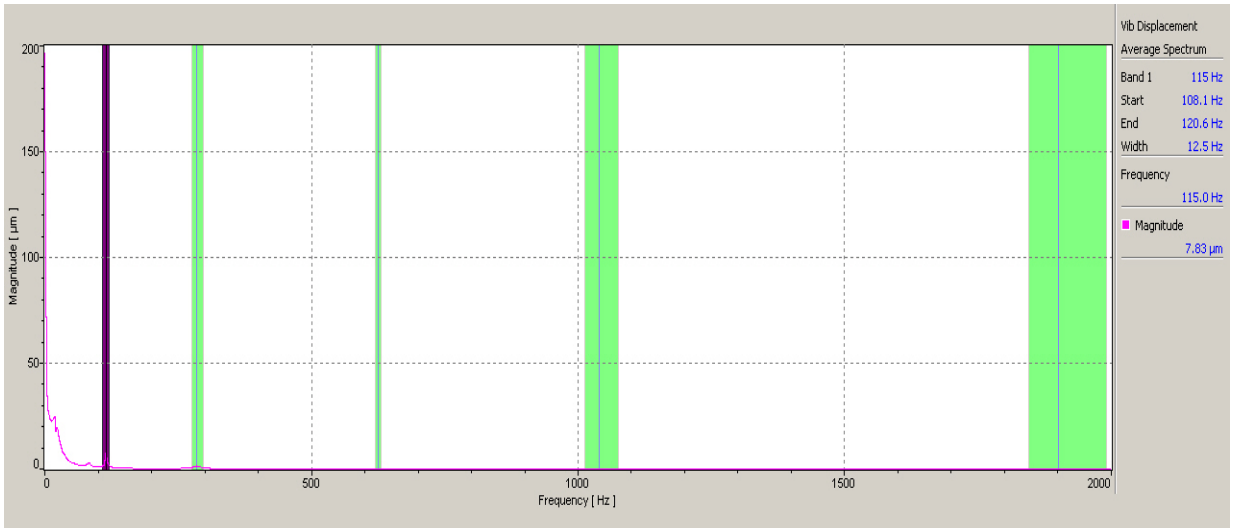


**Figure 4-18: FFT of Sample 4**

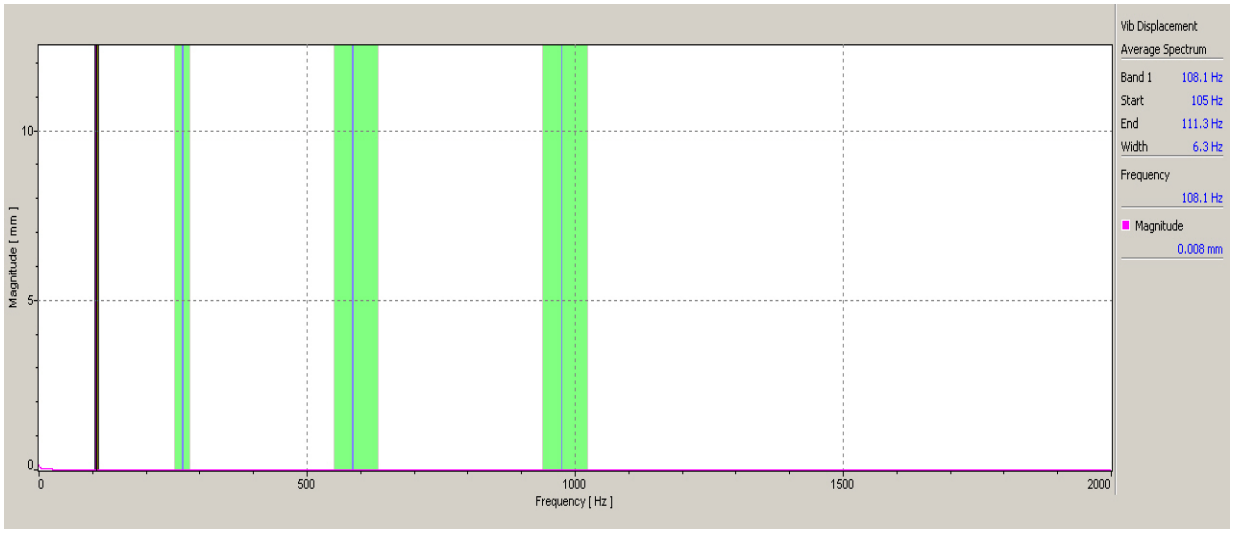


**Figure 4-19: FFT of Sample 5**

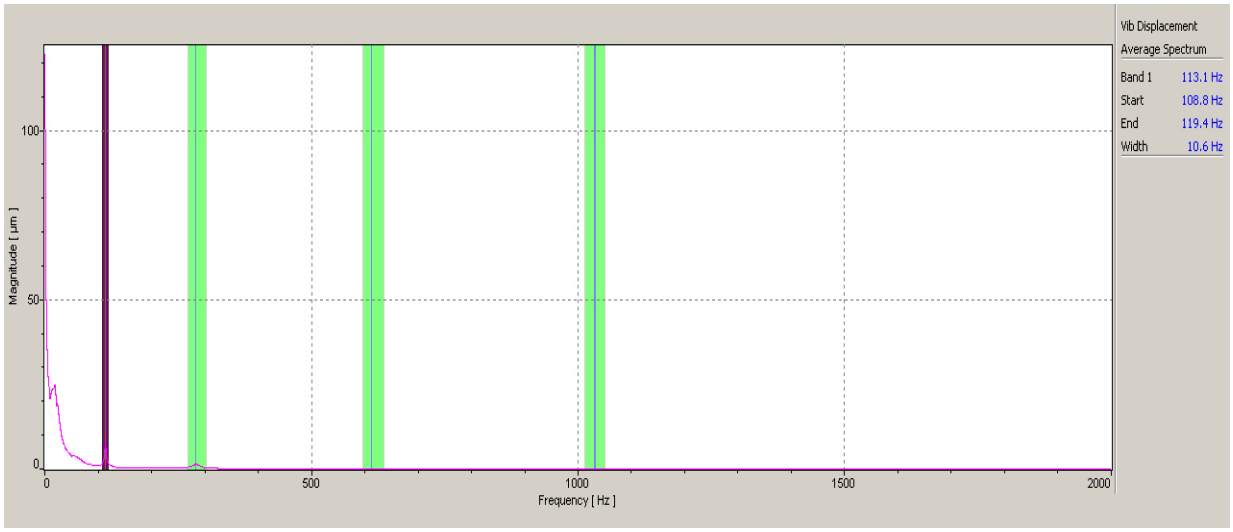


**Figure 4-20: FFT of Sample 6**

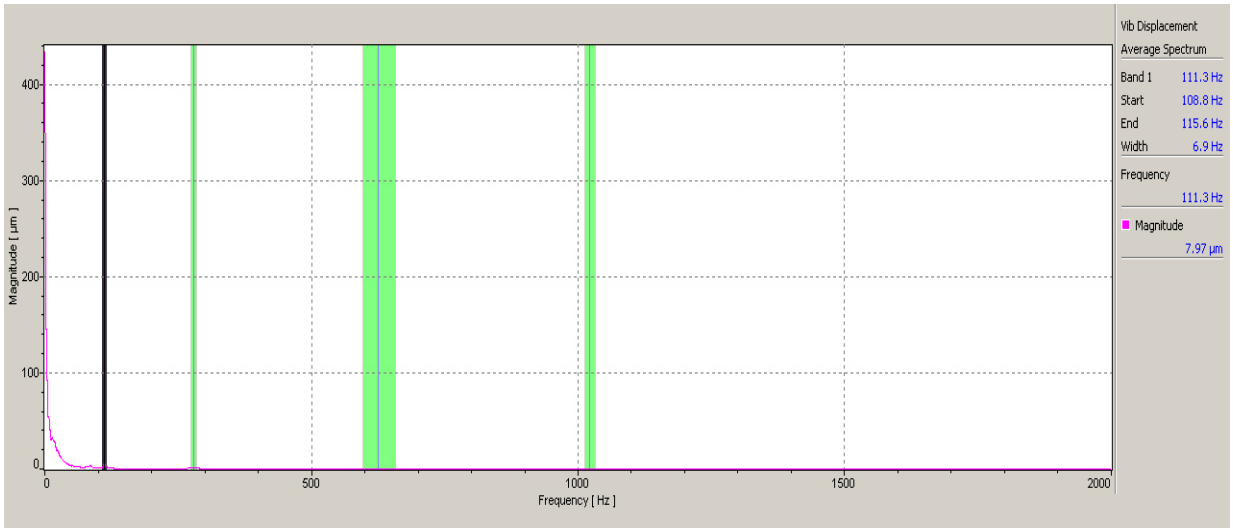


**Figure 4-21: FFT of Sample 7**

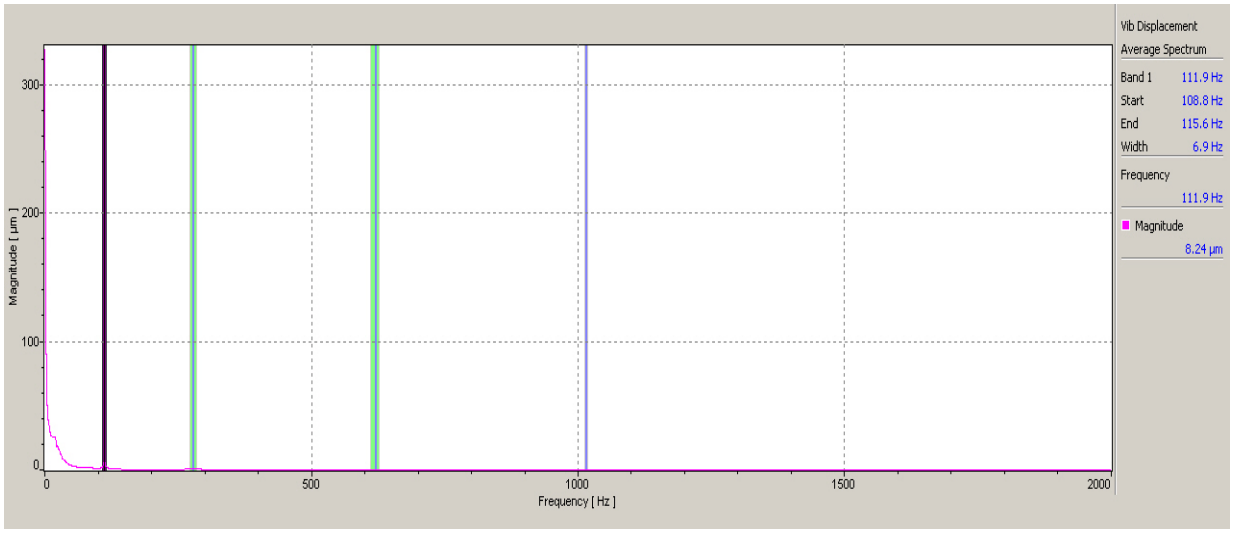


**Figure 4-22: FFT of Sample 8**

As it can seen from the previous figures, there are some shifts and peaks in the graphs of samples with delaminations inside compared with healthy samples which could be used as guidelines for damage detection. It could be observed from the graphs that the general trends are very similar and significant changes in damaged samples graphs lead us to determine the severity and location of damages. Therefore, the new process was obtained to make the gathered results more sensible for damage detection.

## 4.4.1.4. Displacement Mode Shapes

By selecting the regional peaks of ″displacement magnitude/frequency″ and calculating the maximum peak in each region. Then by looking at the graphical spectrum of each sample at peak points, the displacement mode shapes of samples are obtained. However, some of the selected peaks are not acceptable due to the serious effect of noise on the related spectrum of these peaks. All the gathered mode shapes 1, 2, 3 and 4 for each sample were shown in Figures 4.23 to 4.30.

For Sample 1, the four highest peaks in the Frequency-Displacement Magnitude were gathered in Table 4-2. Then at each peak, the displacement mode shape was plotted.

**Table 4-2: Selected peaks in Displacement Magnitude – Sample 1 - Frequency Graph**

| Peak no. | Frequency(Hz) | Displacement Magnitude(µm) |
|---|---|---|
| 1 | 111.3 | 14.250 |
| 2 | 278.1 | 2.922 |
| 3 | 540 | 0.0678 |
| 4 | 1005 | 0.109 |

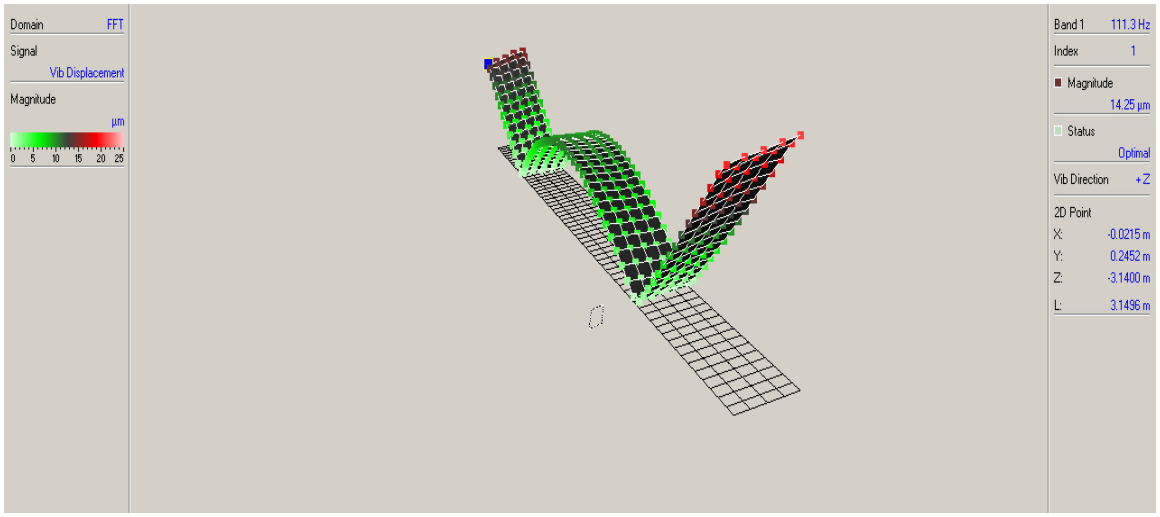


**Figure 4-23-a: Displacement Mode 1 for sample 1**

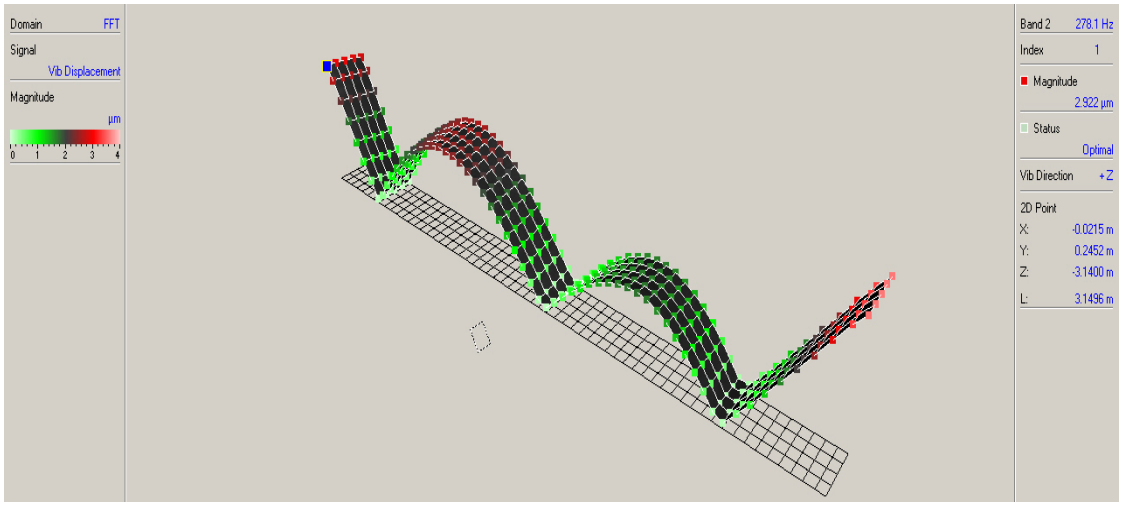


**Figure 4-20-b: Displacement Mode 2 for Sample 1**

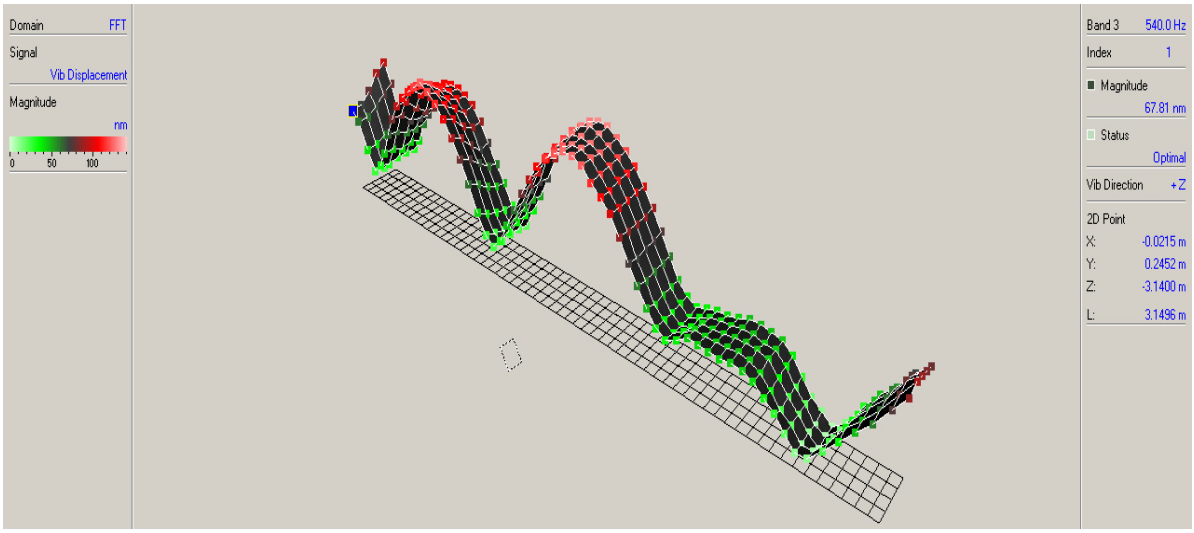


**Figure 4-20-c: Displacement Mode 3 for Sample 1**

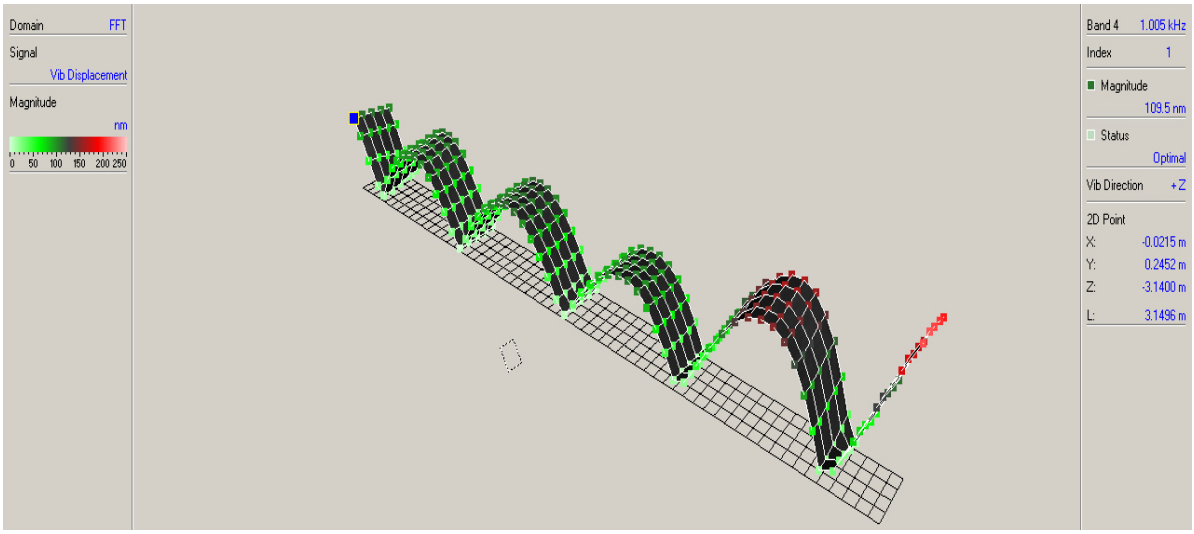


**Figure 4-20-d: Displacement Mode 4 for Sample 1**

**Figure 4.20 Displacement mode shapes of sample 1: (a) Mode 1, (b) Mode 2, (c) Mode 3 and (d) Mode 4.**

Generally speaking, mode 1 has the most noise compared with other mode shapes and mode would be the most reliable mode for damage detection. The right hand side of the samples was connected to the shaker, so it could be predictable that the magnitude of displacement in this area was in the red zone. Table 4-3 shows the frequency peaks and displacement magnitude at each peak for Sample 2.

**Table 4-3: Selected peaks in Displacement Magnitude – Sample 2 - Frequency Graph**

| Peak no. | Frequency(Hz) | Displacement Magnitude(μm) |
|---|---|---|
| 1 | 111.9 | 8.270 |
| 2 | 278.8 | 1.320 |
| 3 | 549.4 | 0.100 |
| 4 | 1015.6 | 0.070 |

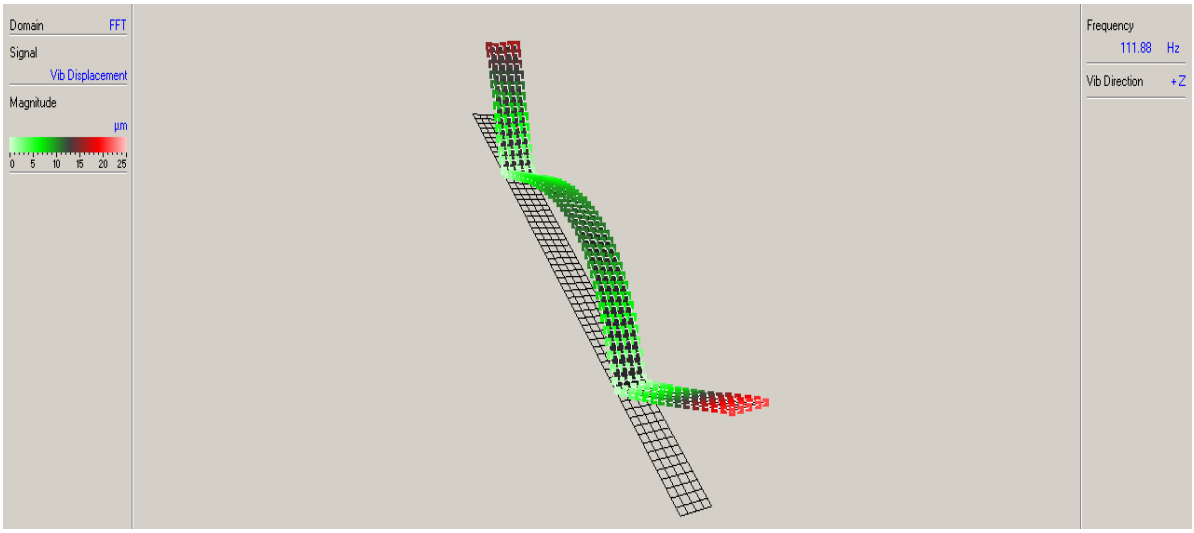


**Figure 4-24-a: Displacement Mode 1 for Sample 2**

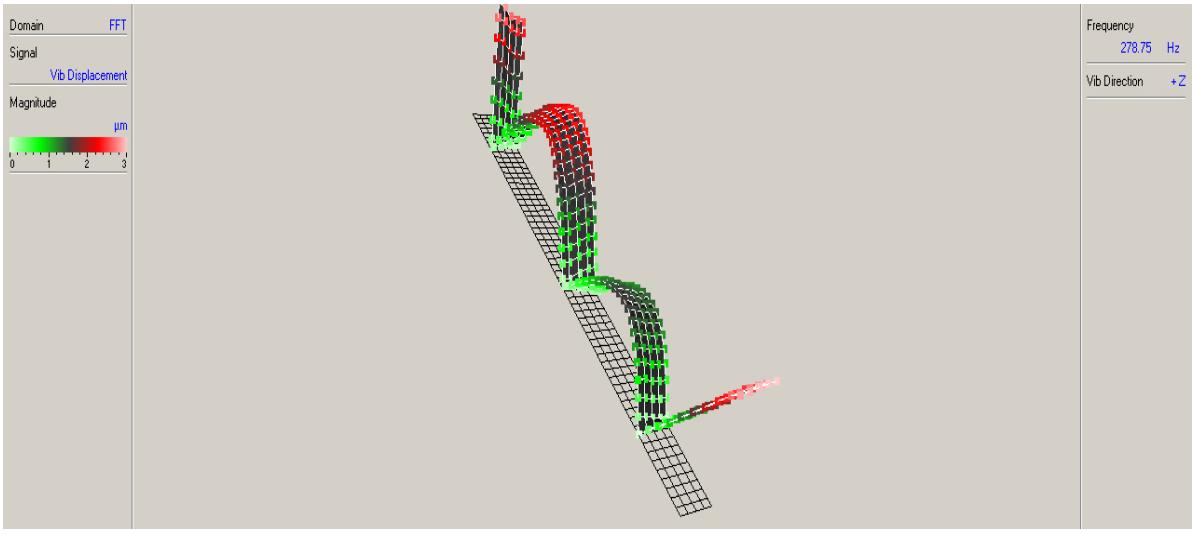


**Figure 4-21-b: Displacement Mode 2 for Sample 2**

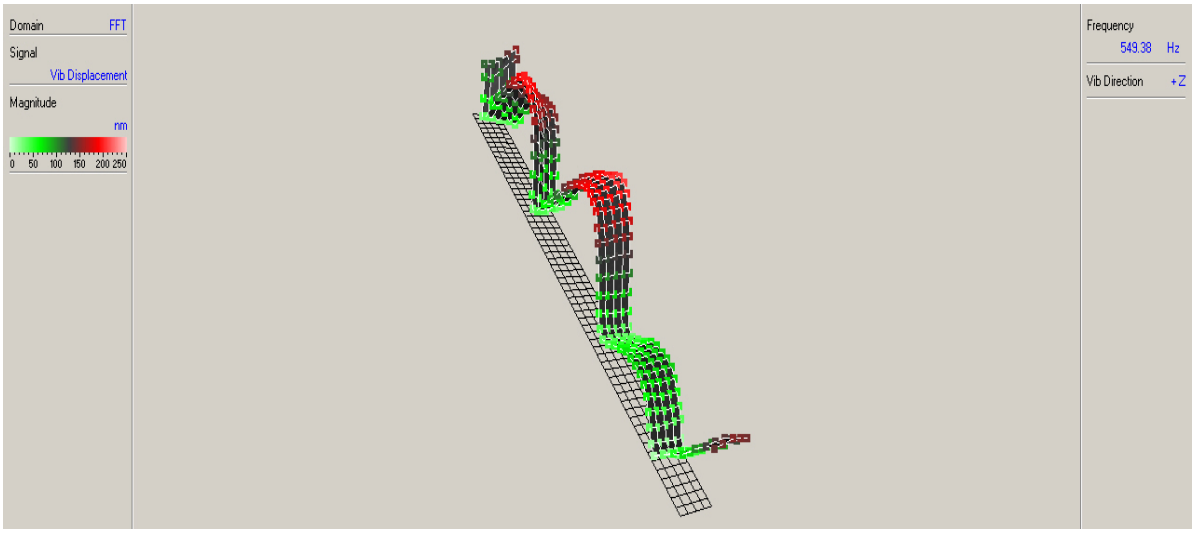


**Figure 4-21-c: Displacement Mode 3 for Sample 2**

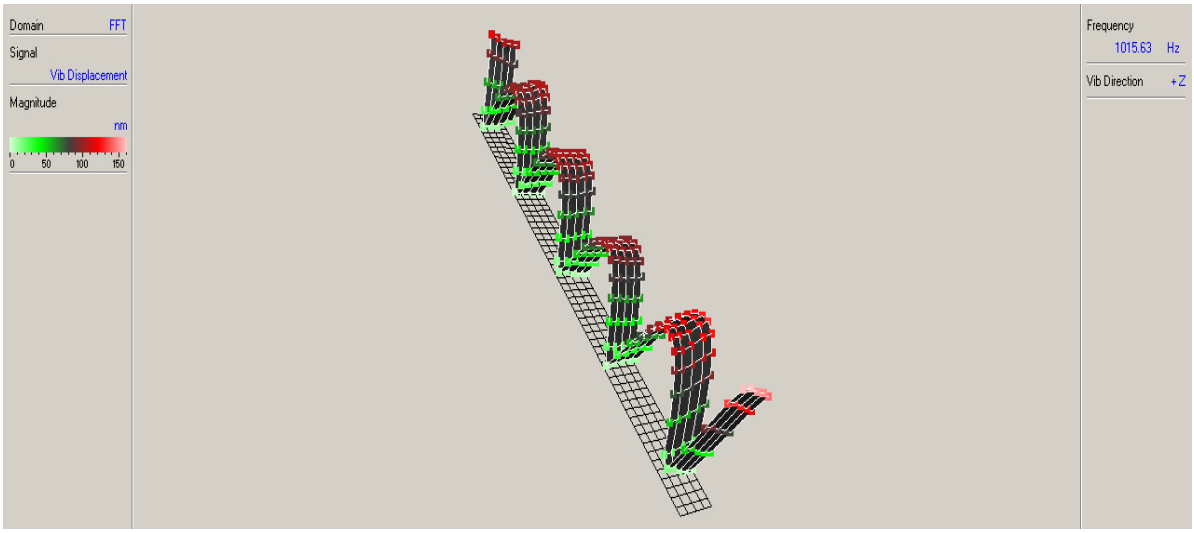


**Figure 4-21-d: Displacement Mode 4 for Sample 2**

**Figure 4.21 Displacement mode shapes of sample 2: (a) Mode 1, (b) Mode 2, (c) Mode 3 and (d) Mode 4.**

Sample 3, is the healthy sample without any delaminations inside. Of course it could have some manufacture damage i.e. Shift, Bubbles etc. the selected Peaks are shown in Table 4-4.

**Table 4-4 Selected peaks in Displacement Magnitude – Sample 3 - Frequency Graph**

| Peak no. | Frequency(Hz) | Displacement Magnitude(μm) |
|---|---|---|
| 1 | 111.9 | 7.560 |
| 2 | 279.4 | 1.080 |
| 3 | 620 | 0.090 |
| 4 | 1010.6 | 0.060 |

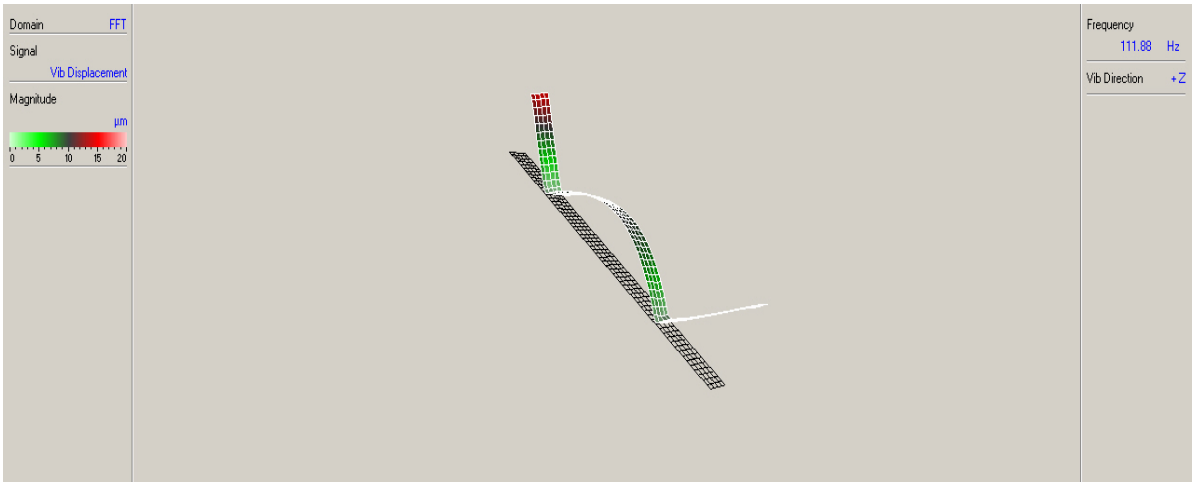


**Figure 4-25-a: Displacement Mode 1 for Sample 3**

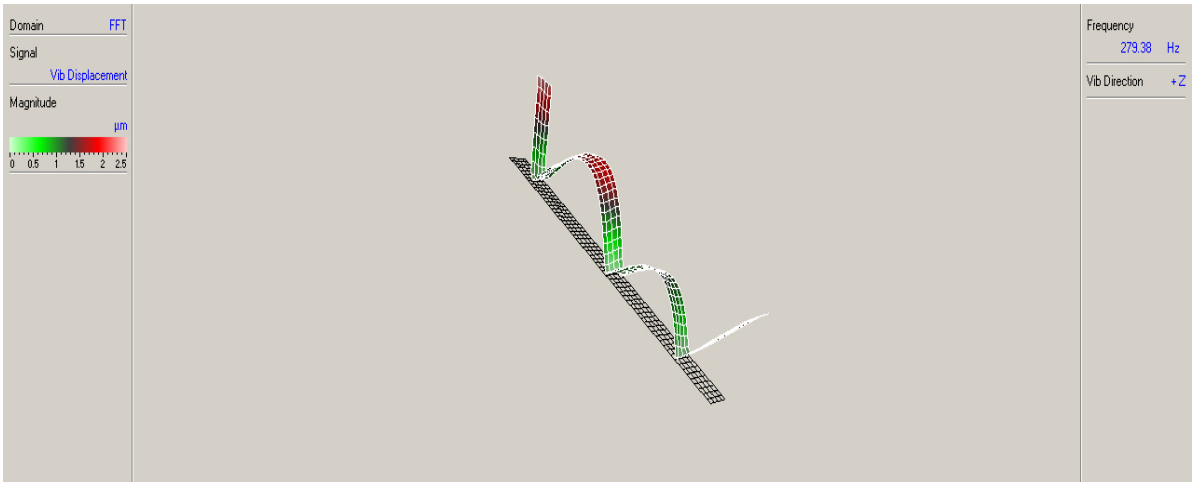


**Figure 4-22-b: Displacement Mode 2 for Sample 3**

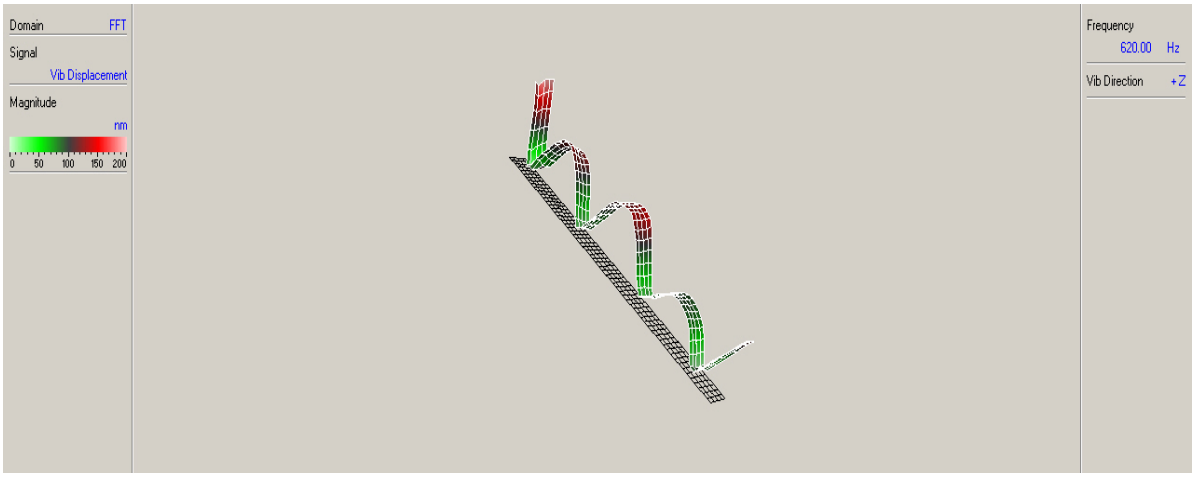


**Figure 4-22-c: Displacement Mode 3 for Sample 3**

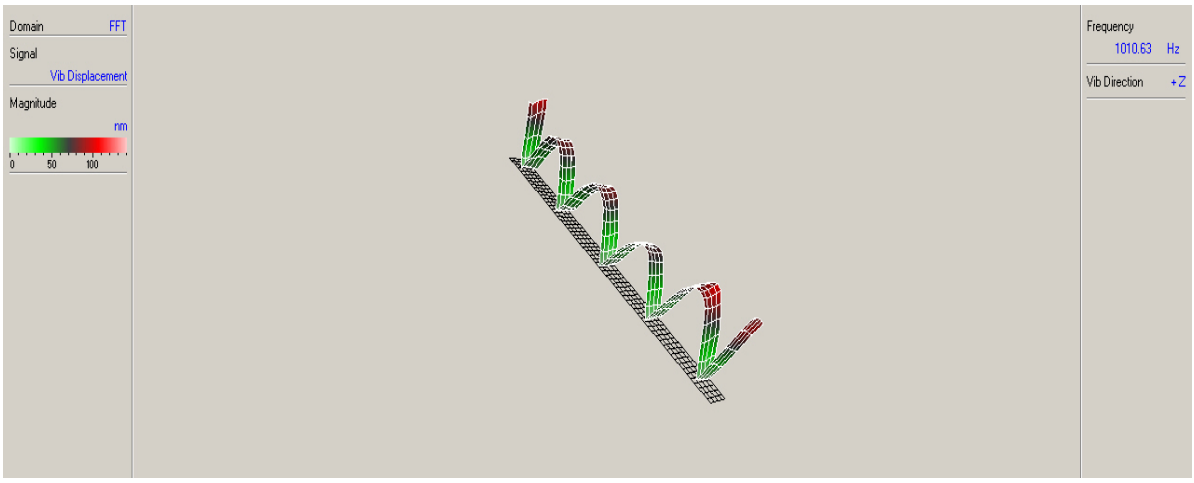


**Figure 4-22-d: Displacement Mode 4 for Sample 3**

**Figure 4.22 Displacement mode shapes of sample 3: (a) Mode 1, (b) Mode 2, (c) Mode 3 and (d) Mode 4.**

Selected Displacement peaks for Sample 4 are shown in Table 4-5:

**Table 4-5: Selected peaks in Displacement Magnitude – Sample 4 - Frequency Graph**

| Peak no. | Frequency(Hz) | Displacement Magnitude(µm) |
|---|---|---|
| 1 | 115 | 7.830 |
| 2 | 285 | 1.440 |
| 3 | 625 | 0.130 |
| 4 | 1039.4 | 0.080 |

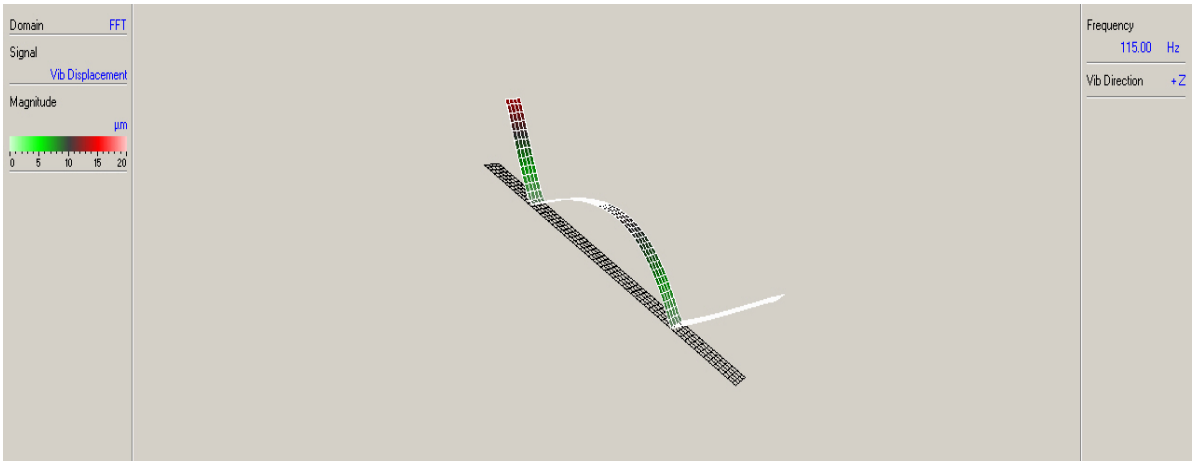


**Figure 4-26-a: Displacement Mode 1 for Sample 4**

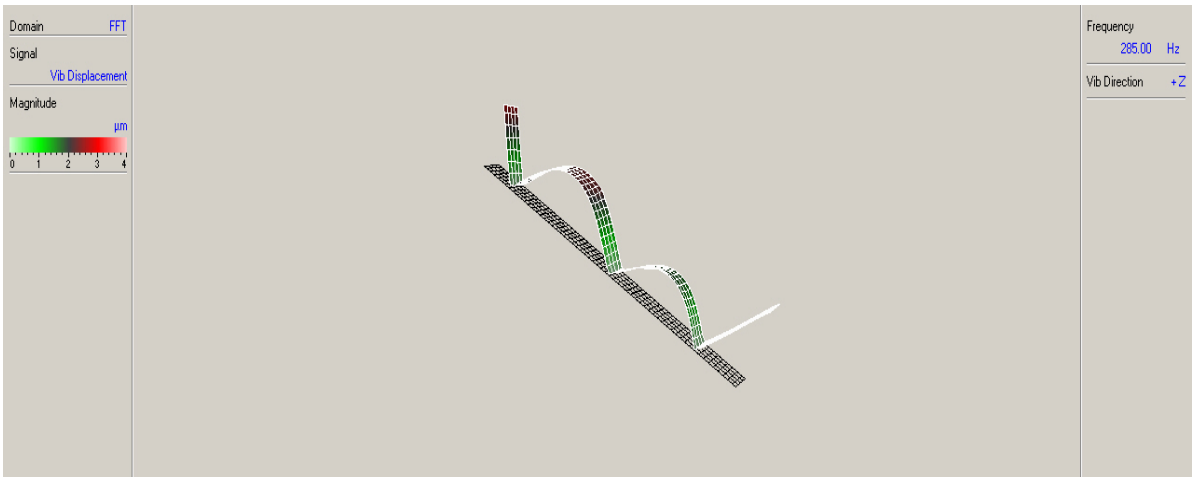


**Figure 4-23-b: Displacement Mode 2 for Sample 4**

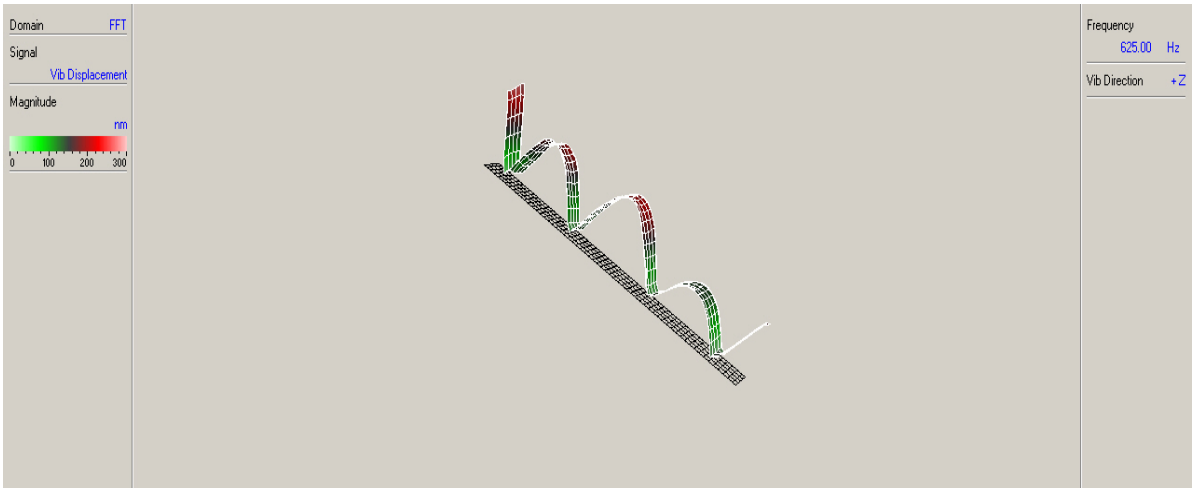


**Figure 4-23-c: Displacement Mode 3 for Sample 4**

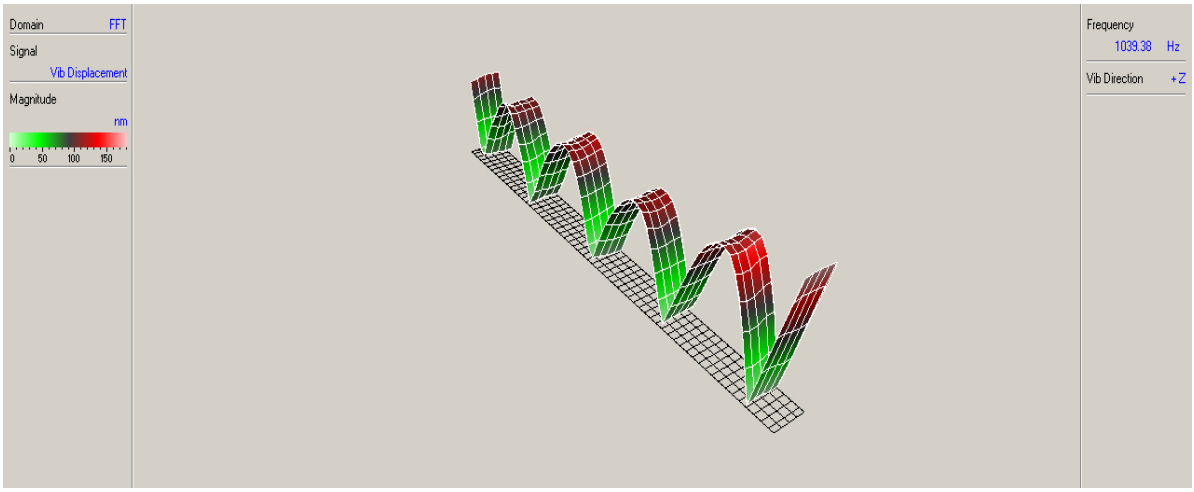


**Figure 4-23-d: Displacement Mode 4 for Sample 4**

**Figure 4.23 Displacement mode shapes of sample 4: (a) Mode 1, (b) Mode 2, (c) Mode 3 and (d) Mode 4.**

Selected Displacement peaks for Sample 5 are shown in Table 4-6:

**Table 4-6: Selected peaks in Displacement Magnitude - Sample 5 - Frequency Graph**

| Peak no. | Frequency(Hz) | Displacement Magnitude(µm) |
|---|---|---|
| 1 | 108.1 | 8.000 |
| 2 | 268.1 | 1.000 |
| 3 | 585 | 0.100 |
| 4 | 974.4 | 0.100 |

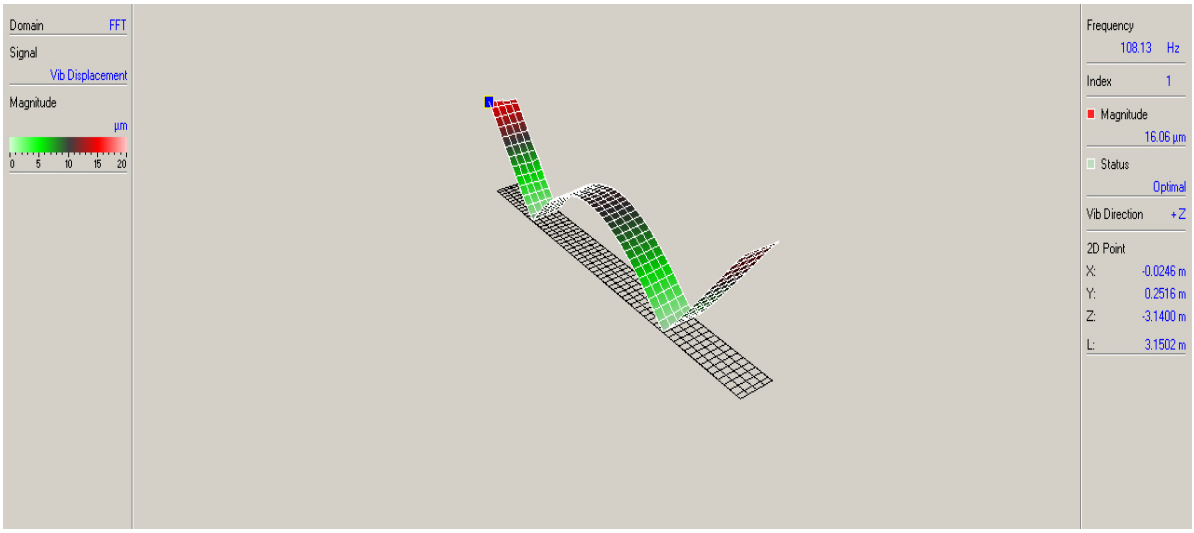


**Figure 4-27-a: Displacement Mode 1 for Sample 5**

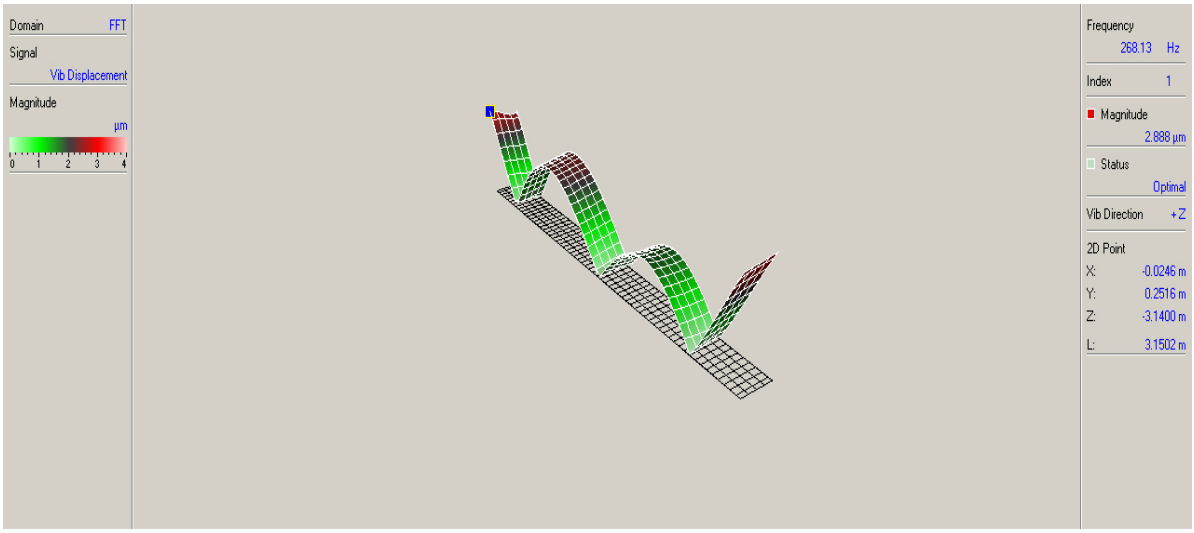


**Figure 4-24-b: Displacement Mode 2 for Sample 5**

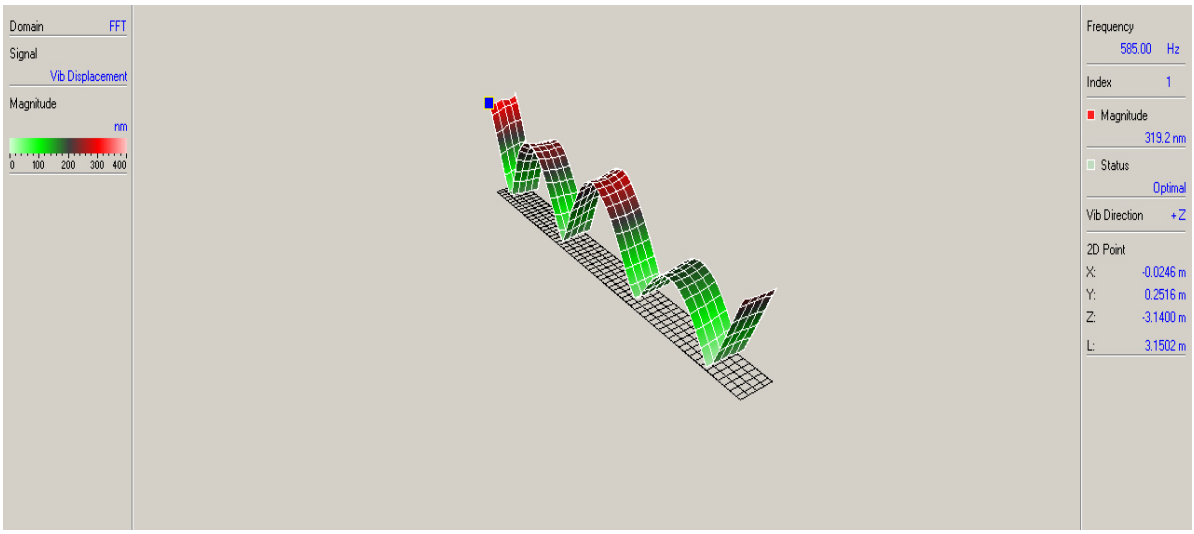


**Figure 4-24-c: Displacement Mode 3 for Sample 5**

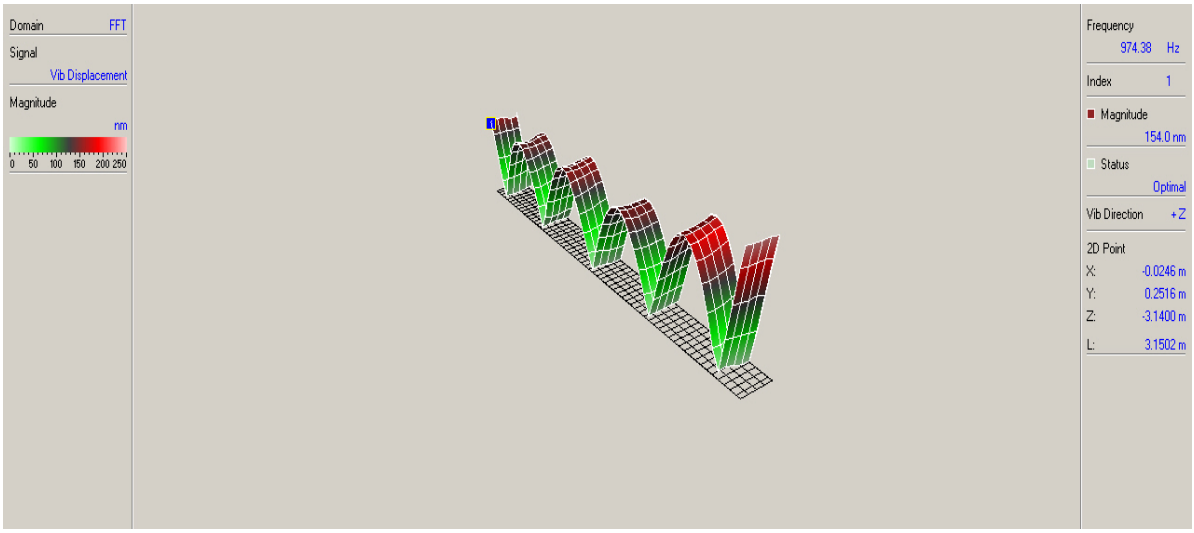


**Figure 4-24-d: Displacement Mode 4 for Sample 5**

**Figure4.24. Displacement mode shapes of sample 5: (a) Mode 1, (b) Mode 2, (c) Mode 3 and (d) Mode 4.**

Selected Displacement peaks for Sample 6 are shown in Table 4-7:

**Table 4-7: Selected peaks in Displacement Magnitude – Sample 6 - Frequency Graph**

| Peak no. | Frequency(Hz) | Displacement Magnitude(µm) |
|---|---|---|
| 1 | 113.1 | 8.560 |
| 2 | 283.1 | 1.370 |
| 3 | 612.5 | 0.140 |
| 4 | 1031.3 | 0.080 |

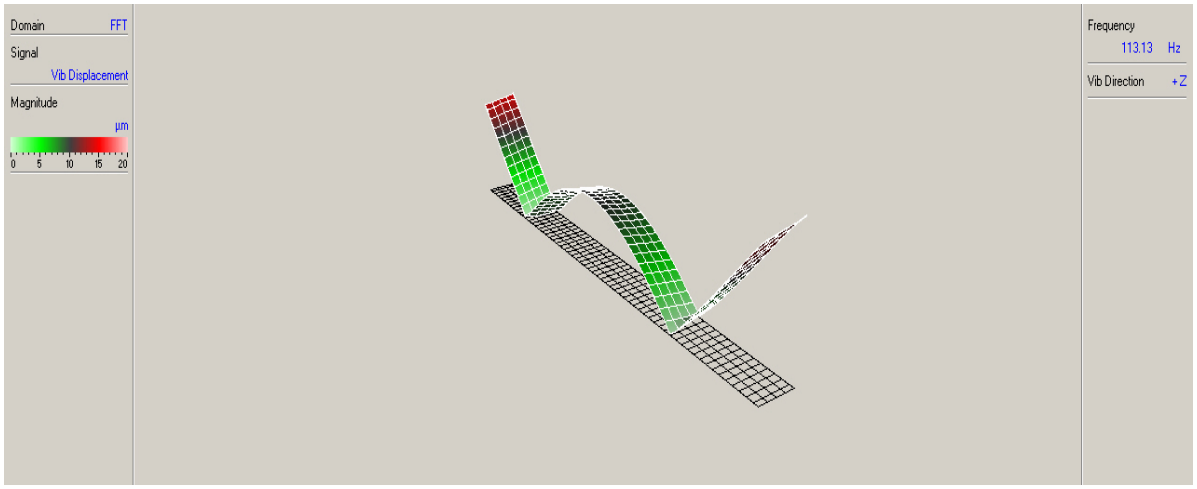


**Figure 4-28- a: Displacement Mode 1 for Sample 6**

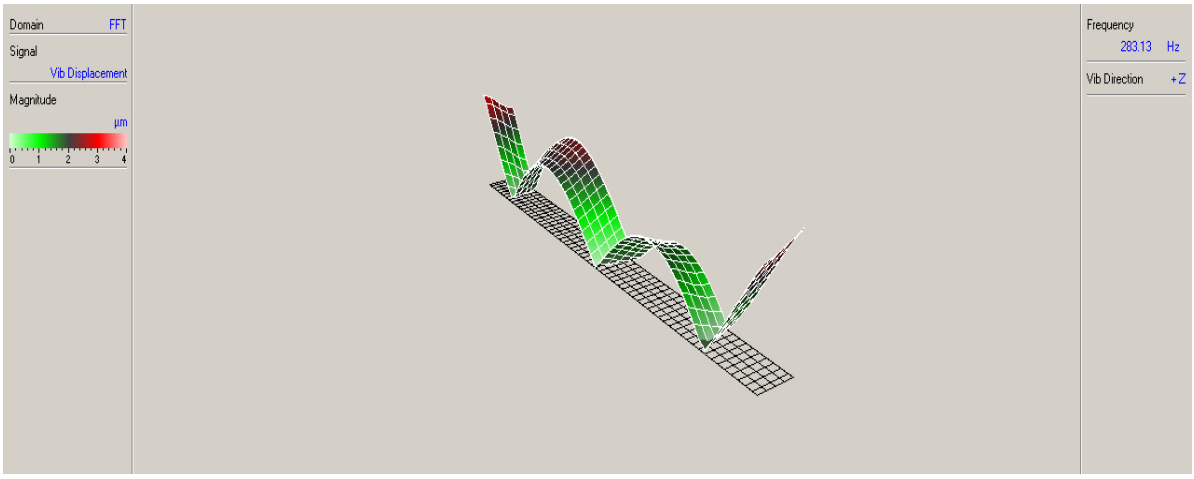


**Figure 4-25-b: Displacement Mode 2 for Sample 6**

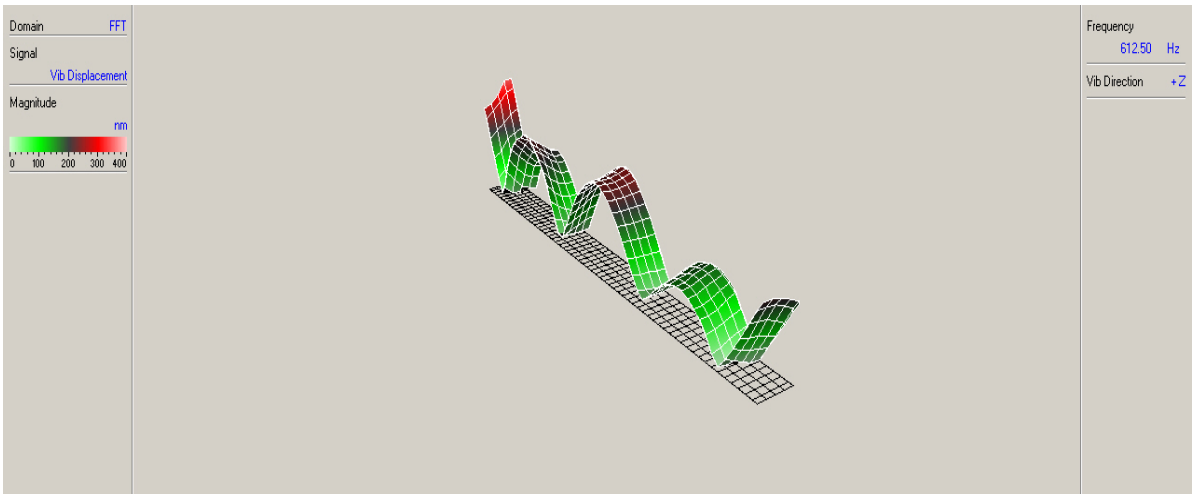


**Figure 4-25-c: Displacement Mode 3 for Sample 6**

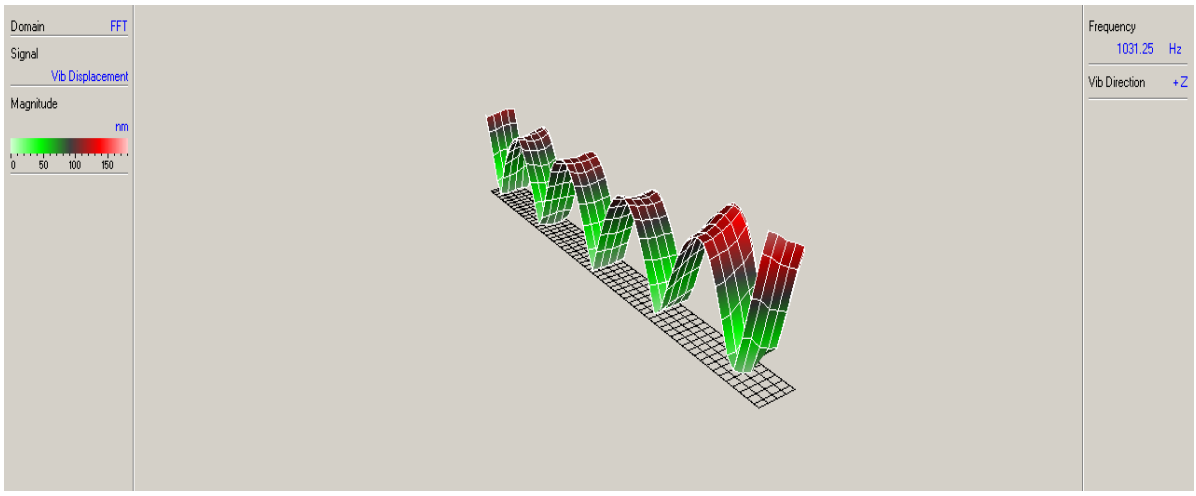


**Figure 4-25-d: Displacement Mode 4 for Sample 6**

**Figure4.25. Displacement mode shapes of sample 6: (a) Mode 1, (b) Mode 2, (c) Mode 3 and (d) Mode 4.**

Selected Displacement peaks for Sample 7 are shown in Table 4-8:

**Table 4-8: Selected peaks in Displacement Magnitude- Sample 7 - Frequency Graph**

| Peak no. | Frequency(Hz) | Displacement Magnitude(μm) |
|---|---|---|
| 1 | 111.3 | 7.970 |
| 2 | 278.8 | 1.160 |
| 3 | 625 | 0.060 |
| 4 | 1021.3 | 0.050 |

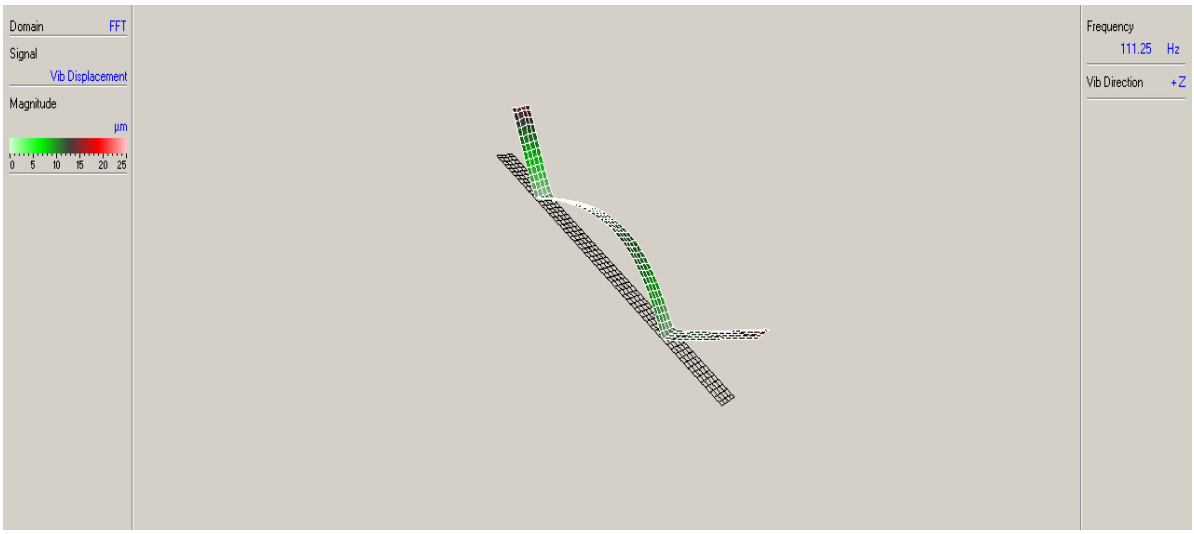


**Figure 4-29-a: Displacement Mode 1 for Sample 7**

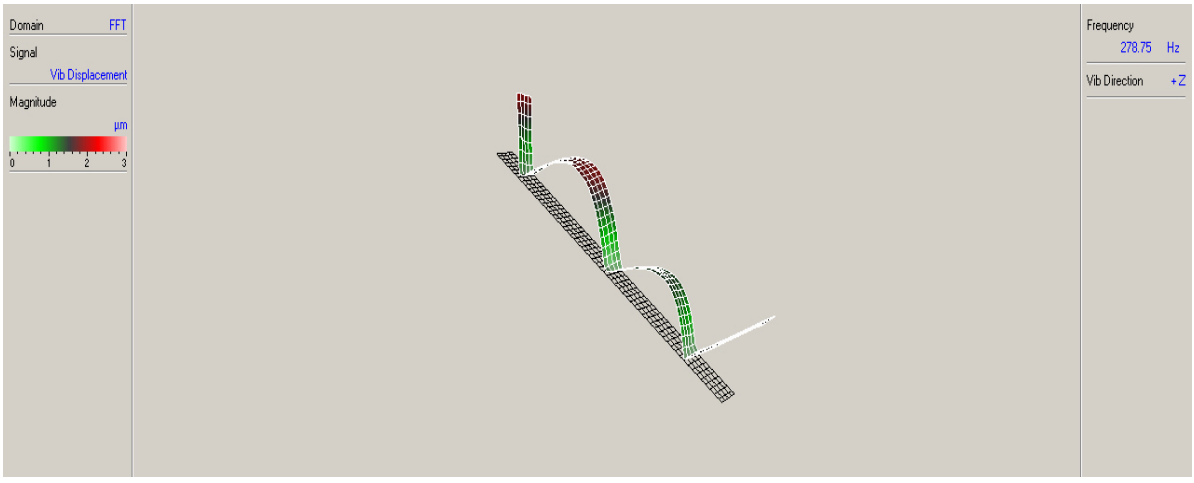


**Figure 4-26-b: Displacement Mode 2 for Sample 7**

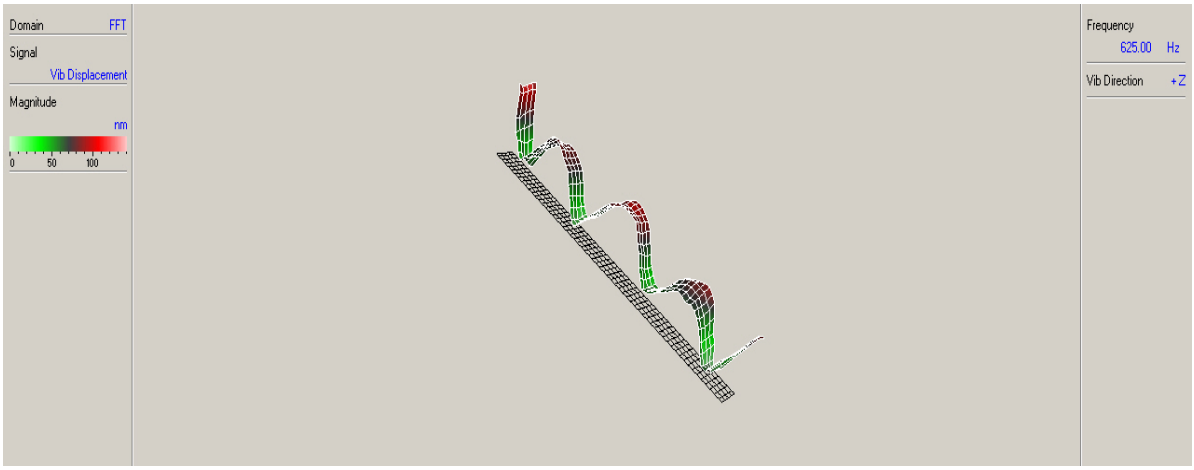


**Figure 4-26-c: Displacement Mode 3 for Sample 7**

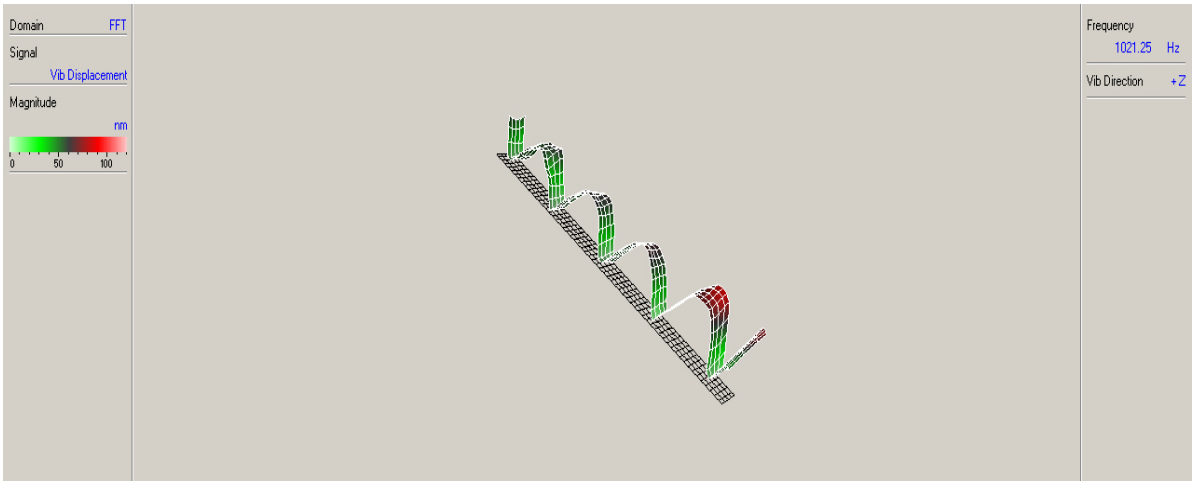


**Figure 4-26-d: Displacement Mode 4 for Sample 7**

**Figure4.26. Displacement mode shapes of sample 7: (a) Mode 1, (b) Mode 2, (c) Mode 3 and (d) Mode 4.**

Selected Displacement peaks for Sample 8 are shown in Table 4-9:

**Table 4-9: Selected peaks in Displacement Magnitude-sample 8 - Frequency Graph**

| Peak no. | Frequency(Hz) | Displacement Magnitude(µm) |
|---|---|---|
| 1 | 111.9 | 8.240 |
| 2 | 278.1 | 1.400 |
| 3 | 620.6 | 0.080 |
| 4 | 1015.6 | 0.080 |

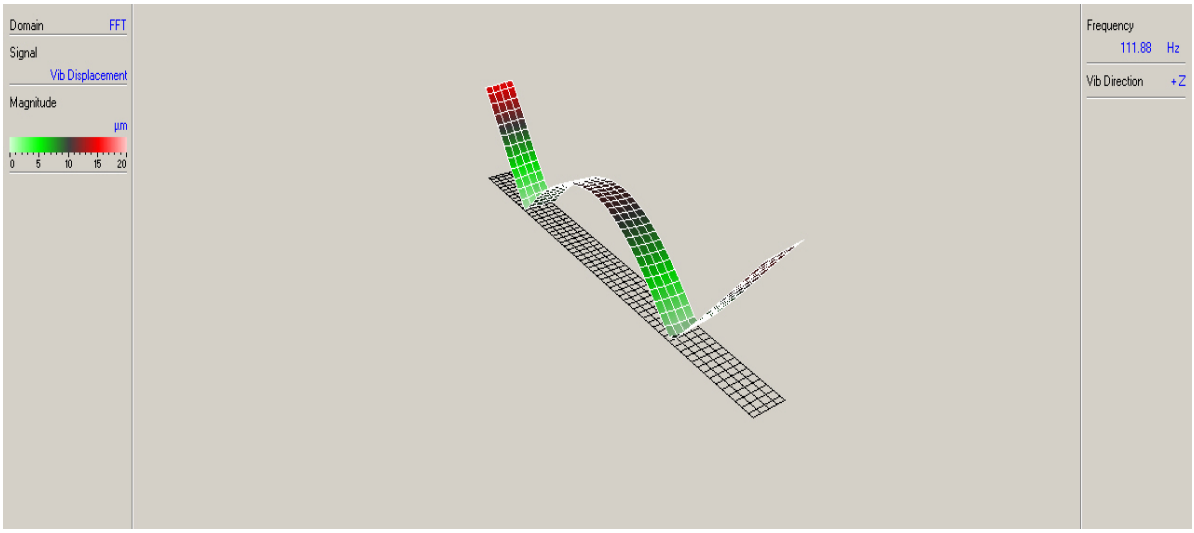


**Figure 4-30-a: Displacement Mode 1 for Sample 8**

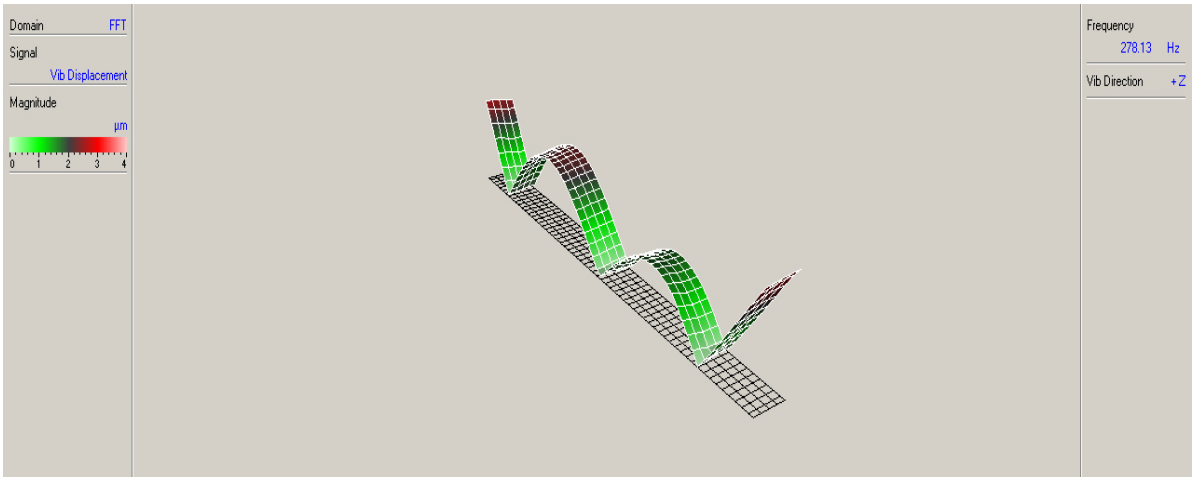


**Figure 4-27-b: Displacement Mode 2 for Sample 8**

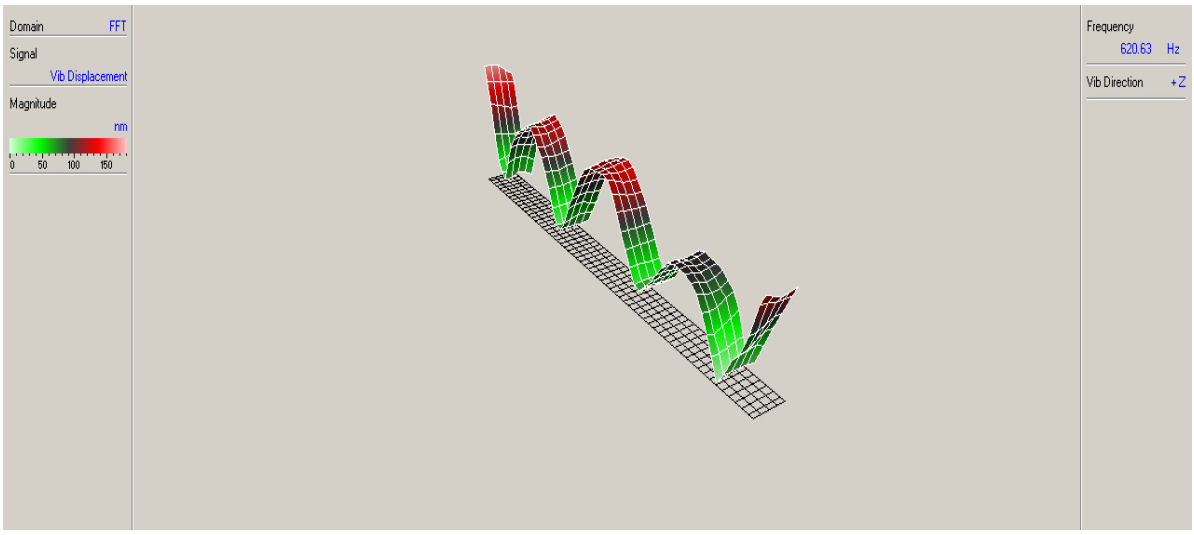


**Figure 4-27-c: Displacement Mode 3 for Sample 8**

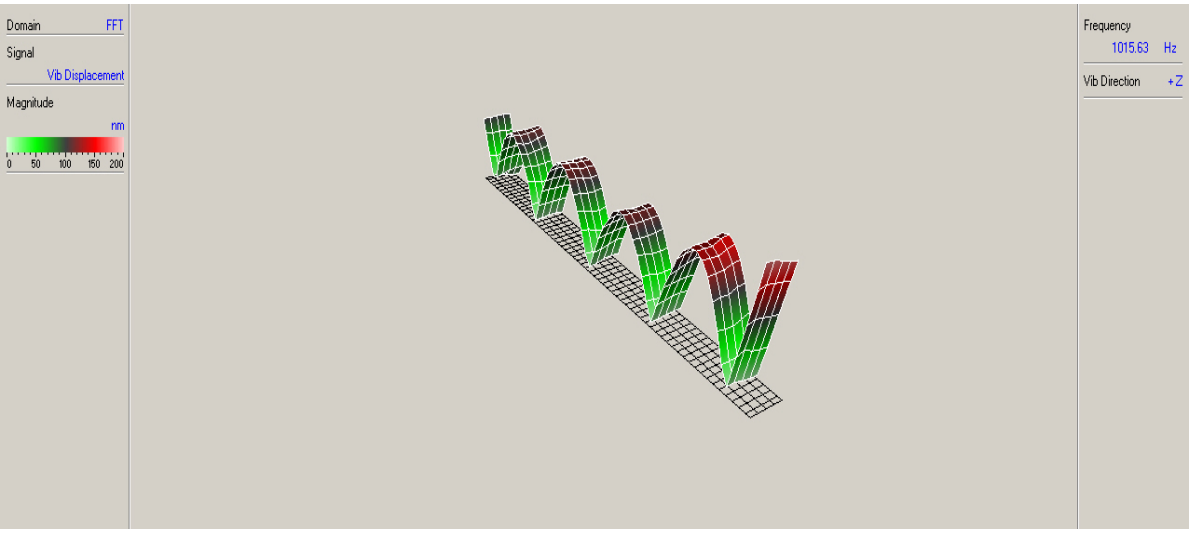


**Figure 4-27-d: Displacement Mode 4 for Sample 8**

**Figure4.27. Displacement mode shapes of sample 8: (a) Mode 1, (b) Mode 2, (c) Mode 3 and (d) Mode 4.**

By comparing the displacement mode shapes (DMS) of intact and damaged structures, it was clear that the DMS is very sensitive to noise and interference. On the other hand, displacement mode shape doesn`t have a local nature. Thus, detection of severity and location of damage in a structure by using DMS is not applied in this project directly and some extra calculations were obtained to find an appropriate scalability factor.

The Displacement Magnitudes for all the points of the samples are presented in Appendix B.

## 4.5. Absolute Difference between the Displacement Mode Shapes for the intact and damaged Samples

The first five natural frequencies of the intact samples and of the damaged samples are listed in Table 4-9. From the percentage change in the frequency, from the intact to the damaged case, a state of damage could be discernible, but no indication of the location of damage is obtained from this, without further analysis.

**Table 4-10: Natural frequencies of the first five modes for the intact sample 3 and the damaged sample 1**

| Mode no. | Intact(sample 3) | Damaged (Sample1) | Percentage change in Frequency |
|---|---|---|---|
| 1 | 111.9 | 111.3 | 0.006 |
| 2 | 279.4 | 278.1 | 0.013 |
| 3 | 620 | 540 | 0.8 |
| 4 | 1010.6 | 1005 | 0.056 |

**Table 4-11: Natural frequencies of the first five modes for the intact sample 3 and the damaged sample2**

| Mode no. | Intact(sample 3) | Damaged (Sample2) | Percentage change in Frequency |
|---|---|---|---|
| 1 | 111.9 | 111.9 | 0 |
| 2 | 279.4 | 278.8 | 0.006 |
| 3 | 620 | 549.4 | 0.706 |
| 4 | 1010.6 | 1015.6 | 0.05 |

**Table 4-12: Natural frequencies of the first five modes for the intact sample 3 and the damaged sample4**

| Mode no. | Intact(sample 3) | Damaged (Sample4) | Percentage change in Frequency |
|---|---|---|---|
| 1 | 111.9 | 115 | 0.031 |
| 2 | 279.4 | 285 | 0.056 |
| 3 | 620 | 625 | 0.05 |
| 4 | 1010.6 | 1039.4 | 0.288 |

**Table 4-13: Natural frequencies of the first five modes for the intact sample 3 and the damaged sample5**

| Mode no. | Intact(sample 3) | Damaged (Sample5) | Percentage change in Frequency |
|---|---|---|---|
| 1 | 111.9 | 108.1 | 0.038 |
| 2 | 279.4 | 268.1 | 0.113 |
| 3 | 620 | 585 | 0.35 |
| 4 | 1010.6 | 974.4 | 0.362 |

**Table 4-14: Natural frequencies of the first five modes for the intact sample 3 and the damaged sample6**

| Mode no. | Intact(sample 3) | Damaged (Sample6) | Percentage change in Frequency |
|---|---|---|---|
| 1 | 111.9 | 113.1 | 0.012 |
| 2 | 279.4 | 283.1 | 0.037 |
| 3 | 620 | 612.5 | 0.075 |
| 4 | 1010.6 | 1031.3 | 0.207 |

**Table 4-15: Natural frequencies of the first five modes for the intact sample 3 and the damaged sample7**

| Mode no. | Intact(sample 3) | Damaged (Sample7) | Percentage change in Frequency |
|---|---|---|---|
| 1 | 111.9 | 111.3 | 0.006 |
| 2 | 279.4 | 278.8 | 0.006 |
| 3 | 620 | 625 | 0.05 |
| 4 | 1010.6 | 1021.3 | 0.107 |

**Table 4-16: Natural frequencies of the first five modes for the intact sample 3 and the damaged samples**

| Mode no. | Intact(sample 3) | Damaged (Sample8) | Percentage change in Frequency |
|---|---|---|---|
| 1 | 111.9 | 111.9 | 0 |
| 2 | 279.4 | 278.1 | 0.013 |
| 3 | 620 | 620.6 | 0.006 |
| 4 | 1010.6 | 1015.6 | 0.05 |

## 4.6. C-SCAN results for Carbon/Epoxy Composite Beams

Although we tried to make the samples as accurate as possible, manufacturing error is inevitable. Therefore all samples should be scanned by C-SCAN machine. In this process, c-scan machine scanned all the samples through soft and tough surface to distinguish if there is any shift or manufacturing error in the samples or not. Therefore three samples were put together under the water and the scanner started scanning the samples (Figure 4.28). A monitor which connected to the scanner shows the condition of the samples and the place of the delaminations could be seen by some extra peaks (Figure 4.29)

**Figure 4-31: The C-Scan machine scanning the samples**

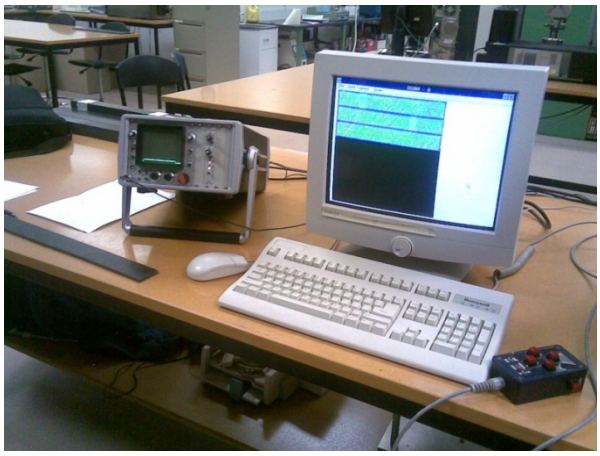

**Figure 4-32: The monitor connected to the c-scan machine to show the condition of samples**

Fortunately, after gathering the results and comparing the c-scan results with the real position of delaminations inside the samples, it was shown that errors were not remarkable and all samples were reliable for testing. The c-scan results are shown in Figure 4.30.

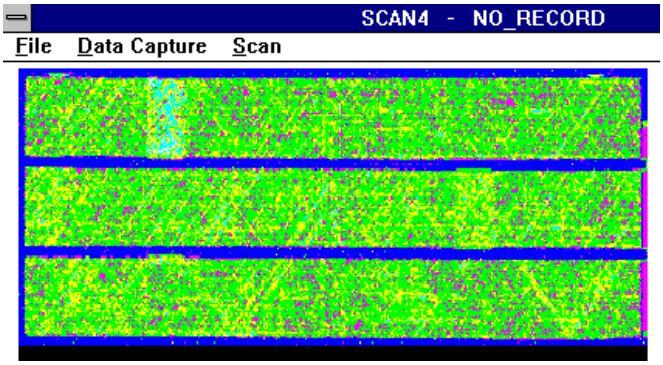


**Figure 4-33-a: Samples 1, 2, 3(Healthy)**

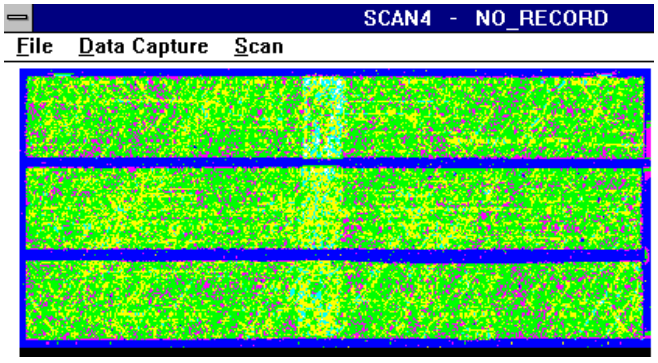


**Figure 4-30-b: Samples 4, 5, 6**

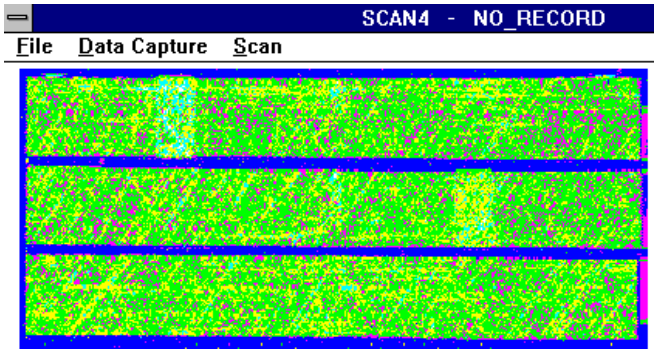


**Figure 4-30-c: Samples 7, 8, 9(Healthy)**

**Figure 4.30 the c-scanning results: (a) samples 1, 2, 3(Healthy) –**

**(b) Samples 4, 5, 6 – (c) samples 7, 8, 9 (healthy)**

## 4.7. Conclusion

The prepared Carbon/Epoxy samples from the last chapter were used for a series of experiments. The POLYTEC® Laser Vibrometer was used to scan all the samples with embedded delamination as well as healthy samples. The principles of plywood composites tests were used to setup the experiment and the physical properties of each samples i.e. FFT, displacement and velocity data were determined. The aim was to evaluate the damage status (severity and location) of the damaged samples by comparing their FFTs and displacement magnitudes with the results from healthy samples. Due to the nature of the natural frequency as well as displacement, further analysis was needed in order to get the damage severity in following chapters. By looking at the peaks in FFT Domains, the location of the delamination was predicted and C-SCAN test was used to confirm the location of the delaminations inside the samples. A good accuracy was observed which validates our manufacturing technique as well as the experimental modeling.

# CHAPTER 5

# Curvature mode shapes of Carbon/Epoxy Composite Beams

## 5.1. Introduction

Any crack or localized damage in a structure reduces the stiffness and increases the damping in the structure. Reduction in stiffness is associated with decreases in the natural frequencies and modification of the modes of vibration of the structure. Many researchers have used one or more of the above characteristics to detect and locate a crack. Most of the emphasis has been on using the decrease in frequency or the increase in damping to detect the crack. Very little work has been done on using the changes in the mode shapes to detect the crack. Adams et al used the decrease in natural frequencies and increase in damping to detect cracks in fiber-reinforced plastics. Loland *et al.* and Vandiver used the same principle to detect damage in offshore structures. From relative changes in the natural frequencies of different modes, Loland *et al.* could predict the location of the damage. They demonstrated the use of their technique on some platforms in the North Sea. The essence of the methods developed by the other researchers is similar, but different methods of data analysis were used. Adams et al developed a theoretical model to predict the damage and its location based on reacceptance analysis. The analysis was done by using axial modes of vibration and is valid for structures which can be treated as one-dimensional. Adams and Cawley employed sensitivity analysis to deduce the location of damage in two-dimensional structures, based on a finite element analysis method. Flexural modes of vibration were used in this case. The method was applied to the case of a flat plate with the assumption that the modulus of elasticity in the damage area was equal to zero. For each element of the model, the sensitivity of the change was evaluated. The results of the analysis agreed well with the experimental results. The drawback of this method is that a lot of computation has to be performed subsequent to data collection to predict the location of the damage. Very little use has been made of the changes in the mode shapes in detecting a crack or damage in a structure. Yuen in his paper showed for a cantilever beam that there is a systematic change in the first mode shape with respect to the damage location. He used finite element analysis to obtain the natural frequencies and the mode shapes of the damaged structure.

From changes in frequency one can easily determine the presence of crack or damage in a structure. But determining the location of the crack, knowing the changes in the frequencies, is a completely different question. This is because cracks at two different locations associated with certain crack lengths may cause the same amount of frequency change. Other parameters need to be determined which will directly identify the location of crack or damage in a structure.

In this paper, a new parameter called “curvature mode shape” is introduced. The difference in the curvature mode shapes between the intact and the damaged case is utilized to detect the location of the crack. The changes in the curvature mode shapes are shown to be localized in the region of damage compared to the changes in the displacement mode shapes. A cantilever and a simply supported beam model are used to demonstrate this characteristic of the curvature mode shapes. Different ways of comparing mode shapes include the Modal Assurance Criterion (MAC) and the Co-ordinate Modal Assurance Criterion (COMAC). MAC indicates the correlation between two sets of mode shapes. It is used to study overall differences in the mode shapes. COMAC compares mode shapes in a point-wise manner. It indicates the correlation between the mode shapes at a selected measurement point of a structure.

Curvature mode shapes are related to the flexural stiffness of beam cross-sections. Curvature at a point is given by

$$\nu'' = M / EI \qquad (5\text{-}1)$$

In which $\nu''$ is the curvature at a section, $M$ is the bending moment at a section, $E$ is the modulus of elasticity and $''I''$ is the second moment of the cross-sectional area. If a crack or other damage is introduced in a structure, it reduces the (EI) of the structure at the cracked section or in the damaged region, which increases the magnitude of curvature at that section of the structure. The changes in the curvature are local in nature and hence can be used to detect and locate a crack or damage in the structure. The change in curvature increases with reduction in the value of (EI), and therefore the amount of damage can be obtained from the magnitude of change in curvature.

## 5.2. Curvature Mode Shapes Calculation Methods

There are different methods to calculate Curvature Mode Shapes from other physical properties. Curvature mode shape could be obtained either directly from laser vibrometer by using Piezoelectric material, or by applying some numerical and analytical methods to calculate them from displacement mode shape. The following sections will outline each method.

## 5.2.1. Piezoelectric material

By using piezoelectric material and I-DEAS Software, curvature mode shapes could be directly calculated after scanning the specimens with Laser Vibrometer. The process consists of two general steps: First, digital analog converter d-SPACE system could be used to acquire data from both the actuator and the sensors. Then the FRFs should be transferred to MATLAB and the modal analysis of the experimental results to generate the curvature mode shapes is performed by using I-DEAS Test module (Figure 5.1). For detailed procedures of data processing and experimental results, see W. Lestari *et al.* (2006).

**Figure 5-1: Application of piezoelectric material to obtain curvature mode shapes**

## 5.2.2. Numerical

In the numerical method of calculating curvature mode shapes, displacement mode shapes are taken as the basic factor for calculations. As a matter of fact, curvature mode shape is the second derivative of displacement mode shape, so by applying a numerical formulation called "Central Difference Approximation" on displacement mode shapes; curvature mode shapes could be calculated. Following is the Central Difference Approximation (CDF) Formula:

$$v''_i = \frac{(v_{i+1} - 2v_i + v_{i-1})}{h^2} \qquad (5\text{-}2)$$

Where h is the element length, ν″ is the curvature and ν is the displacement and h is the length of $i_{th}$ element. After gathering all the results by scanning samples with embedded delaminations in different locations and levels, the results were exported to Excel for numerical calculations.

## 5.2.3. Finite Element Method Analysis

In this study, Finite element analysis (FEA) was initiated to complement and validate the damage detection algorithms. Initial FE models were created by modelling the composite with the solid element (8node82) in ANSYS. A load was applied (in the $F_y$ direction) at 400mm from the left end of the beam, node numbering was used to get x = 0.4 m, y = 0.0 m as shown in Figure 5.2 A bilinear element (Link10) in ANSYS was used to model the delamination as shown in Figure 5.2 A delamination was simulated using Link10 which is a 3-D spar element designed as compression-only element, which means that the stiffness is zero if the element is under tension.

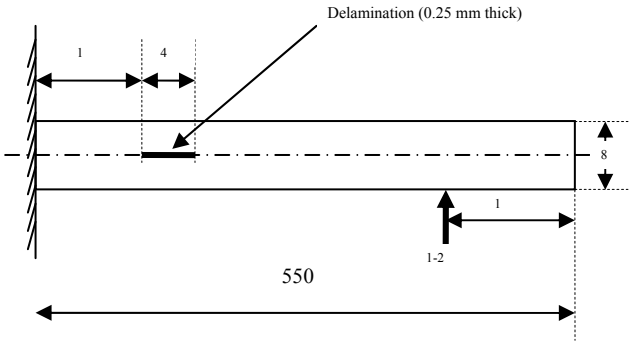


**Figure 5-2: FE model describing damage**

The initial results from the FE analysis that were obtained for various natural frequencies and displacement mode shapes were very encouraging. Table 5.1 describes the comparison between natural frequencies obtained experimentally and that using FEA.

**Table 5-1: Comparison between Natural Frequencies obtained from FE model and LSV system**

| Mode | FEA $\omega_n$ (Hz) | Laser Vibrometer $\omega_n$ (Hz) |
|---|---|---|
| 1 | 136.795 | 111.3 |
| 2 | 336.526 | 278.1 |
| 3 | 468.86 | 540 |
| 4 | 1207 | 1005 |

The mode shapes acquired from FEA were very similar and nodal displacements were very close to the experimental results. Figures 5.3 & 5.4 shows the displacement mode shapes for mode 1 acquired by both FEA and SLV system as an example.

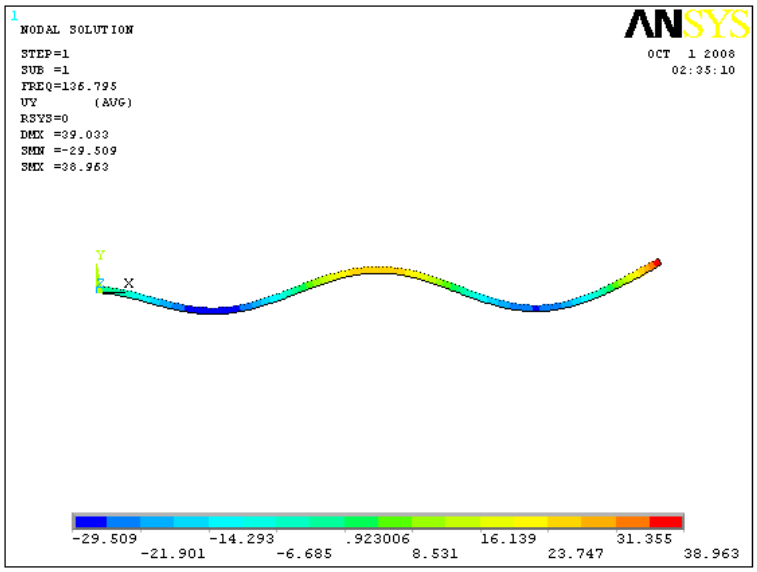


**Figure 5-3: Displacement Mode Shape Gathered from ANSYS**

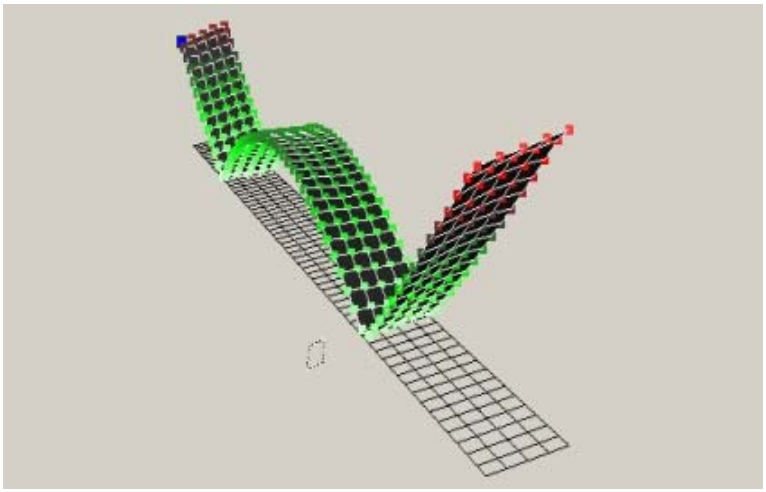

**Figure 5-4: Displacement Mode Shape Gathered from Laser Vibrometer**

Using the Curvature Mode Shapes Calculations method, we can calculate the related curvatures to the gathered displacement mode shapes which could validate experimental and theoretical results.

## 5.2.4. Curvature Mode Shape Calculations

The method which is used in this research project, is the numerical method based on CDA. The following is the process of these calculations.

### 5.2.4.1. Data Sorting

As it was mentioned in chapter 4, the laser vibrometer scanned the points which were defined on the surface of the samples. The movement of laser point was horizontally through the width. But for curvature calculations, a series of points through the length of samples was needed, so a Visual Basic code, Figure 5.5, was obtained to sort the data in a way that would be appropriate for further calculations. Thus, five lines were obtained and by using CDA formulation, the curvature for each line was calculated and by merging all lines together, the final curvature graph for each mode was introduced (Figure 5.6). As it can seen from Figure 5.7 the curvature mode 1 was made by merging 5 curvature lines which calculated from displacement lines for mode 1.

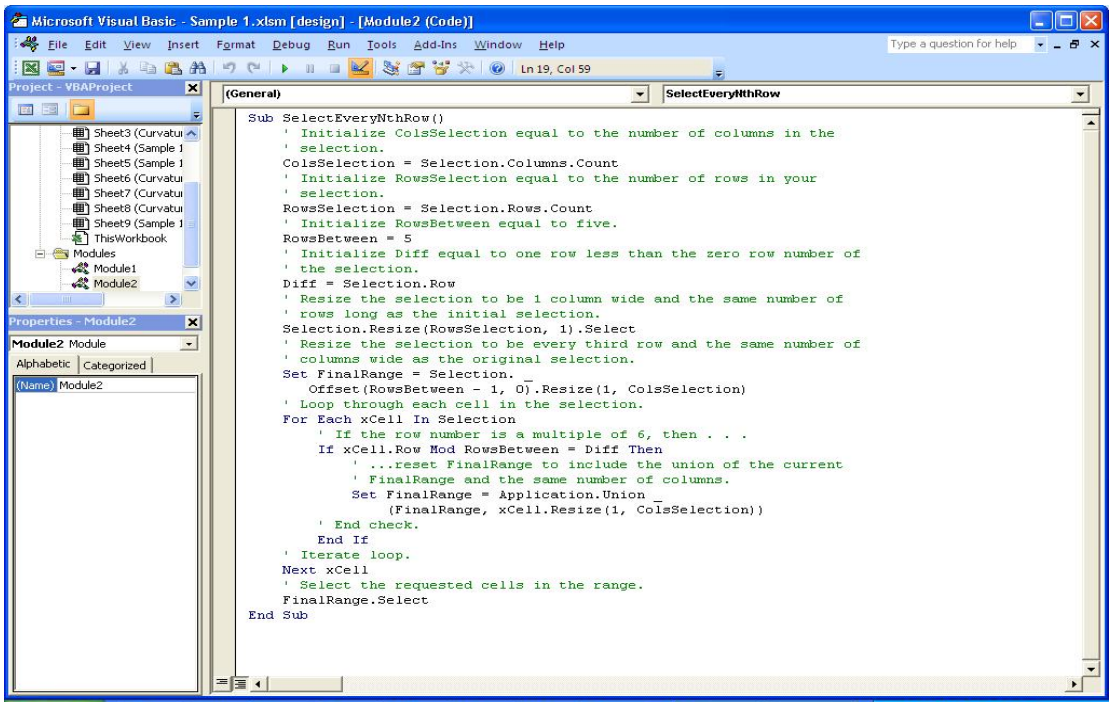


**Figure 5-5: Visual Basic Sorting Program**

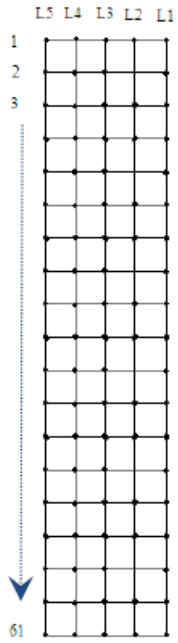


**Figure 5-6: Point Position matrix used to generate curvature mode shapes for Carbon/Epoxy**

In the next step, the same procedure was applied on modes 1 to 4 of defect and healthy samples. As it is mentioned before, sample 9 was selected for physicalproperties tests.The results of these tests were required for FEM Analysis. Thus, for each sample, four curvature modes were available for further analysis.

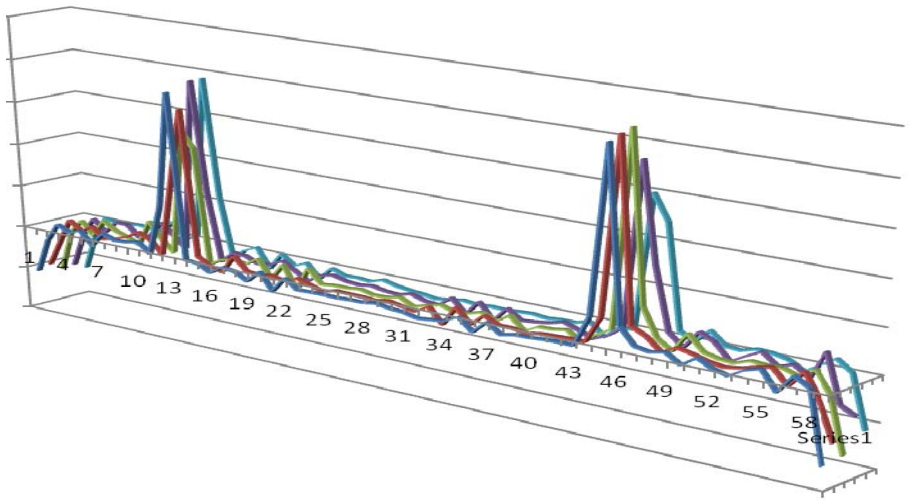


**Figure 5-7: The Curvature Mode Shape made by 5 curvature lines**

## 5.5. Curvature mode shapes for Healthy Beams

In the following graph, Figure 5.8,there are two considerable peaks between points 10-15 and 44-49. Thus the damage zone is estimated approximately as 38.68 mm similar to the estimation from displacement mode shapes.

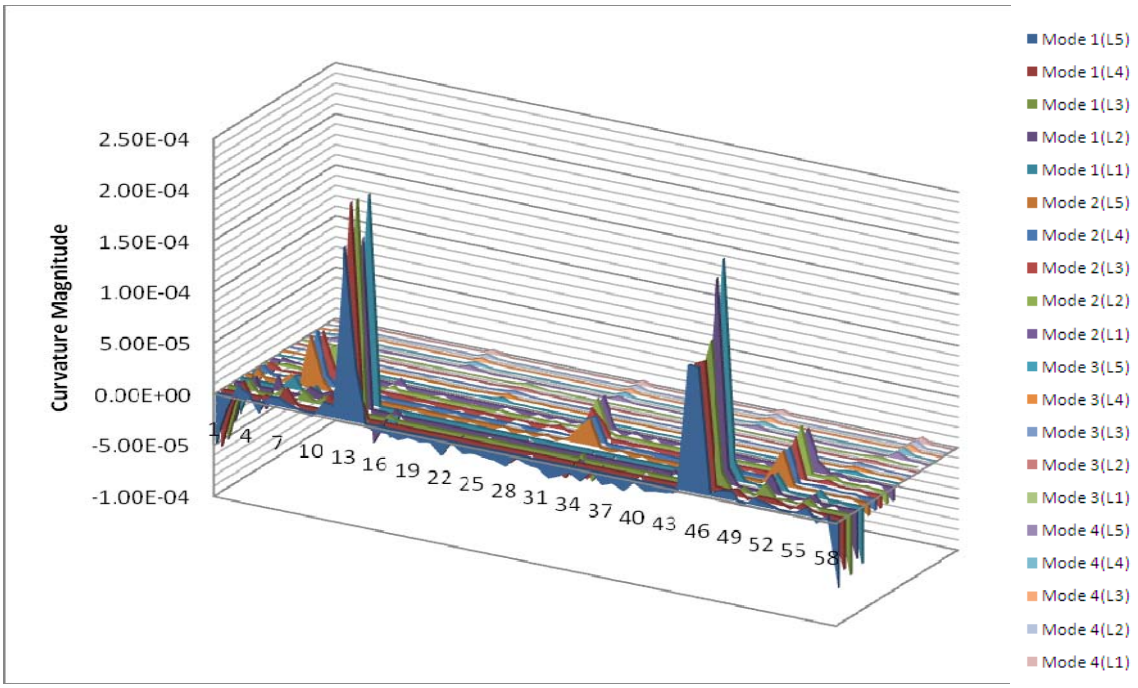


**Figure 5-8: Curvature Mode Shapes of Sample 3 (Healthy sample)**

According to C-SCAN result for sample 3 there is a small delamination on this sample caused by manufacture errors and teflon shifting during curing process. (Figure5.9)

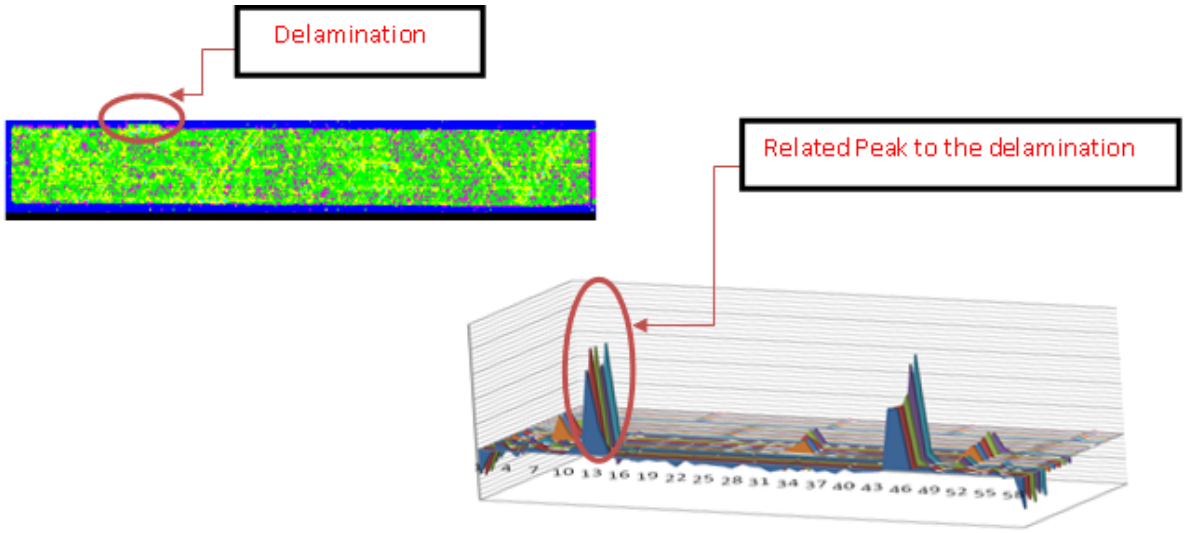


**Figure 5-9: Manufacture error in Healthy sample**

Although this extra delamination is a considerable manufacture error in the healthy sample, it is still usable due to the comparative nature of this detection method. On the other hand, it could be proof of acceptance for this method to detect a small delamination in sample 3 which was not observed at previous stages. The second peak in this graph is related to the excitation point where the shaker was attached to the sample.

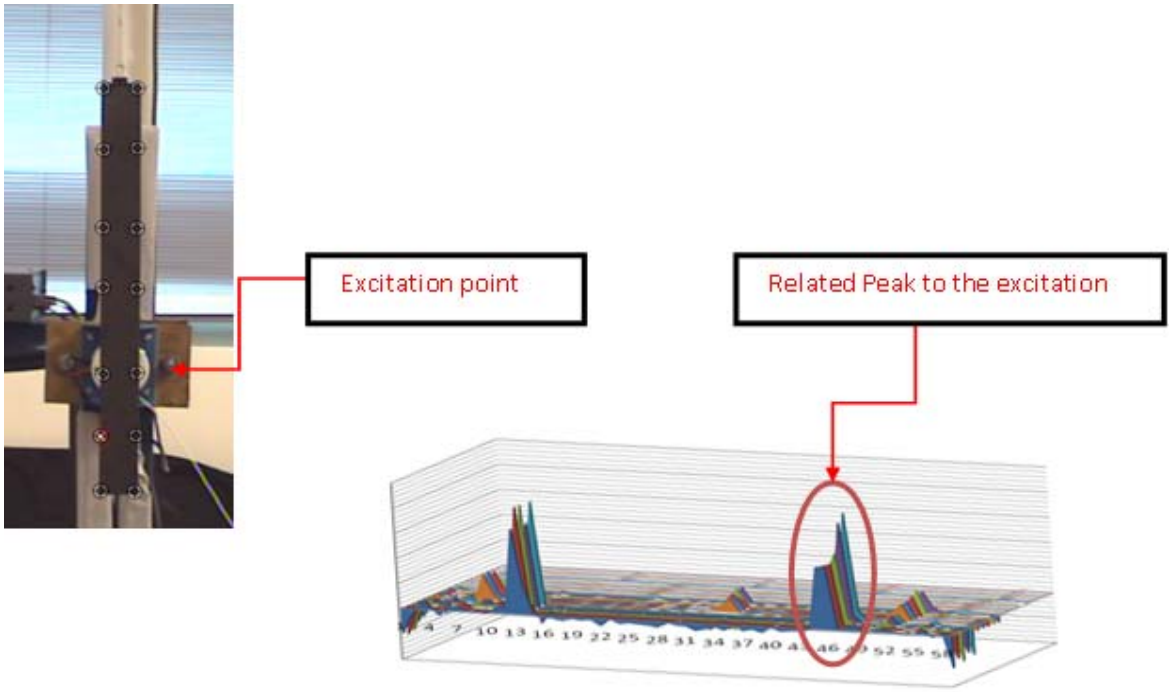


**Figure 5-10: Excitation point in Healthy sample**

As an illustration, one of the peaks in the displacement graph is at the excitation point because of the high magnitude of displacement at this point. Therefore a peak in the curvature graph, which is the second derivative of displacement, was obtained at this point (Figure 5.10). There are other peaks in the curvature mode shapes, however none of them were considerable compared to mentioned peaks. In fact, peaks were observed from modes 1 and 2 which could be a guideline for obtaining possible relationship between the types of damages i.e. impact, delamination, saw-cut etc.

## 5.6. Curvature mode shapes of Defect Beams

The curvature mode shapes for defect samples were calculated as well. Samples 1, 7 and 8 were selected as defect samples with the delaminations in different locations and levels. The method of calculation was as same as healthy samples for better comparison. The important point in making appropriate comparison between different samples is the same number of scanned points for all samples.

### 5.6.1. Curvature mode shapes of sample 1

The curvature mode shapes for sample 1 were calculated based on Central Difference Approximation (CDA) Method. As it can seen from the Figure 5.11, the possibility of extracting damage status is higher in Mode 1 therefore only this mode was analyzed to indicate

the presence of damage within the specimen as higher modes produce results which were less convincing. As the graph illustrates, two distinct peaks were observed which were related to the excitation point and delamination region in sample 1 according to the C-Scan results and experimental modellings. All four curvature mode shapes of sample 1 are gathered in the following graph.

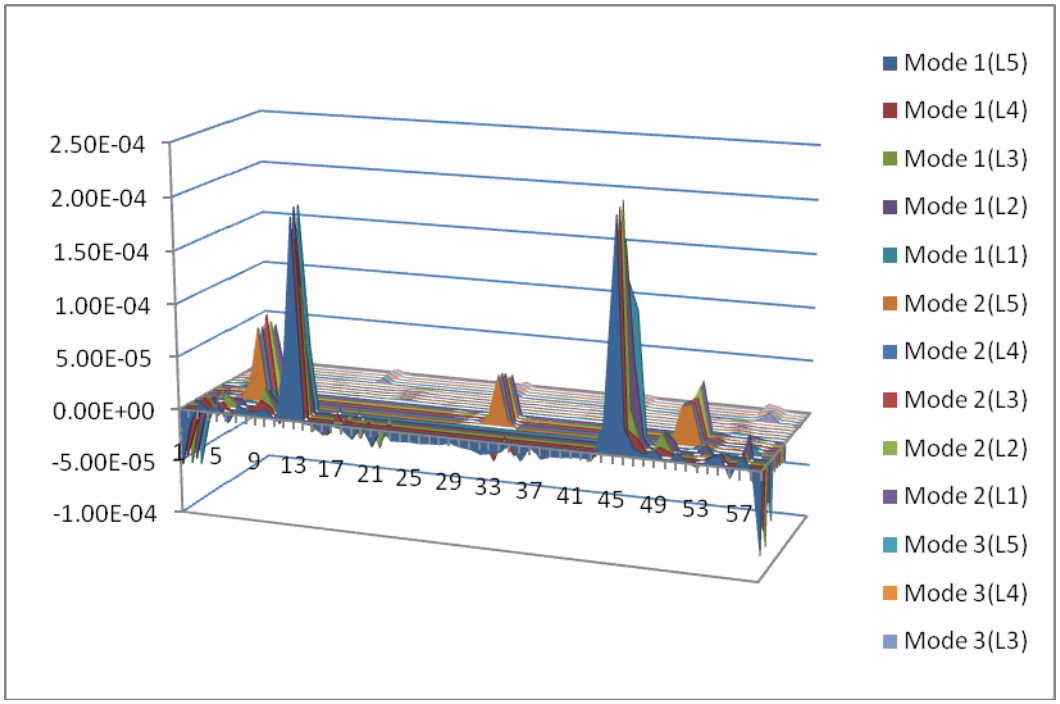


**Figure 5-11: Curvature Mode Shapes of Sample 1**

For better analysis of results, the location of peaks in curvature mode shapes were compared with C-SCAN results and Manufacture plot. As it is shown in Figure 5.12, the location of the peak in curvature mode shapes was matched with the C-SCAN result.

The table of all curvature magnitudes for every sample as well as absolute difference magnitudes are presented in Appendex C.

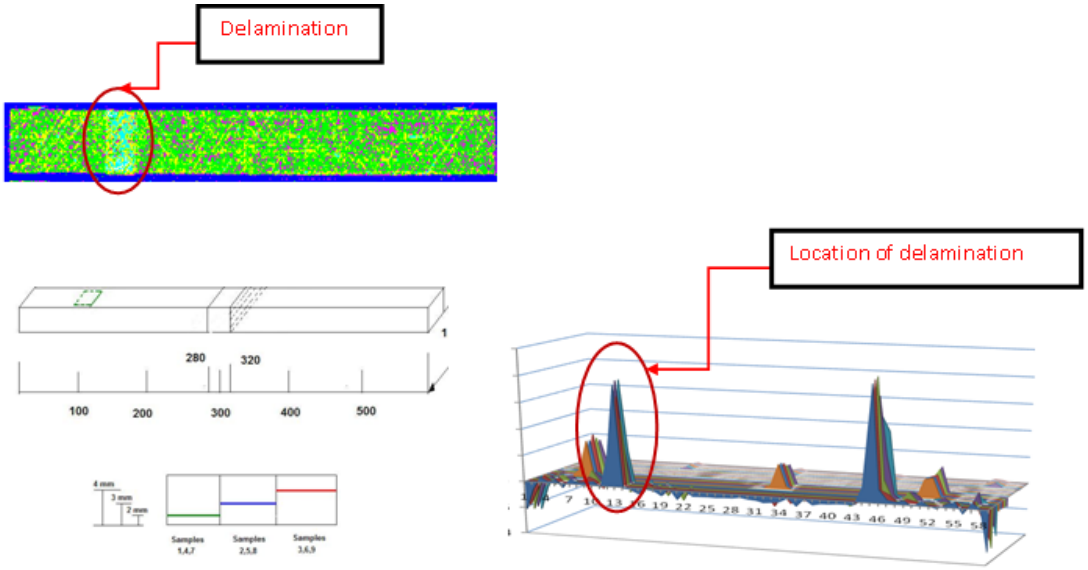


**Figure 5-12: Delamination region in Sample 1**

The location of the peak in the curvature mode shape is between points 11-15 which is acceptable.

## 5.6.2. Curvature mode shapes of sample 7

The same method was applied to calculate the curvature mode shapes of sample 7 (Figure 5.13). As seen from the graph, two main peaks were observed. The left hand peak was happened due to the delamination effect and the right hand one caused by the shaker which was connected to the sample at this point. By comparing the exact locations of the delamination and excitation with the location of the peaks, the accuracy of the experiments was confirmed.

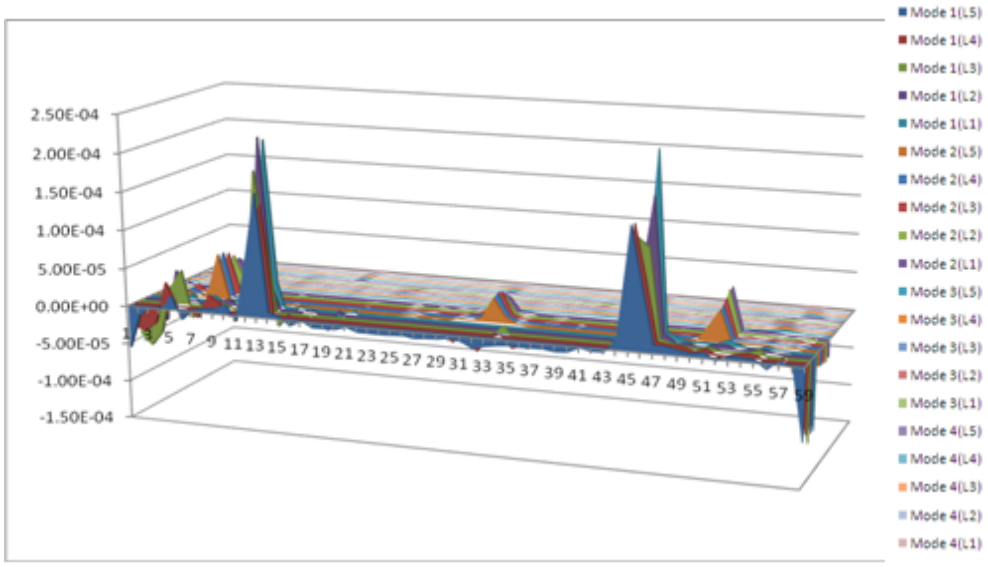


**Figure 5-13: Curvature Mode Shapes of Sample 7**

The Figure 5.14 shows the comparison between the real location of delamination and obtained location of delamination according to curvature mode shape result for sample 7.

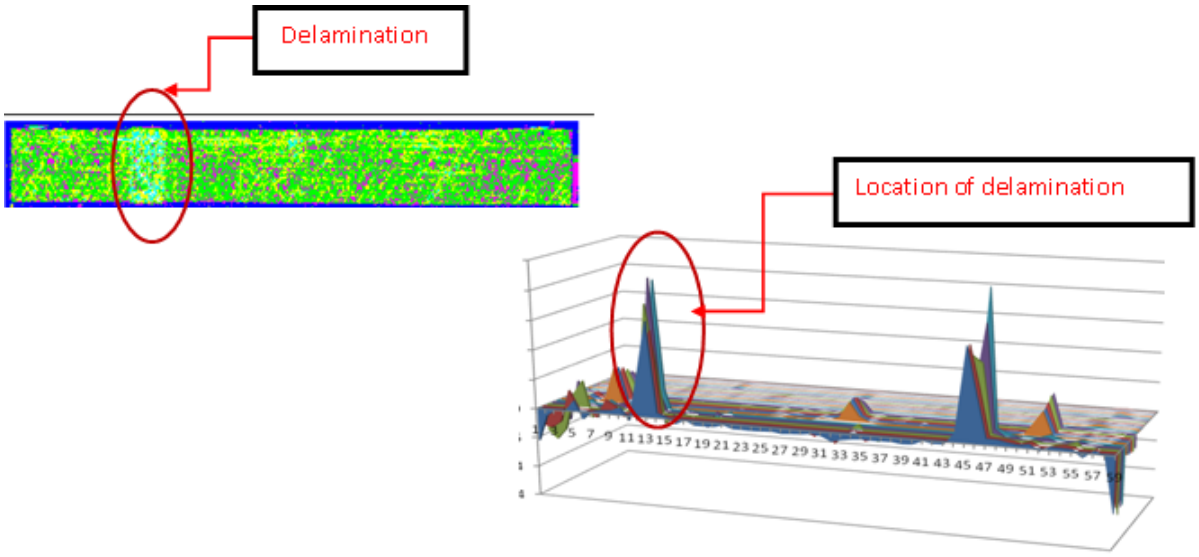


**Figure 5-14: Delamination region in Sample 7**

The location of delamination in sample 1 and 7 are the same, but the levels are different. In fact, the Teflon in sample 1 was placed at the first level with 2 mm distance from the surface, but in sample 7 it was located at the second level with the depth of 3 mm. It is predictable that the magnitudes of peaks in curvature mode shapes of these samples would be different according to the level of delaminations. In other words, the more distance from surface is, the less the magnitude of curvature.

## 5.6.3. Curvature mode shapes of sample 8

As illustrated in Figure 5.15, two main peaks were observed for sample 8 as well with the same magnitude as sample 1. However, the locations are reversed due to the different location of the delamination and shaker in samples 1 and 8. By comparing the following Figure with Figure 5.11 for sample 1, it was observed that the related peak to the delamination at sample 8 has the same magnitude as sample 1(due to the same level of delamination) and reverse location of the peak (due to the difference location of the delamination).

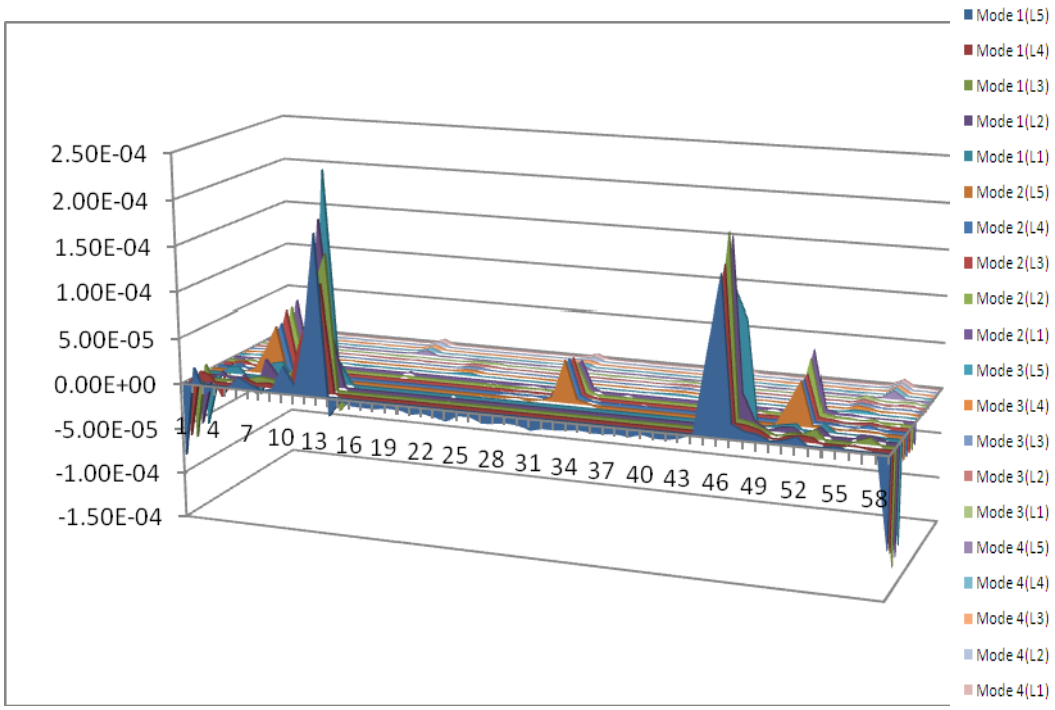


**Figure 5-15: Curvature Mode Shapes of Sample 8**

The comparison between the real location of delamination and obtained location of delamination according to curvature mode shape result for sample 8 is shown in Figure 5.16

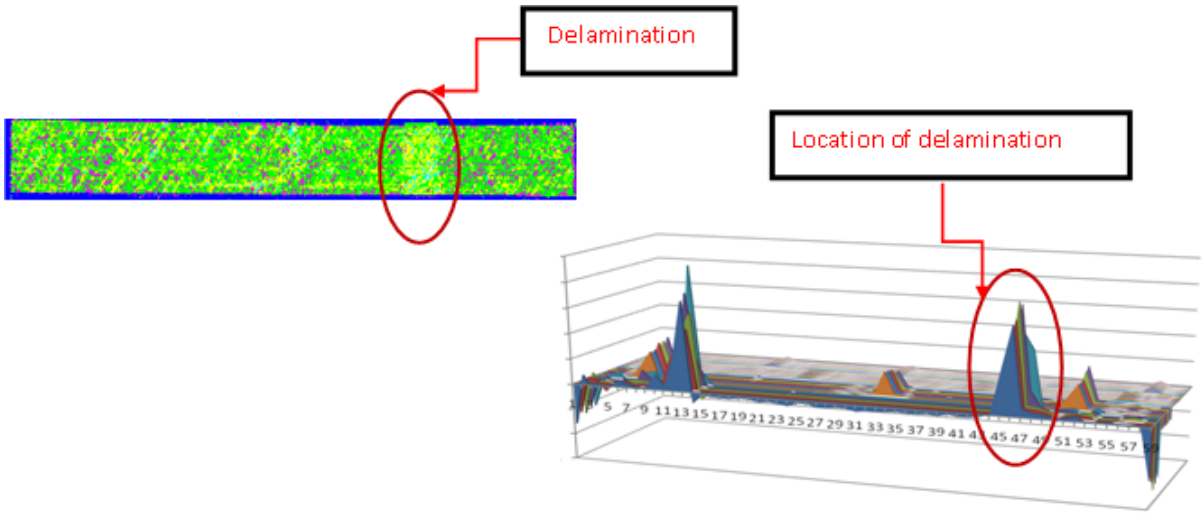


**Figure 5-16: Delamination region in Sample 8**

## 5.7. Comparison the Curvatures of intact and damaged Composite Beams

The curvature mode shapes of healthy and damaged samples were plotted in previous sections however, when detecting the exact location of the damage, an absolute difference between the curvatures of healthy and defect samples is needed. Hence, the absolute difference of samples 1, 7 and 8 as defect samples with sample 3 as healthy sample were calculated. The results were plotted in Figure 5.17 to establish the location and severity of delamination in each sample. The results are below:

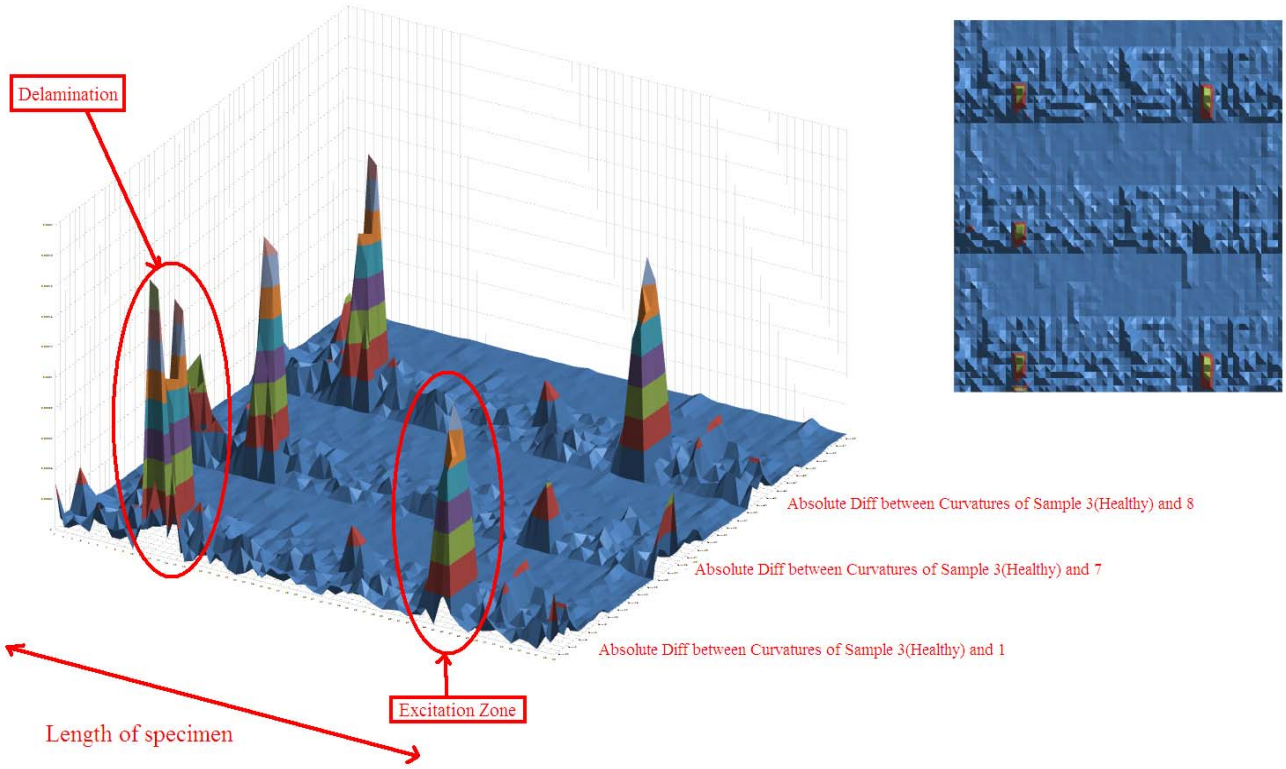


**Figure 5-17: Absolute Difference between the curvature mode shapes of healthy and defect samples**

As it can seen from above plot, there are two considerable peaks in the absolute difference graphs of samples 1 and 8. The left hand side peaks are related to the delaminations and the right hand peaks are related to the excitation point. The magnitudes of peaks are different due to different levels of delaminations but the locations are almost the same. For sample 7, the shaker was attached on the delamination zone. Thus the peak caused by excitation is eliminated by the peak made by delamination. In fact, in all absolute graphs, there is a peak at the left hand side which is related to the manufacture error of sample 3.

## 5.8. Conclusion

The damage within the Carbon/Epoxy beams could be identified successfully by both the displacement mode shape analysis as well as curvature mode shape analysis. The displacement mode shape, which gives a global snapshot the frequency domain range, is a positive method for a globalised technique of damage identification. The curvature mode shape being the derivative of the displacement mode shape is more of a localized technique. The size and location of the delamination in one place was successfully identified by both these techniques and validated using the C-scan results.

In order to calculate the curvature mode shapes, three different ways of data gathering were used: Experiments and FEM. The Central Difference Approximation (CDA) was applied for these calculations. In the experimental results, frequency responses as well as displacement mode shapes of beams were captured. The curvature mode shapes were then calculated with the CDA method. In the FEM technique, the ANSYS Software was used to analyze and calculate the displacement mode shapes. The curvature mode shapes from these two techniques compared favorably.

# CHAPTER 6

# Sample Preparation and Curing For Fatigue Crack Propagation Test

## 6.1. Introduction

Fatigue behavior of composite materials has been the subject of intense research in recent years since fatigue is known to be responsible for the majority of failures of structural components. Local damage in isotropic materials, such as metals and polymers, usually develops monotonically leading to material failure. In contrast, in composite materials, , a combination of four main damage modes have been observed under fatigue loading, namely, matrix cracking, fiber-matrix deboning, delamination, and fiber fracture. Carbon-fiber reinforced polymer (CFRP) composites are attractive in that they combine high strength, high modulus, and low density. Among many studies regarding CFRPs, some were concerned with their fatigue behavior. For instance, Miyano *et al.* carried out fatigue tests of unidirectional CFRPs at various temperatures and loading rates. Harris et al observed for angle ply CFRPs that the combination of tensile and compressive fatigue loading is more damaging than purely tensile or compressive stress cycling. Wang and Chung achieved self-monitoring of fatigue damage in a cross ply CFRP by electrical resistance measurement. Studies were engaged in comparison of tensile fatigue behavior of unidirectional and quasi-isotropic CFRPs with thermoplastic and thermosetting matrices. By using a thorough fracto-graphic analysis, Shin and Jang investigated delamination features in woven CFRPs.

The influence of the material properties, processing conditions, and design on the resulting fatigue performance of composites invalidates any generalization of the experimental results for nominally identical composites. Since coupon specimens are sensitive to the free edge effects, they seem more susceptible to fatigue damage than the entire structure. Although more desirable, testing of a complete structural part is costly, complicated, and not easy to standardize, which leaves coupon specimen testing still in use for its simplicity and ease. Curtis *et al.* surmise that low-frequency fatigue experiments, in which a particular material response is recorded, might provide a better depiction of the component performance than higher frequency

laboratory tests. In fatigue tests at higher frequencies, the material of a structure may be subjected to a more complex stress state than in an idealized coupon.

However, the necessity for defining suitable tests at a coupon-level, which could be used as a part of the methodology for a reliable fatigue design, leads to a need for high-frequency fatigue tests. The literature recognizes the possibility of temperature rise during fatigue of composites that depends primarily on the level and frequency of cyclic load and can be attributed to a number of various heat sources. This study characterizes the high-frequency fatigue behavior of a cross ply and angle ply carbon-fiber reinforced epoxy by $S–N$ testing and by analysis of crack growth. In order to minimize the effect of residual strains due to temperature rise, which may disturb fatigue measurements, we propose a method for determining a more realistic value of the fatigue strength designated in this study as the real fatigue strength.

## 6.2. Sample Preparation

To start the test, the first step would be preparing the carbon/epoxy beams in order to apply the designated fatigue propagation test on them. Generally speaking; there are 3 steps as described below:

### 6.2.1. Locating the Embedded Delamination Using Microscope

As is mentioned in previous chapters, the C-Scan test was done on all Healthy and Damaged Samples to figure out the exact location of Embedded Delaminations in them. The results gathered from this test, validated the real location of delaminations according to manufacturing process.


**Figure 7-1: Vision MANTIS Electronic Inspection**

However, as the main aim in fatigue crack propagation test would be extending the current length of crack (Delamination) in both sides, we need to highlight two ends of the crack with white pen to check the progress of the crack length with Microscope during the test. For this purpose, a **Vision MANTIS Electronic Inspection** (Figure 6.1) is used to locate the delamination in Samples. As it can be seen above, the sample is put under the lens and embedded delamination is observed and highlighted. (Figure 6.2)

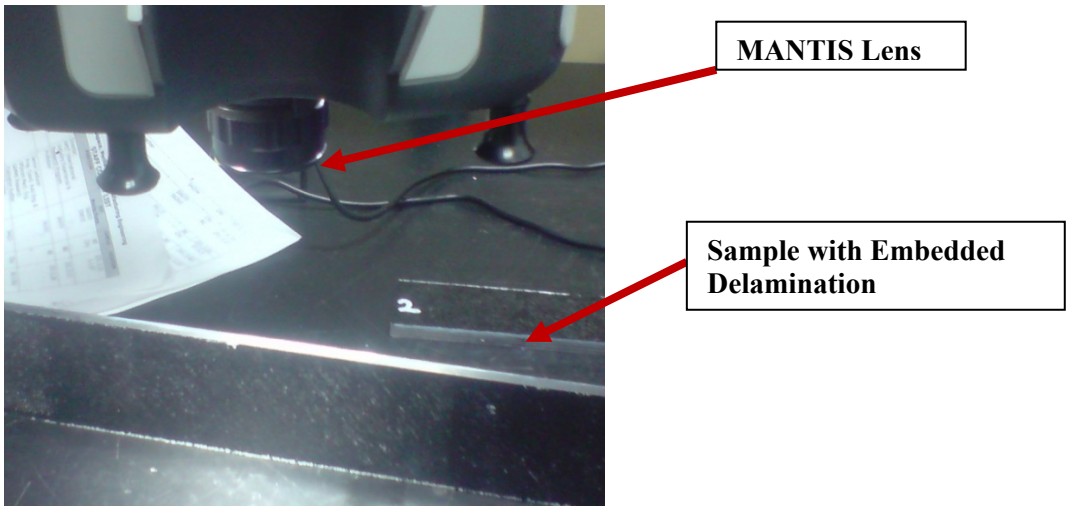


**Figure 7-2: Locating the Embedded Delamination using MANTIS**

## 6.2.2. Attachment of Inserts and Preparation

### 6.2.2.1. Inserts Manufacture

As it is mentioned before, the method which used to propagate the crack is based on pulling test. Therefore; two inserts are designed and manufactured to bond to the samples. They are screwed on the other side in order to fix to the INSTRON Fatigue test JARS. These Inserts are shown in Figure 6.3.

**Figure 7-3: Inserts for bonding to the Sample**

## 6.2.2.2. Inserts Surface Preparation

The stronger inserts bond to the sample, the better results we get. As a matter of fact, it is very important to prepare surfaces of both sample and inserts in order to have stronger attachment and more accurate results. To do that, an Abrasive Blasting (Figure 6.4) is used to clean the Surface of the inserts.


**Figure 7-4: Abrasive Blasting Cabinet Machine**

The inserts are put inside the Blast Cabinet and the operation of cleaning or preparing the surface is done by forcibly propelling a stream of abrasive material against it. A blast cabinet is essentially a closed loop system that allows the operator to blast the part and recycle the abrasive.

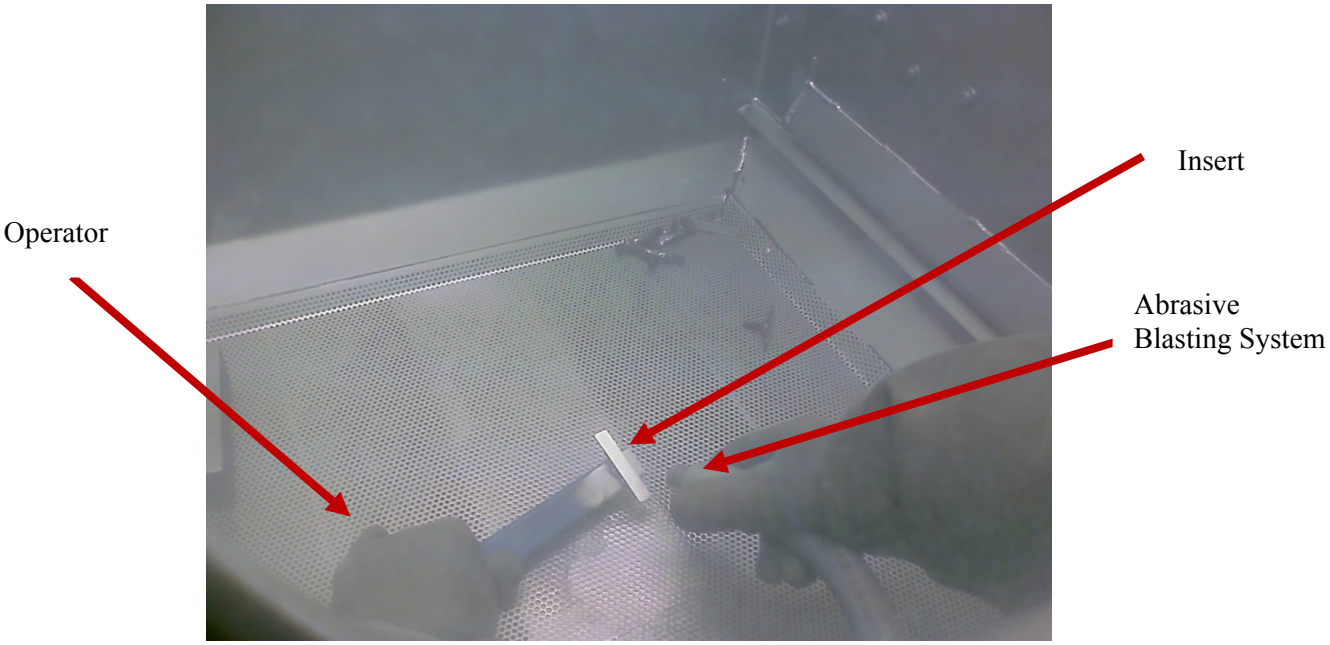


**Figure 7-5: Different Parts of Blasting Machine**

A typical blast cabinet consists of four components; the containment (cabinet), the abrasive blasting system, the abrasive recycling system and the dust collection. The operator blasts the parts from the outside of the cabinet by placing his arms in gloves attached to glove holes on the cabinet, viewing the part through a view window and, typically, turning the blast on and off using a foot pedal or treadle.(Figure 6.5)

After the Blasting Process finished, inserts are ready to bond to the Sample as it is shown in Figure 6.6.

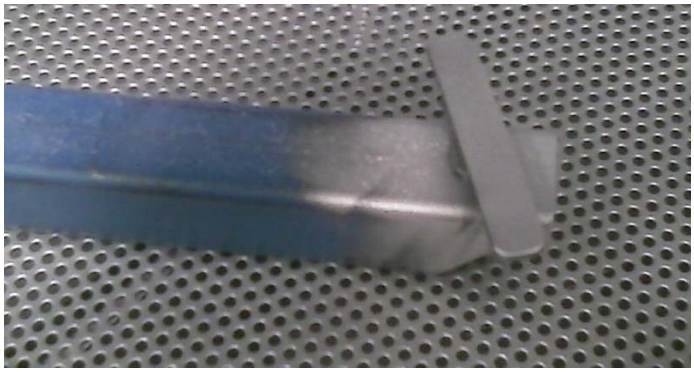

**Figure 7-6: Cleaned and Prepared Sample**

## 6.2.2.3. Samples Surface Preparation

In the previous section, it was described how the surfaces of inserts are prepared. On the other hand, Samples surface should be cleaned from dust and prepared to make the roughness of the surface normal. Figures 6.7 show the process of surface preparation for Carbon/Epoxy beams.

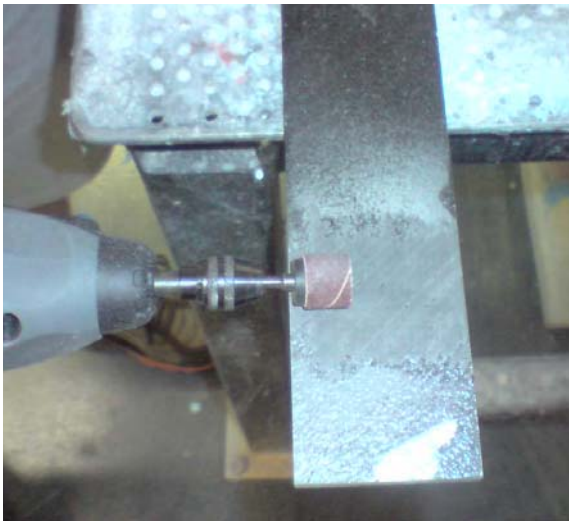

**Figure 7-7: Preparing the Sample**

After this step, both bonding surfaces of the beam are cleaned using UN1090 Acetone. A plunger is filled with Acetone and a tissue is moistened with that to clean the surface of the beam (Figure 6.8)


**Figure 7-8: Cleaning Process with UN1090 Acetone**

## 6.2.2.4. Attachment

After the previous steps, both samples and Inserts are ready for the next step which is fabricating and affixing inserts onto the beam using aerospace grade epoxy adhesive. Aerospace grade epoxy Adhesive has a wide range of application in Composite field as it is strong and easy to cure. It is generally made of two parts; Glue and Hardener. In our project, we mix 3

Units (2.4 grams) of Araldite® 420 A with 1 Unit (0.8 grams) of Catalyst® as it is shown in Figure 5.9 to make the Adhesive (Figure 6.9).

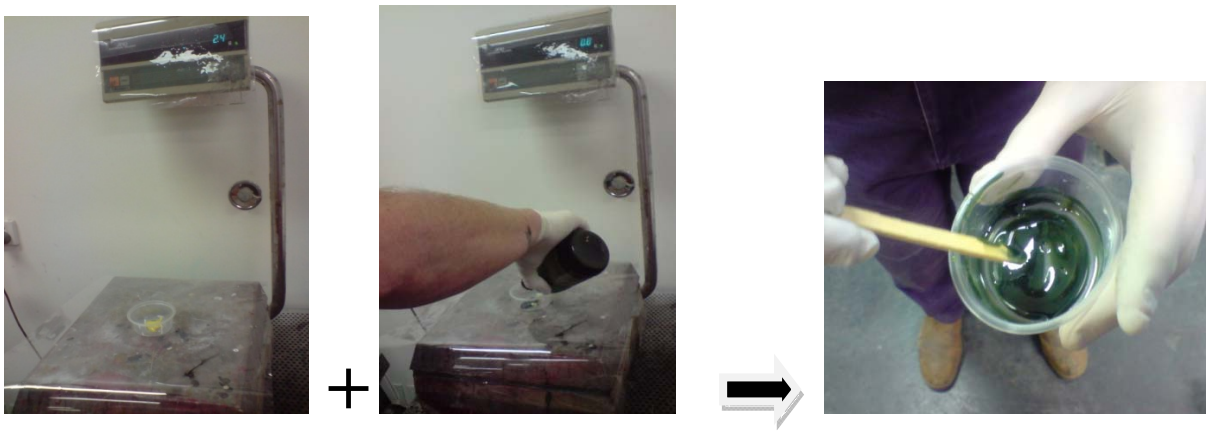

(a) 2.4 grams of Araldite 420 A (b) 0.8 grams of Catalyst (c) Aerospace grade epoxy adhesive

**Figure 7-9: Mixing Adhesive**

After the previous step, we are ready to bond the inserts onto the samples. As it is mentioned before, the inserts are bonded above the location of the delamination, hence the bonding position on the samples as well as inserts surface are covered with the glue and bonded together (Figure 6.10). A clip is used to fix them together until the glue became strong enough to place in the curing Chamber. (Figure 6.11)

**Figure 7-10: Covering Surface of inserts and Samples with Glue**

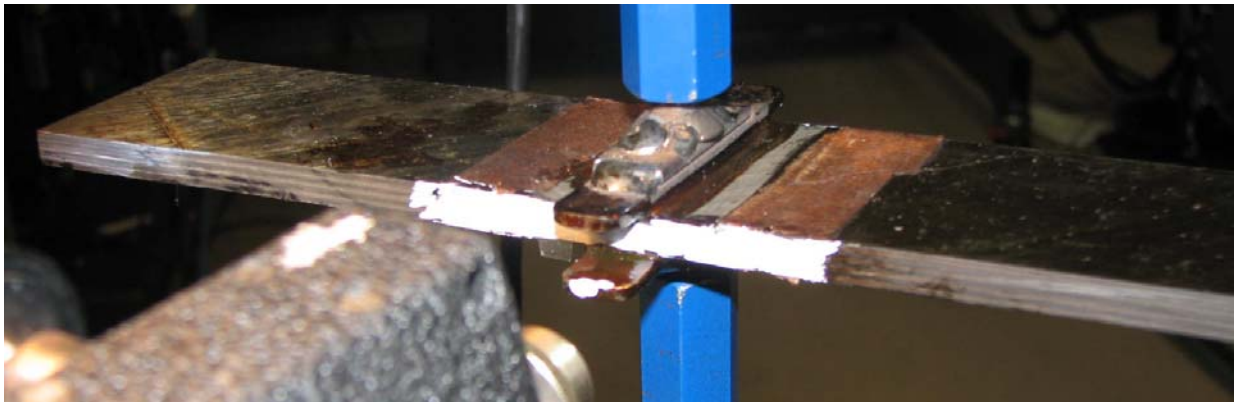

**Figure 7-11: Bonding the Insert to the Sample**

## 6.2.3. Curing and Machining

Now, the sample is ready for the Curing Process. One of the advantages of epoxy glue is its easiness to cure. In fact, it is even possible to cure it at room temperature. However, it is recommended to cure the sample with a Curing Oven in 100°C and for 1 hour (Figure 6.12). After this time, the sample was left in the oven to decrease the temperature gently and become stronger.

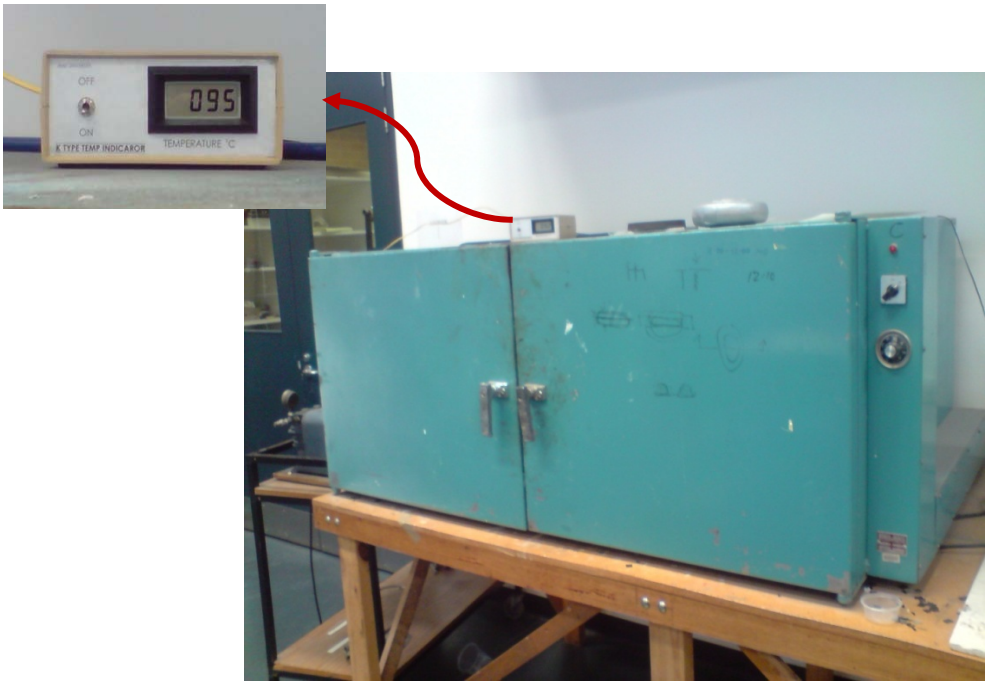


**Figure 7-12: Curing Oven**

By finishing the Curing Process, the sample is ready to start the test. It was a main aim in the whole manufacture and preparing process to make the sample as accurate as possible to observe better results.

## 6.3. Conclusion

This chapter is proposed the process of manufacturing the samples need for fatigue crack propagation test. First, inserts were manufactured and blasted using Blasting Machine to fix the samples to the testing machine. Then these inserts were attached to the samples using Aerospace grade epoxy Adhesive. As the load should be applied above the delamination point in damaged samples, the locations of the embedded delamination were highlighted under the microscope and inserts were attached there. It is also necessary that the surface of the samples were well prepared to have stronger joints and better results.

Finally, the prepared samples with attached inserts were cured in 100°C for 1 hour using Curing Oven and leave samples after while to cool down and prepare for experiments.

# CHAPTER 7

# Fatigue Propagation Test on Carbon/Epoxy Beams

## 7.1. Introduction

Fatigue delamination in brittle-matrix composite laminates is usually accompanied by localized damage accumulation in the form of matrix micro cracking and fiber deboning, as shown schematically in Figure 7.1 (after Friedrich). Process zone forms at the tip of a steadily propagating crack. The damage in this zone affects the energy release rate, stress distribution in the crack tip vicinity, and crack growth rate, leading to a complex interaction between the macro crack and micro cracks (Bolotin, V. V. 1999). In analytical models a common simplifying assumption is the replacement of the actual micro crack field by an equivalent continuum damage measure of tensorial or scalar nature. Further, a damage rate equation is introduced to model the damage accumulation. As it was described in Jun Zhao et al the crack advancement condition relates to the damage measure or a certain function of it (Bolotin, V. V. 1999) reaching a critical value at the crack tip.

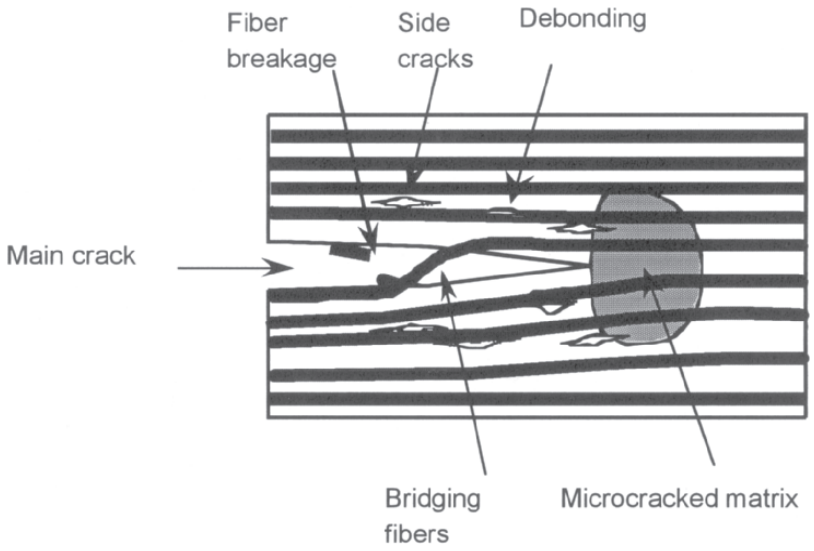


**Figure 8-1: Schematic view of a delamination (Mehdizadeh *et al.* 2009)**

The effect of the process zone on the stress distribution in an elastic material is accounted for by means of various complexities. In Reference, a scalar damage parameter is incorporated in the constitutive material relations. In Reference, it is assumed that the damage affects stress distribution in the crack tip vicinity only by altering the crack tip radius. We follow a simple assumption made in Reference, that the stress in the crack plane forms a plateau within the process zone as shown schematically in Figure 7.2. Consider an interlaminar crack subjected to mode I cyclic loading characterized by maximum stress intensity factor *KI*. For brittle matrix laminates plasticity effects can be neglected, and the stress within the process zone taken proportional to the SIF. All fiber bridging effects, if present, are to be incorporated in the crack tip stress intensity factor by suitably reducing the applied SIF. It is reasonable to choose the proportionality factor as the ratio of the interlaminar strength and fracture toughness.

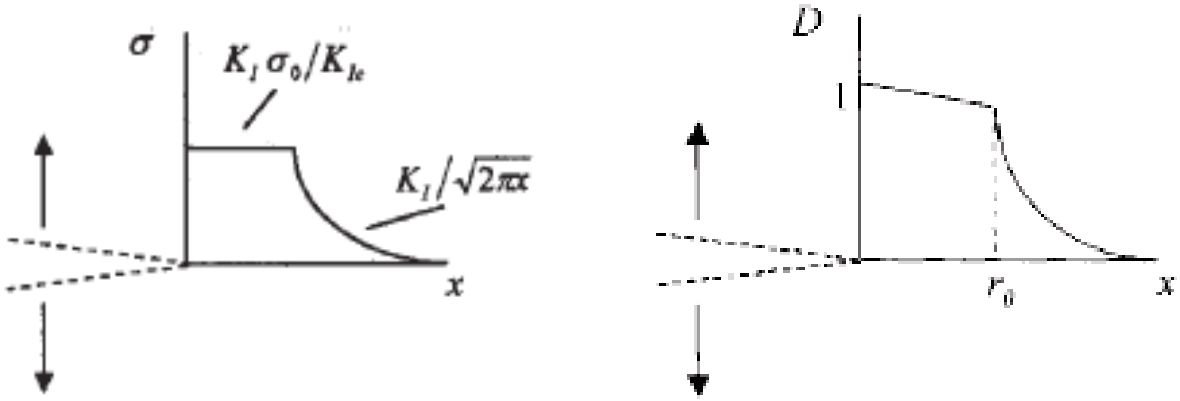


(a) (b)

**Figure 8-2: The assumed stress distribution in the crack plane (a) and the resulting damage distribution (b).**

Thus, when the applied stress intensity factor becomes equal to fracture toughness, the stress in the process zone becomes equal to the interlaminar strength, so that fracture mechanics and strength of materials failure criteria are met simultaneously. Finally, the stress distribution ahead of the crack is expressed as below (7-1):

$$\sigma(x) = \begin{cases} k_1\sigma_s/k_{1c}, & x < r_0 \\ k_1/\sqrt{2\pi x}, & x \geq r_0 \end{cases} \qquad (7\text{-}1)$$

Where $r_0 = (K_{Ic}/\sigma_s)^2/2\pi$, $K_{Ic}$ is fracture toughness, and $\sigma s$ is interlaminar static tensile strength. As it was described before, the method we use for fatigue crack propagation is based on ASTM E399-90 (1997) Standard. Therefore the principles of this standard should be applied. A pure theoretical analysis based on this standard is done elsewhere by another member of this

research project, Krishna Oruganti. However, the baselines and final results will be described below.

## 7.2. Pulling Test Results

The sample for the pulling test (Figure 7.3) was prepared, bonded and cured similar to the main sample and common inserts are applied. Initial experimentation was conducted on a sample with a delamination (damaged) to find out the maximum load based on ASTM E399-90 (1997) standard. A series of experiments are induced by other members of this research project on carbon/epoxy beams with delamination inside based on pulling test to establish the maximum load to apply in actual fatigue propagation test. In fact, the maximum load is needed to calculate the load ranges to be applied on samples and the number of Load cycles.

**Figure 8-3: Prepared Sample for Pulling Test**

An INSTRON Pulling Machine is used for this test by bonding the sample to JARS of the machine and pulling it up to Rupture point. A PC connected to the machine produced the Load-Extension graphs of the experiment. It was observed that the rupture started at the location of delamination. Once the sample ruptured, the machine automatically stopped the experiment. The cracked sample is shown in Figure 7.4.

**Figure 8-4: The cracked sample after pulling test**

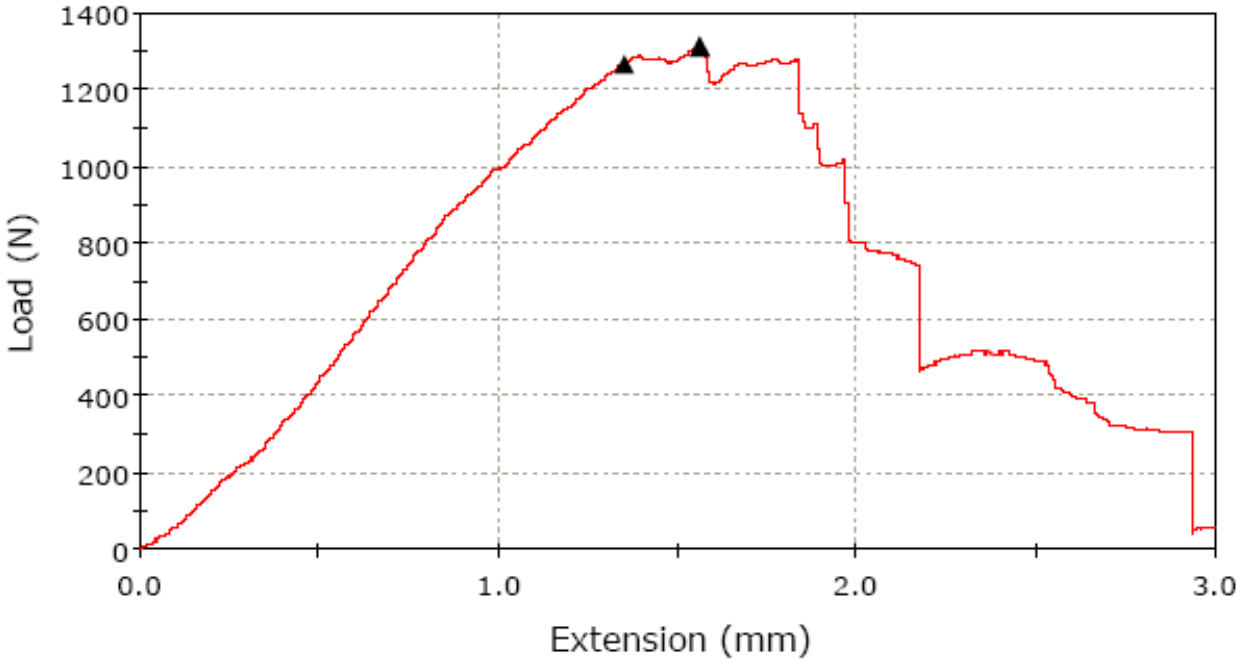


**Figure 8-5: Pulling Test Result**

As it can be seen in Figure 7.5, the maximum load occurred at 1311.95 (N) which is considerably less than the maximum load for the sample without defect. All the information gathered from the experiment is shown in Table 7.1; it shows the Tensile Stress at Maximum Load and Break Point.

**Table 8-1: Pulling Test Results**

| | Specimen label | Maximum Load (N) | Tensile stress at Maximum Load (MPa) | Tensile strain at Maximum Load (%) | Load at Break (Standard) (N) | Tensile stress at Break (Standard) (MPa) | Tensile strain at Break (Standard) (%) |
|---|---|---|---|---|---|---|---|
| 1 | #2 | 1311.95 | 16.70 | -34.38 | 52.94 | 0.67 | -34.37 |
| Minimum | | 1311.95 | 16.70 | -34.38 | 52.94 | 0.67 | -34.37 |
| Coefficient of Variation | | ----- | ----- | ----- | ----- | ----- | ----- |
| Maximum | | 1311.95 | 16.70 | -34.38 | 52.94 | 0.67 | -34.37 |
| Mean | | 1311.95 | 16.70 | -34.38 | 52.94 | 0.67 | -34.37 |
| Median | | 1311.95 | 16.70 | -34.38 | 52.94 | 0.67 | -34.37 |
| Range | | 0.00 | 0.00 | 0.00 | 0.00 | 0.00 | 0.00 |
| Mean + 1 SD | | ----- | ----- | ----- | ----- | ----- | ----- |
| Mean - 1 SD | | ----- | ----- | ----- | ----- | ----- | ----- |
| Standard Deviation | | ----- | ----- | ----- | ----- | ----- | ----- |

According to the graph, the trend is quite linear from 0-200 which could be considered as the beginning load range for fatigue test. This test also confirmed that the extension in actual sample will be started at the location of delamination.

## 7.2. Installation and Setup

The Embedded delamination was extended using a Stress intensity factor (K) - based fatigue crack growth procedure. A test rig was set up where inserts were fabricated to the carbon/epoxy beams. The surface of the samples with the defect embedded within were prepared as it was described in last section and mounted onto an INSTRON machine under displacement control using inserts fabricated and affixed onto the beam using aerospace grade epoxy adhesive. The most important challenge in this experiment would be how to control the amount of Load-Displacement to get the smooth and in-line with delamination extension in the sample.

In order to do that, two connectors are designed as it is shown in Figure 7.6 to fix the inserts, which are bonded at the position of embedded delamination to the sample, to the INSTRON Fatigue test machine JARS.

**Figure 8-6: Connectors**

The inserts are screwed into the connectors and connectors are fixed at the upper and lower JARS of INSTRON Machine (Figure 7.7). The next step is to bond the sample to INSTRON Fatigue Test Machine and place a Microscope in front of the Delamination Location which is highlighted with a white pen to observe the propagation. A study light is used for lightening the experiment point for better observation. The experiment Installation is shown in Figure 7.8.

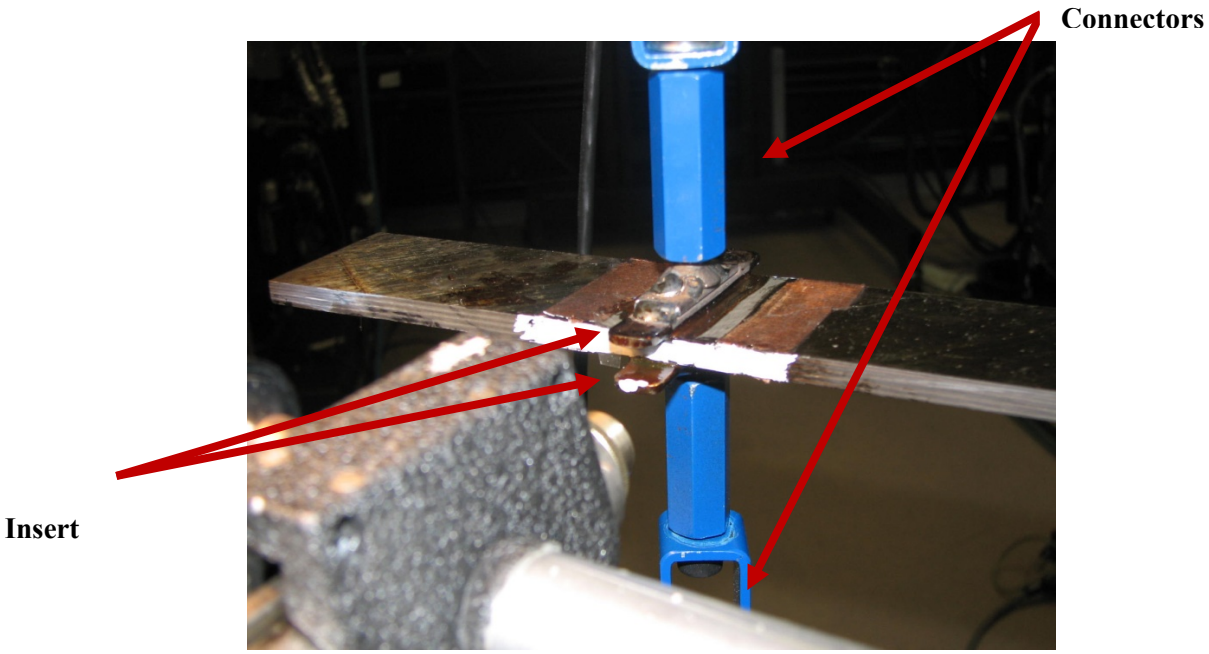


**Figure 8-7: Sample Installation**

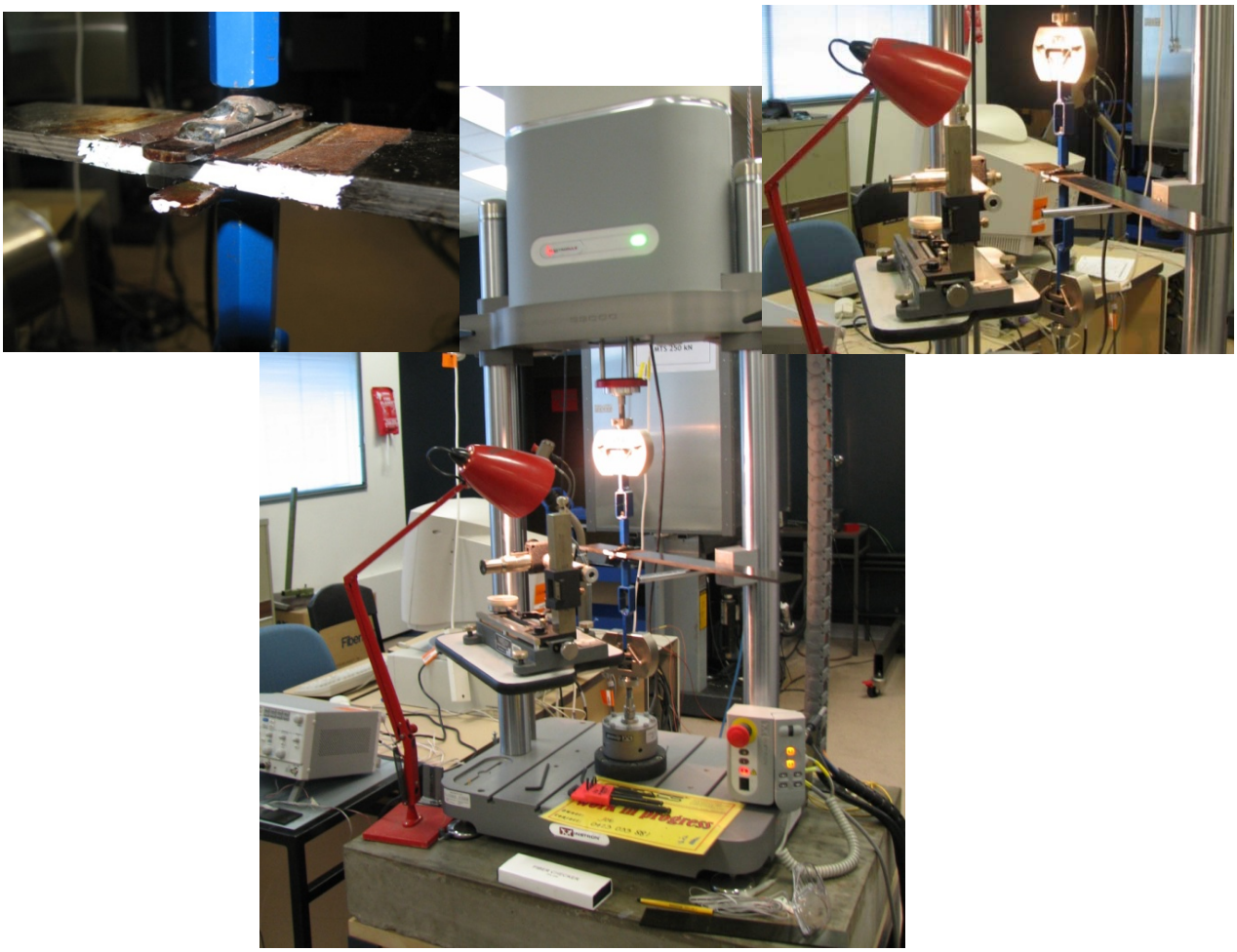

**Figure 8-8: Experiment Setup**

The arrangement shown in Figure 7.8 attempted to induce a near mode 1 opening mode of failure. In reality however, because of inadvertent minute misalignments of the pulling tabs, a mixed mode 1 and 2 might have been induced. The consequence of this might be a slower crack growth rate and is therefore considered a minor consequence.

## 7.3. Applying Load Cycles

After we installed the sample and setup the experiment, it is possible to start the experiment. A PC which is connected to the INSTRON could control the test in terms of Load Cycles, Maximum Load, and Maximum Displacement etc. However it is vital to choose an appropriate controlling factor for the duration of the experiment. In other words, as it is the first time that the fatigue crack extension test is applied on Carbon/Epoxy composite beams, we need to control and supervise the test to make sure that the extension is smooth and along delamination extend. Once there is a dramatic increase in the amount of Maximum Load, it might be a sign for crack extension. Furthermore, it would be a change in designated load range as the experiment continues due to the effect of cyclic load on the sample as well as embedded

delamination. Therefore, load couldn`t be a suitable controlling factor and another factor is needed to control the experiment and load range. For this case, displacement is selected as a controlling factor. To ensure that the propagation will be as smooth as possible and it won`t lead to sample breakage, the test is started with the safest load range of 10-100 (N) for 1000 cycles according to the ASTM Standard as well as pulling test results. The Load/Cycles which applied are shown in Table 7.2.

**Table 8-2: Load/Cycle values for Fatigue Crack Propagation**

| | Number of Cycles | Min Load | Max Load |
|---|---|---|---|
| **1** | 1000 | 10 | 100 |
| **2** | 1000 | 15 | 150 |
| **3** | 3000 | 20 | 200 |
| **4** | 6000 | 25 | 250 |
| **5** | 10000 | 30 | 300 |
| **6** | 10000 | 35 | 350 |
| **7** | 10000 | 40 | 400 |
| **8** | 10000 | 45 | 450 |
| **9** | 3500 | 45 | 450 |

As an example, the first row of the table indicates the periodic load applied between 10(N) and 100(N) for 1000 cycles and observed the changes in sample by checking the changes in Maximum and Minimum Load Magnitude in the PC as well as via microscope. As it wasn't enough excitation for the sample to be propagated in this load range, using pulling test results and ASTM Equations, we selected a new range of 10-100 (N) for 1000 cycles.
As previously mentioned, the controlling factor in this experiment is Displacement which is calculated by using the information observed from PC.

The calculated displacement ranges which are used to control the experiment are shown in Table 7.3.

**Table 8-3: Displacement/Cycle values for Fatigue Crack Propagation**

| | Number of Cycles | Max Displacement | Min Displacement |
|---|---|---|---|
| **1** | 1000 | 0.293 | 0.07 |
| **2** | 1000 | 0.238 | 0.076 |
| **3** | 2000 | 0.273 | 0.111 |
| **4** | 2000 | 0.278 | 0.078 |
| **5** | 2000 | 0.293 | 0.07 |
| **6** | 3000 | 0.3525 | 0.078 |
| **7** | 10000 | 0.238 | 0.076 |
| **8** | 10000 | 0.381 | 0.111 |
| **9** | 3500 | 0.3865 | 0.107 |

After 21000 cycles, the first sign of crack opening was observed. However, there wasn`t a considerable crack extension in the sample by looking at the load changes as well as microscopic view. The delamination status at the time of crack opening is shown in Figure 7.9.

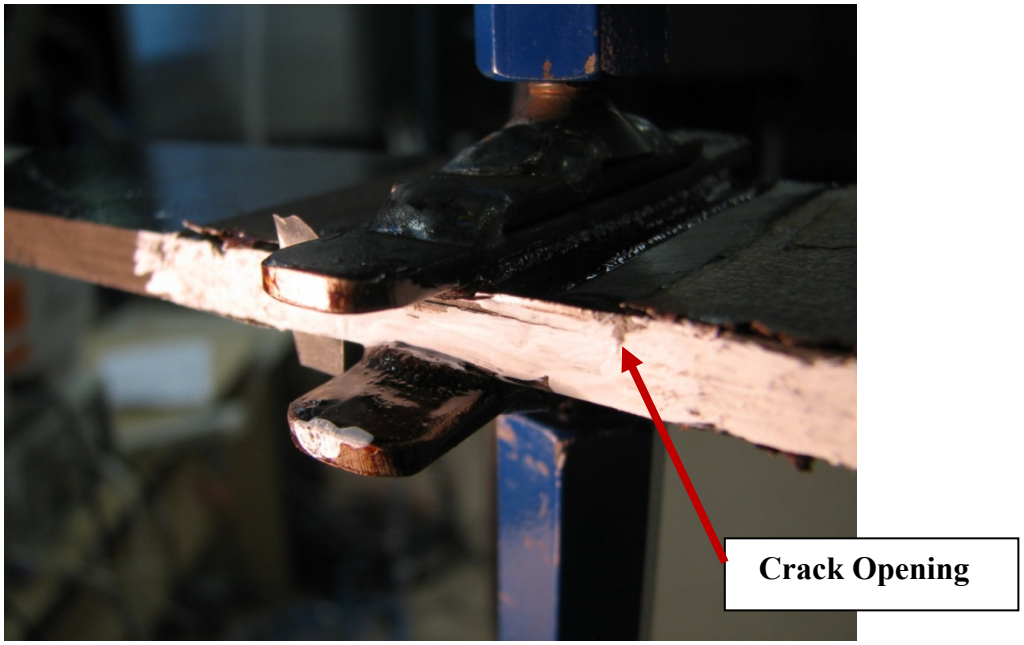


**Figure 8-9: Crack Opening at the location of delamination**

At the final stage, the machine was set for 10000 cycles for the designated displacement range, but after 3500 cycles a dramatic decrease in the maximum load was observed down to 145 (N) and the crack started and grow from both sides.

## 7.4. Conclusion

The prepared samples were then tested for their maximum failure load on an INSTRON® pulling test machine as shown in order to determine the maximum load of the healthy and damaged samples. This value is needed to calculate the fatigue load based on ASTM E399-90 Standard. A computer connected to the machine plotted the increasing load and the extension of the sample up to the failure. The maximum load for defect sample occurred at 1311.95 (N) which is considerably less than the maximum load for the sample without a defect.

A load range of 200- 400 N was chosen for fatigue testing from the linear range within the load and extension curve obtained from the INSTRON machine. The $K_{max}$ chosen to facilitate fatigue growth should be far lower compared to the anticipated $K_{Ic}$ as per ASTM E399-90 (1997) standard. Then, the sample was fixed on the INSTRON fatigue test machine and a range of Cycle/Load values within the designated load range were applied to extend the crack. The key point in this experiment was the controlling factor which was implemented under displacement control.

The crack was extended under control from both sides with the total length of 4 mm and the table of load/cycle values were obtained. In the next chapter these results will be analysed to extract the damage status.

# CHAPTER 8

# Curvature Mode Shapes of Propagated Samples

## 8.1. Introduction

A crack or flaw within a structure reduces the stiffness and increases the damping in the structure. Such a reduction in stiffness is linked with a decrease in the natural frequency and an alteration of the modes of vibration of the structure. Various workers have used one or more of the above characteristics to detect and locate a crack. Systematic change in the first mode shape with respect to the damage location within a cantilever beam was observed during the analysis of various mode shapes. They established their findings using finite element analysis to obtain the natural frequencies and the mode shapes of a damaged structure. From changes in frequency they could determine the presence of crack or damage in a structure. Several researchers have explored the utility of displacement mode shapes and curvature mode shapes in damage detection [Hamey, *et al.* 2004]. The difference in the displacement and curvature mode shapes between the intact and the damaged specimen is utilized to detect the location of the defect. The difference in the signal between the healthy and defect sample would potentially indicate the presence and location of the damage. A difference algorithm was used to estimate the change in displacement between the healthy and the defective sample. The resultant value (δ) described below highlighted the change in signatures.

$$\sigma = \frac{|x_H - x_D|}{x_H} \qquad (8\text{-}1)$$

Where, $x_H$ - Magnitude of displacement of a point on the reference specimen acquired. $x_D$ - Magnitude of displacement of the same point over specimen under test (defect sample). $\delta$ - Ratio of absolute difference of displacement magnitudes between Healthy and Defect specimen to the reference displacement magnitude from a healthy specimen. $\delta$ was computed for modes 1, 2 and 3 respectively. Lestari *et al*. 2005 used few lower order modes to identify damage

location based on the difference between the acquired data of healthy and damaged structures.. Lower order modes were preferred in the damage assessment as the nodal points of damaged structures at high modes may shift significantly from the original undamaged case. This could generate misleading results. The resultant curve could be used to estimate the approximate damage size and location within the specimen under test. Only results from mode 1 were applicable for damage assessment as higher modes produced misleading peaks. Other researchers have studied the systematic change in the first mode shape with respect to damage identification [Yan *et al.* 2006]. From the resultant displacement mode shapes acquired for mode 1 of sample 1 before and after crack propagation, the damage zone is estimated approximately as 36.67 mm and 57.84 mm respectively.

## 8.2. Laser Vibrometer Results

Using POLYTEC Laser Vibrometer as it was described in Chapter 4, the FRF Domain and displacement mode shapes for the sample before propagation and after propagation are gathered. The test was done on sample 1 before and after propagation with same setup and modification in order to make the final comparison between them as accurate as possible. The process of experiment installation and data acquisition is the same as what is described in Chapter 4. The FRF Domains as well as first four Displacement Mode Shapes are gathered using Laser Vibrometer. Then, first four Curvature Mode Shapes which are the second derivatives of Displacement Mode Shapes calculated using Central Difference Approximation as it was explained in Introduction as well as Chapter 4.

### 8.2.1. FRF Domain

It was discussed in Chapter 4 that the application of frequency responses for global damage detection has many considerable advantages as it is very sensitive to interference especially at low order modes. Examples of interferences include fiber misalignment during manufacturing, introduction of non-negligible mass by sensors, and simulated approximate boundary conditions that prompt the largest error in the frequency measurement (Kessler *et al.*, 2002). Nevertheless, the natural frequency can be used as an early warning system of global structural condition.

It was also mentioned that the location of the defect can be estimated with the percentage of change in the natural frequencies of intact and damaged structures which depend on the

position of the defect for a particular mode of vibration. The magnitudes of displacement through the range of frequencies for sample 1 before and after propagation were displayed in Figures 7.1 and 7.2. For better comparison, the changes in different graphs were highlighted for further discussions. As it can be seen from the figures, there are four highlighted areas in each graph which are the selected peaks to calculate four displacement mode shapes of each sample. These graphs are made by the PC connected to the shaker to save data.

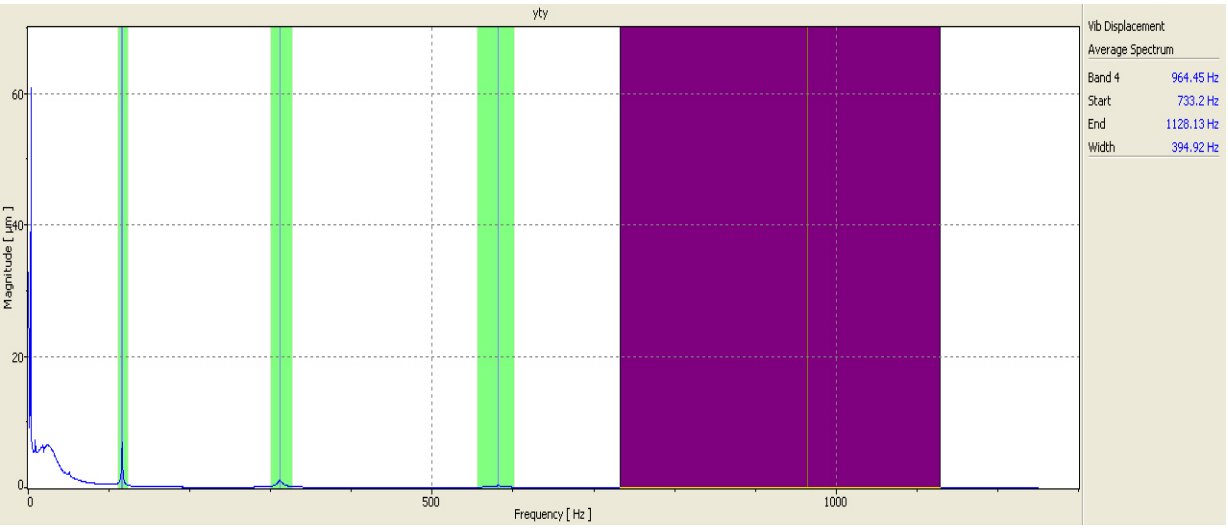


**Figure 8-9-1: FRF Domain of Sample 1 before Propagation**

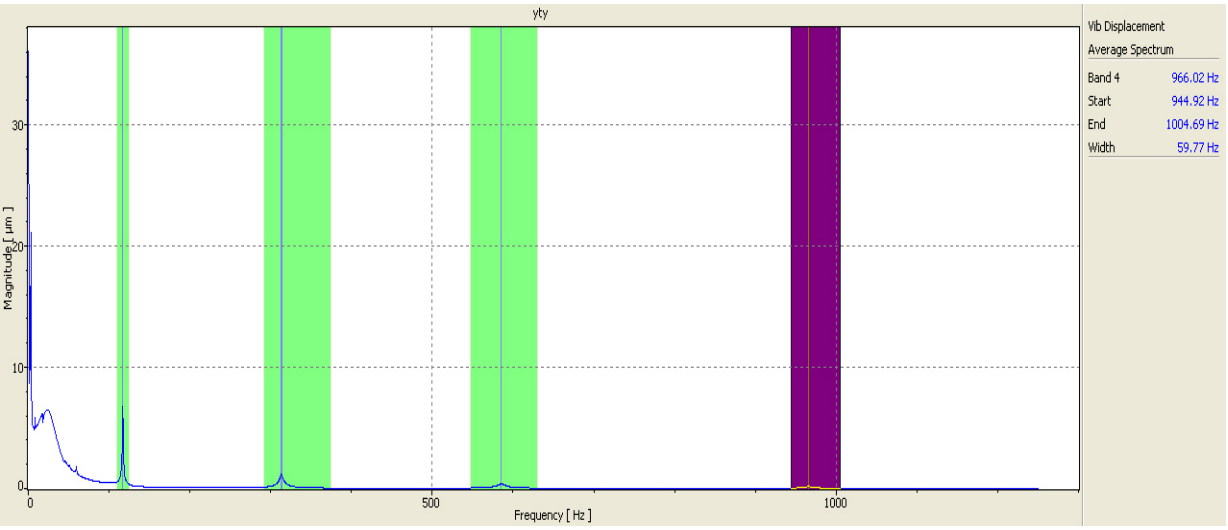


**Figure 8-9-2: FRF Domain of Sample 1 after Propagation**

It can be seen from the graphs that there are some differences at the location of peaks (Shift) as well as magnitudes of peak points especially in peak number 1 which could be considered as an initial sign of crack propagation. In fact, by comparing above graphs, we can propose the propagation of the crack as well as rough location of this extension in the sample. However, Curvature Mode Shapes are needed to determine the exact damage status.

## 8.2.2. Displacement Mode Shapes

By selecting the regional peaks of ″displacement magnitude/frequency″ and calculating the maximum peak in each region and looking at the graphical spectrum of each sample at peak points, the displacement mode shapes of samples obtained. However, some of the selected peaks are not acceptable due to the serious effect of noise on the related spectrum of these peaks. All the gathered mode shapes 1, 2, 3 and 4 for each sample 1 before and after propagation were shown in Figures 7.3 and 7.4.

For each status of Sample 1, the 4 highest peaks in the Frequency-Displacement Magnitude were gathered in Table 7.1 and 7.2. Then at each peak, the displacement mode shape was plotted as below.

**Table 9-1: Selected peaks in Displacement –- Frequency Graph for Sample 1 Before Propagation**

| Peak no. | Frequency(Hz) | Displacement Magnitude(µm) |
|---|---|---|
| 1 | 111.3 | 14.250 |
| 2 | 278.1 | 2.922 |
| 3 | 540 | 0.0678 |
| 4 | 1005 | 0.109 |

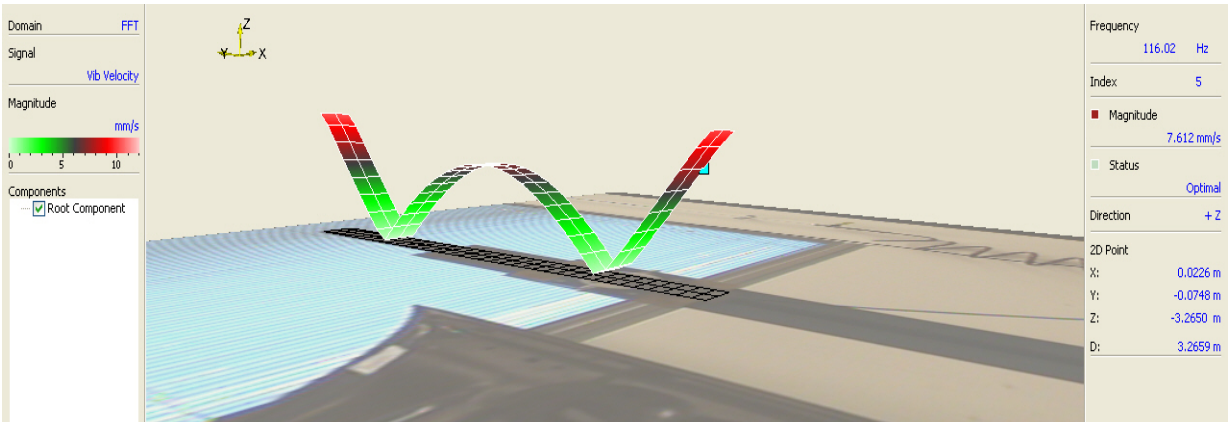


**Figure 9-3: Displacement Mode 1 of Sample 1 before Propagation**

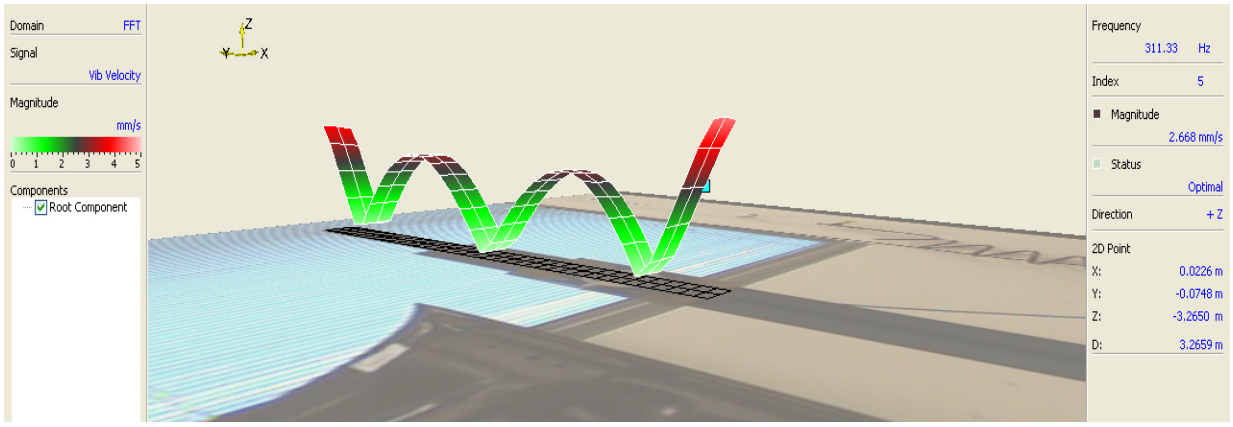


**Figure 9-4: Displacement Mode 2 of Sample 1 before Propagation**

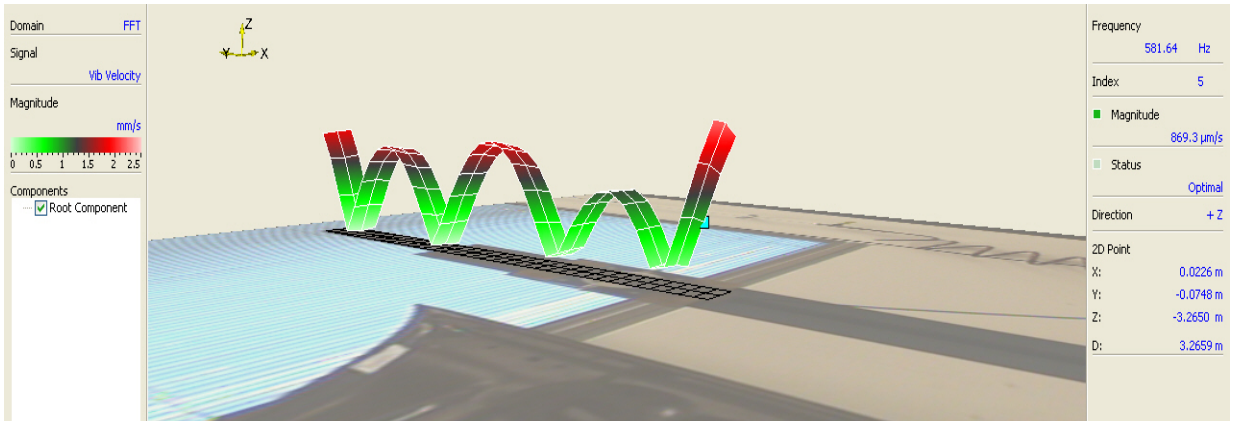


**Figure 9-5: Displacement Mode 3 of Sample 1 before Propagation**

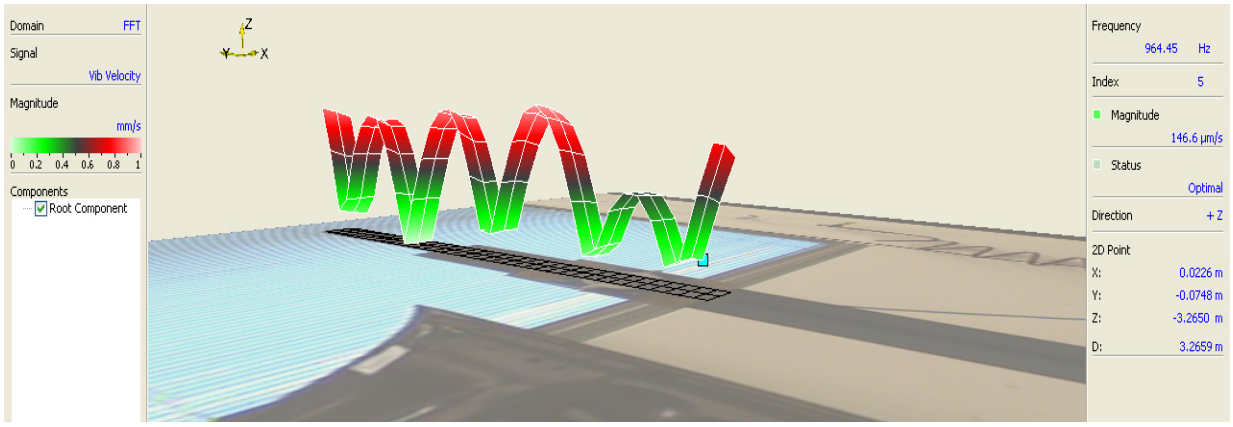


**Figure 9-6: Displacement Mode 4 of Sample 1 before propagation**

Table 8-2 is shown the selected peaks to get displacement mode shapes for sample 1 after propagation.

**Table 9-2: Selected peaks in Displacement –- Frequency Graph for Sample 1 After Propagation**

| Peak no. | Frequency(Hz) | Displacement Magnitude(µm) |
|---|---|---|
| 1 | 116.8 | 6.870 |
| 2 | 311.33 | 0.395 |
| 3 | 585.55 | 0.247 |
| 4 | 964.45 | 0.054 |

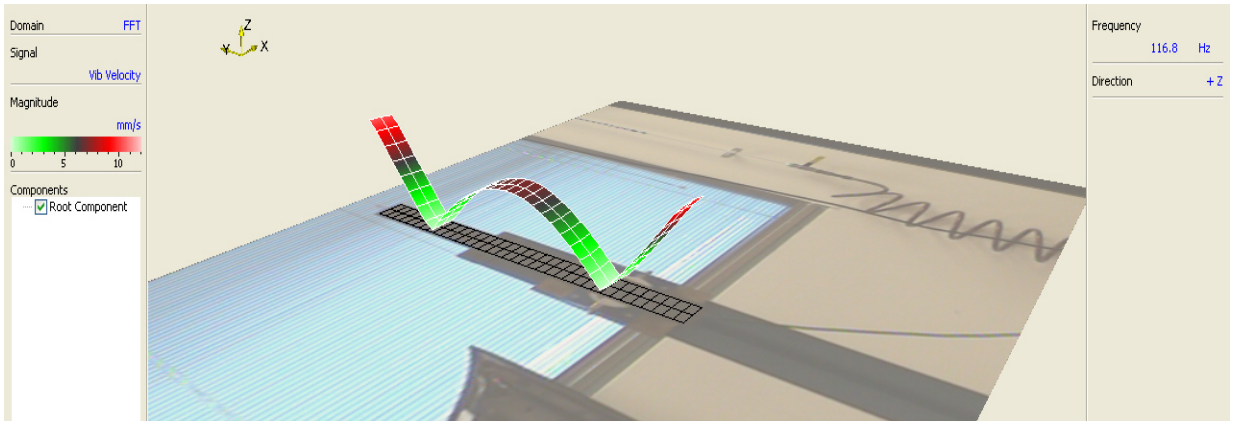


**Figure 9-7: Displacement Mode 1 of Sample after Propagation**

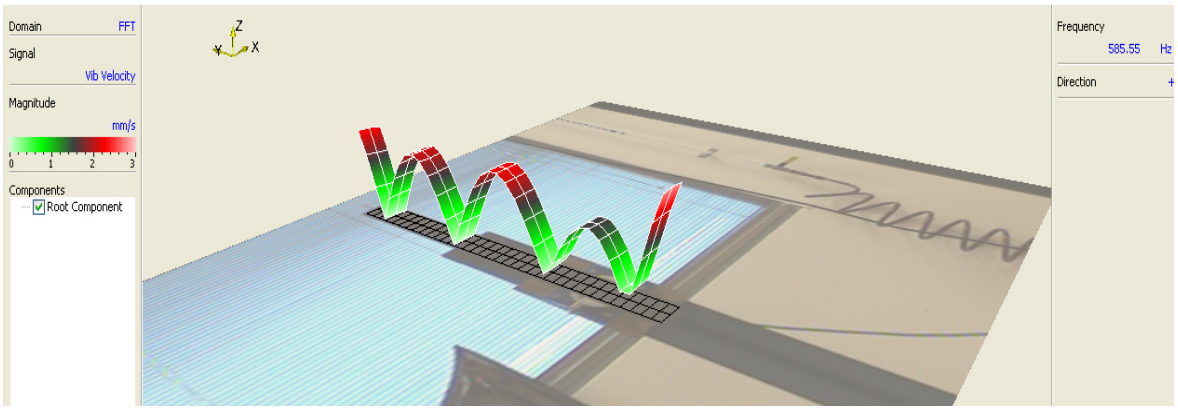


**Figure 9-8: Displacement Mode 3 of Sample after Propagation**

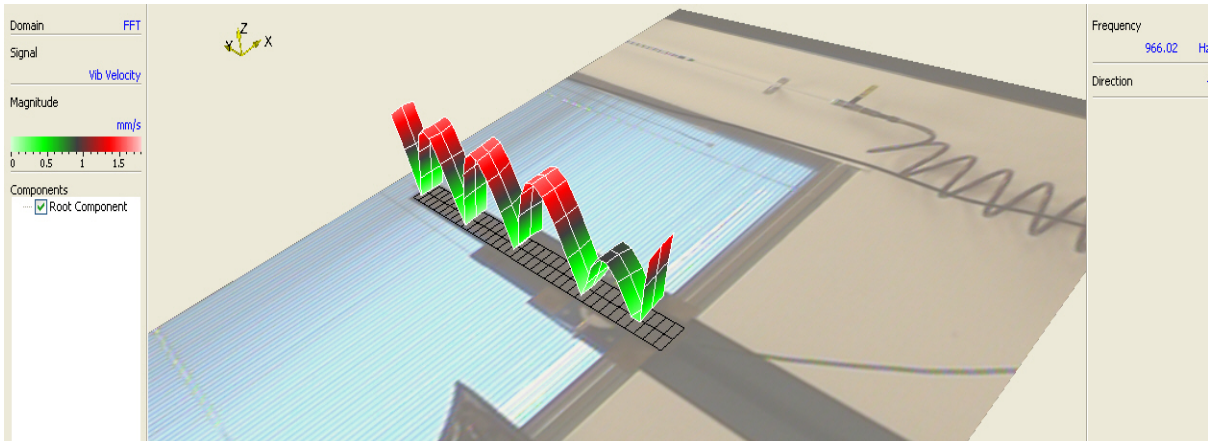


**Figure 9-9: Displacement Mode 4 of Sample after Propagation**

## 8.3. Curvature Mode Shapes

Numerous workers have explored the use of curvature mode shapes in damage detection [Hamey *et al.* 2004]. The difference in the curvature mode shapes between the intact and the damaged specimen is utilized to detect the location of the defect.

The Curvature ( ) at a point is given by:

$$\phi = \frac{M}{EI} \qquad (8\text{-}2)$$

Where,

$\phi$ is the curvature at a section, $M$ is the bending moment at the section, E is the modulus of elasticity and I is the second moment of the cross-sectional area. Curvature mode shape can be obtained by using piezoelectric sensors mounted on the sample [20] or by the application of a numerical algorithm to convert displacement mode shapes to curvature mode shapes. Curvature mode shape is the second derivative of a displacement mode shape. By using the Central Difference Approximation (CDA) technique over displacement mode shapes; curvature mode shapes can be generated. Equation below estimates the curvature at a point using the central difference approximation method.

$$\phi_i = \left(\frac{x_1 + x_3 - 2x_1}{h^2}\right) \qquad (8\text{-}3)$$

Where,

$\phi$ Is the curvature at a section or nodal point, $x_1, x_2, x_3$ – the magnitudes of displacements at nodal points 1, 2 and 3 respectively and *h* is the distance between 2 consecutive nodal points.

Using the central difference approximation method the curvatures for the samples were calculated from the displacement data obtained from the PSV-400 Laser Vibrometer System. A subtracting algorithm was employed to compute the absolute difference between the healthy and defect curvature magnitudes both before and after crack propagation. The resultant curvature plots indicate the presence and location of damage. As observed from the curvature plots for individual samples shown in Figure 11 and Figure 12, only Mode 1 was analysed to indicate the presence of damage within the specimen as higher modes produce results which were less convincing – probably due to an increasing Signal-to-Noise Ratio (SNR). From these resultant curves in Figures 11 and 12, using the subtracting algorithm, the sudden spike in magnitudes extends between points 11 and 15 and 6 and 9. Thus the damage zone is approximately 36.67 mm and 57.84 mm similar to the estimation from displacement mode shapes.

## 8.3.1. Resultant curvature plot

In the final section, displacement mode shapes for sample 1 before and after propagation is presented. However, as it was illustrated in Chapter 4 displacement mode shape by itself won`t be enough for damage detection due to its weakness in detecting local changes in physical properties. Therefore, Curvature Mode Shapes are calculated for sample 1 before and after propagation as well as sample 3 as healthy sample without embedded delamination.
As a matter of fact, the best prediction of damage status will be gathered when the Absolute difference between the curvatures of sample before and after propagation is calculated. Therefore, the resultant curvature plots between sample 1 and sample 3 (Healthy Sample) before and after propagation are plotted. These graphs are presented in Figures 8.10 and 8.11.

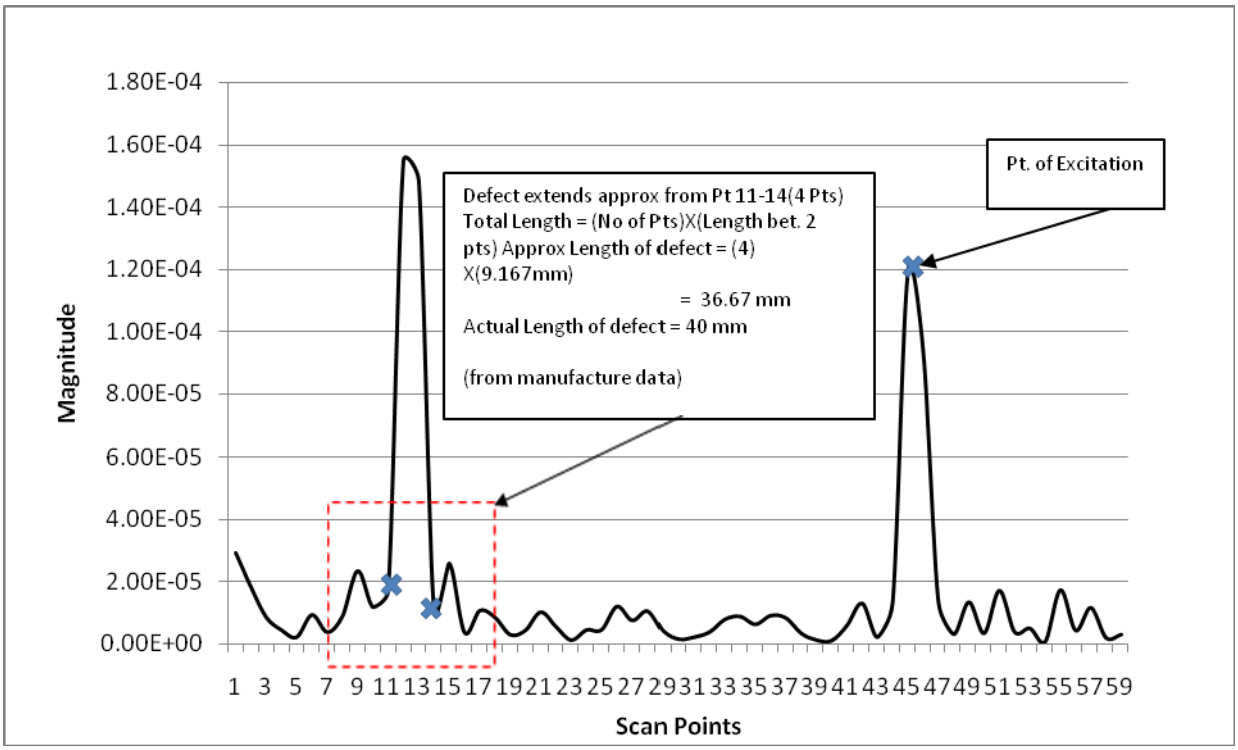


**Figure 9-10: Resultant curvature plot between defect sample #1 and Healthy sample before crack propagation**

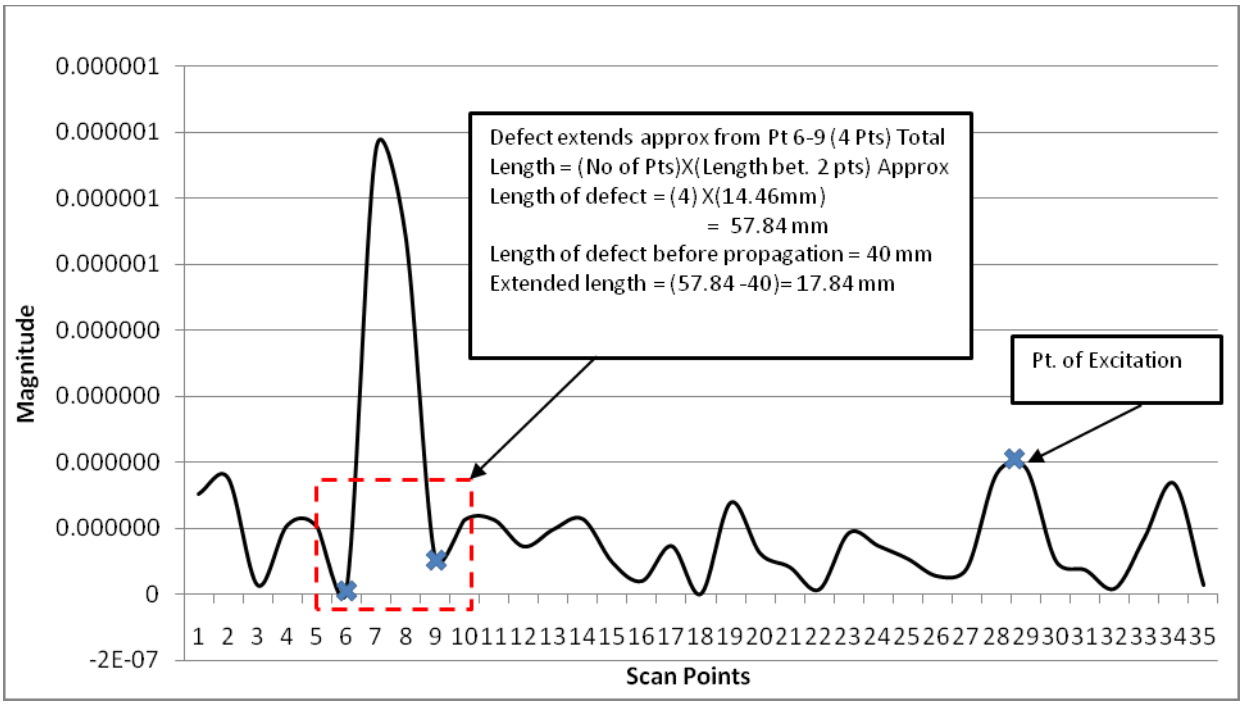


**Figure 9-11: Resultant curvature plot between defect sample #1 and Healthy sample after crack propagation**

## 8.4. Discussion

The damage within the Carbon/Epoxy beams could be identified successfully by both the displacement mode shape analysis as well as curvature mode shape analysis before and after crack propagation using an innovative fatigue-based crack extension process. The detailed stress intensity factor (K) calculations used to determine the optimal fatigue loading for stable crack growth will be discussed in another paper. For the purposes of this paper, a range of 200N to 400N was found to be suitable to extend a 40 mm delamination in an 8 mm thick carbon-epoxy beam in stable and controlled manner. The displacement mode shape, which gives a global snapshot through the frequency domain range, is an effective method for a globalised technique of damage identification, provided the damage is significant relative to the structure being analyses. The curvature mode shape being the derivative of the displacement mode shape is more of a localized technique. In the case examined here however, both the displacement and curvature mode shape analyses were able to identify and quantify the extent of the damage for both the pre- and post-crack extension case.

The size and location of the delamination in one place was successfully identified by both these techniques and validated using the C-scan results as reported by Mehdizadeh *et al.* 2008 a & 2008 b. A denser scanning mesh is employed by the use of the Laser Vibrometer system as compared to a system using a PZT-PVDF system. It can measure the displacement response at individual scan points, thus generating the displacement mode shapes. The present study focuses on the identification of the presence, location, and size of delamination in the laminated composite plates by extracting the modal parameters obtained from the SLV measurement system. In the results presented here, the actual crack growth measurements seen in the side of the specimen measured about 4 mm on either side of the crack, giving a total of about 8 mm. This contrasts with the 17.8 mm extension as determined by the curvature plots from the SLV tests shown in Figure 12 above.

# CHAPTER 9

# Conclusion

## 9.1. Overview

The aim of this research project is to find a damage detection method which could be used to determine the damage status (location and severity) of a composite structure by applying the dynamic responses of the structure to the excitations.

## 9.2. Preferred Damage Detection Method

A comprehensive study was conducted on the various types of damage detection methods. The scalability Curvature Mode Shape plays a key role in the developed method. This is mainly due to its local nature and ability to show the location and severity of the damage without further analyses. By using the absolute difference of the curvatures between intact and damaged structures, the damage status was obtained. Also, a series of fatigue crack propagation tests were induced to extend the damage in Carbon/Epoxy beams with a pre-existing embedded delamination under cyclic load.

## 9.3. Outcomes

At first, the FFT Domains of the intact and damaged structures were gathered and displacement mode shapes were obtained. Then, the curvature mode shapes which are the second derivative of displacement mode shape were calculated using the Central Difference Approximation method. Finally, the absolute difference between the curvatures of the intact and damaged structures was extracted to find the damage status.

The highest peak in the graph is the location of the damage and the magnitude was considered as the damage severity. An average accuracy of 90% was observed. Finally, a sample with embedded delamination is prepared and cured for fatigue crack propagation test to validate our developed technique under fatigue conditions. The total extension of 17 mm was observed from the Microscope. Then, by using the Laser Vibrometer, the same principles were applied to calculate the curvature mode shapes and absolute difference between the curvatures of sample 1 before and after propagation were determined. An accuracy of 96% was observed.

## 9.4. Manufacture of Carbon/Epoxy Beams

After the appropriate set up of the system by using Plywood samples, the process of manufacturing Carbon/Epoxy beams started. The specimens were made of carbon fiber and epoxy resins and had a [0/90/±45] lay-up of a total of six layers, with each layer thickness of 1.25mm and a total thickness of 7.5 mm. Each beam specimen has a width of 50 mm and a length of 550 mm. During manufacture, seven Teflon layers were inserted to simulate the delamination in the sample at different levels in the thickness direction and at different locations . Two beams were designed to be undamaged (Healthy samples).

## 9.5. Finite Element Method (FEM) Analysis

The ANSYS Software was applied to model the beams and analyze it under identical conditions as the experiment in order to calculate Displacement mode shapes as well as Curvature mode shapes of beams.

## 9.6. Curvature Mode Shapes Calculation

In order to calculate the curvature mode shapes, three different ways of data gathering were used: Experiments, FEM, and Fatigue Test. The Central Difference Approximation (CDA) was applied for calculations. In the experimental results, frequency responses as well as displacement mode shapes of beams were captured. The curvature mode shapes were then calculated with the CDA method. In the FEM technique, the ANSYS Software was used to analyze and calculate the displacement mode shapes. The curvature mode shapes from these two techniques compared favorably. Finally, in the fatigue test, a prepared sample with an embedded delamination was tested under fatigue conditions to extend the crack. To finish, the curvature mode shapes of the sample before and after the propagation was compared to determine the growth of the damage.

## 9.7. Fatigue Crack Propagation Test.

A technique was satisfactorily developed to advance an embedded delamination without necessarily inducing other modes of damage during the process. This fatigue-based delamination advance procedure enabled a proper comparison of damage sizes within a given damage type or genre.

## 9.8. Future Work

1. In this research project, delamination as one of the more important type of damage is studied. The possible future work would be generalizing the invented technique for other types of damage such as impact, thermally loaded cracks and layer misaligned cracks.

2. Applying the obtained fatigue propagation technique for more complicated structures with multi-cracks.
3. Develop an analytical model to accurately account for damage in a polymeric composite structure, especially in relation to its detection using its structural response.

# References


[1] Abdo, M. A. B. and M. Hori (2002). "A numerical study of structural damage detection using changes in the rotation of mode shapes." Journal of Sound and Vibration **251**(2): 227-239.

[2] Aimmanee, S. (2004). Deformation and force characteristics of laminated piezoelectric actuators. United States -- Virginia, Virginia Polytechnic Institute and State University.

[3] Araujo dos Santos, J. V., H. M. R. Lopes, *et al.* (2006). "Damage localization in laminated composite plates using mode shapes measured by pulsed TV holography." Composite Structures **76**(3): 272-81.

[4] Chang, J., C. Zheng, *et al.* (2006). "The ultrasonic wave propagation in composite material and its characteristic evaluation." Composite Structures **75**(1-4): 451-456.

[5] Chen, J. and F. Xiong (2007). "Curvature mode shapes-based damage identification method." Journal of Wuhan University of Technology (Information & Management Engineering) **29**(3): 99-102.

[6] Crane, R. M. and C. P. Ratcliffe (2007). Structural health monitoring of A 1/2 scale composite corvette hull section subjected to undex loading, Baltimore, MD, United States, Soc. for the Advancement of Material and Process Engineering, Covina, CA 91724-3748, United States.

[7] Edmonds, J., M. S. Resner, *et al.* (2000). Detection of precursor wear debris in lubrication systems. 2000 IEEE Aerospace Conference, Mar 18-25 2000, Big Sky, MT.

[8] Elaldi, F. (2005). An overview for structural health monitoring of composites in aerospace applications, Istanbul, Turkey, IEEE.

[9] Fujimoto, S.-e. and H. Sekine (2007). "Identification of crack and disbond fronts in repaired aircraft structural panels with bonded FRP composite patches." Composite Structures **77**(4): 533-545.

[10] Ghoshal, A., A. Chattopadhyay, *et al.* (2003). "Experimental investigation of damage detection in composite material structures using a laser vibrometer and piezoelectric actuators." Journal of Intelligent Material Systems and Structures **14**(8): 521-37.

[11] Guennam, A. E. and B. M. Luccioni (2006). "FE modelling of a closed box beam with piezoelectric fiber composite patches." Smart Materials and Structures **15**(6): 1605-15.

[12] Hamey, C. S., W. Lestari, *et al.* (2004). Damage Detection of Composite Laminates Using Smart Piezoelectric Materials, League City/Houston, TX, United States, American Society of Civil Engineers, Reston, VA 20191-4400, United States.

[13] Herszberg, I., B. Whittingham, *et al.* (2006). "Disbond detection in adhesively bonded composite structures using vibration signatures." Composite Structures **75**(1-4): 351-63.

[14] Jiang, H., L. Zhang, *et al.* (2007). "Research on finite element optimal design of precision horizontal machining center(MC) based on FDP." China Mechanical Engineering **18**(3): 317-20.

[15] Kang, Y., P.-C. Shen, *et al.* (2007). "Modified determination of fluid resistance for membrane-type restrictors." Industrial Lubrication and Tribology **59**(3): 123-131.

[16] Kesavan, A., M. Deivasigamani, *et al.* (2006). Structural health monitoring of composite T-joints for assessing the integrity of damage zones, San Diego, CA, United States, International Society for Optical Engineering, Bellingham WA, WA 98227-0010, United States.

[17] Kesavan, A., S. John, *et al.* (2008). "Structural health monitoring of composite structures using artificial intelligence protocols." Journal of Intelligent Material Systems and Structures **19**(1): 63-72.

[18] Kim, C.-G., J. Han, *et al.* (2006). "The propagation of Lamb waves in a laminated composite plate with a variable stepped thickness." Composite Structures **76**(4): 388-96.

[19] Lanza Discalea, F., H. Matt, *et al.* (2007). "Health Monitoring of UAV Wing Skin-to-spar Joints using Guided Waves and Macro Fiber Composite Transducers."

[20] Lestari, W. and Q. Pizhong (2005). Experimental investigation of damage detection on composite plates using wave analysis, San Diego, CA, USA, SPIE-Int. Soc. Opt. Eng.

[21] Lestari, W. and P. Qiao (2005). Damage identification for carbon/epoxy laminated composite structures based on wave propagation analysis, Austin, TX, United States, American Inst. Aeronautics and Astronautics Inc., Reston, VA 20191-4344, United States.

[22] Lestari, W., P. Qiao, *et al.* (2007). "Curvature mode shape-based damage assessment of carbon/epoxy composite beams." Journal of Intelligent Material Systems and Structures **18**(3): 189-208.

[23] Li, H. C. H., F. Beck, *et al.* (2006). "Strain-based health assessment of bonded composite repairs." Composite Structures **76**(3): 234-42.

[24] Montalvao, D., N. M. M. Maia, *et al.* (2006). "A review of vibration-based structural health monitoring with special emphasis on composite materials." Shock and Vibration Digest **38**(4): 295-324.

[25] Mouritz, A. P., A. Kousourakis, *et al.* (2006). "Interlaminar properties of polymer laminates containing internal sensor cavities." Composite Structures **75**(1-4): 610-18.

[26] Nag, A., D. R. Mahapatra, *et al.* (2003). Identification of delaminations in composite: structural health monitoring software based on spectral estimation and hierarchical genetic algorithm, Bangalore, India, SPIE-Int. Soc. Opt. Eng.

[27] Palacz, M. and M. Krawczuk (2002). "Vibration parameters for damage detection in structures." Journal of Sound and Vibration **249**(5): 999-1010.

[28] Pandey, A. K., M. Biswas, *et al.* (1991). "Damage detection from changes in curvature mode shapes." Journal of Sound and Vibration **145**(2): 321-32.

[29] Pawar, P. M. and R. Ganguli (2007). "On the effect of progressive damage on composite helicopter rotor system behavior." Composite Structures **78**(3): 410-423.

[30] Pawar, P. M., K. Venkatesulu Reddy, *et al.* (2007) "Damage Detection in Beams using Spatial Fourier Analysis and Neural Networks."

[31] Qiao, P., K. Lu, *et al.* (2007). "Curvature mode shape-based damage detection in composite laminated plates." Composite Structures **80**(3): 409-428.

[32] Qiao, P. Z., K. Lu, *et al.* (2008). "A combined static/dynamic technique for damage detection of laminated composite plates." Experimental Mechanics **48**(1): 17-35.

[33] Rosalie, C., A. Chan, *et al.* (2005). "Structural health monitoring of composite structures using stress wave methods." Composite Structures **67**(2): 157-66.

[34] Sharma, V. K., S. Hanagud, *et al.* (2006). "Damage index estimation in beams and plates using laser vibrometry." AIAA Journal **44**(4): 919-23.

[35] Sohi, M. M. (1989). Compressive strength and modes of failure in polymeric composites. United States -- Missouri, Washington University.

[36] Takeda, S., Y. Aoki, *et al.* (2007). "Structural health monitoring of composite wing structure during durability test." Composite Structures **79**(1): 133-9.

[37] Verijenko, B. and V. Verijenko (2006). "The use of strain memory alloys in structural health monitoring systems." Composite Structures **76**(1-2): 190-6.

[38] Wang, J. and Z.-N. Li (2006). "Finite element analysis and experiment research on SMA smart composite structure." Hangkong Xuebao/Acta Aeronautica et Astronautica Sinica **27**(4): 610-613.

[39] Wang, X. and K. Dong (2007). "Wave propagation characteristics in piezoelectric cylindrical laminated shells under large deformation." Composite Structures **77**(2): 171-81.

[40] Wong, C. K. W., W. K. Chiu, *et al.* (2006). "Can stress waves be used for monitoring sub-surface defects in repaired structures?" Composite Structures **76**(3): 199-208.

[41] Yam, L. H., Y. J. Yan, *et al.* (2003). "Vibration-based damage detection for composite structures using wavelet transform and neural network identification." Composite Structures **60**(4): 403-12.

[42] Yan, Y. J., L. Cheng, *et al.* (2007). "Development in vibration-based structural damage detection technique." Mechanical Systems and Signal Processing **21**(5): 2198-2211.

[43] Yan, Y. J., L. H. Yam, *et al.* (2006). "FEM modeling method of damage structures for structural damage detection." Composite Structures **72**(2): 193-199.

[44] Yi-Lan, K., Q. Wei, *et al.* (2007). "Study for multilayer piezoelectric composite structure as displacement actuator by Moiré interferometry and infrared thermography experiments." Materials Science & Engineering A (Structural Materials: Properties, Microstructure and Processing) **452-453**: 228-34.

[45] Yu, L., L. Cheng, *et al.* (2007). "Experimental validation of vibration-based damage detection for static laminated composite shells partially filled with fluid." Composite Structures **79**(2): 288-299.

[46] Zou, Y., L. Tong, *et al.* (2000). "Vibration-based model-dependent damage (delamination) identification and health monitoring for composite structures - a review." Journal of Sound and Vibration **230**(2): 357-378.

[47] Autar K. Kaw (2005). *Mechanics of Composite Materials*, 2nd edition, CRC. ISBN 0-84-931343-0.

[48] J.H. CHOU, J. G. (2001) Genetic algorithm in structural damage detection. *Computers & Structures,* 79**,** 1335–1353.

[49] J.T. KIM, Y. S. R., H.M. CHO, N. STUBBS (2003) Damage identification in beam-type structures: frequency-based method vs. mode-shape based method. *Engineering Structures,* 25**,** 57–67.

[50] K. MOSLEM, R. N. (2002) Structural damage detection by genetic algorithms. *AIAA Journal,* 40**,** 1395–1401.

[51] L.H. YAM, Y. J. Y., L. CHENG1, J.S. JIANG (2003) Identification of complex crack damage for honeycomb sandwich plate using wavelet analysis and neural networks. *Smart Materials & Structures,* 12**,** 661–671.

[52] L.H. YAM, Y. J. Y., J.S. JIANG (2003) Vibration-based damage detection for composite structures using wavelet transform and neural network identification. *Composite Structures,* 60**,** 403–412.

[53] LEE, J. K., JD (2002) Health-Monitoring Method for Bridges under Ordinary Traffic Loadings. *Journal of Sound and Vibration,* 257**,** 247-264.

[54] LEE, J. T., H (2005) A Novel Fibre Bragg Grating Acoustic Emission Sensor Head for Mechanical Tests. *Scripta Materialia,* 53**,** 1181-1186.

[55] LI, H., HERSZBERG I, MOURITZ, AP & DAVIS, CE (2004) Disbond Detection in Bonded Composite Ship Joints Using Embedded Bragg Grating Sensors. *Proceedings of the 2nd Australasian Workshop on Structural Health Monitoring.* Monash University, Melbourne, Australia.

[56] LI, H., HERSZBERG I, MOURITZ, AP, DAVIS CE & GALEA, SC (2004) Sensitivity of Embedded Fibre Optic Bragg Grating Sensors to Disbonds in Bonded Composite Ship Joints. *Journal of Composite Structures,* 66**,** 239-248.

[57] MALLICK (1988) *Fibre-Reinforced Composites: Materials, Manufacturing & Design*, Marcel Dekker Inc, USA.

[58] MARTARELLI M, R. G., SANTOLINI C (2001) Automated modal analysis by scanning laser vibrometry: Problems and uncertainties associated with the scanning system calibration. *Mechanical Systems and Signal Processing,* 15**,** 581–601.

[59] A. K. PANDEY, M. BISWAS and M. M. SAMMAN 1991 *Journal of Sound and* v*ibration* 145,321}332. Damage detection form changes in curvature mode shapes.

[60] C. P. RATCLIFFE and W. J. BAGARIA 1998 *AIAA Journal* 36, 1074}1077. Vibration technique for locating delamination in a composite plates.

[61] M Mehdizadeh, K Oruganti, M Bannister, I Herszberg & S John (2009), 'Vibration-based Analysis of an Increasing Delamination in a Polymeric Composite Structure', Submitted to the
Journal of Int. Mat, Systems & Structures', (Under Review).

[62] K Oruganti, M Mehdizadeh, S John, I Herszberg (2008), *Damage Detection in Composites using Vibration signatures and Mode Shapes*, Proceedings of SMASIS08 ASME Conference on Smart Materials, Adaptive Structures and Intelligent Systems October 28-30, 2008, Ellicott City, Maryland, USA, Paper SMASIS2008-404, ISBN 978-0-7918-3839-6.

# APPENDIX A - Principle of Laser Doppler Vibrometery

A laser Doppler Vibrometer is based on the principle of the detection of the Doppler shift of coherent laser light that is scattered from a small area of the test object. The object scatters or reflects light from the laser beam and the Doppler frequency shift is used to measure the component of velocity which lies along the axis of the laser beam. As the laser light has a very high frequency W (approx. 4.74 x$10^{14}$ Hz), a direct demodulation of the light is not possible. An optical interferometer is therefore used to mix the scattered light coherently with a reference beam. The photo detector measures the intensity of the mixed light whose (beat) frequency is equal to the difference frequency between the reference and the measurement beam. Such an arrangement can be a Michelson interferometer as shown below:

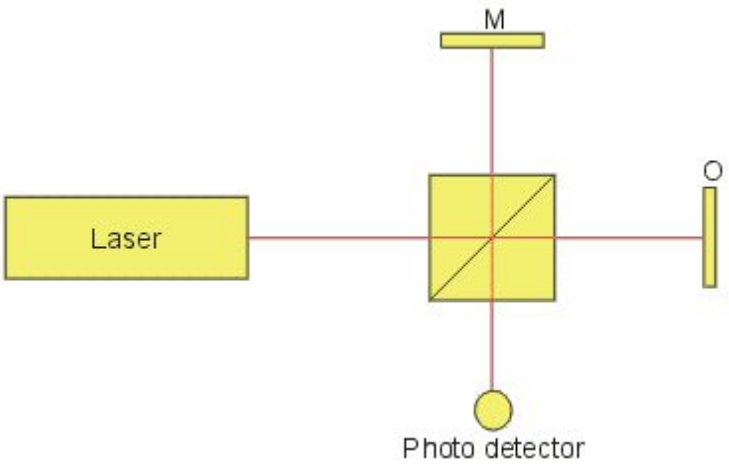


A laser beam is divided at a beam splitter into a measurement beam and a reference beam which propagates in the arms of the interferometer. The distances the light travels between the beam splitter and each reflector are xR and xM for the reference mirror M and object O respectively.

The corresponding optical phase of the beams in the interferometer is:

Reference $F_R = 2kx_R$

Measurement $F_M = 2kx_M$

With k = 2p/l. One usually defines $F(t) = F_R - F_M$

The photo detector measures the time dependant intensity I(t) at the point where the measurement and reference beams interfere.

$$I(t) = I_R I_M R + 2K\sqrt{I_R I_S R}\cos(2\pi f_D t + \Phi)$$

Where $I_R$ and $I_M$ are the intensities of the reference and measurement beams, K is a mixing efficiency coefficient and R is the effective reflectivity of the surface.

The phase F = 2pDL/l where DL is the vibrational displacement of the object and l the wavelength of the laser light.

If DL changes continuously the light intensity I (t) varies in a periodic manner. A phase change F of 2p corresponds to a displacement DL of l/2.

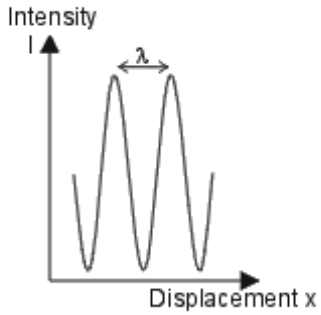


The rate of change of phase F is proportional to the rate of change of position which is the vibrational velocity v of the surface. This leads to the well known formula for the Doppler frequency $F_D$:

$F_D = 2\ v/\lambda$

Due to the sinusoidal nature of the detector signal, the direction of the vibration is ambiguous. There are two ways to introduce a directional sensitivity:

- Solution 1: Introduction of an optical frequency shift into one arm of the interferometer to obtain a virtual velocity offset.

- Solution 2: Adding polarization components and an additional photo receiver in such a way that at the interferometer output a second homodyne signal occurs being in quadrature to the primary photo detector output.

The most common form is the first solution. An acousto optic modulator (Bragg cell) is incorporated into one arm of the interferometer. The Bragg cell is driven at frequencies of 40 MHz or higher and generates a carrier signal at the RF drive (centre) frequency. The movement

of the object frequency modulates the carrier signal. The signed object velocity determines sign and amount of frequency deviation with respect to the centre frequency $F_B$. This type of interferometer is called heterodyne interferometer.

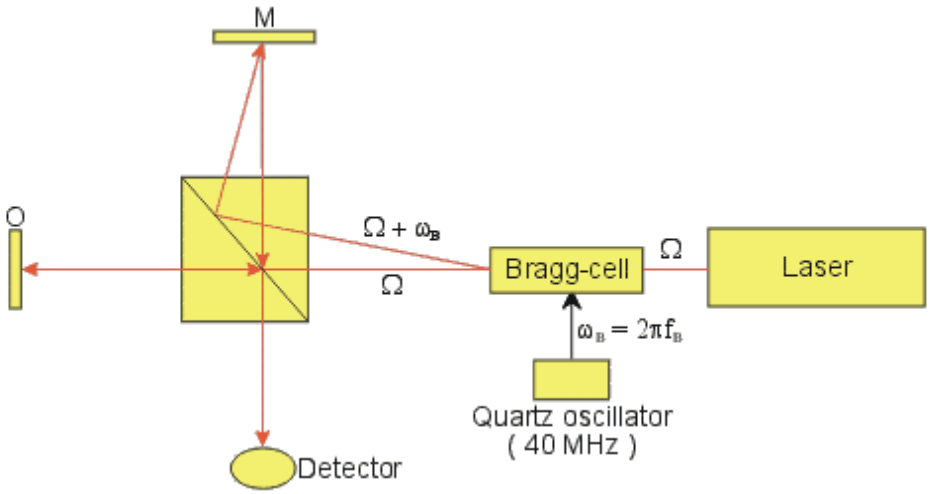


With the introduction of a shift frequency $F_B$ the intensity at the detector changes to:

$$I(t) = I_R\, I_M R + 2\, k \sqrt{I_R\, I_S R}\, \cos\left(2\pi[f_B - f_D]t + \Phi\right)$$

The heterodyne solution has significant advantages. As only high frequency AC signals are transmitted there is no disturbance from hum and noise, introduced from all types of power supplies. Non-linear effects of the photo detector as well as of all signal pre-processing stages do not affect the integrity of the Doppler modulation content. The high efficiency of the Bragg cells used by Polytec (>98%) produce less losses than the polarisers needed for solution 2.

The second solution known as the quadrature homodyne interferometer can be designed by adding wave retardation plates, a polarizing beam splitter and a second detector for example as in the optical system as shown below. The interferometer uses a linear polarized laser oriented to give a 45° polarization state. The light in the reference arm passes twice through the eighth wave retardation plate and the light coming back to the beam splitter BS is circularly polarized. This can be described as the vector sum of two orthogonal polarization states. A polarizing beam splitter PBS placed in front of the detectors 1 and 2 separates the two orthogonal components. The result is a quadrature relationship at the detectors (sine and cosine output). A quadrature homodyne interferometer is much easier to design as simple low frequency photo

detectors and amplifiers can be used. The non-linear behaviour of these elements on the other hand causes harmonic distortions of the measurement signal.

To decode signals from homodyne interferometers the baseband signals of both detector chains are fed into a modulator block which generates a modulated RF carrier with the help of an oscillator at the frequency $F_B$

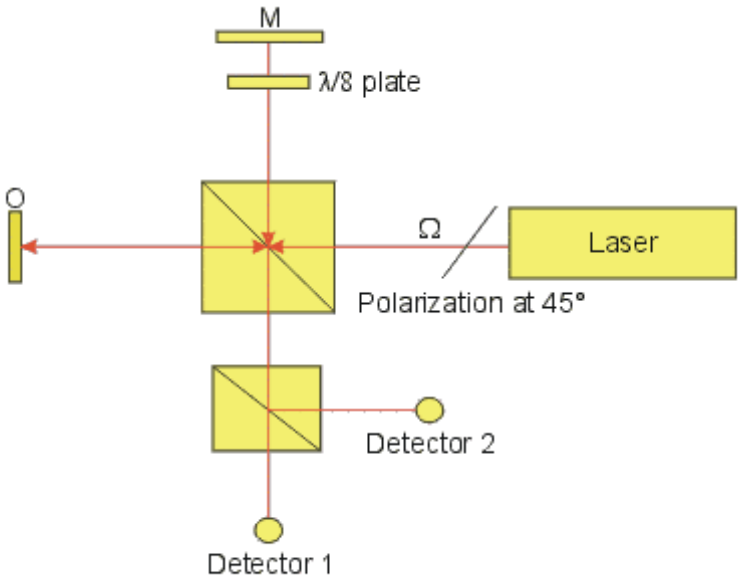


For signal decoding one can process the phase to produce a displacement output or carry out an FM demodulation to provide the vibrational velocity.

# APPENDIX B – Displacement Magnitudes

**Table 1: Displacements – Sample 1(Mode 1)**

| pt | L5 | L4 | L3 | L2 | L1 |
|---|---|---|---|---|---|
| 1 | 1.53E-05 | 1.52E-05 | 1.48E-05 | 1.44E-05 | 1.42E-05 |
| 2 | 1.46E-05 | 1.44E-05 | 1.41E-05 | 1.38E-05 | 1.37E-05 |
| 3 | 1.33E-05 | 1.32E-05 | 1.29E-05 | 1.27E-05 | 1.26E-05 |
| 4 | 1.2E-05 | 1.18E-05 | 1.16E-05 | 1.14E-05 | 1.13E-05 |
| 5 | 1.07E-05 | 1.05E-05 | 1.04E-05 | 1.01E-05 | 1E-05 |
| 6 | 9.37E-06 | 9.24E-06 | 9.02E-06 | 8.8E-06 | 8.76E-06 |
| 7 | 8.14E-06 | 8.01E-06 | 7.78E-06 | 7.52E-06 | 7.48E-06 |
| 8 | 6.82E-06 | 6.74E-06 | 6.56E-06 | 6.3E-06 | 6.22E-06 |
| 9 | 5.58E-06 | 5.45E-06 | 5.31E-06 | 5.01E-06 | 4.97E-06 |
| 10 | 4.37E-06 | 4.19E-06 | 3.98E-06 | 3.72E-06 | 3.7E-06 |
| 11 | 3.19E-06 | 3.05E-06 | 2.85E-06 | 2.58E-06 | 2.57E-06 |
| 12 | 2.07E-06 | 1.97E-06 | 1.74E-06 | 1.48E-06 | 1.4E-06 |
| 13 | 9.23E-07 | 8.11E-07 | 5.47E-07 | 3E-07 | 2.65E-07 |
| 14 | 2.69E-07 | 3.72E-07 | 5.9E-07 | 8.49E-07 | 8.56E-07 |
| 15 | 1.31E-06 | 1.43E-06 | 1.71E-06 | 1.95E-06 | 1.96E-06 |
| 16 | 2.33E-06 | 2.48E-06 | 2.69E-06 | 2.91E-06 | 2.91E-06 |
| 17 | 3.31E-06 | 3.43E-06 | 3.61E-06 | 3.86E-06 | 3.85E-06 |
| 18 | 4.19E-06 | 4.25E-06 | 4.5E-06 | 4.79E-06 | 4.82E-06 |
| 19 | 5.05E-06 | 5.13E-06 | 5.34E-06 | 5.63E-06 | 5.62E-06 |
| 20 | 5.86E-06 | 5.95E-06 | 6.22E-06 | 6.41E-06 | 6.45E-06 |
| 21 | 6.57E-06 | 6.69E-06 | 6.93E-06 | 7.2E-06 | 7.19E-06 |
| 22 | 7.29E-06 | 7.37E-06 | 7.68E-06 | 7.91E-06 | 7.91E-06 |
| 23 | 7.85E-06 | 7.97E-06 | 8.2E-06 | 8.47E-06 | 8.47E-06 |
| 24 | 8.41E-06 | 8.53E-06 | 8.76E-06 | 8.96E-06 | 9E-06 |
| 25 | 8.89E-06 | 9.02E-06 | 9.22E-06 | 9.42E-06 | 9.45E-06 |
| 26 | 9.27E-06 | 9.4E-06 | 9.6E-06 | 9.8E-06 | 9.84E-06 |
| 27 | 9.58E-06 | 9.7E-06 | 9.9E-06 | 1.01E-05 | 1.01E-05 |
| 28 | 9.79E-06 | 9.92E-06 | 1.01E-05 | 1.03E-05 | 1.04E-05 |
| 29 | 9.93E-06 | 1.01E-05 | 1.03E-05 | 1.05E-05 | 1.06E-05 |
| 30 | 9.99E-06 | 1.01E-05 | 1.03E-05 | 1.05E-05 | 1.07E-05 |
| 31 | 9.99E-06 | 1.01E-05 | 1.03E-05 | 1.05E-05 | 1.07E-05 |
| 32 | 9.91E-06 | 9.98E-06 | 1.01E-05 | 1.04E-05 | 1.06E-05 |
| 33 | 9.75E-06 | 9.76E-06 | 9.9E-06 | 1.02E-05 | 1.04E-05 |
| 34 | 9.46E-06 | 9.5E-06 | 9.6E-06 | 9.92E-06 | 1.01E-05 |
| 35 | 9.06E-06 | 9.04E-06 | 9.21E-06 | 9.5E-06 | 9.75E-06 |
| 36 | 8.58E-06 | 8.6E-06 | 8.74E-06 | 9.09E-06 | 9.29E-06 |
| 37 | 8.08E-06 | 8.03E-06 | 8.23E-06 | 8.51E-06 | 8.74E-06 |
| 38 | 7.43E-06 | 7.45E-06 | 7.61E-06 | 7.92E-06 | 8.11E-06 |
| 39 | 6.78E-06 | 6.78E-06 | 6.98E-06 | 7.22E-06 | 7.42E-06 |
| 40 | 6.01E-06 | 6.04E-06 | 6.21E-06 | 6.44E-06 | 6.64E-06 |
| 41 | 5.17E-06 | 5.2E-06 | 5.37E-06 | 5.6E-06 | 5.8E-06 |
| 42 | 4.25E-06 | 4.28E-06 | 4.46E-06 | 4.72E-06 | 4.88E-06 |
| 43 | 3.26E-06 | 3.3E-06 | 3.51E-06 | 3.77E-06 | 3.93E-06 |
| 44 | 2.22E-06 | 2.25E-06 | 2.42E-06 | 2.68E-06 | 2.83E-06 |
| 45 | 1.11E-06 | 1.14E-06 | 1.3E-06 | 1.51E-06 | 1.69E-06 |
| 46 | 2.48E-07 | 2.38E-07 | 2.37E-07 | 3.81E-07 | 5.41E-07 |
| 47 | 1.3E-06 | 1.3E-06 | 1.17E-06 | 9.23E-07 | 7.2E-07 |
| 48 | 2.57E-06 | 2.54E-06 | 2.43E-06 | 2.15E-06 | 1.98E-06 |
| 49 | 3.89E-06 | 3.89E-06 | 3.75E-06 | 3.46E-06 | 3.3E-06 |
| 50 | 5.24E-06 | 5.23E-06 | 5.03E-06 | 4.74E-06 | 4.6E-06 |
| 51 | 6.66E-06 | 6.65E-06 | 6.47E-06 | 6.15E-06 | 6.02E-06 |
| 52 | 8.03E-06 | 8.09E-06 | 7.93E-06 | 7.65E-06 | 7.45E-06 |
| 53 | 9.48E-06 | 9.54E-06 | 9.38E-06 | 9.06E-06 | 8.86E-06 |
| 54 | 1.09E-05 | 1.1E-05 | 1.08E-05 | 1.05E-05 | 1.03E-05 |
| 55 | 1.23E-05 | 1.24E-05 | 1.22E-05 | 1.2E-05 | 1.18E-05 |
| 56 | 1.38E-05 | 1.38E-05 | 1.37E-05 | 1.34E-05 | 1.32E-05 |
| 57 | 1.53E-05 | 1.53E-05 | 1.52E-05 | 1.49E-05 | 1.46E-05 |
| 58 | 1.68E-05 | 1.68E-05 | 1.66E-05 | 1.63E-05 | 1.6E-05 |
| 59 | 1.83E-05 | 1.83E-05 | 1.81E-05 | 1.79E-05 | 1.75E-05 |
| 61 | 1.98E-05 | 1.96E-05 | 1.95E-05 | 1.92E-05 | 1.9E-05 |
| 62 | 2.07E-05 | 2.06E-05 | 2.03E-05 | 2.02E-05 | 2E-05 |

**Table 2: Displacements – Sample 1(Mode 2)**

| pt | L5 | L4 | L3 | L2 | L1 |
|---|---|---|---|---|---|
| 1 | 2.78E-06 | 2.85E-06 | 2.88E-06 | 2.92E-06 | 2.92E-06 |
| 2 | 2.5E-06 | 2.54E-06 | 2.57E-06 | 2.61E-06 | 2.63E-06 |
| 3 | 2.06E-06 | 2.09E-06 | 2.12E-06 | 2.17E-06 | 2.2E-06 |
| 4 | 1.62E-06 | 1.63E-06 | 1.68E-06 | 1.72E-06 | 1.76E-06 |
| 5 | 1.19E-06 | 1.19E-06 | 1.24E-06 | 1.29E-06 | 1.32E-06 |
| 6 | 7.58E-07 | 7.53E-07 | 8.16E-07 | 8.79E-07 | 8.99E-07 |
| 7 | 3.43E-07 | 3.34E-07 | 4.05E-07 | 4.67E-07 | 4.85E-07 |
| 8 | 7.12E-08 | 7.37E-08 | 4.88E-08 | 8.72E-08 | 1.06E-07 |
| 9 | 4.34E-07 | 4.41E-07 | 4.02E-07 | 3.38E-07 | 3.08E-07 |
| 10 | 7.8E-07 | 7.81E-07 | 7.58E-07 | 6.96E-07 | 6.63E-07 |
| 11 | 1.1E-06 | 1.09E-06 | 1.06E-06 | 1.01E-06 | 9.86E-07 |
| 12 | 1.41E-06 | 1.4E-06 | 1.36E-06 | 1.31E-06 | 1.28E-06 |
| 13 | 1.69E-06 | 1.69E-06 | 1.65E-06 | 1.59E-06 | 1.56E-06 |
| 14 | 1.91E-06 | 1.91E-06 | 1.87E-06 | 1.81E-06 | 1.79E-06 |
| 15 | 2.11E-06 | 2.1E-06 | 2.06E-06 | 2.02E-06 | 2E-06 |
| 16 | 2.27E-06 | 2.26E-06 | 2.22E-06 | 2.18E-06 | 2.16E-06 |
| 17 | 2.4E-06 | 2.4E-06 | 2.35E-06 | 2.3E-06 | 2.29E-06 |
| 18 | 2.5E-06 | 2.5E-06 | 2.46E-06 | 2.41E-06 | 2.38E-06 |
| 19 | 2.56E-06 | 2.54E-06 | 2.49E-06 | 2.45E-06 | 2.42E-06 |
| 20 | 2.58E-06 | 2.55E-06 | 2.48E-06 | 2.44E-06 | 2.43E-06 |
| 21 | 2.57E-06 | 2.52E-06 | 2.46E-06 | 2.42E-06 | 2.41E-06 |
| 22 | 2.49E-06 | 2.44E-06 | 2.39E-06 | 2.35E-06 | 2.34E-06 |
| 23 | 2.38E-06 | 2.33E-06 | 2.28E-06 | 2.24E-06 | 2.23E-06 |
| 24 | 2.25E-06 | 2.19E-06 | 2.14E-06 | 2.1E-06 | 2.09E-06 |
| 25 | 2.07E-06 | 2.02E-06 | 1.97E-06 | 1.94E-06 | 1.94E-06 |
| 26 | 1.87E-06 | 1.82E-06 | 1.78E-06 | 1.75E-06 | 1.74E-06 |
| 27 | 1.64E-06 | 1.61E-06 | 1.56E-06 | 1.52E-06 | 1.51E-06 |
| 28 | 1.4E-06 | 1.36E-06 | 1.31E-06 | 1.28E-06 | 1.27E-06 |
| 29 | 1.13E-06 | 1.1E-06 | 1.06E-06 | 1.02E-06 | 1.02E-06 |
| 30 | 8.55E-07 | 8.23E-07 | 7.91E-07 | 7.52E-07 | 7.46E-07 |
| 31 | 5.72E-07 | 5.49E-07 | 5.19E-07 | 4.8E-07 | 4.67E-07 |
| 32 | 2.9E-07 | 2.61E-07 | 2.3E-07 | 1.93E-07 | 1.87E-07 |
| 33 | 7.84E-08 | 7.46E-08 | 8.51E-08 | 1.07E-07 | 1.12E-07 |
| 34 | 2.93E-07 | 3.1E-07 | 3.37E-07 | 3.66E-07 | 3.72E-07 |
| 35 | 5.55E-07 | 5.73E-07 | 5.97E-07 | 6.25E-07 | 6.3E-07 |
| 36 | 8.01E-07 | 8.14E-07 | 8.4E-07 | 8.66E-07 | 8.71E-07 |
| 37 | 1.03E-06 | 1.04E-06 | 1.06E-06 | 1.1E-06 | 1.09E-06 |
| 38 | 1.23E-06 | 1.24E-06 | 1.27E-06 | 1.3E-06 | 1.3E-06 |
| 39 | 1.41E-06 | 1.41E-06 | 1.43E-06 | 1.46E-06 | 1.46E-06 |
| 40 | 1.54E-06 | 1.54E-06 | 1.55E-06 | 1.58E-06 | 1.58E-06 |
| 41 | 1.63E-06 | 1.63E-06 | 1.64E-06 | 1.66E-06 | 1.67E-06 |
| 42 | 1.68E-06 | 1.68E-06 | 1.69E-06 | 1.71E-06 | 1.72E-06 |
| 43 | 1.68E-06 | 1.68E-06 | 1.69E-06 | 1.71E-06 | 1.74E-06 |
| 44 | 1.64E-06 | 1.64E-06 | 1.65E-06 | 1.67E-06 | 1.7E-06 |
| 45 | 1.55E-06 | 1.55E-06 | 1.55E-06 | 1.58E-06 | 1.6E-06 |
| 46 | 1.41E-06 | 1.41E-06 | 1.42E-06 | 1.44E-06 | 1.46E-06 |
| 47 | 1.23E-06 | 1.23E-06 | 1.23E-06 | 1.26E-06 | 1.27E-06 |
| 48 | 1.01E-06 | 1.01E-06 | 1.01E-06 | 1.03E-06 | 1.05E-06 |
| 49 | 7.63E-07 | 7.57E-07 | 7.6E-07 | 7.83E-07 | 7.99E-07 |
| 50 | 4.82E-07 | 4.78E-07 | 4.83E-07 | 5.09E-07 | 5.2E-07 |
| 51 | 1.72E-07 | 1.67E-07 | 1.73E-07 | 2.05E-07 | 2.12E-07 |
| 52 | 1.75E-07 | 1.78E-07 | 1.67E-07 | 1.32E-07 | 1.22E-07 |
| 53 | 5.2E-07 | 5.19E-07 | 5.12E-07 | 4.86E-07 | 4.8E-07 |
| 54 | 8.88E-07 | 8.9E-07 | 8.79E-07 | 8.63E-07 | 8.54E-07 |
| 55 | 1.28E-06 | 1.28E-06 | 1.28E-06 | 1.26E-06 | 1.25E-06 |
| 56 | 1.68E-06 | 1.68E-06 | 1.67E-06 | 1.66E-06 | 1.64E-06 |
| 57 | 2.08E-06 | 2.08E-06 | 2.08E-06 | 2.05E-06 | 2.04E-06 |
| 58 | 2.49E-06 | 2.49E-06 | 2.49E-06 | 2.46E-06 | 2.46E-06 |
| 59 | 2.91E-06 | 2.91E-06 | 2.9E-06 | 2.89E-06 | 2.88E-06 |
| 61 | 3.31E-06 | 3.32E-06 | 3.31E-06 | 3.3E-06 | 3.3E-06 |
| 62 | 3.59E-06 | 3.61E-06 | 3.6E-06 | 3.59E-06 | 3.57E-06 |

## Table 3: Displacements – Sample 1(Mode 3)

| pt | L5 | L4 | L3 | L2 | L1 |
|---|---|---|---|---|---|
| 1 | 9.54E-08 | 9E-08 | 7.76E-08 | 6.97E-08 | 6.78E-08 |
| 2 | 7.96E-08 | 7.39E-08 | 6.7E-08 | 6.14E-08 | 6.08E-08 |
| 3 | 5.3E-08 | 5.04E-08 | 4.5E-08 | 4.07E-08 | 4E-08 |
| 4 | 3.34E-08 | 2.94E-08 | 2.84E-08 | 2.31E-08 | 2.45E-08 |
| 5 | 3.07E-08 | 3.18E-08 | 3.14E-08 | 2.98E-08 | 3.22E-08 |
| 6 | 4.14E-08 | 4.47E-08 | 4.25E-08 | 4.62E-08 | 4.61E-08 |
| 7 | 5.9E-08 | 5.86E-08 | 5.9E-08 | 6.37E-08 | 6.45E-08 |
| 8 | 6.95E-08 | 7.02E-08 | 7.24E-08 | 8.04E-08 | 8.03E-08 |
| 9 | 7.86E-08 | 7.91E-08 | 8.54E-08 | 9.42E-08 | 9.34E-08 |
| 10 | 9.2E-08 | 9.35E-08 | 9.88E-08 | 1.06E-07 | 1.03E-07 |
| 11 | 1.03E-07 | 1.04E-07 | 1.07E-07 | 1.11E-07 | 1.1E-07 |
| 12 | 1.04E-07 | 1.06E-07 | 1.08E-07 | 1.14E-07 | 1.16E-07 |
| 13 | 1.04E-07 | 1.05E-07 | 1.1E-07 | 1.17E-07 | 1.22E-07 |
| 14 | 1.01E-07 | 1.02E-07 | 1.06E-07 | 1.13E-07 | 1.18E-07 |
| 15 | 9.66E-08 | 9.42E-08 | 1.01E-07 | 1.07E-07 | 1.12E-07 |
| 16 | 8.65E-08 | 8.54E-08 | 9.01E-08 | 9.95E-08 | 1.03E-07 |
| 17 | 7.26E-08 | 7.03E-08 | 7.85E-08 | 8.76E-08 | 9.18E-08 |
| 18 | 5.88E-08 | 6.09E-08 | 6.71E-08 | 7.46E-08 | 7.86E-08 |
| 19 | 4.62E-08 | 4.69E-08 | 5.13E-08 | 5.76E-08 | 6.22E-08 |
| 20 | 3.08E-08 | 3.11E-08 | 3.34E-08 | 3.73E-08 | 4.27E-08 |
| 21 | 1.88E-08 | 1.98E-08 | 2.24E-08 | 2.49E-08 | 2.8E-08 |
| 22 | 2.08E-08 | 2.24E-08 | 2.36E-08 | 2.27E-08 | 2.26E-08 |
| 23 | 3.72E-08 | 3.75E-08 | 3.71E-08 | 3.41E-08 | 3.12E-08 |
| 24 | 5.21E-08 | 5.38E-08 | 5.15E-08 | 4.87E-08 | 4.64E-08 |
| 25 | 6.98E-08 | 7.12E-08 | 6.89E-08 | 6.42E-08 | 6.23E-08 |
| 26 | 8.8E-08 | 9.23E-08 | 8.66E-08 | 8.1E-08 | 7.81E-08 |
| 27 | 1.02E-07 | 1.03E-07 | 1E-07 | 9.33E-08 | 9.2E-08 |
| 28 | 1.11E-07 | 1.12E-07 | 1.1E-07 | 1.06E-07 | 1.05E-07 |
| 29 | 1.2E-07 | 1.21E-07 | 1.18E-07 | 1.15E-07 | 1.13E-07 |
| 30 | 1.27E-07 | 1.27E-07 | 1.25E-07 | 1.21E-07 | 1.2E-07 |
| 31 | 1.3E-07 | 1.3E-07 | 1.26E-07 | 1.25E-07 | 1.24E-07 |
| 32 | 1.29E-07 | 1.27E-07 | 1.25E-07 | 1.25E-07 | 1.25E-07 |
| 33 | 1.24E-07 | 1.22E-07 | 1.21E-07 | 1.22E-07 | 1.21E-07 |
| 34 | 1.18E-07 | 1.17E-07 | 1.16E-07 | 1.14E-07 | 1.13E-07 |
| 35 | 1.1E-07 | 1.1E-07 | 1.09E-07 | 1.06E-07 | 1.06E-07 |
| 36 | 9.97E-08 | 9.95E-08 | 9.86E-08 | 9.8E-08 | 9.84E-08 |
| 37 | 8.8E-08 | 8.63E-08 | 8.58E-08 | 8.57E-08 | 8.62E-08 |
| 38 | 7.43E-08 | 7.26E-08 | 7.16E-08 | 7E-08 | 7.2E-08 |
| 39 | 6.02E-08 | 5.96E-08 | 5.88E-08 | 5.81E-08 | 5.91E-08 |
| 40 | 4.63E-08 | 4.6E-08 | 4.58E-08 | 4.48E-08 | 4.76E-08 |
| 41 | 3.82E-08 | 3.78E-08 | 3.65E-08 | 3.72E-08 | 3.73E-08 |
| 42 | 3.42E-08 | 3.19E-08 | 3.14E-08 | 3.23E-08 | 3.28E-08 |
| 43 | 3.71E-08 | 3.58E-08 | 3.48E-08 | 3.71E-08 | 3.72E-08 |
| 44 | 3.98E-08 | 4.07E-08 | 4.16E-08 | 4.36E-08 | 4.39E-08 |
| 45 | 4.06E-08 | 4.24E-08 | 4.23E-08 | 4.32E-08 | 4.35E-08 |
| 46 | 4.31E-08 | 4.36E-08 | 4.35E-08 | 4.38E-08 | 4.3E-08 |
| 47 | 4.7E-08 | 4.55E-08 | 4.53E-08 | 4.43E-08 | 4.26E-08 |
| 48 | 4.76E-08 | 4.61E-08 | 4.6E-08 | 4.57E-08 | 4.43E-08 |
| 49 | 4.64E-08 | 4.39E-08 | 4.57E-08 | 4.44E-08 | 4.39E-08 |
| 50 | 4.49E-08 | 4.4E-08 | 4.39E-08 | 4.03E-08 | 4.07E-08 |
| 51 | 3.83E-08 | 3.71E-08 | 3.53E-08 | 3.29E-08 | 3.42E-08 |
| 52 | 2.78E-08 | 2.66E-08 | 2.64E-08 | 2.34E-08 | 2.81E-08 |
| 53 | 1.79E-08 | 1.88E-08 | 1.86E-08 | 1.81E-08 | 1.91E-08 |
| 54 | 1.19E-08 | 8.7E-09 | 9.96E-09 | 8.99E-09 | 1.05E-08 |
| 55 | 5.44E-09 | 5.26E-09 | 3.57E-09 | 9.54E-09 | 1.17E-08 |
| 56 | 1.39E-08 | 1.58E-08 | 1.7E-08 | 2.21E-08 | 2.31E-08 |
| 57 | 3.12E-08 | 3.3E-08 | 3.61E-08 | 3.8E-08 | 3.54E-08 |
| 58 | 4.56E-08 | 4.79E-08 | 5.01E-08 | 4.84E-08 | 4.77E-08 |
| 59 | 5.58E-08 | 6.02E-08 | 6.17E-08 | 6.14E-08 | 5.87E-08 |
| 61 | 7.04E-08 | 7.5E-08 | 7.87E-08 | 7.64E-08 | 7.36E-08 |
| 62 | 7.88E-08 | 8.23E-08 | 8.61E-08 | 8.95E-08 | 8.56E-08 |

## Table 4: Displacements – Sample 1(Mode 4)

| pt | L5 | L4 | L3 | L2 | L1 |
|---|---|---|---|---|---|
| 1 | 1.01E-07 | 1.03E-07 | 1.07E-07 | 1.09E-07 | 1.09E-07 |
| 2 | 7.87E-08 | 8.06E-08 | 8.36E-08 | 8.61E-08 | 8.68E-08 |
| 3 | 4.37E-08 | 4.43E-08 | 4.87E-08 | 5.27E-08 | 5.42E-08 |
| 4 | 9.72E-09 | 1.02E-08 | 1.49E-08 | 1.86E-08 | 1.99E-08 |
| 5 | 2.09E-08 | 1.94E-08 | 1.47E-08 | 1.18E-08 | 1.14E-08 |
| 6 | 4.67E-08 | 4.68E-08 | 4.4E-08 | 4.27E-08 | 4.09E-08 |
| 7 | 6.85E-08 | 6.87E-08 | 6.73E-08 | 6.67E-08 | 6.48E-08 |
| 8 | 8.89E-08 | 8.83E-08 | 8.65E-08 | 8.54E-08 | 8.29E-08 |
| 9 | 1.01E-07 | 1E-07 | 9.82E-08 | 9.8E-08 | 9.6E-08 |
| 10 | 1.08E-07 | 1.07E-07 | 1.03E-07 | 1.03E-07 | 1.02E-07 |
| 11 | 1.09E-07 | 1.08E-07 | 1.04E-07 | 1.04E-07 | 1.06E-07 |
| 12 | 1.04E-07 | 1.04E-07 | 9.95E-08 | 9.87E-08 | 9.95E-08 |
| 13 | 9.18E-08 | 9.02E-08 | 8.71E-08 | 8.52E-08 | 8.64E-08 |
| 14 | 7.28E-08 | 7.07E-08 | 6.81E-08 | 6.76E-08 | 6.79E-08 |
| 15 | 5.1E-08 | 4.95E-08 | 4.81E-08 | 4.64E-08 | 4.62E-08 |
| 16 | 2.84E-08 | 2.73E-08 | 2.6E-08 | 2.33E-08 | 2.24E-08 |
| 17 | 2.19E-09 | 1.54E-09 | 2.3E-09 | 3.4E-09 | 3.06E-09 |
| 18 | 2.47E-08 | 2.59E-08 | 2.53E-08 | 2.5E-08 | 2.48E-08 |
| 19 | 4.85E-08 | 4.92E-08 | 5.04E-08 | 5.1E-08 | 5.09E-08 |
| 20 | 6.87E-08 | 7E-08 | 7E-08 | 7.14E-08 | 7.13E-08 |
| 21 | 8.84E-08 | 8.89E-08 | 8.87E-08 | 8.88E-08 | 8.9E-08 |
| 22 | 1.01E-07 | 1.03E-07 | 1.01E-07 | 1.02E-07 | 1.02E-07 |
| 23 | 1.1E-07 | 1.1E-07 | 1.08E-07 | 1.09E-07 | 1.1E-07 |
| 24 | 1.12E-07 | 1.12E-07 | 1.09E-07 | 1.11E-07 | 1.13E-07 |
| 25 | 1.1E-07 | 1.09E-07 | 1.07E-07 | 1.09E-07 | 1.1E-07 |
| 26 | 1.02E-07 | 1E-07 | 9.79E-08 | 9.9E-08 | 9.94E-08 |
| 27 | 8.85E-08 | 8.74E-08 | 8.5E-08 | 8.52E-08 | 8.53E-08 |
| 28 | 6.97E-08 | 6.84E-08 | 6.67E-08 | 6.69E-08 | 6.71E-08 |
| 29 | 4.74E-08 | 4.63E-08 | 4.52E-08 | 4.51E-08 | 4.55E-08 |
| 30 | 2.29E-08 | 2.18E-08 | 2.02E-08 | 2.01E-08 | 2.03E-08 |
| 31 | 3.98E-09 | 4.75E-09 | 5.69E-09 | 6.41E-09 | 5.53E-09 |
| 32 | 2.74E-08 | 2.78E-08 | 2.9E-08 | 3.04E-08 | 2.98E-08 |
| 33 | 5.09E-08 | 5.13E-08 | 5.22E-08 | 5.36E-08 | 5.29E-08 |
| 34 | 7.15E-08 | 7.21E-08 | 7.2E-08 | 7.39E-08 | 7.29E-08 |
| 35 | 8.76E-08 | 8.77E-08 | 8.83E-08 | 9E-08 | 8.94E-08 |
| 36 | 9.79E-08 | 9.83E-08 | 9.94E-08 | 1.01E-07 | 1E-07 |
| 37 | 1.02E-07 | 1.01E-07 | 1.02E-07 | 1.05E-07 | 1.05E-07 |
| 38 | 1.02E-07 | 1.01E-07 | 1.01E-07 | 1.05E-07 | 1.06E-07 |
| 39 | 9.61E-08 | 9.47E-08 | 9.58E-08 | 9.93E-08 | 1.01E-07 |
| 40 | 8.41E-08 | 8.34E-08 | 8.28E-08 | 8.51E-08 | 8.67E-08 |
| 41 | 6.61E-08 | 6.5E-08 | 6.42E-08 | 6.47E-08 | 6.63E-08 |
| 42 | 4.06E-08 | 4.04E-08 | 4E-08 | 4.07E-08 | 4.13E-08 |
| 43 | 1.09E-08 | 1.05E-08 | 1.14E-08 | 1.3E-08 | 1.35E-08 |
| 44 | 2.23E-08 | 2.28E-08 | 2.19E-08 | 1.93E-08 | 1.88E-08 |
| 45 | 5.4E-08 | 5.51E-08 | 5.35E-08 | 5.16E-08 | 5.07E-08 |
| 46 | 8.62E-08 | 8.71E-08 | 8.52E-08 | 8.26E-08 | 8.15E-08 |
| 47 | 1.14E-07 | 1.16E-07 | 1.13E-07 | 1.1E-07 | 1.09E-07 |
| 48 | 1.38E-07 | 1.4E-07 | 1.37E-07 | 1.33E-07 | 1.31E-07 |
| 49 | 1.54E-07 | 1.54E-07 | 1.51E-07 | 1.47E-07 | 1.45E-07 |
| 50 | 1.63E-07 | 1.6E-07 | 1.56E-07 | 1.51E-07 | 1.5E-07 |
| 51 | 1.64E-07 | 1.61E-07 | 1.54E-07 | 1.5E-07 | 1.49E-07 |
| 52 | 1.57E-07 | 1.52E-07 | 1.44E-07 | 1.4E-07 | 1.4E-07 |
| 53 | 1.38E-07 | 1.34E-07 | 1.25E-07 | 1.21E-07 | 1.22E-07 |
| 54 | 1.13E-07 | 1.09E-07 | 1.01E-07 | 9.48E-08 | 9.39E-08 |
| 55 | 7.77E-08 | 7.19E-08 | 6.42E-08 | 5.82E-08 | 5.88E-08 |
| 56 | 3.71E-08 | 3.21E-08 | 2.34E-08 | 1.82E-08 | 1.71E-08 |
| 57 | 8.44E-09 | 1.29E-08 | 2.07E-08 | 2.7E-08 | 2.73E-08 |
| 58 | 5.83E-08 | 6.08E-08 | 6.83E-08 | 7.54E-08 | 7.54E-08 |
| 59 | 1.09E-07 | 1.12E-07 | 1.18E-07 | 1.25E-07 | 1.26E-07 |
| 61 | 1.64E-07 | 1.68E-07 | 1.72E-07 | 1.77E-07 | 1.76E-07 |
| 62 | 1.96E-07 | 2.03E-07 | 2.08E-07 | 2.14E-07 | 2.12E-07 |

## Table 5: Displacements – Sample 3(Mode 1)

| pt | L5 | L4 | L3 | L2 | L1 |
|---|---|---|---|---|---|
| 1 | 1.57E-05 | 1.55E-05 | 1.52E-05 | 1.49E-05 | 1.48E-05 |
| 2 | 1.49E-05 | 1.47E-05 | 1.45E-05 | 1.41E-05 | 1.40E-05 |
| 3 | 1.37E-05 | 1.35E-05 | 1.32E-05 | 1.28E-05 | 1.28E-05 |
| 4 | 1.23E-05 | 1.22E-05 | 1.19E-05 | 1.16E-05 | 1.16E-05 |
| 5 | 1.10E-05 | 1.10E-05 | 1.07E-05 | 1.04E-05 | 1.03E-05 |
| 6 | 9.81E-06 | 9.66E-06 | 9.39E-06 | 9.04E-06 | 9.00E-06 |
| 7 | 8.49E-06 | 8.38E-06 | 8.09E-06 | 7.80E-06 | 7.71E-06 |
| 8 | 7.24E-06 | 7.10E-06 | 6.86E-06 | 6.52E-06 | 6.52E-06 |
| 9 | 6.04E-06 | 5.94E-06 | 5.56E-06 | 5.22E-06 | 5.30E-06 |
| 10 | 4.87E-06 | 4.78E-06 | 4.36E-06 | 4.01E-06 | 4.16E-06 |
| 11 | 3.68E-06 | 3.55E-06 | 3.17E-06 | 2.85E-06 | 2.93E-06 |
| 12 | 2.46E-06 | 2.30E-06 | 2.06E-06 | 1.77E-06 | 1.78E-06 |
| 13 | 1.36E-06 | 1.20E-06 | 9.95E-07 | 6.74E-07 | 8.11E-07 |
| 14 | 3.45E-07 | 1.64E-07 | 2.01E-07 | 4.01E-07 | 1.77E-07 |
| 15 | 8.50E-07 | 1.00E-06 | 1.28E-06 | 1.63E-06 | 1.39E-06 |
| 16 | 1.83E-06 | 2.01E-06 | 2.25E-06 | 2.58E-06 | 2.55E-06 |
| 17 | 2.78E-06 | 2.93E-06 | 3.12E-06 | 3.42E-06 | 3.46E-06 |
| 18 | 3.69E-06 | 3.86E-06 | 4.04E-06 | 4.31E-06 | 4.37E-06 |
| 19 | 4.55E-06 | 4.70E-06 | 4.93E-06 | 5.16E-06 | 5.21E-06 |
| 20 | 5.33E-06 | 5.51E-06 | 5.73E-06 | 5.95E-06 | 5.99E-06 |
| 21 | 6.07E-06 | 6.23E-06 | 6.48E-06 | 6.68E-06 | 6.72E-06 |
| 22 | 6.74E-06 | 6.90E-06 | 7.13E-06 | 7.35E-06 | 7.39E-06 |
| 23 | 7.38E-06 | 7.48E-06 | 7.73E-06 | 7.94E-06 | 7.99E-06 |
| 24 | 7.87E-06 | 7.99E-06 | 8.23E-06 | 8.47E-06 | 8.51E-06 |
| 25 | 8.36E-06 | 8.48E-06 | 8.73E-06 | 8.92E-06 | 8.96E-06 |
| 26 | 8.76E-06 | 8.91E-06 | 9.12E-06 | 9.32E-06 | 9.39E-06 |
| 27 | 9.09E-06 | 9.23E-06 | 9.44E-06 | 9.70E-06 | 9.78E-06 |
| 28 | 9.35E-06 | 9.49E-06 | 9.70E-06 | 9.93E-06 | 1.00E-05 |
| 29 | 9.53E-06 | 9.64E-06 | 9.83E-06 | 1.01E-05 | 1.01E-05 |
| 30 | 9.59E-06 | 9.67E-06 | 9.86E-06 | 1.01E-05 | 1.02E-05 |
| 31 | 9.62E-06 | 9.66E-06 | 9.86E-06 | 1.01E-05 | 1.03E-05 |
| 32 | 9.60E-06 | 9.64E-06 | 9.78E-06 | 1.01E-05 | 1.02E-05 |
| 33 | 9.50E-06 | 9.50E-06 | 9.63E-06 | 9.89E-06 | 1.01E-05 |
| 34 | 9.26E-06 | 9.28E-06 | 9.41E-06 | 9.70E-06 | 9.84E-06 |
| 35 | 8.91E-06 | 8.90E-06 | 9.04E-06 | 9.33E-06 | 9.45E-06 |
| 36 | 8.51E-06 | 8.53E-06 | 8.71E-06 | 8.95E-06 | 9.07E-06 |
| 37 | 8.00E-06 | 8.04E-06 | 8.20E-06 | 8.45E-06 | 8.54E-06 |
| 38 | 7.49E-06 | 7.51E-06 | 7.68E-06 | 7.89E-06 | 8.01E-06 |
| 39 | 6.87E-06 | 6.90E-06 | 7.02E-06 | 7.24E-06 | 7.35E-06 |
| 40 | 6.19E-06 | 6.18E-06 | 6.29E-06 | 6.48E-06 | 6.63E-06 |
| 41 | 5.38E-06 | 5.36E-06 | 5.47E-06 | 5.69E-06 | 5.85E-06 |
| 42 | 4.55E-06 | 4.55E-06 | 4.66E-06 | 4.87E-06 | 5.01E-06 |
| 43 | 3.64E-06 | 3.65E-06 | 3.74E-06 | 3.93E-06 | 4.08E-06 |
| 44 | 2.67E-06 | 2.69E-06 | 2.76E-06 | 3.02E-06 | 3.12E-06 |
| 45 | 1.65E-06 | 1.65E-06 | 1.76E-06 | 2.04E-06 | 2.15E-06 |
| 46 | 5.88E-07 | 5.88E-07 | 6.79E-07 | 9.32E-07 | 1.04E-06 |
| 47 | 6.37E-07 | 6.09E-07 | 5.05E-07 | 2.69E-07 | 1.97E-07 |
| 48 | 1.79E-06 | 1.76E-06 | 1.61E-06 | 1.39E-06 | 1.27E-06 |
| 49 | 2.96E-06 | 2.95E-06 | 2.85E-06 | 2.65E-06 | 2.53E-06 |
| 50 | 4.19E-06 | 4.18E-06 | 4.07E-06 | 3.90E-06 | 3.79E-06 |
| 51 | 5.49E-06 | 5.47E-06 | 5.33E-06 | 5.13E-06 | 5.05E-06 |
| 52 | 6.76E-06 | 6.75E-06 | 6.58E-06 | 6.35E-06 | 6.29E-06 |
| 53 | 8.08E-06 | 8.06E-06 | 7.93E-06 | 7.74E-06 | 7.66E-06 |
| 54 | 9.44E-06 | 9.41E-06 | 9.29E-06 | 9.12E-06 | 9.04E-06 |
| 55 | 1.08E-05 | 1.08E-05 | 1.07E-05 | 1.05E-05 | 1.04E-05 |
| 56 | 1.22E-05 | 1.21E-05 | 1.20E-05 | 1.18E-05 | 1.17E-05 |
| 57 | 1.35E-05 | 1.35E-05 | 1.34E-05 | 1.33E-05 | 1.32E-05 |
| 58 | 1.49E-05 | 1.49E-05 | 1.48E-05 | 1.46E-05 | 1.45E-05 |
| 59 | 1.63E-05 | 1.63E-05 | 1.62E-05 | 1.60E-05 | 1.59E-05 |
| 61 | 1.77E-05 | 1.76E-05 | 1.75E-05 | 1.73E-05 | 1.73E-05 |
| 62 | 1.86E-05 | 1.86E-05 | 1.84E-05 | 1.83E-05 | 1.82E-05 |

**Table 6: Displacements – Sample 3(Mode 2)**

| pt | L5 | L4 | L3 | L2 | L1 |
|---|---|---|---|---|---|
| 1 | 2.27E-06 | 2.32E-06 | 2.38E-06 | 2.45E-06 | 2.47E-06 |
| 2 | 2.02E-06 | 2.04E-06 | 2.13E-06 | 2.20E-06 | 2.24E-06 |
| 3 | 1.65E-06 | 1.66E-06 | 1.73E-06 | 1.83E-06 | 1.86E-06 |
| 4 | 1.34E-06 | 1.33E-06 | 1.39E-06 | 1.47E-06 | 1.52E-06 |
| 5 | 9.93E-07 | 9.89E-07 | 1.04E-06 | 1.12E-06 | 1.18E-06 |
| 6 | 6.32E-07 | 6.48E-07 | 7.08E-07 | 7.99E-07 | 8.36E-07 |
| 7 | 3.40E-07 | 3.33E-07 | 3.87E-07 | 4.68E-07 | 5.09E-07 |
| 8 | 6.75E-08 | 6.52E-08 | 8.86E-08 | 1.82E-07 | 2.24E-07 |
| 9 | 2.44E-07 | 2.59E-07 | 2.17E-07 | 1.39E-07 | 1.19E-07 |
| 10 | 5.26E-07 | 5.38E-07 | 4.75E-07 | 3.92E-07 | 3.58E-07 |
| 11 | 7.90E-07 | 8.04E-07 | 7.24E-07 | 6.43E-07 | 6.00E-07 |
| 12 | 1.03E-06 | 1.03E-06 | 9.52E-07 | 8.69E-07 | 8.25E-07 |
| 13 | 1.22E-06 | 1.21E-06 | 1.15E-06 | 1.07E-06 | 1.01E-06 |
| 14 | 1.38E-06 | 1.39E-06 | 1.34E-06 | 1.23E-06 | 1.16E-06 |
| 15 | 1.55E-06 | 1.57E-06 | 1.51E-06 | 1.43E-06 | 1.37E-06 |
| 16 | 1.69E-06 | 1.70E-06 | 1.62E-06 | 1.57E-06 | 1.54E-06 |
| 17 | 1.78E-06 | 1.79E-06 | 1.70E-06 | 1.65E-06 | 1.63E-06 |
| 18 | 1.86E-06 | 1.84E-06 | 1.77E-06 | 1.70E-06 | 1.69E-06 |
| 19 | 1.91E-06 | 1.88E-06 | 1.82E-06 | 1.75E-06 | 1.74E-06 |
| 20 | 1.93E-06 | 1.89E-06 | 1.83E-06 | 1.77E-06 | 1.76E-06 |
| 21 | 1.91E-06 | 1.88E-06 | 1.82E-06 | 1.75E-06 | 1.75E-06 |
| 22 | 1.88E-06 | 1.85E-06 | 1.79E-06 | 1.72E-06 | 1.71E-06 |
| 23 | 1.82E-06 | 1.78E-06 | 1.71E-06 | 1.65E-06 | 1.64E-06 |
| 24 | 1.73E-06 | 1.70E-06 | 1.62E-06 | 1.54E-06 | 1.52E-06 |
| 25 | 1.62E-06 | 1.59E-06 | 1.52E-06 | 1.44E-06 | 1.41E-06 |
| 26 | 1.47E-06 | 1.44E-06 | 1.36E-06 | 1.29E-06 | 1.29E-06 |
| 27 | 1.32E-06 | 1.29E-06 | 1.21E-06 | 1.12E-06 | 1.12E-06 |
| 28 | 1.14E-06 | 1.13E-06 | 1.05E-06 | 9.58E-07 | 9.53E-07 |
| 29 | 9.59E-07 | 9.28E-07 | 8.42E-07 | 7.62E-07 | 7.61E-07 |
| 30 | 7.50E-07 | 7.20E-07 | 6.37E-07 | 5.76E-07 | 5.78E-07 |
| 31 | 5.55E-07 | 5.22E-07 | 4.58E-07 | 3.79E-07 | 3.72E-07 |
| 32 | 3.34E-07 | 3.24E-07 | 2.57E-07 | 1.87E-07 | 1.71E-07 |
| 33 | 1.46E-07 | 1.26E-07 | 8.14E-08 | 5.88E-08 | 6.16E-08 |
| 34 | 9.46E-08 | 1.04E-07 | 1.45E-07 | 2.20E-07 | 2.32E-07 |
| 35 | 2.79E-07 | 3.03E-07 | 3.47E-07 | 4.13E-07 | 4.24E-07 |
| 36 | 4.56E-07 | 4.87E-07 | 5.22E-07 | 5.85E-07 | 5.77E-07 |
| 37 | 6.04E-07 | 6.34E-07 | 6.80E-07 | 7.45E-07 | 7.51E-07 |
| 38 | 7.57E-07 | 7.75E-07 | 8.14E-07 | 8.90E-07 | 8.84E-07 |
| 39 | 8.74E-07 | 8.97E-07 | 9.35E-07 | 1.01E-06 | 1.02E-06 |
| 40 | 9.88E-07 | 1.00E-06 | 1.04E-06 | 1.09E-06 | 1.10E-06 |
| 41 | 1.06E-06 | 1.07E-06 | 1.11E-06 | 1.15E-06 | 1.16E-06 |
| 42 | 1.11E-06 | 1.11E-06 | 1.15E-06 | 1.20E-06 | 1.22E-06 |
| 43 | 1.12E-06 | 1.12E-06 | 1.15E-06 | 1.21E-06 | 1.24E-06 |
| 44 | 1.10E-06 | 1.10E-06 | 1.13E-06 | 1.18E-06 | 1.22E-06 |
| 45 | 1.05E-06 | 1.06E-06 | 1.07E-06 | 1.12E-06 | 1.16E-06 |
| 46 | 9.61E-07 | 9.55E-07 | 9.75E-07 | 1.02E-06 | 1.07E-06 |
| 47 | 8.46E-07 | 8.44E-07 | 8.64E-07 | 9.11E-07 | 9.59E-07 |
| 48 | 7.00E-07 | 7.00E-07 | 7.25E-07 | 7.84E-07 | 8.18E-07 |
| 49 | 5.34E-07 | 5.35E-07 | 5.65E-07 | 6.29E-07 | 6.67E-07 |
| 50 | 3.51E-07 | 3.50E-07 | 3.68E-07 | 4.28E-07 | 4.61E-07 |
| 51 | 1.46E-07 | 1.44E-07 | 1.68E-07 | 2.20E-07 | 2.59E-07 |
| 52 | 8.18E-08 | 8.64E-08 | 5.59E-08 | 1.92E-08 | 4.81E-08 |
| 53 | 3.20E-07 | 3.34E-07 | 3.01E-07 | 2.40E-07 | 2.03E-07 |
| 54 | 5.75E-07 | 5.81E-07 | 5.42E-07 | 4.79E-07 | 4.55E-07 |
| 55 | 8.35E-07 | 8.35E-07 | 7.88E-07 | 7.37E-07 | 7.21E-07 |
| 56 | 1.11E-06 | 1.11E-06 | 1.07E-06 | 1.03E-06 | 1.01E-06 |
| 57 | 1.38E-06 | 1.38E-06 | 1.35E-06 | 1.32E-06 | 1.29E-06 |
| 58 | 1.65E-06 | 1.66E-06 | 1.62E-06 | 1.59E-06 | 1.56E-06 |
| 59 | 1.94E-06 | 1.94E-06 | 1.91E-06 | 1.87E-06 | 1.83E-06 |
| 61 | 2.20E-06 | 2.19E-06 | 2.17E-06 | 2.14E-06 | 2.11E-06 |
| 62 | 2.37E-06 | 2.36E-06 | 2.33E-06 | 2.31E-06 | 2.29E-06 |

## Table 7: Displacements – Sample 3(Mode 3)

| pt | L5 | L4 | L3 | L2 | L1 |
|---|---|---|---|---|---|
| 1 | 1.98E-07 | 1.96E-07 | 1.92E-07 | 1.76E-07 | 1.84E-07 |
| 2 | 1.74E-07 | 1.72E-07 | 1.66E-07 | 1.56E-07 | 1.63E-07 |
| 3 | 1.39E-07 | 1.37E-07 | 1.35E-07 | 1.26E-07 | 1.34E-07 |
| 4 | 1.05E-07 | 1.02E-07 | 9.57E-08 | 9.13E-08 | 9.09E-08 |
| 5 | 7.55E-08 | 6.78E-08 | 6.14E-08 | 4.95E-08 | 5.44E-08 |
| 6 | 5.46E-08 | 4.96E-08 | 3.83E-08 | 2.26E-08 | 2.37E-08 |
| 7 | 3.33E-08 | 2.84E-08 | 2.02E-08 | 1.96E-08 | 2.45E-08 |
| 8 | 3.72E-08 | 3.58E-08 | 3.83E-08 | 5.05E-08 | 5.30E-08 |
| 9 | 5.76E-08 | 6.11E-08 | 6.34E-08 | 7.26E-08 | 7.42E-08 |
| 10 | 8.04E-08 | 8.18E-08 | 8.36E-08 | 9.08E-08 | 9.36E-08 |
| 11 | 9.89E-08 | 1.02E-07 | 1.03E-07 | 1.12E-07 | 1.14E-07 |
| 12 | 1.16E-07 | 1.17E-07 | 1.17E-07 | 1.25E-07 | 1.27E-07 |
| 13 | 1.25E-07 | 1.24E-07 | 1.26E-07 | 1.35E-07 | 1.39E-07 |
| 14 | 1.27E-07 | 1.27E-07 | 1.30E-07 | 1.40E-07 | 1.43E-07 |
| 15 | 1.28E-07 | 1.26E-07 | 1.33E-07 | 1.40E-07 | 1.43E-07 |
| 16 | 1.25E-07 | 1.23E-07 | 1.25E-07 | 1.32E-07 | 1.33E-07 |
| 17 | 1.19E-07 | 1.15E-07 | 1.17E-07 | 1.19E-07 | 1.23E-07 |
| 18 | 1.04E-07 | 1.04E-07 | 1.04E-07 | 1.08E-07 | 1.09E-07 |
| 19 | 8.62E-08 | 8.59E-08 | 8.79E-08 | 9.06E-08 | 9.40E-08 |
| 20 | 6.57E-08 | 6.65E-08 | 6.99E-08 | 7.41E-08 | 7.68E-08 |
| 21 | 4.10E-08 | 4.12E-08 | 4.61E-08 | 5.08E-08 | 5.45E-08 |
| 22 | 2.15E-08 | 2.17E-08 | 2.55E-08 | 2.85E-08 | 3.19E-08 |
| 23 | 1.18E-08 | 1.34E-08 | 1.62E-08 | 1.75E-08 | 1.71E-08 |
| 24 | 3.35E-08 | 3.42E-08 | 3.26E-08 | 2.75E-08 | 2.60E-08 |
| 25 | 5.42E-08 | 5.59E-08 | 5.56E-08 | 5.29E-08 | 4.81E-08 |
| 26 | 7.71E-08 | 7.74E-08 | 7.76E-08 | 7.28E-08 | 6.82E-08 |
| 27 | 9.93E-08 | 1.01E-07 | 9.94E-08 | 9.86E-08 | 9.45E-08 |
| 28 | 1.17E-07 | 1.18E-07 | 1.16E-07 | 1.16E-07 | 1.17E-07 |
| 29 | 1.29E-07 | 1.31E-07 | 1.30E-07 | 1.30E-07 | 1.32E-07 |
| 30 | 1.39E-07 | 1.40E-07 | 1.39E-07 | 1.39E-07 | 1.39E-07 |
| 31 | 1.45E-07 | 1.44E-07 | 1.42E-07 | 1.42E-07 | 1.40E-07 |
| 32 | 1.47E-07 | 1.45E-07 | 1.44E-07 | 1.44E-07 | 1.43E-07 |
| 33 | 1.46E-07 | 1.43E-07 | 1.43E-07 | 1.44E-07 | 1.43E-07 |
| 34 | 1.42E-07 | 1.38E-07 | 1.35E-07 | 1.35E-07 | 1.34E-07 |
| 35 | 1.30E-07 | 1.24E-07 | 1.22E-07 | 1.20E-07 | 1.22E-07 |
| 36 | 1.14E-07 | 1.10E-07 | 1.08E-07 | 1.07E-07 | 1.09E-07 |
| 37 | 9.60E-08 | 9.41E-08 | 9.18E-08 | 8.90E-08 | 9.19E-08 |
| 38 | 7.52E-08 | 7.50E-08 | 7.26E-08 | 7.17E-08 | 7.22E-08 |
| 39 | 5.50E-08 | 5.48E-08 | 5.36E-08 | 5.32E-08 | 5.52E-08 |
| 40 | 3.62E-08 | 3.61E-08 | 3.82E-08 | 3.74E-08 | 3.86E-08 |
| 41 | 2.22E-08 | 2.36E-08 | 2.74E-08 | 2.80E-08 | 2.80E-08 |
| 42 | 3.14E-08 | 3.11E-08 | 3.31E-08 | 3.55E-08 | 3.57E-08 |
| 43 | 4.76E-08 | 4.82E-08 | 4.77E-08 | 4.99E-08 | 4.86E-08 |
| 44 | 6.10E-08 | 6.27E-08 | 6.19E-08 | 6.34E-08 | 6.31E-08 |
| 45 | 7.31E-08 | 7.40E-08 | 7.30E-08 | 7.39E-08 | 7.43E-08 |
| 46 | 8.36E-08 | 8.38E-08 | 8.14E-08 | 8.25E-08 | 8.30E-08 |
| 47 | 8.95E-08 | 8.69E-08 | 8.68E-08 | 8.82E-08 | 9.01E-08 |
| 48 | 9.09E-08 | 8.81E-08 | 8.89E-08 | 9.10E-08 | 9.22E-08 |
| 49 | 8.81E-08 | 8.59E-08 | 8.78E-08 | 8.91E-08 | 9.02E-08 |
| 50 | 8.28E-08 | 8.22E-08 | 8.37E-08 | 8.60E-08 | 8.59E-08 |
| 51 | 7.63E-08 | 7.57E-08 | 7.59E-08 | 7.89E-08 | 7.99E-08 |
| 52 | 6.67E-08 | 6.63E-08 | 6.55E-08 | 6.84E-08 | 6.93E-08 |
| 53 | 4.99E-08 | 4.98E-08 | 4.88E-08 | 5.12E-08 | 5.14E-08 |
| 54 | 3.24E-08 | 3.13E-08 | 2.99E-08 | 3.17E-08 | 3.21E-08 |
| 55 | 1.24E-08 | 9.37E-09 | 9.36E-09 | 1.38E-08 | 1.61E-08 |
| 56 | 9.59E-09 | 1.28E-08 | 1.54E-08 | 1.44E-08 | 1.41E-08 |
| 57 | 3.31E-08 | 3.75E-08 | 3.74E-08 | 3.63E-08 | 3.39E-08 |
| 58 | 5.88E-08 | 6.27E-08 | 6.61E-08 | 6.29E-08 | 6.10E-08 |
| 59 | 8.42E-08 | 8.76E-08 | 9.14E-08 | 8.46E-08 | 8.26E-08 |
| 61 | 1.11E-07 | 1.15E-07 | 1.16E-07 | 1.08E-07 | 1.05E-07 |
| 62 | 1.28E-07 | 1.30E-07 | 1.33E-07 | 1.26E-07 | 1.26E-07 |

## Table 8: Displacements – Sample 3(Mode 4)

| pt | L5 | L4 | L3 | L2 | L1 |
|---|---|---|---|---|---|
| 1 | 1.07E-07 | 1.05E-07 | 1.01E-07 | 9.35E-08 | 9.69E-08 |
| 2 | 8.83E-08 | 8.89E-08 | 8.31E-08 | 7.51E-08 | 7.60E-08 |
| 3 | 5.32E-08 | 5.34E-08 | 5.11E-08 | 4.40E-08 | 4.82E-08 |
| 4 | 2.20E-08 | 2.11E-08 | 1.93E-08 | 1.70E-08 | 1.85E-08 |
| 5 | 4.95E-09 | 5.71E-09 | 6.94E-09 | 9.34E-09 | 5.46E-09 |
| 6 | 3.05E-08 | 3.22E-08 | 3.05E-08 | 2.89E-08 | 2.46E-08 |
| 7 | 4.80E-08 | 4.95E-08 | 4.95E-08 | 5.27E-08 | 4.99E-08 |
| 8 | 6.26E-08 | 6.29E-08 | 6.23E-08 | 6.75E-08 | 6.86E-08 |
| 9 | 7.95E-08 | 7.81E-08 | 7.87E-08 | 8.15E-08 | 8.24E-08 |
| 10 | 8.64E-08 | 8.57E-08 | 8.45E-08 | 8.74E-08 | 8.72E-08 |
| 11 | 8.76E-08 | 8.62E-08 | 8.68E-08 | 8.67E-08 | 8.93E-08 |
| 12 | 8.28E-08 | 8.28E-08 | 8.11E-08 | 8.18E-08 | 8.35E-08 |
| 13 | 7.46E-08 | 7.47E-08 | 7.35E-08 | 7.39E-08 | 7.56E-08 |
| 14 | 6.30E-08 | 6.11E-08 | 5.89E-08 | 5.98E-08 | 6.26E-08 |
| 15 | 4.69E-08 | 4.49E-08 | 4.19E-08 | 4.45E-08 | 4.68E-08 |
| 16 | 2.63E-08 | 2.47E-08 | 2.47E-08 | 2.51E-08 | 2.74E-08 |
| 17 | 4.74E-09 | 4.53E-09 | 4.99E-09 | 5.22E-09 | 5.37E-09 |
| 18 | 1.47E-08 | 1.52E-08 | 1.62E-08 | 1.85E-08 | 1.77E-08 |
| 19 | 3.47E-08 | 3.49E-08 | 3.67E-08 | 3.86E-08 | 3.85E-08 |
| 20 | 5.16E-08 | 5.24E-08 | 5.47E-08 | 5.81E-08 | 5.55E-08 |
| 21 | 6.25E-08 | 6.34E-08 | 6.80E-08 | 7.10E-08 | 6.91E-08 |
| 22 | 7.40E-08 | 7.44E-08 | 7.69E-08 | 8.02E-08 | 7.82E-08 |
| 23 | 8.48E-08 | 8.41E-08 | 8.49E-08 | 8.55E-08 | 8.65E-08 |
| 24 | 8.89E-08 | 8.72E-08 | 8.58E-08 | 8.66E-08 | 8.79E-08 |
| 25 | 8.79E-08 | 8.59E-08 | 8.36E-08 | 8.33E-08 | 8.48E-08 |
| 26 | 8.13E-08 | 7.94E-08 | 7.74E-08 | 7.72E-08 | 8.01E-08 |
| 27 | 7.00E-08 | 6.87E-08 | 6.65E-08 | 6.90E-08 | 7.20E-08 |
| 28 | 5.79E-08 | 5.62E-08 | 5.39E-08 | 5.38E-08 | 5.71E-08 |
| 29 | 4.41E-08 | 4.24E-08 | 3.82E-08 | 3.63E-08 | 3.90E-08 |
| 30 | 2.34E-08 | 2.21E-08 | 1.85E-08 | 1.81E-08 | 2.09E-08 |
| 31 | 3.75E-09 | 2.77E-09 | 2.52E-10 | 1.92E-09 | 8.88E-10 |
| 32 | 1.86E-08 | 1.94E-08 | 2.00E-08 | 2.05E-08 | 1.93E-08 |
| 33 | 3.74E-08 | 3.77E-08 | 3.66E-08 | 3.75E-08 | 3.66E-08 |
| 34 | 5.25E-08 | 5.35E-08 | 5.11E-08 | 5.22E-08 | 5.27E-08 |
| 35 | 6.43E-08 | 6.53E-08 | 6.41E-08 | 6.43E-08 | 6.46E-08 |
| 36 | 7.12E-08 | 7.27E-08 | 7.29E-08 | 7.28E-08 | 7.24E-08 |
| 37 | 7.58E-08 | 7.52E-08 | 7.73E-08 | 7.72E-08 | 7.74E-08 |
| 38 | 7.81E-08 | 7.71E-08 | 7.80E-08 | 7.99E-08 | 8.08E-08 |
| 39 | 7.67E-08 | 7.53E-08 | 7.57E-08 | 7.80E-08 | 7.94E-08 |
| 40 | 6.78E-08 | 6.76E-08 | 6.73E-08 | 6.99E-08 | 7.05E-08 |
| 41 | 5.47E-08 | 5.43E-08 | 5.37E-08 | 5.40E-08 | 5.51E-08 |
| 42 | 3.81E-08 | 3.80E-08 | 3.75E-08 | 3.68E-08 | 3.74E-08 |
| 43 | 1.75E-08 | 1.80E-08 | 1.87E-08 | 1.82E-08 | 1.88E-08 |
| 44 | 5.92E-09 | 6.22E-09 | 5.25E-09 | 4.12E-09 | 3.28E-09 |
| 45 | 2.59E-08 | 2.63E-08 | 2.71E-08 | 2.62E-08 | 2.54E-08 |
| 46 | 4.70E-08 | 4.70E-08 | 4.68E-08 | 4.60E-08 | 4.55E-08 |
| 47 | 6.83E-08 | 6.81E-08 | 6.65E-08 | 6.59E-08 | 6.56E-08 |
| 48 | 8.60E-08 | 8.59E-08 | 8.40E-08 | 8.23E-08 | 8.16E-08 |
| 49 | 9.53E-08 | 9.52E-08 | 9.25E-08 | 9.12E-08 | 9.04E-08 |
| 50 | 1.04E-07 | 1.03E-07 | 9.90E-08 | 9.75E-08 | 9.72E-08 |
| 51 | 1.08E-07 | 1.05E-07 | 1.00E-07 | 9.83E-08 | 9.82E-08 |
| 52 | 1.05E-07 | 1.01E-07 | 9.69E-08 | 9.44E-08 | 9.56E-08 |
| 53 | 9.17E-08 | 8.89E-08 | 8.69E-08 | 8.57E-08 | 8.72E-08 |
| 54 | 7.63E-08 | 7.42E-08 | 7.17E-08 | 6.82E-08 | 6.89E-08 |
| 55 | 5.88E-08 | 5.69E-08 | 5.10E-08 | 4.78E-08 | 4.72E-08 |
| 56 | 3.27E-08 | 3.06E-08 | 2.54E-08 | 2.52E-08 | 2.56E-08 |
| 57 | 3.45E-09 | 1.32E-09 | 3.82E-09 | 5.58E-09 | 5.56E-09 |
| 58 | 2.87E-08 | 2.99E-08 | 3.49E-08 | 3.83E-08 | 3.90E-08 |
| 59 | 6.04E-08 | 6.30E-08 | 6.65E-08 | 7.03E-08 | 7.06E-08 |
| 61 | 9.40E-08 | 9.74E-08 | 1.02E-07 | 1.04E-07 | 1.04E-07 |
| 62 | 1.17E-07 | 1.22E-07 | 1.26E-07 | 1.29E-07 | 1.28E-07 |

## Table 9: Displacements – Sample 7(Mode 1)

| pt | L5 | L4 | L3 | L2 | L1 |
|---|---|---|---|---|---|
| 1 | 1.52E-05 | 1.50E-05 | 1.47E-05 | 1.44E-05 | 1.43E-05 |
| 2 | 1.46E-05 | 1.43E-05 | 1.43E-05 | 1.37E-05 | 1.36E-05 |
| 3 | 1.34E-05 | 1.34E-05 | 1.35E-05 | 1.26E-05 | 1.23E-05 |
| 4 | 1.21E-05 | 1.21E-05 | 1.21E-05 | 1.13E-05 | 1.10E-05 |
| 5 | 1.08E-05 | 1.05E-05 | 1.04E-05 | 9.73E-06 | 9.76E-06 |
| 6 | 9.46E-06 | 9.29E-06 | 8.87E-06 | 8.53E-06 | 8.52E-06 |
| 7 | 8.28E-06 | 8.05E-06 | 7.74E-06 | 7.33E-06 | 7.33E-06 |
| 8 | 6.99E-06 | 6.80E-06 | 6.46E-06 | 6.14E-06 | 6.05E-06 |
| 9 | 5.70E-06 | 5.43E-06 | 5.19E-06 | 4.88E-06 | 4.83E-06 |
| 10 | 4.45E-06 | 4.24E-06 | 3.98E-06 | 3.65E-06 | 3.59E-06 |
| 11 | 3.26E-06 | 3.13E-06 | 2.82E-06 | 2.50E-06 | 2.39E-06 |
| 12 | 2.16E-06 | 1.95E-06 | 1.64E-06 | 1.30E-06 | 1.26E-06 |
| 13 | 9.93E-07 | 7.88E-07 | 3.77E-07 | 1.79E-07 | 1.72E-07 |
| 14 | 4.64E-07 | 5.23E-07 | 7.47E-07 | 1.05E-06 | 1.03E-06 |
| 15 | 1.36E-06 | 1.53E-06 | 1.88E-06 | 2.16E-06 | 2.15E-06 |
| 16 | 2.32E-06 | 2.55E-06 | 2.84E-06 | 3.15E-06 | 3.12E-06 |
| 17 | 3.29E-06 | 3.49E-06 | 3.82E-06 | 4.05E-06 | 4.11E-06 |
| 18 | 4.19E-06 | 4.40E-06 | 4.69E-06 | 4.97E-06 | 5.10E-06 |
| 19 | 5.08E-06 | 5.28E-06 | 5.56E-06 | 5.89E-06 | 6.03E-06 |
| 20 | 5.89E-06 | 6.08E-06 | 6.35E-06 | 6.61E-06 | 6.75E-06 |
| 21 | 6.63E-06 | 6.84E-06 | 7.11E-06 | 7.39E-06 | 7.44E-06 |
| 22 | 7.30E-06 | 7.51E-06 | 7.81E-06 | 8.09E-06 | 8.15E-06 |
| 23 | 7.94E-06 | 8.16E-06 | 8.44E-06 | 8.72E-06 | 8.77E-06 |
| 24 | 8.49E-06 | 8.70E-06 | 8.98E-06 | 9.26E-06 | 9.32E-06 |
| 25 | 8.97E-06 | 9.17E-06 | 9.46E-06 | 9.73E-06 | 9.77E-06 |
| 26 | 9.37E-06 | 9.55E-06 | 9.84E-06 | 1.01E-05 | 1.01E-05 |
| 27 | 9.68E-06 | 9.87E-06 | 1.02E-05 | 1.04E-05 | 1.05E-05 |
| 28 | 9.93E-06 | 1.01E-05 | 1.04E-05 | 1.07E-05 | 1.08E-05 |
| 29 | 1.01E-05 | 1.03E-05 | 1.05E-05 | 1.08E-05 | 1.10E-05 |
| 30 | 1.02E-05 | 1.03E-05 | 1.06E-05 | 1.09E-05 | 1.12E-05 |
| 31 | 1.02E-05 | 1.03E-05 | 1.05E-05 | 1.09E-05 | 1.12E-05 |
| 32 | 1.01E-05 | 1.02E-05 | 1.04E-05 | 1.08E-05 | 1.11E-05 |
| 33 | 1.00E-05 | 1.01E-05 | 1.02E-05 | 1.06E-05 | 1.09E-05 |
| 34 | 9.76E-06 | 9.74E-06 | 9.85E-06 | 1.03E-05 | 1.06E-05 |
| 35 | 9.39E-06 | 9.36E-06 | 9.45E-06 | 9.92E-06 | 1.02E-05 |
| 36 | 8.94E-06 | 8.98E-06 | 9.13E-06 | 9.52E-06 | 9.78E-06 |
| 37 | 8.41E-06 | 8.47E-06 | 8.69E-06 | 8.99E-06 | 9.24E-06 |
| 38 | 7.81E-06 | 7.85E-06 | 8.08E-06 | 8.38E-06 | 8.63E-06 |
| 39 | 7.13E-06 | 7.17E-06 | 7.38E-06 | 7.67E-06 | 7.94E-06 |
| 40 | 6.37E-06 | 6.41E-06 | 6.60E-06 | 6.90E-06 | 7.16E-06 |
| 41 | 5.52E-06 | 5.56E-06 | 5.77E-06 | 6.05E-06 | 6.30E-06 |
| 42 | 4.59E-06 | 4.64E-06 | 4.86E-06 | 5.16E-06 | 5.37E-06 |
| 43 | 3.63E-06 | 3.67E-06 | 3.88E-06 | 4.15E-06 | 4.38E-06 |
| 44 | 2.62E-06 | 2.66E-06 | 2.84E-06 | 3.12E-06 | 3.35E-06 |
| 45 | 1.57E-06 | 1.59E-06 | 1.74E-06 | 2.00E-06 | 2.24E-06 |
| 46 | 6.44E-07 | 6.34E-07 | 6.73E-07 | 8.81E-07 | 1.09E-06 |
| 47 | 1.10E-06 | 1.05E-06 | 7.92E-07 | 4.57E-07 | 1.90E-07 |
| 48 | 2.26E-06 | 2.22E-06 | 1.99E-06 | 1.66E-06 | 1.40E-06 |
| 49 | 3.51E-06 | 3.48E-06 | 3.28E-06 | 2.98E-06 | 2.72E-06 |
| 50 | 4.84E-06 | 4.80E-06 | 4.61E-06 | 4.32E-06 | 4.07E-06 |
| 51 | 6.21E-06 | 6.17E-06 | 5.97E-06 | 5.69E-06 | 5.42E-06 |
| 52 | 7.61E-06 | 7.56E-06 | 7.34E-06 | 7.05E-06 | 6.80E-06 |
| 53 | 9.06E-06 | 9.01E-06 | 8.76E-06 | 8.44E-06 | 8.19E-06 |
| 54 | 1.05E-05 | 1.04E-05 | 1.02E-05 | 9.88E-06 | 9.65E-06 |
| 55 | 1.19E-05 | 1.19E-05 | 1.16E-05 | 1.13E-05 | 1.11E-05 |
| 56 | 1.34E-05 | 1.33E-05 | 1.31E-05 | 1.28E-05 | 1.26E-05 |
| 57 | 1.49E-05 | 1.49E-05 | 1.46E-05 | 1.43E-05 | 1.41E-05 |
| 58 | 1.63E-05 | 1.63E-05 | 1.60E-05 | 1.58E-05 | 1.56E-05 |
| 59 | 1.78E-05 | 1.77E-05 | 1.75E-05 | 1.73E-05 | 1.70E-05 |
| 61 | 1.92E-05 | 1.91E-05 | 1.88E-05 | 1.86E-05 | 1.84E-05 |
| 62 | 2.01E-05 | 1.99E-05 | 1.96E-05 | 1.93E-05 | 1.92E-05 |

**Table 10: Displacements – Sample 7(Mode 2)**

| pt | L5 | L4 | L3 | L2 | L1 |
|---|---|---|---|---|---|
| 1 | 2.07E-06 | 2.11E-06 | 2.15E-06 | 2.20E-06 | 2.20E-06 |
| 2 | 1.89E-06 | 1.90E-06 | 1.95E-06 | 2.00E-06 | 2.01E-06 |
| 3 | 1.55E-06 | 1.55E-06 | 1.60E-06 | 1.69E-06 | 1.71E-06 |
| 4 | 1.22E-06 | 1.20E-06 | 1.26E-06 | 1.37E-06 | 1.43E-06 |
| 5 | 8.62E-07 | 8.52E-07 | 9.04E-07 | 1.05E-06 | 1.12E-06 |
| 6 | 5.68E-07 | 5.70E-07 | 6.27E-07 | 7.23E-07 | 7.67E-07 |
| 7 | 2.68E-07 | 2.77E-07 | 3.27E-07 | 4.05E-07 | 4.31E-07 |
| 8 | 3.20E-08 | 4.28E-08 | 5.57E-08 | 9.72E-08 | 1.30E-07 |
| 9 | 3.19E-07 | 3.26E-07 | 2.69E-07 | 2.21E-07 | 2.01E-07 |
| 10 | 6.06E-07 | 6.02E-07 | 5.31E-07 | 4.82E-07 | 4.64E-07 |
| 11 | 8.57E-07 | 8.57E-07 | 7.89E-07 | 7.56E-07 | 7.28E-07 |
| 12 | 1.11E-06 | 1.09E-06 | 1.03E-06 | 9.85E-07 | 9.55E-07 |
| 13 | 1.30E-06 | 1.29E-06 | 1.24E-06 | 1.19E-06 | 1.17E-06 |
| 14 | 1.47E-06 | 1.47E-06 | 1.43E-06 | 1.36E-06 | 1.33E-06 |
| 15 | 1.62E-06 | 1.63E-06 | 1.59E-06 | 1.52E-06 | 1.50E-06 |
| 16 | 1.76E-06 | 1.77E-06 | 1.72E-06 | 1.65E-06 | 1.63E-06 |
| 17 | 1.85E-06 | 1.87E-06 | 1.81E-06 | 1.76E-06 | 1.75E-06 |
| 18 | 1.92E-06 | 1.93E-06 | 1.88E-06 | 1.83E-06 | 1.82E-06 |
| 19 | 1.97E-06 | 1.95E-06 | 1.91E-06 | 1.86E-06 | 1.84E-06 |
| 20 | 1.98E-06 | 1.94E-06 | 1.91E-06 | 1.85E-06 | 1.83E-06 |
| 21 | 1.97E-06 | 1.92E-06 | 1.88E-06 | 1.82E-06 | 1.81E-06 |
| 22 | 1.94E-06 | 1.88E-06 | 1.83E-06 | 1.77E-06 | 1.77E-06 |
| 23 | 1.85E-06 | 1.80E-06 | 1.74E-06 | 1.70E-06 | 1.71E-06 |
| 24 | 1.74E-06 | 1.69E-06 | 1.64E-06 | 1.59E-06 | 1.59E-06 |
| 25 | 1.60E-06 | 1.56E-06 | 1.50E-06 | 1.45E-06 | 1.45E-06 |
| 26 | 1.45E-06 | 1.41E-06 | 1.36E-06 | 1.31E-06 | 1.32E-06 |
| 27 | 1.30E-06 | 1.27E-06 | 1.20E-06 | 1.14E-06 | 1.14E-06 |
| 28 | 1.11E-06 | 1.10E-06 | 1.03E-06 | 9.62E-07 | 9.58E-07 |
| 29 | 9.16E-07 | 8.94E-07 | 8.39E-07 | 7.69E-07 | 7.52E-07 |
| 30 | 6.92E-07 | 6.64E-07 | 6.21E-07 | 5.61E-07 | 5.45E-07 |
| 31 | 4.78E-07 | 4.39E-07 | 4.05E-07 | 3.38E-07 | 3.25E-07 |
| 32 | 2.62E-07 | 2.40E-07 | 2.05E-07 | 1.27E-07 | 1.16E-07 |
| 33 | 9.75E-08 | 8.59E-08 | 8.17E-08 | 1.12E-07 | 1.26E-07 |
| 34 | 2.12E-07 | 2.30E-07 | 2.51E-07 | 3.03E-07 | 3.11E-07 |
| 35 | 4.03E-07 | 4.29E-07 | 4.59E-07 | 5.09E-07 | 5.09E-07 |
| 36 | 6.00E-07 | 6.23E-07 | 6.64E-07 | 7.12E-07 | 7.15E-07 |
| 37 | 7.79E-07 | 8.00E-07 | 8.30E-07 | 8.78E-07 | 8.76E-07 |
| 38 | 9.35E-07 | 9.56E-07 | 9.81E-07 | 1.02E-06 | 1.02E-06 |
| 39 | 1.07E-06 | 1.09E-06 | 1.12E-06 | 1.16E-06 | 1.16E-06 |
| 40 | 1.17E-06 | 1.18E-06 | 1.21E-06 | 1.27E-06 | 1.26E-06 |
| 41 | 1.25E-06 | 1.26E-06 | 1.30E-06 | 1.34E-06 | 1.34E-06 |
| 42 | 1.30E-06 | 1.30E-06 | 1.34E-06 | 1.38E-06 | 1.38E-06 |
| 43 | 1.30E-06 | 1.31E-06 | 1.34E-06 | 1.38E-06 | 1.40E-06 |
| 44 | 1.29E-06 | 1.29E-06 | 1.31E-06 | 1.35E-06 | 1.38E-06 |
| 45 | 1.22E-06 | 1.22E-06 | 1.25E-06 | 1.28E-06 | 1.32E-06 |
| 46 | 1.12E-06 | 1.12E-06 | 1.14E-06 | 1.18E-06 | 1.21E-06 |
| 47 | 9.86E-07 | 9.83E-07 | 1.01E-06 | 1.05E-06 | 1.08E-06 |
| 48 | 8.27E-07 | 8.10E-07 | 8.34E-07 | 8.84E-07 | 9.05E-07 |
| 49 | 6.34E-07 | 6.25E-07 | 6.42E-07 | 6.99E-07 | 7.16E-07 |
| 50 | 4.16E-07 | 4.01E-07 | 4.33E-07 | 4.88E-07 | 5.05E-07 |
| 51 | 1.71E-07 | 1.78E-07 | 1.97E-07 | 2.55E-07 | 2.65E-07 |
| 52 | 8.74E-08 | 8.51E-08 | 6.18E-08 | 2.82E-08 | 2.60E-08 |
| 53 | 3.73E-07 | 3.71E-07 | 3.60E-07 | 3.06E-07 | 2.92E-07 |
| 54 | 6.72E-07 | 6.75E-07 | 6.57E-07 | 5.99E-07 | 5.68E-07 |
| 55 | 9.81E-07 | 9.84E-07 | 9.66E-07 | 9.05E-07 | 8.67E-07 |
| 56 | 1.30E-06 | 1.29E-06 | 1.27E-06 | 1.23E-06 | 1.19E-06 |
| 57 | 1.62E-06 | 1.62E-06 | 1.59E-06 | 1.55E-06 | 1.53E-06 |
| 58 | 1.94E-06 | 1.94E-06 | 1.90E-06 | 1.87E-06 | 1.85E-06 |
| 59 | 2.28E-06 | 2.27E-06 | 2.23E-06 | 2.18E-06 | 2.17E-06 |
| 61 | 2.58E-06 | 2.58E-06 | 2.55E-06 | 2.51E-06 | 2.50E-06 |
| 62 | 2.77E-06 | 2.76E-06 | 2.72E-06 | 2.69E-06 | 2.68E-06 |

**Table 11: Displacements – Sample 7(Mode 3)**

| pt | L5 | L4 | L3 | L2 | L1 |
|---|---|---|---|---|---|
| 1 | 1.21E-07 | 1.20E-07 | 1.16E-07 | 1.14E-07 | 1.19E-07 |
| 2 | 1.11E-07 | 1.14E-07 | 1.09E-07 | 1.06E-07 | 1.08E-07 |
| 3 | 8.43E-08 | 8.23E-08 | 7.86E-08 | 7.03E-08 | 7.18E-08 |
| 4 | 6.62E-08 | 6.34E-08 | 5.88E-08 | 5.67E-08 | 5.27E-08 |
| 5 | 4.70E-08 | 4.15E-08 | 3.96E-08 | 4.42E-08 | 4.58E-08 |
| 6 | 2.30E-08 | 1.96E-08 | 2.25E-08 | 3.04E-08 | 3.22E-08 |
| 7 | 8.79E-09 | 1.15E-08 | 1.98E-08 | 2.52E-08 | 2.40E-08 |
| 8 | 3.22E-08 | 3.26E-08 | 3.41E-08 | 3.31E-08 | 3.63E-08 |
| 9 | 5.21E-08 | 5.17E-08 | 4.77E-08 | 4.67E-08 | 4.88E-08 |
| 10 | 6.21E-08 | 6.57E-08 | 6.49E-08 | 6.27E-08 | 6.47E-08 |
| 11 | 6.99E-08 | 7.37E-08 | 7.79E-08 | 7.72E-08 | 7.59E-08 |
| 12 | 8.01E-08 | 8.42E-08 | 8.85E-08 | 9.24E-08 | 9.25E-08 |
| 13 | 8.63E-08 | 8.66E-08 | 8.91E-08 | 9.45E-08 | 9.79E-08 |
| 14 | 8.74E-08 | 8.72E-08 | 8.74E-08 | 9.21E-08 | 9.48E-08 |
| 15 | 8.65E-08 | 8.70E-08 | 8.72E-08 | 8.92E-08 | 9.02E-08 |
| 16 | 8.20E-08 | 8.18E-08 | 8.20E-08 | 8.13E-08 | 8.31E-08 |
| 17 | 7.65E-08 | 7.69E-08 | 7.67E-08 | 7.80E-08 | 7.76E-08 |
| 18 | 7.03E-08 | 7.08E-08 | 7.31E-08 | 7.26E-08 | 7.23E-08 |
| 19 | 5.77E-08 | 5.77E-08 | 5.76E-08 | 5.94E-08 | 5.76E-08 |
| 20 | 4.24E-08 | 4.23E-08 | 4.30E-08 | 4.49E-08 | 4.58E-08 |
| 21 | 3.04E-08 | 3.08E-08 | 2.87E-08 | 3.15E-08 | 3.22E-08 |
| 22 | 2.31E-08 | 1.97E-08 | 1.66E-08 | 1.85E-08 | 2.01E-08 |
| 23 | 2.21E-08 | 2.15E-08 | 1.95E-08 | 1.55E-08 | 1.46E-08 |
| 24 | 2.97E-08 | 3.04E-08 | 3.13E-08 | 2.83E-08 | 2.75E-08 |
| 25 | 4.21E-08 | 4.28E-08 | 4.30E-08 | 4.30E-08 | 4.19E-08 |
| 26 | 5.75E-08 | 5.81E-08 | 5.91E-08 | 5.90E-08 | 5.81E-08 |
| 27 | 7.01E-08 | 7.12E-08 | 7.13E-08 | 7.45E-08 | 7.19E-08 |
| 28 | 8.13E-08 | 8.10E-08 | 8.32E-08 | 8.60E-08 | 8.39E-08 |
| 29 | 9.27E-08 | 9.29E-08 | 9.09E-08 | 9.23E-08 | 8.77E-08 |
| 30 | 9.98E-08 | 9.88E-08 | 9.52E-08 | 9.48E-08 | 9.40E-08 |
| 31 | 1.01E-07 | 1.00E-07 | 9.53E-08 | 9.79E-08 | 9.93E-08 |
| 32 | 1.01E-07 | 9.93E-08 | 9.57E-08 | 9.66E-08 | 9.95E-08 |
| 33 | 9.63E-08 | 9.62E-08 | 9.51E-08 | 9.74E-08 | 9.92E-08 |
| 34 | 9.16E-08 | 9.17E-08 | 9.16E-08 | 9.41E-08 | 9.74E-08 |
| 35 | 8.33E-08 | 8.14E-08 | 8.07E-08 | 8.36E-08 | 8.67E-08 |
| 36 | 6.97E-08 | 6.81E-08 | 6.83E-08 | 7.22E-08 | 7.48E-08 |
| 37 | 5.63E-08 | 5.55E-08 | 5.83E-08 | 6.29E-08 | 6.43E-08 |
| 38 | 4.34E-08 | 4.16E-08 | 4.28E-08 | 4.68E-08 | 4.85E-08 |
| 39 | 3.50E-08 | 3.33E-08 | 3.23E-08 | 3.54E-08 | 3.76E-08 |
| 40 | 2.81E-08 | 2.58E-08 | 2.63E-08 | 2.51E-08 | 2.75E-08 |
| 41 | 2.74E-08 | 2.81E-08 | 2.99E-08 | 3.04E-08 | 2.88E-08 |
| 42 | 3.58E-08 | 3.56E-08 | 3.57E-08 | 3.43E-08 | 3.41E-08 |
| 43 | 4.94E-08 | 4.90E-08 | 4.73E-08 | 4.68E-08 | 4.40E-08 |
| 44 | 6.46E-08 | 6.53E-08 | 6.05E-08 | 5.55E-08 | 5.20E-08 |
| 45 | 7.30E-08 | 7.49E-08 | 6.85E-08 | 6.41E-08 | 6.01E-08 |
| 46 | 7.90E-08 | 8.05E-08 | 7.56E-08 | 6.97E-08 | 6.85E-08 |
| 47 | 8.38E-08 | 8.34E-08 | 7.82E-08 | 7.27E-08 | 6.83E-08 |
| 48 | 8.73E-08 | 8.19E-08 | 7.66E-08 | 6.94E-08 | 6.52E-08 |
| 49 | 8.89E-08 | 8.19E-08 | 7.58E-08 | 7.24E-08 | 6.85E-08 |
| 50 | 8.37E-08 | 7.47E-08 | 6.82E-08 | 6.79E-08 | 6.67E-08 |
| 51 | 7.64E-08 | 6.89E-08 | 6.09E-08 | 5.82E-08 | 6.04E-08 |
| 52 | 5.99E-08 | 5.43E-08 | 4.98E-08 | 4.90E-08 | 5.12E-08 |
| 53 | 4.23E-08 | 3.85E-08 | 3.79E-08 | 3.39E-08 | 3.95E-08 |
| 54 | 3.15E-08 | 2.88E-08 | 2.64E-08 | 2.35E-08 | 2.56E-08 |
| 55 | 1.29E-08 | 1.15E-08 | 1.19E-08 | 1.12E-08 | 1.44E-08 |
| 56 | 4.64E-10 | 8.52E-10 | 1.01E-08 | 1.49E-08 | 1.37E-08 |
| 57 | 1.36E-08 | 1.88E-08 | 2.85E-08 | 3.61E-08 | 3.24E-08 |
| 58 | 4.05E-08 | 4.38E-08 | 4.95E-08 | 4.96E-08 | 4.90E-08 |
| 59 | 6.32E-08 | 6.70E-08 | 6.75E-08 | 6.88E-08 | 6.58E-08 |
| 61 | 8.59E-08 | 9.17E-08 | 9.34E-08 | 9.16E-08 | 8.65E-08 |
| 62 | 9.36E-08 | 9.99E-08 | 1.02E-07 | 1.05E-07 | 1.00E-07 |

**Table 12: Displacements – Sample 8(Mode 1)**

| pt | L5 | L4 | L3 | L2 | L1 |
|---|---|---|---|---|---|
| 1 | 5.55E-08 | 5.16E-08 | 4.99E-08 | 5.31E-08 | 5.69E-08 |
| 2 | 4.40E-08 | 4.03E-08 | 3.96E-08 | 4.14E-08 | 4.43E-08 |
| 3 | 2.52E-08 | 2.29E-08 | 2.40E-08 | 2.57E-08 | 2.67E-08 |
| 4 | 9.72E-09 | 9.42E-09 | 1.06E-08 | 8.75E-09 | 1.09E-08 |
| 5 | 8.97E-09 | 9.54E-09 | 1.18E-08 | 1.24E-08 | 1.03E-08 |
| 6 | 1.86E-08 | 2.06E-08 | 2.08E-08 | 2.48E-08 | 2.16E-08 |
| 7 | 3.64E-08 | 3.53E-08 | 3.59E-08 | 3.43E-08 | 3.45E-08 |
| 8 | 4.91E-08 | 5.01E-08 | 4.78E-08 | 4.55E-08 | 4.49E-08 |
| 9 | 5.55E-08 | 5.55E-08 | 5.54E-08 | 5.24E-08 | 5.20E-08 |
| 10 | 5.64E-08 | 5.62E-08 | 5.63E-08 | 5.42E-08 | 5.51E-08 |
| 11 | 5.88E-08 | 5.83E-08 | 5.60E-08 | 5.53E-08 | 5.61E-08 |
| 12 | 6.22E-08 | 6.03E-08 | 5.44E-08 | 4.83E-08 | 5.01E-08 |
| 13 | 5.34E-08 | 5.31E-08 | 4.60E-08 | 3.98E-08 | 4.12E-08 |
| 14 | 3.90E-08 | 3.73E-08 | 3.59E-08 | 3.45E-08 | 3.75E-08 |
| 15 | 2.71E-08 | 2.51E-08 | 2.51E-08 | 2.59E-08 | 2.84E-08 |
| 16 | 1.56E-08 | 1.36E-08 | 1.36E-08 | 1.29E-08 | 1.43E-08 |
| 17 | 5.95E-10 | 1.51E-09 | 7.99E-10 | 1.47E-09 | 3.76E-09 |
| 18 | 1.54E-08 | 1.70E-08 | 1.35E-08 | 1.25E-08 | 1.16E-08 |
| 19 | 2.75E-08 | 2.98E-08 | 2.74E-08 | 2.76E-08 | 2.77E-08 |
| 20 | 3.85E-08 | 4.04E-08 | 3.91E-08 | 4.00E-08 | 3.96E-08 |
| 21 | 4.74E-08 | 4.83E-08 | 4.72E-08 | 4.83E-08 | 4.78E-08 |
| 22 | 5.37E-08 | 5.43E-08 | 5.58E-08 | 5.92E-08 | 5.81E-08 |
| 23 | 5.71E-08 | 5.76E-08 | 5.91E-08 | 6.27E-08 | 6.29E-08 |
| 24 | 6.22E-08 | 6.17E-08 | 6.04E-08 | 6.26E-08 | 6.37E-08 |
| 25 | 6.35E-08 | 6.22E-08 | 5.87E-08 | 6.04E-08 | 6.20E-08 |
| 26 | 6.06E-08 | 5.97E-08 | 5.69E-08 | 5.74E-08 | 5.85E-08 |
| 27 | 5.10E-08 | 5.07E-08 | 4.99E-08 | 5.08E-08 | 5.11E-08 |
| 28 | 4.11E-08 | 4.07E-08 | 3.97E-08 | 3.80E-08 | 3.74E-08 |
| 29 | 2.77E-08 | 2.72E-08 | 2.42E-08 | 2.24E-08 | 2.16E-08 |
| 30 | 1.37E-08 | 1.19E-08 | 9.17E-09 | 8.03E-09 | 8.61E-09 |
| 31 | 2.37E-09 | 3.05E-09 | 6.50E-09 | 7.51E-09 | 7.72E-09 |
| 32 | 1.90E-08 | 2.02E-08 | 2.04E-08 | 2.12E-08 | 2.11E-08 |
| 33 | 3.29E-08 | 3.39E-08 | 3.47E-08 | 3.60E-08 | 3.68E-08 |
| 34 | 4.53E-08 | 4.68E-08 | 4.71E-08 | 4.93E-08 | 4.96E-08 |
| 35 | 5.49E-08 | 5.67E-08 | 5.69E-08 | 6.00E-08 | 6.01E-08 |
| 36 | 6.14E-08 | 6.17E-08 | 6.18E-08 | 6.46E-08 | 6.60E-08 |
| 37 | 6.47E-08 | 6.54E-08 | 6.46E-08 | 6.83E-08 | 6.94E-08 |
| 38 | 6.49E-08 | 6.37E-08 | 6.45E-08 | 6.74E-08 | 6.85E-08 |
| 39 | 6.05E-08 | 5.90E-08 | 5.94E-08 | 6.14E-08 | 6.26E-08 |
| 40 | 5.53E-08 | 5.47E-08 | 5.47E-08 | 5.48E-08 | 5.47E-08 |
| 41 | 4.56E-08 | 4.54E-08 | 4.58E-08 | 4.49E-08 | 4.51E-08 |
| 42 | 3.56E-08 | 3.48E-08 | 3.52E-08 | 3.22E-08 | 3.13E-08 |
| 43 | 1.98E-08 | 1.94E-08 | 1.83E-08 | 1.54E-08 | 1.38E-08 |
| 44 | 1.03E-08 | 1.17E-08 | 1.13E-08 | 8.40E-09 | 5.68E-09 |
| 45 | 2.32E-08 | 2.36E-08 | 2.45E-08 | 2.23E-08 | 1.98E-08 |
| 46 | 3.88E-08 | 3.98E-08 | 4.01E-08 | 3.85E-08 | 3.54E-08 |
| 47 | 5.36E-08 | 5.56E-08 | 5.41E-08 | 5.19E-08 | 4.96E-08 |
| 48 | 6.72E-08 | 6.94E-08 | 6.75E-08 | 6.49E-08 | 6.35E-08 |
| 49 | 7.82E-08 | 7.85E-08 | 7.56E-08 | 7.35E-08 | 7.25E-08 |
| 50 | 8.73E-08 | 8.37E-08 | 7.90E-08 | 7.57E-08 | 7.44E-08 |
| 51 | 8.93E-08 | 8.48E-08 | 7.92E-08 | 7.57E-08 | 7.43E-08 |
| 52 | 8.71E-08 | 8.39E-08 | 7.85E-08 | 7.32E-08 | 7.37E-08 |
| 53 | 8.19E-08 | 7.81E-08 | 7.01E-08 | 6.53E-08 | 6.56E-08 |
| 54 | 6.77E-08 | 6.02E-08 | 5.42E-08 | 5.17E-08 | 5.45E-08 |
| 55 | 4.94E-08 | 4.10E-08 | 3.68E-08 | 3.66E-08 | 3.73E-08 |
| 56 | 3.29E-08 | 2.38E-08 | 1.98E-08 | 1.54E-08 | 1.46E-08 |
| 57 | 1.26E-08 | 8.19E-09 | 6.91E-09 | 9.17E-09 | 1.01E-08 |
| 58 | 1.89E-08 | 2.48E-08 | 2.90E-08 | 3.19E-08 | 3.29E-08 |
| 59 | 4.74E-08 | 5.24E-08 | 5.88E-08 | 5.97E-08 | 5.90E-08 |
| 61 | 7.22E-08 | 7.86E-08 | 8.32E-08 | 8.51E-08 | 8.51E-08 |
| 62 | 8.70E-08 | 9.23E-08 | 9.89E-08 | 1.03E-07 | 1.03E-07 |

**Table 13: Displacements – Sample 8(Mode 2)**

| pt | L5 | L4 | L3 | L2 | L1 |
|---|---|---|---|---|---|
| 1 | 1.58E-05 | 1.58E-05 | 1.56E-05 | 1.55E-05 | 1.55E-05 |
| 2 | 1.51E-05 | 1.49E-05 | 1.48E-05 | 1.47E-05 | 1.47E-05 |
| 3 | 1.36E-05 | 1.35E-05 | 1.34E-05 | 1.34E-05 | 1.34E-05 |
| 4 | 1.23E-05 | 1.21E-05 | 1.21E-05 | 1.20E-05 | 1.20E-05 |
| 5 | 1.09E-05 | 1.08E-05 | 1.08E-05 | 1.07E-05 | 1.06E-05 |
| 6 | 9.45E-06 | 9.40E-06 | 9.35E-06 | 9.26E-06 | 9.34E-06 |
| 7 | 8.03E-06 | 8.00E-06 | 7.95E-06 | 7.90E-06 | 7.99E-06 |
| 8 | 6.71E-06 | 6.67E-06 | 6.58E-06 | 6.40E-06 | 6.45E-06 |
| 9 | 5.44E-06 | 5.36E-06 | 5.27E-06 | 5.10E-06 | 5.05E-06 |
| 10 | 4.16E-06 | 4.10E-06 | 4.01E-06 | 3.87E-06 | 3.81E-06 |
| 11 | 2.90E-06 | 2.86E-06 | 2.76E-06 | 2.62E-06 | 2.58E-06 |
| 12 | 1.91E-06 | 1.63E-06 | 1.70E-06 | 1.36E-06 | 1.33E-06 |
| 13 | 9.82E-07 | 8.64E-07 | 7.11E-07 | 3.56E-07 | 1.28E-07 |
| 14 | 6.70E-07 | 8.74E-07 | 7.03E-07 | 9.69E-07 | 9.94E-07 |
| 15 | 1.92E-06 | 1.94E-06 | 2.01E-06 | 2.09E-06 | 2.10E-06 |
| 16 | 2.98E-06 | 3.01E-06 | 3.12E-06 | 3.22E-06 | 3.24E-06 |
| 17 | 4.01E-06 | 4.04E-06 | 4.15E-06 | 4.27E-06 | 4.30E-06 |
| 18 | 4.97E-06 | 5.01E-06 | 5.11E-06 | 5.23E-06 | 5.27E-06 |
| 19 | 5.87E-06 | 5.91E-06 | 6.01E-06 | 6.17E-06 | 6.22E-06 |
| 20 | 6.70E-06 | 6.76E-06 | 6.84E-06 | 6.98E-06 | 7.03E-06 |
| 21 | 7.48E-06 | 7.55E-06 | 7.62E-06 | 7.75E-06 | 7.78E-06 |
| 22 | 8.21E-06 | 8.28E-06 | 8.35E-06 | 8.47E-06 | 8.50E-06 |
| 23 | 8.85E-06 | 8.92E-06 | 9.00E-06 | 9.10E-06 | 9.12E-06 |
| 24 | 9.43E-06 | 9.48E-06 | 9.56E-06 | 9.64E-06 | 9.64E-06 |
| 25 | 9.92E-06 | 9.98E-06 | 1.01E-05 | 1.02E-05 | 1.02E-05 |
| 26 | 1.03E-05 | 1.04E-05 | 1.05E-05 | 1.06E-05 | 1.06E-05 |
| 27 | 1.06E-05 | 1.07E-05 | 1.08E-05 | 1.09E-05 | 1.09E-05 |
| 28 | 1.09E-05 | 1.09E-05 | 1.10E-05 | 1.12E-05 | 1.12E-05 |
| 29 | 1.10E-05 | 1.11E-05 | 1.12E-05 | 1.13E-05 | 1.13E-05 |
| 30 | 1.11E-05 | 1.12E-05 | 1.13E-05 | 1.14E-05 | 1.15E-05 |
| 31 | 1.11E-05 | 1.11E-05 | 1.13E-05 | 1.14E-05 | 1.15E-05 |
| 32 | 1.10E-05 | 1.11E-05 | 1.12E-05 | 1.13E-05 | 1.15E-05 |
| 33 | 1.08E-05 | 1.08E-05 | 1.10E-05 | 1.11E-05 | 1.12E-05 |
| 34 | 1.05E-05 | 1.05E-05 | 1.06E-05 | 1.08E-05 | 1.10E-05 |
| 35 | 1.01E-05 | 1.02E-05 | 1.03E-05 | 1.04E-05 | 1.06E-05 |
| 36 | 9.66E-06 | 9.68E-06 | 9.79E-06 | 9.97E-06 | 1.01E-05 |
| 37 | 9.12E-06 | 9.13E-06 | 9.24E-06 | 9.42E-06 | 9.57E-06 |
| 38 | 8.49E-06 | 8.50E-06 | 8.59E-06 | 8.76E-06 | 8.91E-06 |
| 39 | 7.78E-06 | 7.80E-06 | 7.89E-06 | 8.05E-06 | 8.18E-06 |
| 40 | 7.01E-06 | 7.03E-06 | 7.11E-06 | 7.28E-06 | 7.40E-06 |
| 41 | 6.15E-06 | 6.15E-06 | 6.21E-06 | 6.38E-06 | 6.55E-06 |
| 42 | 5.24E-06 | 5.24E-06 | 5.27E-06 | 5.45E-06 | 5.61E-06 |
| 43 | 4.25E-06 | 4.25E-06 | 4.30E-06 | 4.45E-06 | 4.62E-06 |
| 44 | 3.20E-06 | 3.21E-06 | 3.27E-06 | 3.42E-06 | 3.56E-06 |
| 45 | 2.09E-06 | 2.11E-06 | 2.19E-06 | 2.33E-06 | 2.48E-06 |
| 46 | 9.80E-07 | 9.91E-07 | 1.06E-06 | 1.19E-06 | 1.49E-06 |
| 47 | 6.16E-07 | 5.77E-07 | 3.97E-07 | 4.02E-07 | 6.59E-07 |
| 48 | 1.73E-06 | 1.70E-06 | 1.54E-06 | 1.36E-06 | 1.08E-06 |
| 49 | 2.98E-06 | 2.94E-06 | 2.79E-06 | 2.64E-06 | 2.47E-06 |
| 50 | 4.29E-06 | 4.27E-06 | 4.14E-06 | 3.99E-06 | 3.84E-06 |
| 51 | 5.67E-06 | 5.65E-06 | 5.54E-06 | 5.35E-06 | 5.22E-06 |
| 52 | 7.05E-06 | 7.03E-06 | 6.92E-06 | 6.74E-06 | 6.62E-06 |
| 53 | 8.46E-06 | 8.44E-06 | 8.33E-06 | 8.19E-06 | 8.09E-06 |
| 54 | 9.95E-06 | 9.91E-06 | 9.78E-06 | 9.61E-06 | 9.48E-06 |
| 55 | 1.14E-05 | 1.14E-05 | 1.13E-05 | 1.11E-05 | 1.10E-05 |
| 56 | 1.29E-05 | 1.29E-05 | 1.28E-05 | 1.26E-05 | 1.24E-05 |
| 57 | 1.44E-05 | 1.44E-05 | 1.42E-05 | 1.40E-05 | 1.39E-05 |
| 58 | 1.59E-05 | 1.58E-05 | 1.56E-05 | 1.54E-05 | 1.54E-05 |
| 59 | 1.73E-05 | 1.73E-05 | 1.71E-05 | 1.69E-05 | 1.68E-05 |
| 61 | 1.88E-05 | 1.87E-05 | 1.86E-05 | 1.84E-05 | 1.83E-05 |
| 62 | 1.96E-05 | 1.95E-05 | 1.94E-05 | 1.92E-05 | 1.91E-05 |

**Table 13: Displacements – Sample 8(Mode 3)**

| pt | L5 | L4 | L3 | L2 | L1 |
|---|---|---|---|---|---|
| 1 | 2.51E-06 | 2.55E-06 | 2.60E-06 | 2.65E-06 | 2.67E-06 |
| 2 | 2.28E-06 | 2.29E-06 | 2.34E-06 | 2.41E-06 | 2.43E-06 |
| 3 | 1.88E-06 | 1.87E-06 | 1.91E-06 | 2.00E-06 | 2.03E-06 |
| 4 | 1.46E-06 | 1.45E-06 | 1.50E-06 | 1.58E-06 | 1.61E-06 |
| 5 | 1.06E-06 | 1.06E-06 | 1.11E-06 | 1.17E-06 | 1.20E-06 |
| 6 | 6.44E-07 | 6.50E-07 | 7.09E-07 | 7.53E-07 | 7.98E-07 |
| 7 | 2.74E-07 | 2.71E-07 | 3.27E-07 | 3.79E-07 | 4.23E-07 |
| 8 | 1.33E-07 | 1.30E-07 | 8.62E-08 | 7.23E-08 | 6.38E-08 |
| 9 | 4.71E-07 | 4.69E-07 | 4.24E-07 | 3.48E-07 | 3.29E-07 |
| 10 | 7.79E-07 | 7.98E-07 | 7.43E-07 | 6.68E-07 | 6.46E-07 |
| 11 | 1.10E-06 | 1.11E-06 | 1.06E-06 | 9.74E-07 | 9.52E-07 |
| 12 | 1.37E-06 | 1.40E-06 | 1.32E-06 | 1.25E-06 | 1.24E-06 |
| 13 | 1.62E-06 | 1.64E-06 | 1.58E-06 | 1.50E-06 | 1.49E-06 |
| 14 | 1.84E-06 | 1.87E-06 | 1.81E-06 | 1.73E-06 | 1.71E-06 |
| 15 | 2.03E-06 | 2.03E-06 | 1.98E-06 | 1.92E-06 | 1.90E-06 |
| 16 | 2.18E-06 | 2.17E-06 | 2.13E-06 | 2.07E-06 | 2.06E-06 |
| 17 | 2.28E-06 | 2.28E-06 | 2.24E-06 | 2.18E-06 | 2.16E-06 |
| 18 | 2.36E-06 | 2.35E-06 | 2.30E-06 | 2.24E-06 | 2.21E-06 |
| 19 | 2.41E-06 | 2.39E-06 | 2.35E-06 | 2.30E-06 | 2.28E-06 |
| 20 | 2.42E-06 | 2.40E-06 | 2.36E-06 | 2.31E-06 | 2.30E-06 |
| 21 | 2.40E-06 | 2.37E-06 | 2.34E-06 | 2.29E-06 | 2.28E-06 |
| 22 | 2.33E-06 | 2.30E-06 | 2.27E-06 | 2.22E-06 | 2.22E-06 |
| 23 | 2.24E-06 | 2.20E-06 | 2.18E-06 | 2.14E-06 | 2.13E-06 |
| 24 | 2.10E-06 | 2.08E-06 | 2.06E-06 | 2.01E-06 | 2.00E-06 |
| 25 | 1.94E-06 | 1.91E-06 | 1.89E-06 | 1.84E-06 | 1.83E-06 |
| 26 | 1.75E-06 | 1.72E-06 | 1.70E-06 | 1.65E-06 | 1.64E-06 |
| 27 | 1.54E-06 | 1.51E-06 | 1.49E-06 | 1.45E-06 | 1.43E-06 |
| 28 | 1.31E-06 | 1.28E-06 | 1.26E-06 | 1.22E-06 | 1.21E-06 |
| 29 | 1.06E-06 | 1.04E-06 | 1.01E-06 | 9.74E-07 | 9.63E-07 |
| 30 | 8.14E-07 | 7.88E-07 | 7.61E-07 | 7.23E-07 | 7.20E-07 |
| 31 | 5.48E-07 | 5.36E-07 | 5.02E-07 | 4.68E-07 | 4.58E-07 |
| 32 | 2.80E-07 | 2.67E-07 | 2.41E-07 | 1.98E-07 | 1.95E-07 |
| 33 | 6.21E-08 | 6.44E-08 | 7.72E-08 | 1.19E-07 | 1.23E-07 |
| 34 | 2.57E-07 | 2.63E-07 | 2.92E-07 | 3.36E-07 | 3.43E-07 |
| 35 | 4.92E-07 | 5.08E-07 | 5.39E-07 | 5.92E-07 | 5.96E-07 |
| 36 | 7.38E-07 | 7.50E-07 | 7.85E-07 | 8.23E-07 | 8.27E-07 |
| 37 | 9.53E-07 | 9.65E-07 | 9.81E-07 | 1.03E-06 | 1.02E-06 |
| 38 | 1.13E-06 | 1.14E-06 | 1.16E-06 | 1.21E-06 | 1.21E-06 |
| 39 | 1.28E-06 | 1.29E-06 | 1.30E-06 | 1.35E-06 | 1.36E-06 |
| 40 | 1.40E-06 | 1.41E-06 | 1.43E-06 | 1.47E-06 | 1.48E-06 |
| 41 | 1.49E-06 | 1.50E-06 | 1.51E-06 | 1.55E-06 | 1.56E-06 |
| 42 | 1.55E-06 | 1.55E-06 | 1.56E-06 | 1.60E-06 | 1.62E-06 |
| 43 | 1.55E-06 | 1.56E-06 | 1.57E-06 | 1.62E-06 | 1.64E-06 |
| 44 | 1.52E-06 | 1.53E-06 | 1.55E-06 | 1.60E-06 | 1.62E-06 |
| 45 | 1.44E-06 | 1.44E-06 | 1.47E-06 | 1.54E-06 | 1.55E-06 |
| 46 | 1.32E-06 | 1.32E-06 | 1.34E-06 | 1.40E-06 | 1.46E-06 |
| 47 | 1.17E-06 | 1.17E-06 | 1.17E-06 | 1.26E-06 | 1.33E-06 |
| 48 | 9.70E-07 | 9.68E-07 | 9.72E-07 | 1.03E-06 | 1.10E-06 |
| 49 | 7.36E-07 | 7.36E-07 | 7.47E-07 | 8.03E-07 | 8.43E-07 |
| 50 | 4.79E-07 | 4.80E-07 | 4.91E-07 | 5.45E-07 | 5.91E-07 |
| 51 | 2.00E-07 | 1.96E-07 | 2.06E-07 | 2.68E-07 | 3.07E-07 |
| 52 | 1.10E-07 | 1.20E-07 | 1.03E-07 | 4.26E-08 | 2.31E-08 |
| 53 | 4.45E-07 | 4.52E-07 | 4.31E-07 | 3.61E-07 | 3.40E-07 |
| 54 | 7.94E-07 | 8.03E-07 | 7.81E-07 | 7.18E-07 | 6.97E-07 |
| 55 | 1.17E-06 | 1.17E-06 | 1.15E-06 | 1.09E-06 | 1.06E-06 |
| 56 | 1.53E-06 | 1.54E-06 | 1.51E-06 | 1.46E-06 | 1.44E-06 |
| 57 | 1.90E-06 | 1.90E-06 | 1.88E-06 | 1.84E-06 | 1.82E-06 |
| 58 | 2.28E-06 | 2.29E-06 | 2.27E-06 | 2.23E-06 | 2.20E-06 |
| 59 | 2.67E-06 | 2.67E-06 | 2.66E-06 | 2.60E-06 | 2.57E-06 |
| 61 | 3.04E-06 | 3.03E-06 | 3.02E-06 | 2.97E-06 | 2.94E-06 |
| 62 | 3.25E-06 | 3.24E-06 | 3.22E-06 | 3.19E-06 | 3.17E-06 |

**Table 14: Displacements – Sample 8(Mode 3)**

| pt | L5 | L4 | L3 | L2 | L1 |
|---|---|---|---|---|---|
| 1 | 1.54E-07 | 1.61E-07 | 1.70E-07 | 1.73E-07 | 1.72E-07 |
| 2 | 1.43E-07 | 1.46E-07 | 1.49E-07 | 1.50E-07 | 1.51E-07 |
| 3 | 1.11E-07 | 1.10E-07 | 1.14E-07 | 1.18E-07 | 1.22E-07 |
| 4 | 7.67E-08 | 7.43E-08 | 7.70E-08 | 7.90E-08 | 8.04E-08 |
| 5 | 5.08E-08 | 4.71E-08 | 4.90E-08 | 4.62E-08 | 4.49E-08 |
| 6 | 2.77E-08 | 2.67E-08 | 2.83E-08 | 2.77E-08 | 3.10E-08 |
| 7 | 1.99E-08 | 2.65E-08 | 2.96E-08 | 2.27E-08 | 2.34E-08 |
| 8 | 4.62E-08 | 5.31E-08 | 5.69E-08 | 5.64E-08 | 5.13E-08 |
| 9 | 7.52E-08 | 7.61E-08 | 7.81E-08 | 8.12E-08 | 7.83E-08 |
| 10 | 9.35E-08 | 9.41E-08 | 9.26E-08 | 9.67E-08 | 9.39E-08 |
| 11 | 1.07E-07 | 1.08E-07 | 1.07E-07 | 1.07E-07 | 1.06E-07 |
| 12 | 1.18E-07 | 1.17E-07 | 1.16E-07 | 1.15E-07 | 1.14E-07 |
| 13 | 1.31E-07 | 1.28E-07 | 1.24E-07 | 1.24E-07 | 1.21E-07 |
| 14 | 1.36E-07 | 1.31E-07 | 1.29E-07 | 1.29E-07 | 1.27E-07 |
| 15 | 1.32E-07 | 1.29E-07 | 1.27E-07 | 1.29E-07 | 1.30E-07 |
| 16 | 1.26E-07 | 1.23E-07 | 1.21E-07 | 1.21E-07 | 1.23E-07 |
| 17 | 1.16E-07 | 1.13E-07 | 1.10E-07 | 1.08E-07 | 1.11E-07 |
| 18 | 1.01E-07 | 9.81E-08 | 9.72E-08 | 9.89E-08 | 1.00E-07 |
| 19 | 8.50E-08 | 8.40E-08 | 8.09E-08 | 8.24E-08 | 8.37E-08 |
| 20 | 6.69E-08 | 6.58E-08 | 6.38E-08 | 6.42E-08 | 6.45E-08 |
| 21 | 4.47E-08 | 4.35E-08 | 4.24E-08 | 4.21E-08 | 4.14E-08 |
| 22 | 2.37E-08 | 2.15E-08 | 2.05E-08 | 2.16E-08 | 2.22E-08 |
| 23 | 2.03E-08 | 1.94E-08 | 2.04E-08 | 2.03E-08 | 2.03E-08 |
| 24 | 3.80E-08 | 3.93E-08 | 4.01E-08 | 3.68E-08 | 3.34E-08 |
| 25 | 5.58E-08 | 5.78E-08 | 6.25E-08 | 6.11E-08 | 5.84E-08 |
| 26 | 7.69E-08 | 7.76E-08 | 7.98E-08 | 7.91E-08 | 7.68E-08 |
| 27 | 9.69E-08 | 9.78E-08 | 9.84E-08 | 9.73E-08 | 9.69E-08 |
| 28 | 1.13E-07 | 1.14E-07 | 1.15E-07 | 1.15E-07 | 1.14E-07 |
| 29 | 1.27E-07 | 1.29E-07 | 1.30E-07 | 1.29E-07 | 1.28E-07 |
| 30 | 1.37E-07 | 1.38E-07 | 1.38E-07 | 1.36E-07 | 1.34E-07 |
| 31 | 1.40E-07 | 1.40E-07 | 1.40E-07 | 1.36E-07 | 1.35E-07 |
| 32 | 1.41E-07 | 1.41E-07 | 1.39E-07 | 1.38E-07 | 1.36E-07 |
| 33 | 1.37E-07 | 1.35E-07 | 1.35E-07 | 1.37E-07 | 1.38E-07 |
| 34 | 1.25E-07 | 1.25E-07 | 1.27E-07 | 1.32E-07 | 1.35E-07 |
| 35 | 1.14E-07 | 1.14E-07 | 1.15E-07 | 1.19E-07 | 1.22E-07 |
| 36 | 1.01E-07 | 1.01E-07 | 1.02E-07 | 1.03E-07 | 1.05E-07 |
| 37 | 8.33E-08 | 8.30E-08 | 8.30E-08 | 8.37E-08 | 8.41E-08 |
| 38 | 6.69E-08 | 6.64E-08 | 6.68E-08 | 6.71E-08 | 6.66E-08 |
| 39 | 4.77E-08 | 4.70E-08 | 4.85E-08 | 4.97E-08 | 4.97E-08 |
| 40 | 3.35E-08 | 3.33E-08 | 3.34E-08 | 3.39E-08 | 3.29E-08 |
| 41 | 2.92E-08 | 2.93E-08 | 2.93E-08 | 3.03E-08 | 3.04E-08 |
| 42 | 3.80E-08 | 3.82E-08 | 3.95E-08 | 4.05E-08 | 4.08E-08 |
| 43 | 5.25E-08 | 5.29E-08 | 5.29E-08 | 5.34E-08 | 5.21E-08 |
| 44 | 6.50E-08 | 6.52E-08 | 6.50E-08 | 6.73E-08 | 6.65E-08 |
| 45 | 7.99E-08 | 7.88E-08 | 7.78E-08 | 8.06E-08 | 8.04E-08 |
| 46 | 9.22E-08 | 9.08E-08 | 8.95E-08 | 9.23E-08 | 9.18E-08 |
| 47 | 9.59E-08 | 9.35E-08 | 9.24E-08 | 9.48E-08 | 9.52E-08 |
| 48 | 9.39E-08 | 9.07E-08 | 9.13E-08 | 9.54E-08 | 9.52E-08 |
| 49 | 9.26E-08 | 9.10E-08 | 8.93E-08 | 9.30E-08 | 9.41E-08 |
| 50 | 8.97E-08 | 8.48E-08 | 8.28E-08 | 8.75E-08 | 8.94E-08 |
| 51 | 8.28E-08 | 7.75E-08 | 7.57E-08 | 7.84E-08 | 8.24E-08 |
| 52 | 7.60E-08 | 7.18E-08 | 6.53E-08 | 6.43E-08 | 6.64E-08 |
| 53 | 5.93E-08 | 5.35E-08 | 4.85E-08 | 4.33E-08 | 4.75E-08 |
| 54 | 3.34E-08 | 3.23E-08 | 2.90E-08 | 2.68E-08 | 2.69E-08 |
| 55 | 1.02E-08 | 6.51E-09 | 7.13E-09 | 3.70E-09 | 2.69E-09 |
| 56 | 1.40E-08 | 1.69E-08 | 1.69E-08 | 1.77E-08 | 1.80E-08 |
| 57 | 4.04E-08 | 4.66E-08 | 4.50E-08 | 4.40E-08 | 4.20E-08 |
| 58 | 6.74E-08 | 6.89E-08 | 6.31E-08 | 5.66E-08 | 5.52E-08 |
| 59 | 9.05E-08 | 9.10E-08 | 8.64E-08 | 8.25E-08 | 8.18E-08 |
| 61 | 1.15E-07 | 1.16E-07 | 1.16E-07 | 1.20E-07 | 1.21E-07 |
| 62 | 1.29E-07 | 1.28E-07 | 1.26E-07 | 1.31E-07 | 1.36E-07 |

**Table 15: Displacements – Sample 8(Mode 4)**

| pt | L5 | L4 | L3 | L2 | L1 |
|---|---|---|---|---|---|
| 1 | 1.02E-07 | 1.03E-07 | 1.04E-07 | 1.03E-07 | 1.04E-07 |
| 2 | 7.69E-08 | 7.77E-08 | 7.96E-08 | 7.94E-08 | 8.10E-08 |
| 3 | 4.05E-08 | 4.04E-08 | 4.55E-08 | 4.43E-08 | 4.79E-08 |
| 4 | 8.83E-09 | 9.00E-09 | 1.29E-08 | 1.57E-08 | 1.75E-08 |
| 5 | 2.51E-08 | 2.67E-08 | 2.40E-08 | 2.17E-08 | 1.80E-08 |
| 6 | 5.36E-08 | 5.42E-08 | 5.41E-08 | 5.29E-08 | 4.85E-08 |
| 7 | 7.39E-08 | 7.35E-08 | 7.48E-08 | 7.51E-08 | 7.22E-08 |
| 8 | 9.36E-08 | 9.41E-08 | 9.52E-08 | 9.89E-08 | 9.55E-08 |
| 9 | 1.07E-07 | 1.06E-07 | 1.07E-07 | 1.07E-07 | 1.07E-07 |
| 10 | 1.16E-07 | 1.14E-07 | 1.14E-07 | 1.15E-07 | 1.14E-07 |
| 11 | 1.17E-07 | 1.14E-07 | 1.13E-07 | 1.12E-07 | 1.15E-07 |
| 12 | 1.09E-07 | 1.06E-07 | 1.02E-07 | 1.02E-07 | 1.05E-07 |
| 13 | 9.48E-08 | 9.32E-08 | 9.14E-08 | 9.00E-08 | 9.37E-08 |
| 14 | 7.54E-08 | 7.46E-08 | 7.33E-08 | 7.50E-08 | 7.64E-08 |
| 15 | 5.13E-08 | 5.10E-08 | 5.14E-08 | 5.54E-08 | 5.73E-08 |
| 16 | 2.25E-08 | 2.24E-08 | 2.14E-08 | 2.51E-08 | 2.60E-08 |
| 17 | 4.67E-09 | 5.50E-09 | 6.48E-09 | 5.07E-09 | 4.55E-09 |
| 18 | 3.30E-08 | 3.32E-08 | 3.37E-08 | 3.36E-08 | 3.34E-08 |
| 19 | 5.88E-08 | 6.02E-08 | 6.03E-08 | 6.14E-08 | 6.14E-08 |
| 20 | 7.93E-08 | 8.07E-08 | 8.22E-08 | 8.35E-08 | 8.22E-08 |
| 21 | 1.01E-07 | 1.03E-07 | 1.03E-07 | 1.04E-07 | 1.01E-07 |
| 22 | 1.16E-07 | 1.16E-07 | 1.15E-07 | 1.15E-07 | 1.14E-07 |
| 23 | 1.21E-07 | 1.22E-07 | 1.21E-07 | 1.23E-07 | 1.24E-07 |
| 24 | 1.21E-07 | 1.22E-07 | 1.22E-07 | 1.25E-07 | 1.26E-07 |
| 25 | 1.17E-07 | 1.17E-07 | 1.17E-07 | 1.21E-07 | 1.22E-07 |
| 26 | 1.07E-07 | 1.06E-07 | 1.08E-07 | 1.11E-07 | 1.12E-07 |
| 27 | 9.19E-08 | 9.01E-08 | 9.06E-08 | 9.35E-08 | 9.43E-08 |
| 28 | 6.87E-08 | 6.60E-08 | 6.81E-08 | 7.25E-08 | 7.45E-08 |
| 29 | 4.42E-08 | 4.10E-08 | 4.45E-08 | 4.96E-08 | 5.19E-08 |
| 30 | 1.92E-08 | 1.69E-08 | 1.82E-08 | 2.12E-08 | 2.22E-08 |
| 31 | 1.17E-08 | 1.33E-08 | 1.20E-08 | 8.74E-09 | 8.06E-09 |
| 32 | 4.13E-08 | 4.31E-08 | 4.01E-08 | 3.67E-08 | 3.52E-08 |
| 33 | 6.46E-08 | 6.59E-08 | 6.46E-08 | 6.32E-08 | 6.21E-08 |
| 34 | 8.57E-08 | 8.76E-08 | 8.66E-08 | 8.52E-08 | 8.36E-08 |
| 35 | 1.01E-07 | 1.02E-07 | 1.01E-07 | 1.02E-07 | 9.93E-08 |
| 36 | 1.11E-07 | 1.11E-07 | 1.12E-07 | 1.14E-07 | 1.16E-07 |
| 37 | 1.19E-07 | 1.19E-07 | 1.18E-07 | 1.20E-07 | 1.22E-07 |
| 38 | 1.19E-07 | 1.19E-07 | 1.19E-07 | 1.19E-07 | 1.21E-07 |
| 39 | 1.11E-07 | 1.11E-07 | 1.11E-07 | 1.11E-07 | 1.12E-07 |
| 40 | 9.79E-08 | 9.67E-08 | 9.57E-08 | 9.65E-08 | 9.78E-08 |
| 41 | 7.70E-08 | 7.61E-08 | 7.66E-08 | 7.98E-08 | 8.17E-08 |
| 42 | 5.35E-08 | 5.30E-08 | 5.34E-08 | 5.71E-08 | 5.82E-08 |
| 43 | 2.70E-08 | 2.63E-08 | 2.61E-08 | 2.89E-08 | 3.03E-08 |
| 44 | 8.32E-09 | 8.66E-09 | 8.17E-09 | 7.15E-09 | 6.94E-09 |
| 45 | 4.01E-08 | 4.17E-08 | 4.15E-08 | 3.93E-08 | 3.81E-08 |
| 46 | 6.84E-08 | 7.01E-08 | 6.98E-08 | 6.86E-08 | 6.81E-08 |
| 47 | 9.88E-08 | 1.00E-07 | 9.75E-08 | 9.37E-08 | 9.13E-08 |
| 48 | 1.19E-07 | 1.21E-07 | 1.20E-07 | 1.20E-07 | 1.17E-07 |
| 49 | 1.32E-07 | 1.32E-07 | 1.32E-07 | 1.35E-07 | 1.34E-07 |
| 50 | 1.46E-07 | 1.45E-07 | 1.43E-07 | 1.44E-07 | 1.43E-07 |
| 51 | 1.50E-07 | 1.48E-07 | 1.43E-07 | 1.44E-07 | 1.44E-07 |
| 52 | 1.43E-07 | 1.41E-07 | 1.36E-07 | 1.37E-07 | 1.39E-07 |
| 53 | 1.29E-07 | 1.28E-07 | 1.25E-07 | 1.25E-07 | 1.24E-07 |
| 54 | 1.05E-07 | 1.05E-07 | 1.00E-07 | 1.01E-07 | 9.96E-08 |
| 55 | 7.43E-08 | 7.05E-08 | 6.60E-08 | 6.69E-08 | 6.92E-08 |
| 56 | 3.87E-08 | 3.76E-08 | 3.30E-08 | 3.24E-08 | 3.28E-08 |
| 57 | 5.19E-09 | 5.85E-09 | 8.27E-09 | 1.21E-08 | 1.06E-08 |
| 58 | 4.99E-08 | 5.15E-08 | 5.47E-08 | 6.12E-08 | 5.65E-08 |
| 59 | 9.82E-08 | 1.00E-07 | 1.03E-07 | 1.06E-07 | 1.02E-07 |
| 61 | 1.45E-07 | 1.48E-07 | 1.50E-07 | 1.54E-07 | 1.50E-07 |
| 62 | 1.73E-07 | 1.76E-07 | 1.80E-07 | 1.85E-07 | 1.87E-07 |

# APPENDIX C – Curvature Mode Shape Tables

**Table 17: Curvatures – Sample 1(Mode 1)**

| pt | L5 | L4 | L3 | L2 | L1 |
|---|---|---|---|---|---|
| 1 | -5.48E-05 | -5.01E-05 | -5.96E-05 | -5.79E-05 | -6.5E-05 |
| 2 | -1.50E-05 | -2.03E-05 | -1.10E-05 | -1.74E-05 | -2.2E-05 |
| 3 | 7.60E-06 | 9.75E-06 | 5.58E-06 | 4.76E-06 | 2.16E-06 |
| 4 | 8.89E-07 | -4.72E-07 | -1.01E-05 | -8.91E-06 | -3.3E-07 |
| 5 | 6.11E-06 | 7.49E-06 | 1.11E-05 | 5.70E-06 | 8.57E-08 |
| 6 | -8.93E-06 | -5.02E-06 | 1.97E-06 | 5.74E-06 | 2.12E-06 |
| 7 | 8.25E-06 | -1.40E-06 | -3.19E-06 | -6.83E-06 | 1.22E-06 |
| 8 | 3.00E-06 | 3.77E-06 | -8.96E-06 | -6.86E-07 | -1.6E-06 |
| 9 | 4.05E-06 | 1.25E-05 | 2.21E-05 | 1.71E-05 | 1.48E-05 |
| 10 | 7.02E-06 | 6.52E-06 | 2.70E-06 | 4.30E-06 | -4.1E-06 |
| 11 | -3.94E-06 | -8.44E-06 | -9.61E-06 | -8.52E-06 | 3.8E-06 |
| 12 | 5.53E-05 | 8.02E-05 | 1.38E-04 | 1.92E-04 | 0.000192 |
| 13 | 1.89E-04 | 1.67E-04 | 1.20E-04 | 6.15E-05 | 5.69E-05 |
| 14 | -2.83E-06 | -1.76E-06 | -1.54E-05 | -1.54E-05 | -1.6E-05 |
| 15 | -3.92E-06 | -1.10E-05 | -6.09E-06 | -1.78E-06 | -2.4E-06 |
| 16 | -1.19E-05 | -1.45E-05 | -3.66E-06 | -2.42E-06 | 4.14E-06 |
| 17 | -2.02E-06 | 7.66E-06 | -5.66E-06 | -9.08E-06 | -1.9E-05 |
| 18 | -4.40E-06 | -7.44E-06 | 3.76E-06 | -7.23E-06 | 2.09E-06 |
| 19 | -1.25E-05 | -8.96E-06 | -1.76E-05 | 9.25E-07 | -8.9E-06 |
| 20 | 1.73E-06 | -6.36E-06 | 2.78E-06 | -8.34E-06 | -2.5E-06 |
| 21 | -1.78E-05 | -1.01E-05 | -2.43E-05 | -1.71E-05 | -1.8E-05 |
| 22 | 4.49E-07 | -3.18E-06 | 4.43E-06 | -7.31E-06 | -2.8E-06 |
| 23 | -1.02E-05 | -7.81E-06 | -1.11E-05 | -4.08E-06 | -8.5E-06 |
| 24 | -9.68E-06 | -1.26E-05 | -9.17E-06 | -7.88E-06 | -7.7E-06 |
| 25 | -9.29E-06 | -8.55E-06 | -9.16E-06 | -9.24E-06 | -8.9E-06 |
| 26 | -9.71E-06 | -8.90E-06 | -7.33E-06 | -6.97E-06 | -3.8E-06 |
| 27 | -8.76E-06 | -9.23E-06 | -1.09E-05 | -1.00E-05 | -7.9E-06 |
| 28 | -8.60E-06 | -1.01E-05 | -1.04E-05 | -1.10E-05 | -1E-05 |
| 29 | -6.34E-06 | -7.34E-06 | -6.83E-06 | -6.95E-06 | -1.1E-05 |
| 30 | -8.96E-06 | -1.03E-05 | -1.48E-05 | -1.20E-05 | -1.3E-05 |
| 31 | -9.93E-06 | -1.29E-05 | -9.74E-06 | -1.36E-05 | -1.1E-05 |
| 32 | -1.35E-05 | -4.09E-06 | -5.80E-06 | -1.72E-06 | -8.5E-06 |
| 33 | -1.19E-05 | -2.15E-05 | -1.07E-05 | -1.75E-05 | -1E-05 |
| 34 | -9.82E-06 | 1.90E-06 | -9.29E-06 | 7.90E-08 | -9.1E-06 |
| 35 | -1.99E-06 | -1.49E-05 | -4.62E-06 | -1.88E-05 | -9.5E-06 |
| 36 | -1.60E-05 | -1.15E-06 | -1.14E-05 | -9.08E-07 | -8.6E-06 |
| 37 | -1.39E-06 | -8.73E-06 | -1.49E-06 | -1.13E-05 | -7.6E-06 |
| 38 | -1.20E-05 | -8.91E-06 | -1.59E-05 | -9.70E-06 | -9.4E-06 |
| 39 | -8.76E-06 | -1.12E-05 | -7.84E-06 | -7.52E-06 | -7.9E-06 |
| 40 | -8.48E-06 | -8.31E-06 | -7.31E-06 | -3.19E-06 | -7.8E-06 |
| 41 | -7.14E-06 | -7.69E-06 | -4.38E-06 | -8.86E-06 | -3.2E-06 |
| 42 | -6.76E-06 | -6.89E-06 | -1.59E-05 | -1.51E-05 | -1.7E-05 |
| 43 | -7.06E-06 | -6.96E-06 | -2.92E-06 | -8.18E-06 | -3.4E-06 |
| 44 | 2.78E-05 | 2.32E-05 | 6.18E-06 | 3.85E-06 | -2.1E-06 |
| 45 | 2.13E-04 | 2.18E-04 | 2.22E-04 | 1.86E-04 | 0.000148 |
| 46 | 2.41E-05 | 2.01E-05 | 3.72E-05 | 7.68E-05 | 0.00012 |
| 47 | 5.87E-06 | 1.28E-05 | 6.00E-06 | 8.77E-06 | 6.53E-06 |
| 48 | 3.31E-06 | -1.10E-06 | -4.32E-06 | -4.35E-06 | -2.3E-06 |
| 49 | 6.72E-06 | 7.39E-06 | 1.84E-05 | 1.62E-05 | 1.37E-05 |
| 50 | -3.63E-06 | 4.10E-06 | 1.75E-06 | 8.45E-06 | 1.02E-07 |
| 51 | 7.62E-06 | -4.65E-07 | -1.97E-06 | -8.93E-06 | -1.1E-06 |
| 52 | -3.87E-07 | -3.01E-06 | -2.99E-06 | 2.86E-07 | 3.73E-06 |
| 53 | -4.60E-06 | -5.39E-07 | 2.91E-06 | 8.54E-06 | 2.82E-06 |
| 54 | 5.10E-06 | 3.97E-06 | 1.56E-06 | -3.90E-06 | -8.1E-07 |
| 55 | 9.93E-06 | 7.44E-06 | 2.40E-06 | 1.81E-06 | -9.5E-06 |
| 56 | -1.11E-05 | -8.99E-06 | -3.55E-06 | -8.89E-06 | 8.01E-07 |
| 57 | 9.86E-06 | 1.01E-05 | 8.16E-06 | 2.25E-05 | 1.09E-05 |
| 58 | 3.23E-07 | -1.82E-05 | -1.46E-05 | -3.04E-05 | -8.9E-07 |
| 59 | -7.74E-05 | -5.81E-05 | -7.57E-05 | -3.87E-05 | -5.9E-05 |

## Table 18: Curvatures – Sample 1(Mode 2)

| pt | L5 | L4 | L3 | L2 | L1 |
|---|---|---|---|---|---|
| 1 | -1.7E-05 | -1.6E-05 | -1.6E-05 | -1.42E-05 | -1.5E-05 |
| 2 | -4.7E-07 | -8.1E-07 | 1.61E-07 | -7.48E-07 | -2.3E-06 |
| 3 | 1.27E-06 | 1.85E-06 | 1.26E-06 | 1.72E-06 | 8.82E-07 |
| 4 | 3.8E-07 | 9.3E-07 | 1.45E-06 | 2.36E-06 | 2.49E-06 |
| 5 | 1.44E-06 | 1.62E-06 | 1.51E-06 | -1.96E-07 | 5.09E-07 |
| 6 | 1.6E-05 | 1.76E-05 | 5.95E-06 | 3.59E-06 | 3.79E-06 |
| 7 | 7.06E-05 | 6.99E-05 | 7.9E-05 | 7.02E-05 | 6.46E-05 |
| 8 | -1.8E-06 | -3.1E-06 | 2.98E-07 | 1.18E-05 | 1.72E-05 |
| 9 | -2.6E-06 | -2.9E-06 | -6.1E-06 | -4.51E-06 | -3.8E-06 |
| 10 | -1.6E-06 | -1E-06 | -1.4E-07 | -2.35E-06 | -2.7E-06 |
| 11 | -3.8E-06 | -1.7E-06 | -1E-06 | -1.21E-06 | -2.3E-06 |
| 12 | -5.3E-06 | -7.9E-06 | -7.7E-06 | -7.04E-06 | -5E-06 |
| 13 | -3.7E-06 | -2.5E-06 | -3.6E-06 | -2.12E-06 | -3.1E-06 |
| 14 | -3.3E-06 | -3.8E-06 | -3.5E-06 | -4.76E-06 | -4.7E-06 |
| 15 | -4E-06 | -2.7E-06 | -3E-06 | -3.63E-06 | -4.2E-06 |
| 16 | -3E-06 | -3.6E-06 | -1.9E-06 | -2.82E-06 | -3.5E-06 |
| 17 | -4.8E-06 | -7.3E-06 | -8.9E-06 | -7.06E-06 | -5.5E-06 |
| 18 | -3.3E-06 | -3.6E-06 | -4.9E-06 | -4.49E-06 | -4.1E-06 |
| 19 | -5.1E-06 | -3.8E-06 | -1.6E-06 | -2.72E-06 | -2.9E-06 |
| 20 | -6.4E-06 | -5.2E-06 | -5.5E-06 | -4.65E-06 | -5.6E-06 |
| 21 | -3.4E-06 | -4.3E-06 | -3.5E-06 | -4.83E-06 | -4.1E-06 |
| 22 | -3.6E-06 | -2.9E-06 | -4E-06 | -2.97E-06 | -3.7E-06 |
| 23 | -4E-06 | -3.5E-06 | -2.6E-06 | -2.49E-06 | -2E-06 |
| 24 | -3.2E-06 | -3.2E-06 | -3.5E-06 | -3.39E-06 | -4.3E-06 |
| 25 | -2.3E-06 | -2.1E-06 | -3E-06 | -4.18E-06 | -3.8E-06 |
| 26 | -2.4E-06 | -3E-06 | -2E-06 | -1.68E-06 | -1.5E-06 |
| 27 | -2.1E-06 | -1.7E-06 | -1.6E-06 | -8.96E-07 | -8.9E-07 |
| 28 | -1.7E-06 | -1.8E-06 | -1.4E-06 | -2.26E-06 | -2.1E-06 |
| 29 | -4E-07 | 2.69E-07 | -4.9E-07 | -1.41E-08 | -9.2E-07 |
| 30 | 2.48E-08 | -1.5E-06 | -1.8E-06 | -1.64E-06 | -4.6E-08 |
| 31 | 7.89E-06 | 1.13E-05 | 1.59E-05 | 2.23E-05 | 2.27E-05 |
| 32 | 4.74E-05 | 4.7E-05 | 4.42E-05 | 3.85E-05 | 3.74E-05 |
| 33 | 5.39E-06 | 3.01E-06 | 8.37E-07 | -1.01E-07 | -2.9E-07 |
| 34 | -1.9E-06 | -2.3E-06 | -1.8E-06 | -1.88E-06 | -1.8E-06 |
| 35 | -2E-06 | -1.9E-06 | -2.4E-06 | -1.37E-06 | -2.4E-06 |
| 36 | -2.5E-06 | -2.9E-06 | -1.8E-06 | -2.63E-06 | -1.3E-06 |
| 37 | -3.5E-06 | -2.9E-06 | -5.2E-06 | -4.97E-06 | -5.4E-06 |
| 38 | -4.3E-06 | -4.5E-06 | -3.5E-06 | -4.85E-06 | -3.8E-06 |
| 39 | -4.9E-06 | -4.7E-06 | -4.6E-06 | -3.91E-06 | -4.9E-06 |
| 40 | -4.6E-06 | -4.6E-06 | -4.3E-06 | -4.22E-06 | -3.4E-06 |
| 41 | -5E-06 | -5E-06 | -5E-06 | -4.01E-06 | -3.6E-06 |
| 42 | -5.1E-06 | -4.9E-06 | -4.9E-06 | -5.77E-06 | -6.4E-06 |
| 43 | -6.1E-06 | -6.1E-06 | -5.9E-06 | -5.44E-06 | -7E-06 |
| 44 | -4.9E-06 | -4.8E-06 | -4.4E-06 | -4.61E-06 | -3.9E-06 |
| 45 | -3.9E-06 | -4.5E-06 | -5.9E-06 | -6.17E-06 | -6.1E-06 |
| 46 | -5.1E-06 | -4.6E-06 | -4E-06 | -4.15E-06 | -3.4E-06 |
| 47 | -3.3E-06 | -3.3E-06 | -2.8E-06 | -2.13E-06 | -3.6E-06 |
| 48 | -3.4E-06 | -3.3E-06 | -3.2E-06 | -3.26E-06 | -2.9E-06 |
| 49 | -3.3E-06 | -3.4E-06 | -3.7E-06 | -3.24E-06 | -3.2E-06 |
| 50 | 3.48E-05 | 3.57E-05 | 3.39E-05 | 2.57E-05 | 2.44E-05 |
| 51 | 3.8E-05 | 3.69E-05 | 3.9E-05 | 4.75E-05 | 4.97E-05 |
| 52 | 2.67E-06 | 3.18E-06 | 2.35E-06 | 2.67E-06 | 1.86E-06 |
| 53 | 2.99E-06 | 2.66E-06 | 3.44E-06 | 1.87E-06 | 1.92E-06 |
| 54 | -2.4E-08 | 3.66E-07 | 5.45E-08 | 2.86E-07 | 3.63E-07 |
| 55 | 1.06E-06 | 5.42E-07 | 5.19E-07 | -1.22E-08 | 4.29E-07 |
| 56 | 3.6E-07 | 4.72E-07 | 9.37E-07 | 1.59E-06 | 2.16E-06 |
| 57 | 1.26E-06 | 1.77E-06 | 8.37E-07 | 1.17E-06 | 3.27E-07 |
| 58 | -2.2E-06 | -2E-06 | -1.2E-06 | -7.50E-07 | -4.5E-07 |
| 59 | -1.6E-05 | -1.5E-05 | -1.6E-05 | -1.67E-05 | -1.8E-05 |

## Table 19: Curvatures – Sample 1(Mode 3)

| pt | L5 | L4 | L3 | L2 | L1 |
|---|---|---|---|---|---|
| 1 | -1.2E-06 | -8.3E-07 | -1.3E-06 | -1.4E-06 | -1.5E-06 |
| 2 | 7.94E-07 | 2.91E-07 | 5.95E-07 | 3.31E-07 | 5.95E-07 |
| 3 | 1.87E-06 | 2.59E-06 | 2.18E-06 | 2.72E-06 | 2.57E-06 |
| 4 | 1.5E-06 | 1.18E-06 | 9.03E-07 | 1.07E-06 | 6.92E-07 |
| 5 | 7.63E-07 | 1.05E-07 | 6.11E-07 | 1.21E-07 | 5.12E-07 |
| 6 | -7.9E-07 | -2.6E-07 | -3.6E-07 | -8.5E-08 | -3E-07 |
| 7 | -1.6E-07 | -3E-07 | -3.6E-08 | -3.2E-07 | -2.9E-07 |
| 8 | 4.85E-07 | 6.17E-07 | 3.87E-08 | -2.6E-07 | -4.1E-07 |
| 9 | -2.9E-07 | -4.5E-07 | -5.8E-07 | -6.6E-07 | -3E-07 |
| 10 | -1E-06 | -9.3E-07 | -7.7E-07 | -2.5E-07 | -6.2E-08 |
| 11 | -2.2E-07 | -3.2E-07 | 8.27E-08 | -7.9E-08 | -1.2E-09 |
| 12 | -3.1E-07 | -2.4E-07 | -7.3E-07 | -7.5E-07 | -1.1E-06 |
| 13 | -1.6E-07 | -5.2E-07 | -9.5E-09 | -2.2E-07 | -2.5E-07 |
| 14 | -6.3E-07 | -1.2E-07 | -6.8E-07 | -1.5E-07 | -2.4E-07 |
| 15 | -4.2E-07 | -6.9E-07 | -9.7E-08 | -5.1E-07 | -3.1E-07 |
| 16 | 6.76E-09 | 6.16E-07 | 3.57E-08 | -1.1E-07 | -2.2E-07 |
| 17 | 1.46E-07 | -5E-07 | -5E-07 | -4.6E-07 | -3.5E-07 |
| 18 | -3.2E-07 | -2E-07 | -2.3E-07 | -3.6E-07 | -3.5E-07 |
| 19 | 3.77E-07 | 4.95E-07 | 7.6E-07 | 8.74E-07 | 5.36E-07 |
| 20 | 1.56E-06 | 1.55E-06 | 1.37E-06 | 1.14E-06 | 1.03E-06 |
| 21 | 1.6E-06 | 1.4E-06 | 1.36E-06 | 1.53E-06 | 1.56E-06 |
| 22 | -1.6E-07 | 1.24E-07 | 1.08E-07 | 3.4E-07 | 7.44E-07 |
| 23 | 3.05E-07 | 1.25E-07 | 3.26E-07 | 1.16E-07 | 6.43E-08 |
| 24 | 6.46E-08 | 4.15E-07 | 4.13E-08 | 1.37E-07 | 2.18E-09 |
| 25 | -5E-07 | -1.1E-06 | -4.7E-07 | -5E-07 | -2.2E-07 |
| 26 | -5E-07 | -2.2E-07 | -4.1E-07 | 2.34E-08 | -1.5E-07 |
| 27 | -5.8E-08 | -9.6E-08 | -1.7E-07 | -4.1E-07 | -4.3E-07 |
| 28 | -1.8E-07 | -1.7E-07 | -2E-07 | -2.8E-07 | -2.4E-07 |
| 29 | -5.1E-07 | -4.5E-07 | -5.8E-07 | -2.7E-07 | -2.5E-07 |
| 30 | -3.6E-07 | -5.8E-07 | -2.8E-07 | -4E-07 | -4.5E-07 |
| 31 | -4.9E-07 | -2.7E-07 | -2.5E-07 | -3.9E-07 | -4.2E-07 |
| 32 | -5.9E-08 | -4.5E-08 | -2.4E-07 | -4.7E-07 | -5.1E-07 |
| 33 | -2.6E-07 | -2.2E-07 | -1.4E-07 | -6.2E-08 | 1.43E-07 |
| 34 | -2.8E-07 | -3E-07 | -3.6E-07 | -2.1E-08 | -1.1E-07 |
| 35 | -1.4E-07 | -3.6E-07 | -3E-07 | -4.5E-07 | -4.9E-07 |
| 36 | -2.1E-07 | -4.7E-08 | -1.5E-07 | -3.9E-07 | -2.2E-07 |
| 37 | -4.5E-08 | 8.73E-08 | 1.48E-07 | 4.25E-07 | 1.44E-07 |
| 38 | 7.67E-09 | -7.9E-08 | -1.5E-08 | -1.5E-07 | 1.58E-07 |
| 39 | 6.61E-07 | 5.99E-07 | 4.03E-07 | 6.33E-07 | 1.27E-07 |
| 40 | 4.53E-07 | 2.59E-07 | 4.73E-07 | 3.03E-07 | 6.49E-07 |
| 41 | 7.69E-07 | 1.09E-06 | 9.39E-07 | 1.08E-06 | 9.93E-07 |
| 42 | -2.7E-08 | 1.18E-07 | 3.91E-07 | 1.89E-07 | 2.63E-07 |
| 43 | -2E-07 | -3.6E-07 | -6.9E-07 | -7.6E-07 | -8.1E-07 |
| 44 | 1.79E-07 | -6.4E-08 | 5.78E-08 | 9.99E-08 | 6.47E-09 |
| 45 | 1.6E-07 | 8.99E-08 | 6.16E-08 | -1.3E-08 | 1.38E-09 |
| 46 | -3.6E-07 | -1.5E-07 | -1.1E-07 | 1.1E-07 | 2.39E-07 |
| 47 | -2.1E-07 | -3E-07 | -1.2E-07 | -3E-07 | -2.3E-07 |
| 48 | -2E-08 | 2.43E-07 | -1.6E-07 | -3.2E-07 | -3.1E-07 |
| 49 | -5.8E-07 | -7.8E-07 | -7.6E-07 | -3.6E-07 | -3.7E-07 |
| 50 | -4.2E-07 | -3.9E-07 | -4.1E-08 | -2.4E-07 | 4.47E-08 |
| 51 | 5.48E-08 | 2.94E-07 | 1.4E-07 | 4.69E-07 | -3.2E-07 |
| 52 | 4.48E-07 | -2.6E-07 | -1.1E-07 | -4.2E-07 | 3.54E-08 |
| 53 | -6.1E-08 | 7.46E-07 | 2.55E-07 | 1.07E-06 | 1.1E-06 |
| 54 | 1.67E-06 | 1.55E-06 | 2.21E-06 | 1.34E-06 | 1.14E-06 |
| 55 | 9.79E-07 | 7.43E-07 | 6.24E-07 | 3.71E-07 | 1.04E-07 |
| 56 | -3.2E-07 | -2.5E-07 | -5.7E-07 | -6.1E-07 | -9.1E-09 |
| 57 | -4.7E-07 | -2.9E-07 | -2.6E-07 | 2.78E-07 | -1.4E-07 |
| 58 | 4.92E-07 | 2.77E-07 | 6.01E-07 | 2.3E-07 | 4.28E-07 |
| 59 | -8.1E-07 | -9.8E-07 | -1.3E-06 | -2.5E-07 | -3.7E-07 |

## Table 20: Curvatures – Sample 1(Mode 4)

| pt | L5 | L4 | L3 | L2 | L1 |
|---|---|---|---|---|---|
| 1 | -1.4E-06 | -1.5E-06 | -1.3E-06 | -1.2E-06 | -1.1E-06 |
| 2 | 1.24E-07 | 2.48E-07 | 1.24E-07 | -6.6E-08 | -1.9E-07 |
| 3 | 5.02E-06 | 4.83E-06 | 3.74E-06 | 3.03E-06 | 2.88E-06 |
| 4 | 1.64E-06 | 2.02E-06 | 3.28E-06 | 4.2E-06 | 4.24E-06 |
| 5 | -4.5E-07 | -6.2E-07 | -6.6E-07 | -7.7E-07 | -6.3E-07 |
| 6 | -1.5E-07 | -2.6E-07 | -4.7E-07 | -5.9E-07 | -6.4E-07 |
| 7 | -9.5E-07 | -8.6E-07 | -8.3E-07 | -6.8E-07 | -5.7E-07 |
| 8 | -5.1E-07 | -5.8E-07 | -7.5E-07 | -8E-07 | -7.4E-07 |
| 9 | -7.3E-07 | -6.3E-07 | -4.3E-07 | -5.5E-07 | -3.7E-07 |
| 10 | -6.2E-07 | -5.2E-07 | -6.7E-07 | -6.1E-07 | -1E-06 |
| 11 | -8.4E-07 | -1.1E-06 | -8.4E-07 | -9.5E-07 | -7.9E-07 |
| 12 | -7.5E-07 | -6.5E-07 | -7.3E-07 | -4.5E-07 | -6E-07 |
| 13 | -3E-07 | -1.9E-07 | -1.2E-07 | -4E-07 | -3.5E-07 |
| 14 | -9.5E-08 | -1.1E-07 | -2.3E-07 | -2.2E-07 | -2.5E-07 |
| 15 | -4.1E-07 | -4.1E-07 | -1.8E-07 | 3.56E-07 | 5.07E-07 |
| 16 | 5.42E-06 | 5.59E-06 | 5.19E-06 | 4.62E-06 | 4.57E-06 |
| 17 | 1.54E-07 | -1.2E-07 | 2.41E-07 | 4.9E-07 | 4.89E-07 |
| 18 | -4.1E-07 | -2.7E-07 | -6.1E-07 | -6.1E-07 | -6.3E-07 |
| 19 | -5.8E-08 | -2.2E-07 | -9E-08 | -3.5E-07 | -3.2E-07 |
| 20 | -7.5E-07 | -5.8E-07 | -7.3E-07 | -4.8E-07 | -5.5E-07 |
| 21 | -5.1E-07 | -7.2E-07 | -5.3E-07 | -6.3E-07 | -4.5E-07 |
| 22 | -6.7E-07 | -5.9E-07 | -7.5E-07 | -5.5E-07 | -6.4E-07 |
| 23 | -5E-07 | -5.3E-07 | -3.3E-07 | -5.9E-07 | -6.7E-07 |
| 24 | -6.6E-07 | -6E-07 | -7.6E-07 | -7.6E-07 | -8.5E-07 |
| 25 | -5.5E-07 | -5.3E-07 | -4.4E-07 | -4.6E-07 | -3.7E-07 |
| 26 | -6.3E-07 | -6.6E-07 | -5.9E-07 | -5E-07 | -4.6E-07 |
| 27 | -4E-07 | -3.6E-07 | -3.5E-07 | -4E-07 | -3.9E-07 |
| 28 | -2.5E-07 | -2.5E-07 | -4E-07 | -3.4E-07 | -3.9E-07 |
| 29 | 6.24E-07 | 8.24E-07 | 1.17E-06 | 1.25E-06 | 1.15E-06 |
| 30 | 4.72E-06 | 4.46E-06 | 4.21E-06 | 4.19E-06 | 4.35E-06 |
| 31 | -4.5E-09 | 5.24E-08 | -8.7E-09 | -8.4E-08 | -1.3E-07 |
| 32 | -3.1E-07 | -3E-07 | -3.8E-07 | -3.3E-07 | -3.4E-07 |
| 33 | -5.1E-07 | -5.8E-07 | -3.9E-07 | -4.7E-07 | -3.8E-07 |
| 34 | -6.4E-07 | -5.6E-07 | -5.8E-07 | -5.6E-07 | -6.4E-07 |
| 35 | -6.8E-07 | -8.5E-07 | -9.4E-07 | -8.2E-07 | -6.7E-07 |
| 36 | -4.9E-07 | -3.5E-07 | -3.7E-07 | -3.8E-07 | -3.9E-07 |
| 37 | -6.4E-07 | -6.6E-07 | -5.6E-07 | -7E-07 | -7.7E-07 |
| 38 | -6.8E-07 | -5.7E-07 | -8.3E-07 | -9.2E-07 | -9.4E-07 |
| 39 | -6.7E-07 | -7.9E-07 | -6.1E-07 | -7E-07 | -7.1E-07 |
| 40 | -8.4E-07 | -6.9E-07 | -6.4E-07 | -4E-07 | -5E-07 |
| 41 | -4.8E-07 | -5.9E-07 | -4.8E-07 | -4.1E-07 | -3.2E-07 |
| 42 | 4.58E-06 | 4.71E-06 | 4.35E-06 | 3.78E-06 | 3.69E-06 |
| 43 | 2.26E-06 | 2.21E-06 | 2.36E-06 | 2.89E-06 | 2.95E-06 |
| 44 | 5.01E-08 | -2.7E-08 | -6.9E-09 | -1.4E-07 | -1.2E-07 |
| 45 | -4.4E-07 | -3.1E-07 | -4.6E-07 | -3.8E-07 | -4.1E-07 |
| 46 | -4.7E-07 | -6.3E-07 | -3.3E-07 | -5.3E-07 | -5.5E-07 |
| 47 | -9.8E-07 | -1E-06 | -1.1E-06 | -9E-07 | -8.9E-07 |
| 48 | -6.9E-07 | -1E-06 | -1.1E-06 | -1.2E-06 | -1E-06 |
| 49 | -8.7E-07 | -5E-07 | -7.9E-07 | -5.6E-07 | -6.7E-07 |
| 50 | -9.4E-07 | -1.1E-06 | -8.5E-07 | -1E-06 | -8.9E-07 |
| 51 | -1.3E-06 | -8.7E-07 | -9.4E-07 | -9.8E-07 | -1E-06 |
| 52 | -6.5E-07 | -9.5E-07 | -7E-07 | -8.1E-07 | -1E-06 |
| 53 | -1.3E-06 | -1.2E-06 | -1.3E-06 | -1.1E-06 | -8.2E-07 |
| 54 | -5.3E-07 | -3.4E-07 | -4.9E-07 | -3.8E-07 | -7.3E-07 |
| 55 | 1.32E-06 | 2.3E-06 | 4.24E-06 | 5.43E-06 | 5.78E-06 |
| 56 | 8.75E-06 | 7.46E-06 | 5.6E-06 | 4.41E-06 | 4.22E-06 |
| 57 | 1.3E-07 | 4.01E-07 | 2.12E-07 | 1.74E-07 | 2.86E-07 |
| 58 | 3.84E-07 | 4.67E-07 | 5.21E-07 | 1.82E-07 | -1.1E-07 |
| 59 | -2.8E-06 | -2.6E-06 | -2.3E-06 | -2E-06 | -1.7E-06 |

## Table 21: Curvatures – Sample 3(Mode 1)

| pt | L5 | L4 | L3 | L2 | L1 |
|---|---|---|---|---|---|
| 1 | -4.94E-05 | -5.66E-05 | -5.36E-05 | -4.02E-05 | -3.59E-05 |
| 2 | -1.47E-05 | -1.38E-05 | -1.03E-05 | -4.12E-07 | -3.25E-06 |
| 3 | 1.13E-05 | 1.22E-05 | 9.22E-06 | 7.87E-06 | -6.44E-06 |
| 4 | 5.24E-06 | -8.58E-06 | -5.29E-06 | -2.10E-05 | -4.79E-06 |
| 5 | -1.13E-05 | 2.61E-06 | -2.21E-06 | 1.38E-05 | 2.32E-06 |
| 6 | 6.99E-06 | -3.83E-07 | 8.32E-06 | -5.06E-06 | 1.15E-05 |
| 7 | 7.13E-06 | 1.43E-05 | -7.64E-06 | -1.39E-06 | -2.60E-06 |
| 8 | 1.94E-06 | -8.64E-07 | 1.05E-05 | 9.82E-06 | 7.41E-06 |
| 9 | -1.12E-06 | -7.51E-06 | 1.73E-06 | 4.93E-06 | -8.67E-06 |
| 10 | -3.67E-06 | -1.36E-06 | 8.55E-06 | 9.36E-06 | 7.72E-06 |
| 11 | 1.29E-05 | 1.53E-05 | 5.28E-06 | -2.20E-06 | 2.10E-05 |
| 12 | 1.03E-05 | 8.29E-06 | 3.01E-05 | 9.20E-05 | 3.72E-05 |
| 13 | 1.69E-04 | 2.09E-04 | 2.08E-04 | 1.68E-04 | 2.06E-04 |
| 14 | 5.27E-05 | 1.87E-05 | -1.14E-05 | -3.18E-05 | -5.43E-06 |
| 15 | -2.31E-06 | -1.02E-05 | -1.06E-05 | -1.09E-05 | -2.84E-05 |
| 16 | -5.54E-06 | 2.03E-06 | 4.45E-06 | 5.06E-06 | 3.71E-07 |
| 17 | -5.13E-06 | -9.77E-06 | -2.91E-06 | -4.65E-06 | -7.81E-06 |
| 18 | -9.15E-06 | -5.01E-06 | -1.00E-05 | -7.08E-06 | -6.47E-06 |
| 19 | -4.79E-06 | -8.90E-06 | -5.71E-06 | -5.87E-06 | -5.86E-06 |
| 20 | -6.59E-06 | -5.33E-06 | -1.08E-05 | -7.34E-06 | -6.92E-06 |
| 21 | -4.70E-06 | -1.06E-05 | -5.99E-06 | -8.46E-06 | -8.03E-06 |
| 22 | -1.58E-05 | -7.28E-06 | -1.12E-05 | -7.80E-06 | -8.38E-06 |
| 23 | -8.68E-07 | -2.62E-06 | -1.58E-07 | -7.08E-06 | -7.19E-06 |
| 24 | -9.62E-06 | -6.88E-06 | -1.18E-05 | -7.26E-06 | -3.21E-06 |
| 25 | -6.94E-06 | -1.15E-05 | -7.70E-06 | -1.30E-06 | -4.35E-06 |
| 26 | -8.60E-06 | -7.85E-06 | -7.08E-06 | -1.74E-05 | -1.59E-05 |
| 27 | -9.21E-06 | -1.14E-05 | -1.43E-05 | -1.05E-05 | -1.54E-05 |
| 28 | -1.32E-05 | -1.34E-05 | -1.13E-05 | -9.46E-06 | 5.91E-07 |
| 29 | -2.67E-06 | -4.55E-06 | -3.02E-06 | -3.04E-06 | -7.12E-06 |
| 30 | -6.80E-06 | -1.42E-06 | -9.26E-06 | -9.69E-06 | -1.18E-05 |
| 31 | -7.91E-06 | -1.33E-05 | -8.21E-06 | -1.06E-05 | -1.36E-05 |
| 32 | -1.61E-05 | -8.78E-06 | -6.22E-06 | -3.23E-06 | -4.58E-06 |
| 33 | -1.17E-05 | -1.73E-05 | -1.85E-05 | -1.94E-05 | -1.83E-05 |
| 34 | -5.81E-06 | 8.83E-07 | 5.24E-06 | -2.57E-06 | -2.53E-07 |
| 35 | -1.24E-05 | -1.44E-05 | -2.00E-05 | -1.16E-05 | -1.59E-05 |
| 36 | -1.68E-07 | -3.37E-06 | -8.52E-07 | -7.70E-06 | 5.62E-07 |
| 37 | -1.17E-05 | -9.70E-06 | -1.63E-05 | -9.81E-06 | -1.59E-05 |
| 38 | -7.71E-06 | -1.24E-05 | -7.26E-06 | -1.22E-05 | -5.97E-06 |
| 39 | -1.30E-05 | -9.64E-06 | -9.98E-06 | -3.71E-06 | -6.63E-06 |
| 40 | -2.79E-06 | 3.23E-08 | 5.75E-07 | -2.68E-06 | -6.71E-06 |
| 41 | -9.19E-06 | -1.08E-05 | -1.18E-05 | -1.37E-05 | -9.12E-06 |
| 42 | -6.82E-06 | -5.05E-06 | -6.67E-06 | 2.85E-06 | -4.19E-06 |
| 43 | -6.15E-06 | -1.04E-05 | -3.35E-06 | -6.71E-06 | -1.21E-06 |
| 44 | -3.41E-06 | -1.53E-06 | -7.65E-06 | -1.49E-05 | -1.54E-05 |
| 45 | 1.23E-04 | 1.20E-04 | 1.01E-04 | 4.97E-05 | 2.91E-05 |
| 46 | 1.23E-04 | 1.26E-04 | 1.43E-04 | 1.99E-04 | 2.14E-04 |
| 47 | 2.18E-06 | 5.16E-06 | 1.56E-05 | 1.52E-05 | 2.01E-05 |
| 48 | 6.96E-06 | 3.97E-06 | -3.10E-06 | -4.83E-07 | 9.10E-07 |
| 49 | 8.06E-06 | 6.97E-06 | 4.97E-06 | -2.27E-06 | 1.98E-07 |
| 50 | -3.95E-06 | -1.96E-06 | -2.03E-06 | -1.38E-06 | -3.37E-06 |
| 51 | 5.88E-06 | 4.06E-06 | 1.27E-05 | 1.80E-05 | 1.60E-05 |
| 52 | 3.92E-06 | 3.99E-06 | 1.07E-07 | 6.93E-07 | -1.36E-07 |
| 53 | 1.37E-06 | 2.82E-06 | 1.30E-06 | -2.81E-06 | -2.20E-06 |
| 54 | -2.12E-06 | -2.33E-06 | -1.06E-06 | -7.34E-07 | -1.56E-06 |
| 55 | 9.25E-07 | 5.68E-06 | 6.25E-06 | 6.90E-06 | 7.89E-06 |
| 56 | 7.30E-06 | 8.92E-08 | -4.46E-07 | -4.11E-06 | -3.57E-06 |
| 57 | -6.11E-06 | -1.45E-06 | -7.03E-06 | 8.58E-07 | -7.36E-07 |
| 58 | 4.24E-06 | -8.69E-06 | -2.07E-06 | -8.19E-06 | -2.88E-06 |
| 59 | -6.48E-05 | -5.02E-05 | -5.96E-05 | -4.71E-05 | -5.55E-05 |

## Table 22: Curvatures – Sample 3(Mode 2)

| pt | L5 | L4 | L3 | L2 | L1 |
|---|---|---|---|---|---|
| 1 | -1.51E-05 | -1.26E-05 | -1.65E-05 | -1.29E-05 | -1.61E-05 |
| 2 | 7.76E-06 | 7.07E-06 | 5.99E-06 | -1.78E-08 | 2.91E-06 |
| 3 | -4.06E-06 | -2.33E-06 | 1.03E-07 | 2.76E-06 | 7.94E-07 |
| 4 | -1.83E-06 | 4.09E-07 | 1.31E-06 | 1.72E-06 | -2.40E-08 |
| 5 | 7.71E-06 | 2.81E-06 | 1.28E-06 | -5.60E-07 | 1.51E-06 |
| 6 | 2.22E-06 | 5.34E-06 | 2.55E-06 | 5.05E-06 | 4.66E-06 |
| 7 | 5.00E-05 | 5.15E-05 | 4.75E-05 | 2.71E-05 | 2.00E-05 |
| 8 | 1.18E-05 | 9.45E-06 | 1.45E-05 | 3.30E-05 | 3.84E-05 |
| 9 | -1.95E-06 | -1.47E-06 | -9.53E-07 | -2.39E-07 | 2.97E-07 |
| 10 | -2.24E-06 | -4.15E-06 | -2.44E-06 | -2.83E-06 | -1.94E-06 |
| 11 | -7.03E-06 | -6.10E-06 | -3.43E-06 | -2.79E-06 | -4.84E-06 |
| 12 | -1.50E-06 | 1.65E-06 | -7.43E-07 | -4.03E-06 | -3.07E-06 |
| 13 | 2.89E-07 | -1.55E-06 | -2.48E-06 | 3.70E-06 | 6.26E-06 |
| 14 | -4.46E-06 | -4.43E-06 | -6.15E-06 | -7.00E-06 | -4.10E-06 |
| 15 | -3.78E-06 | -4.87E-06 | -3.19E-06 | -5.85E-06 | -9.30E-06 |
| 16 | -2.54E-06 | -4.75E-06 | -2.22E-06 | -3.02E-06 | -3.42E-06 |
| 17 | -1.96E-06 | -9.97E-07 | -1.68E-06 | -5.94E-07 | -1.11E-06 |
| 18 | -3.87E-06 | -3.22E-06 | -3.85E-06 | -3.86E-06 | -3.13E-06 |
| 19 | -4.56E-06 | -3.18E-06 | -3.33E-06 | -3.71E-06 | -3.92E-06 |
| 20 | -1.19E-06 | -7.47E-07 | -1.71E-06 | -1.30E-06 | -2.67E-06 |
| 21 | -4.26E-06 | -5.22E-06 | -5.32E-06 | -4.93E-06 | -3.75E-06 |
| 22 | -1.79E-06 | -1.23E-06 | -1.08E-06 | -4.14E-06 | -4.49E-06 |
| 23 | -3.39E-06 | -2.48E-06 | -1.53E-06 | 1.11E-06 | 1.88E-07 |
| 24 | -3.92E-06 | -5.72E-06 | -6.05E-06 | -4.71E-06 | -1.75E-06 |
| 25 | 5.73E-07 | 6.69E-07 | 3.34E-09 | -2.90E-06 | -4.65E-06 |
| 26 | -3.84E-06 | -5.02E-07 | -5.03E-07 | 2.77E-07 | 1.04E-07 |
| 27 | -5.25E-07 | -5.61E-06 | -4.90E-06 | -3.25E-06 | -2.87E-06 |
| 28 | -2.74E-06 | -3.12E-07 | -1.49E-07 | 1.08E-06 | 1.09E-06 |
| 29 | 1.44E-06 | 1.02E-06 | 3.03E-06 | -1.23E-06 | -2.53E-06 |
| 30 | -2.75E-06 | 1.12E-07 | -2.50E-06 | 6.18E-07 | 4.64E-07 |
| 31 | 3.59E-06 | -8.93E-08 | 2.79E-06 | 7.05E-06 | 1.03E-05 |
| 32 | 1.52E-05 | 1.97E-05 | 2.67E-05 | 3.22E-05 | 3.11E-05 |
| 33 | 2.64E-05 | 2.46E-05 | 1.54E-05 | 3.61E-06 | 2.52E-06 |
| 34 | -9.01E-07 | -1.71E-06 | -3.06E-06 | -2.36E-06 | -4.43E-06 |
| 35 | -3.21E-06 | -4.10E-06 | -1.81E-06 | -1.40E-06 | 2.28E-06 |
| 36 | 5.53E-07 | -6.51E-07 | -2.76E-06 | -1.66E-06 | -4.42E-06 |
| 37 | -3.96E-06 | -2.13E-06 | -1.34E-06 | -2.68E-06 | 2.31E-08 |
| 38 | -3.44E-07 | -2.05E-06 | -2.22E-06 | -4.17E-06 | -6.15E-06 |
| 39 | -5.11E-06 | -3.33E-06 | -3.40E-06 | -2.56E-06 | -1.41E-06 |
| 40 | -2.01E-06 | -3.75E-06 | -2.79E-06 | -1.99E-06 | -1.11E-06 |
| 41 | -4.50E-06 | -3.45E-06 | -5.36E-06 | -3.24E-06 | -3.71E-06 |
| 42 | -2.79E-06 | -3.42E-06 | -2.55E-06 | -4.97E-06 | -5.18E-06 |
| 43 | -3.85E-06 | -2.55E-06 | -3.12E-06 | -2.89E-06 | -4.21E-06 |
| 44 | -4.52E-06 | -6.61E-06 | -5.13E-06 | -4.57E-06 | -3.11E-06 |
| 45 | -2.81E-06 | -7.75E-07 | -1.33E-06 | -1.46E-06 | -2.32E-06 |
| 46 | -3.41E-06 | -3.72E-06 | -3.18E-06 | -1.74E-06 | -3.46E-06 |
| 47 | -2.16E-06 | -2.31E-06 | -2.26E-06 | -3.14E-06 | -1.12E-06 |
| 48 | -1.97E-06 | -2.32E-06 | -4.26E-06 | -5.09E-06 | -6.18E-06 |
| 49 | -2.50E-06 | -2.27E-06 | -1.44E-07 | -8.18E-07 | 5.08E-07 |
| 50 | 1.58E-05 | 1.65E-05 | 9.67E-06 | 8.12E-07 | -1.02E-06 |
| 51 | 3.37E-05 | 3.40E-05 | 3.98E-05 | 4.70E-05 | 4.08E-05 |
| 52 | 1.86E-06 | 4.30E-08 | -4.08E-07 | 2.00E-06 | 1.09E-05 |
| 53 | 6.09E-07 | 7.54E-07 | 5.37E-07 | 2.10E-06 | 1.48E-06 |
| 54 | 1.48E-06 | 1.92E-06 | 3.85E-06 | 4.31E-06 | 3.05E-06 |
| 55 | 1.61E-07 | 6.14E-07 | -2.76E-08 | -1.18E-06 | -1.75E-06 |
| 56 | -6.71E-07 | -2.92E-07 | -6.78E-07 | -1.60E-06 | -1.23E-06 |
| 57 | 1.56E-06 | 8.30E-07 | 1.34E-06 | 8.29E-07 | 1.16E-06 |
| 58 | -1.76E-06 | -3.37E-06 | -3.18E-06 | -1.44E-06 | 9.81E-08 |
| 59 | -1.25E-05 | -1.09E-05 | -1.26E-05 | -1.18E-05 | -1.33E-05 |

**Table 23: Curvatures – Sample 3(Mode 3)**

| pt | L5 | L4 | L3 | L2 | L1 |
|---|---|---|---|---|---|
| 1 | -1.32E-06 | -1.23E-06 | -4.93E-07 | -1.15E-06 | -8.81E-07 |
| 2 | 1.85E-07 | -3.59E-08 | -1.01E-06 | -4.87E-07 | -1.58E-06 |
| 3 | 4.34E-07 | 6.26E-08 | 5.94E-07 | -7.84E-07 | 7.23E-07 |
| 4 | 9.80E-07 | 1.82E-06 | 1.25E-06 | 1.66E-06 | 6.45E-07 |
| 5 | -3.39E-08 | -3.34E-07 | 5.58E-07 | 2.65E-06 | 3.53E-06 |
| 6 | 2.81E-06 | 3.19E-06 | 4.03E-06 | 3.79E-06 | 3.07E-06 |
| 7 | 1.85E-06 | 1.99E-06 | 7.84E-07 | -9.92E-07 | -8.05E-07 |
| 8 | 2.62E-07 | -5.04E-07 | -5.48E-07 | -4.32E-07 | -1.92E-07 |
| 9 | -4.85E-07 | -6.62E-08 | -1.18E-07 | 2.83E-07 | 8.95E-08 |
| 10 | -9.67E-08 | -5.84E-07 | -5.64E-07 | -8.56E-07 | -8.10E-07 |
| 11 | -1.06E-06 | -8.42E-07 | -5.00E-07 | -2.78E-07 | -7.51E-08 |
| 12 | -6.24E-07 | -4.95E-07 | -6.26E-07 | -6.00E-07 | -1.01E-06 |
| 13 | -1.44E-07 | -3.77E-07 | -1.39E-07 | -6.39E-07 | -3.63E-07 |
| 14 | -4.88E-07 | -3.59E-07 | -1.22E-06 | -7.92E-07 | -1.02E-06 |
| 15 | -3.28E-07 | -4.65E-07 | 9.47E-09 | -6.54E-07 | -1.11E-07 |
| 16 | -9.59E-07 | -2.87E-07 | -5.31E-07 | 2.98E-07 | -4.03E-07 |
| 17 | -3.66E-07 | -8.93E-07 | -3.30E-07 | -7.01E-07 | -1.84E-07 |
| 18 | -2.80E-07 | -1.02E-07 | -2.35E-07 | 7.36E-08 | -2.00E-07 |
| 19 | -4.70E-07 | -6.54E-07 | -6.47E-07 | -7.64E-07 | -5.66E-07 |
| 20 | 5.81E-07 | 6.41E-07 | 3.57E-07 | 1.23E-07 | -4.06E-08 |
| 21 | 1.09E-06 | 1.25E-06 | 1.27E-06 | 1.24E-06 | 8.75E-07 |
| 22 | 3.50E-06 | 3.24E-06 | 2.86E-06 | 2.35E-06 | 2.64E-06 |
| 23 | -9.91E-08 | 1.10E-07 | 7.30E-07 | 1.71E-06 | 1.47E-06 |
| 24 | 2.35E-07 | -3.34E-08 | -1.14E-07 | -6.12E-07 | -2.28E-07 |
| 25 | -8.08E-08 | 2.63E-07 | -1.43E-08 | 6.62E-07 | 6.91E-07 |
| 26 | -5.44E-07 | -7.67E-07 | -5.52E-07 | -9.16E-07 | -4.52E-07 |
| 27 | -5.67E-07 | -4.43E-07 | -3.88E-07 | -3.72E-07 | -7.79E-07 |
| 28 | -2.33E-07 | -4.21E-07 | -4.99E-07 | -6.36E-07 | -9.03E-07 |
| 29 | -4.18E-07 | -5.84E-07 | -5.61E-07 | -6.51E-07 | -6.38E-07 |
| 30 | -4.76E-07 | -3.12E-07 | -2.47E-07 | -3.12E-08 | 9.51E-08 |
| 31 | -3.55E-07 | -4.01E-07 | -3.19E-07 | -3.19E-07 | -2.37E-07 |
| 32 | -3.78E-07 | -3.17E-07 | -7.15E-07 | -9.64E-07 | -9.94E-07 |
| 33 | -8.01E-07 | -8.88E-07 | -6.18E-07 | -6.09E-07 | -3.92E-07 |
| 34 | -4.80E-07 | -7.35E-08 | -1.55E-07 | 1.91E-07 | -6.45E-08 |
| 35 | -2.11E-07 | -2.56E-07 | -1.33E-07 | -6.01E-07 | -4.66E-07 |
| 36 | -3.25E-07 | -3.17E-07 | -3.77E-07 | 9.50E-08 | -2.87E-07 |
| 37 | 6.37E-08 | -1.26E-07 | 1.36E-08 | -1.23E-07 | 2.88E-07 |
| 38 | 1.63E-07 | 1.70E-07 | 4.04E-07 | 2.99E-07 | 4.44E-08 |
| 39 | 5.36E-07 | 6.84E-07 | 5.03E-07 | 7.13E-07 | 6.76E-07 |
| 40 | 2.58E-06 | 2.24E-06 | 1.85E-06 | 1.88E-06 | 2.04E-06 |
| 41 | 7.74E-07 | 1.07E-06 | 9.93E-07 | 7.73E-07 | 5.77E-07 |
| 42 | -2.98E-07 | -3.04E-07 | -5.26E-08 | -9.33E-08 | 1.80E-07 |
| 43 | -1.54E-07 | -3.50E-07 | -3.44E-07 | -3.35E-07 | -3.74E-07 |
| 44 | -1.73E-07 | -1.55E-07 | -2.97E-07 | -2.19E-07 | -2.73E-07 |
| 45 | -5.19E-07 | -7.57E-07 | -3.37E-07 | -3.20E-07 | -1.83E-07 |
| 46 | -4.88E-07 | -2.19E-07 | -3.61E-07 | -3.34E-07 | -5.50E-07 |
| 47 | -4.80E-07 | -3.68E-07 | -3.56E-07 | -5.15E-07 | -4.59E-07 |
| 48 | -2.75E-07 | -1.72E-07 | -3.45E-07 | -1.26E-07 | -2.60E-07 |
| 49 | -1.35E-07 | -3.15E-07 | -4.04E-07 | -4.59E-07 | -1.90E-07 |
| 50 | -3.48E-07 | -3.16E-07 | -3.00E-07 | -3.67E-07 | -5.12E-07 |
| 51 | -8.00E-07 | -7.90E-07 | -6.89E-07 | -7.58E-07 | -8.06E-07 |
| 52 | -7.45E-08 | -2.24E-07 | -2.53E-07 | -2.53E-07 | -1.61E-07 |
| 53 | -2.88E-07 | -3.91E-07 | -1.81E-07 | 1.83E-07 | 3.66E-07 |
| 54 | 1.93E-06 | 2.83E-06 | 2.96E-06 | 2.06E-06 | 1.56E-06 |
| 55 | 2.92E-06 | 2.37E-06 | 1.78E-06 | 2.37E-06 | 2.43E-06 |
| 56 | 2.57E-07 | 4.70E-08 | 7.56E-07 | 5.16E-07 | 8.12E-07 |
| 57 | -4.65E-08 | -1.71E-08 | -3.89E-07 | -5.35E-07 | -6.02E-07 |
| 58 | 2.03E-07 | 2.63E-07 | -8.42E-08 | 1.42E-07 | 4.93E-08 |
| 59 | -1.37E-06 | -1.58E-06 | -9.71E-07 | -5.53E-07 | -9.12E-08 |

## Table 24: Curvatures – Sample 3(Mode 4)

| pt | L5 | L4 | L3 | L2 | L1 |
|---|---|---|---|---|---|
| 1 | -1.83E-06 | -2.14E-06 | -1.61E-06 | -1.42E-06 | -7.66E-07 |
| 2 | 4.50E-07 | 3.47E-07 | 2.08E-08 | 4.48E-07 | -2.23E-07 |
| 3 | 1.57E-06 | 1.88E-06 | 2.17E-06 | 2.16E-06 | 1.87E-06 |
| 4 | 4.75E-06 | 4.67E-06 | 4.01E-06 | 3.03E-06 | 3.58E-06 |
| 5 | -8.97E-07 | -1.01E-06 | -5.16E-07 | 4.75E-07 | 6.84E-07 |
| 6 | -3.29E-07 | -4.45E-07 | -6.84E-07 | -1.01E-06 | -7.35E-07 |
| 7 | 2.57E-07 | 2.08E-07 | 3.93E-07 | -8.48E-08 | -5.46E-07 |
| 8 | -1.11E-06 | -8.49E-07 | -1.18E-06 | -9.00E-07 | -9.96E-07 |
| 9 | -6.36E-07 | -7.93E-07 | -3.82E-07 | -7.27E-07 | -3.06E-07 |
| 10 | -6.82E-07 | -4.40E-07 | -8.99E-07 | -4.81E-07 | -8.86E-07 |
| 11 | -3.66E-07 | -5.17E-07 | -2.03E-07 | -3.30E-07 | -2.31E-07 |
| 12 | -3.76E-07 | -6.18E-07 | -7.92E-07 | -6.89E-07 | -5.65E-07 |
| 13 | -5.10E-07 | -2.87E-07 | -2.58E-07 | -1.39E-07 | -3.11E-07 |
| 14 | -5.04E-07 | -4.48E-07 | -3.11E-08 | -4.52E-07 | -4.12E-07 |
| 15 | -1.04E-07 | 7.23E-09 | -2.72E-07 | -5.64E-08 | -2.85E-07 |
| 16 | 3.52E-06 | 3.44E-06 | 3.45E-06 | 3.70E-06 | 3.83E-06 |
| 17 | 1.12E-06 | 1.01E-06 | 1.03E-06 | 7.54E-07 | 9.36E-07 |
| 18 | -3.52E-07 | -2.53E-07 | -2.79E-07 | -6.56E-08 | -4.07E-07 |
| 19 | -6.68E-07 | -7.12E-07 | -5.22E-07 | -7.36E-07 | -3.95E-07 |
| 20 | 8.08E-08 | -5.81E-09 | -4.98E-07 | -4.21E-07 | -4.96E-07 |
| 21 | -9.60E-08 | -1.47E-07 | -8.68E-08 | -4.18E-07 | -8.75E-08 |
| 22 | -7.34E-07 | -7.30E-07 | -8.02E-07 | -4.75E-07 | -7.70E-07 |
| 23 | -5.76E-07 | -5.03E-07 | -3.43E-07 | -4.93E-07 | -5.04E-07 |
| 24 | -6.20E-07 | -5.72E-07 | -4.40E-07 | -3.15E-07 | -1.74E-07 |
| 25 | -5.27E-07 | -4.68E-07 | -5.29E-07 | -2.28E-07 | -3.82E-07 |
| 26 | -8.74E-08 | -1.94E-07 | -1.92E-07 | -7.78E-07 | -7.53E-07 |
| 27 | -1.86E-07 | -1.57E-07 | -3.48E-07 | -2.68E-07 | -3.68E-07 |
| 28 | -7.77E-07 | -7.12E-07 | -4.35E-07 | -6.10E-08 | 1.00E-08 |
| 29 | 1.24E-07 | 9.59E-08 | 1.52E-07 | 2.11E-07 | -2.14E-07 |
| 30 | 3.84E-06 | 4.02E-06 | 4.24E-06 | 3.88E-06 | 4.28E-06 |
| 31 | 4.44E-07 | 1.86E-07 | -3.58E-07 | -1.70E-07 | -1.12E-07 |
| 32 | -4.11E-07 | -2.89E-07 | -2.30E-07 | -2.59E-07 | -1.38E-07 |
| 33 | -3.73E-07 | -4.38E-07 | -1.67E-07 | -2.92E-07 | -4.73E-07 |
| 34 | -5.43E-07 | -4.89E-07 | -4.75E-07 | -4.09E-07 | -4.51E-07 |
| 35 | -2.50E-07 | -5.42E-07 | -4.77E-07 | -4.46E-07 | -3.23E-07 |
| 36 | -2.70E-07 | -7.67E-08 | -4.29E-07 | -1.86E-07 | -1.70E-07 |
| 37 | -3.99E-07 | -4.04E-07 | -3.19E-07 | -5.20E-07 | -5.36E-07 |
| 38 | -8.42E-07 | -6.66E-07 | -6.88E-07 | -6.87E-07 | -8.34E-07 |
| 39 | -4.66E-07 | -6.15E-07 | -5.83E-07 | -8.82E-07 | -7.26E-07 |
| 40 | -3.93E-07 | -3.35E-07 | -2.82E-07 | -1.30E-07 | -2.56E-07 |
| 41 | -4.51E-07 | -4.20E-07 | -2.96E-07 | -1.61E-07 | -1.09E-07 |
| 42 | 1.02E-06 | 9.20E-07 | 5.96E-07 | 5.03E-07 | 3.54E-07 |
| 43 | 3.51E-06 | 3.55E-06 | 3.94E-06 | 4.03E-06 | 4.19E-06 |
| 44 | 1.28E-07 | 6.31E-08 | -2.39E-07 | -2.59E-07 | -2.27E-07 |
| 45 | 2.14E-08 | 5.06E-08 | 6.72E-09 | 9.15E-09 | 5.29E-09 |
| 46 | -3.94E-07 | -3.62E-07 | -2.58E-07 | -3.91E-07 | -4.62E-07 |
| 47 | -9.41E-07 | -9.54E-07 | -9.89E-07 | -8.32E-07 | -7.93E-07 |
| 48 | -8.17E-08 | -1.97E-07 | -2.30E-07 | -2.90E-07 | -2.27E-07 |
| 49 | -4.63E-07 | -5.39E-07 | -5.73E-07 | -6.10E-07 | -6.49E-07 |
| 50 | -9.16E-07 | -8.02E-07 | -5.39E-07 | -5.25E-07 | -4.04E-07 |
| 51 | -1.00E-06 | -8.48E-07 | -7.28E-07 | -5.37E-07 | -6.44E-07 |
| 52 | -3.01E-07 | -2.79E-07 | -5.73E-07 | -9.85E-07 | -1.10E-06 |
| 53 | -2.14E-07 | -3.05E-07 | -6.15E-07 | -3.23E-07 | -3.84E-07 |
| 54 | -9.77E-07 | -1.00E-06 | -5.46E-07 | -2.40E-07 | 2.85E-09 |
| 55 | -3.39E-07 | -3.27E-07 | 4.39E-07 | 3.34E-07 | 1.87E-07 |
| 56 | 6.07E-06 | 6.45E-06 | 5.87E-06 | 5.83E-06 | 5.96E-06 |
| 57 | 7.24E-07 | 5.04E-07 | 6.52E-08 | -8.18E-08 | -2.07E-07 |
| 58 | 2.10E-07 | 1.43E-07 | 4.20E-07 | 1.93E-07 | 1.65E-07 |
| 59 | -1.39E-06 | -1.21E-06 | -1.41E-06 | -1.08E-06 | -1.16E-06 |

## Table 25: Curvatures – Sample 7(Mode 1)

| pt | L5 | L4 | L3 | L2 | L1 |
|---|---|---|---|---|---|
| 1 | -5.68E-05 | -3.18E-05 | -4.45E-05 | -4.81E-05 | -6.64E-05 |
| 2 | -1.20E-05 | -3.64E-05 | -5.96E-05 | -2.01E-05 | 3.36E-08 |
| 3 | -1.40E-06 | -2.46E-05 | -4.15E-05 | -2.85E-05 | 4.00E-06 |
| 4 | -2.75E-06 | 3.04E-05 | 2.17E-05 | 4.02E-05 | 2.19E-06 |
| 5 | 1.71E-05 | 5.09E-07 | 4.49E-05 | 9.87E-07 | 6.37E-06 |
| 6 | -1.32E-05 | -9.97E-07 | -1.79E-05 | 6.01E-07 | -1.12E-05 |
| 7 | 1.21E-06 | -1.27E-05 | 1.58E-06 | -8.58E-06 | 7.59E-06 |
| 8 | 4.20E-06 | 1.90E-05 | 6.89E-06 | 4.23E-06 | -1.72E-06 |
| 9 | 5.39E-06 | 1.00E-05 | 4.98E-06 | 8.13E-06 | 3.49E-06 |
| 10 | 1.20E-05 | -7.99E-06 | -2.04E-06 | -4.99E-06 | 7.83E-06 |
| 11 | -9.06E-06 | 1.22E-06 | -8.60E-06 | 9.13E-06 | 5.03E-06 |
| 12 | 7.20E-05 | 1.01E-04 | 1.82E-04 | 2.22E-04 | 2.17E-04 |
| 13 | 1.60E-04 | 1.42E-04 | 8.52E-05 | 2.69E-05 | 3.07E-05 |
| 14 | 6.76E-06 | 1.50E-06 | -1.88E-05 | -1.28E-05 | -1.78E-05 |
| 15 | 1.51E-06 | -7.89E-06 | 1.29E-06 | -1.10E-05 | 1.55E-06 |
| 16 | -8.65E-06 | -4.10E-06 | -1.09E-05 | 2.19E-06 | 8.24E-07 |
| 17 | -7.50E-07 | -3.93E-06 | -1.08E-06 | 7.92E-07 | -5.85E-06 |
| 18 | -8.45E-06 | -8.14E-06 | -8.57E-06 | -2.28E-05 | -2.48E-05 |
| 19 | -8.10E-06 | -4.94E-06 | -3.90E-06 | 6.03E-06 | -3.33E-06 |
| 20 | -7.95E-06 | -9.83E-06 | -6.03E-06 | -7.62E-06 | 3.23E-06 |
| 21 | -3.67E-06 | -2.22E-06 | -7.89E-06 | -8.76E-06 | -1.05E-05 |
| 22 | -8.92E-06 | -1.30E-05 | -1.00E-05 | -9.95E-06 | -8.59E-06 |
| 23 | -8.88E-06 | -6.34E-06 | -7.72E-06 | -7.83E-06 | -9.72E-06 |
| 24 | -9.23E-06 | -1.13E-05 | -9.81E-06 | -1.06E-05 | -1.02E-05 |
| 25 | -8.73E-06 | -6.43E-06 | -8.40E-06 | -6.48E-06 | -2.10E-06 |
| 26 | -7.58E-06 | -9.10E-06 | -9.37E-06 | -5.77E-06 | -5.77E-06 |
| 27 | -1.02E-05 | -9.20E-06 | -1.07E-05 | -1.37E-05 | -7.92E-06 |
| 28 | -8.77E-06 | -1.01E-05 | -8.74E-06 | -7.38E-06 | -8.73E-06 |
| 29 | -7.97E-06 | -6.18E-06 | -7.44E-06 | -5.50E-06 | -1.08E-05 |
| 30 | -5.71E-06 | -1.44E-05 | -9.81E-06 | -1.63E-05 | -1.67E-05 |
| 31 | -8.50E-06 | -1.78E-06 | -1.31E-05 | -4.16E-06 | -1.49E-05 |
| 32 | -1.57E-05 | -2.34E-05 | -1.81E-05 | -1.99E-05 | -5.40E-06 |
| 33 | -1.20E-05 | -4.66E-06 | -2.34E-06 | -6.90E-06 | -9.61E-06 |
| 34 | -9.62E-06 | 9.17E-07 | 9.21E-06 | -1.01E-08 | -9.29E-06 |
| 35 | -8.20E-06 | -1.55E-05 | -1.34E-05 | -1.47E-05 | -9.96E-06 |
| 36 | -8.90E-06 | -1.08E-05 | -1.87E-05 | -9.15E-06 | -7.93E-06 |
| 37 | -8.57E-06 | -8.20E-06 | -1.12E-05 | -1.12E-05 | -9.84E-06 |
| 38 | -8.36E-06 | -8.35E-06 | -8.56E-06 | -7.25E-06 | -9.32E-06 |
| 39 | -1.04E-05 | -1.05E-05 | -5.26E-06 | -8.07E-06 | -7.91E-06 |
| 40 | -9.45E-06 | -6.96E-06 | -8.40E-06 | -5.38E-06 | -9.33E-06 |
| 41 | -2.66E-06 | -5.83E-06 | -8.02E-06 | -1.20E-05 | -5.70E-06 |
| 42 | -5.70E-06 | -5.14E-06 | -8.00E-06 | -3.78E-06 | -5.22E-06 |
| 43 | -5.25E-06 | -6.09E-06 | -5.79E-06 | -8.60E-06 | -8.32E-06 |
| 44 | 1.49E-05 | 1.28E-05 | 4.04E-06 | -1.03E-06 | -5.71E-06 |
| 45 | 1.54E-04 | 1.53E-04 | 1.32E-04 | 7.80E-05 | 2.92E-05 |
| 46 | 7.96E-05 | 8.50E-05 | 1.21E-04 | 1.82E-04 | 2.36E-04 |
| 47 | 9.05E-06 | 9.31E-06 | 9.72E-06 | 1.35E-05 | 1.09E-05 |
| 48 | 8.78E-06 | 7.37E-06 | 5.23E-06 | 1.62E-06 | 4.47E-06 |
| 49 | 5.29E-06 | 5.92E-06 | 2.55E-06 | 3.49E-06 | 6.33E-07 |
| 50 | 3.05E-06 | 1.61E-06 | 2.07E-06 | -1.36E-06 | 2.08E-06 |
| 51 | 5.60E-06 | 6.33E-06 | 4.38E-06 | 4.01E-06 | 1.72E-06 |
| 52 | -4.12E-06 | -2.89E-06 | 1.19E-06 | 5.50E-06 | 7.45E-06 |
| 53 | 3.79E-06 | 1.75E-06 | 1.37E-06 | -4.03E-07 | 2.15E-06 |
| 54 | 3.62E-06 | 4.93E-06 | 2.15E-06 | 2.92E-06 | -1.83E-06 |
| 55 | 2.76E-06 | 3.55E-06 | 7.51E-06 | 3.80E-06 | 3.03E-06 |
| 56 | -8.73E-06 | -9.63E-06 | -8.28E-06 | 2.24E-07 | 2.68E-07 |
| 57 | 3.38E-06 | 3.22E-06 | 9.29E-07 | -3.07E-06 | -1.44E-06 |
| 58 | -2.95E-06 | -1.20E-05 | -1.35E-05 | -1.62E-05 | -1.35E-05 |
| 59 | -9.39E-05 | -8.83E-05 | -1.04E-04 | -9.57E-05 | -9.64E-05 |

## Table 26: Curvatures – Sample 7(Mode 2)

| pt | L5 | L4 | L3 | L2 | L1 |
|---|---|---|---|---|---|
| 1 | -1.84E-05 | -1.59E-05 | -1.74E-05 | -1.24E-05 | -1.32E-05 |
| 2 | 1.85E-06 | -8.39E-08 | 1.46E-06 | -1.56E-06 | 2.34E-06 |
| 3 | -3.05E-06 | -2.97E-07 | -2.55E-06 | -1.06E-07 | -2.83E-06 |
| 4 | 6.90E-06 | 7.80E-06 | 9.34E-06 | -7.96E-07 | -4.58E-06 |
| 5 | -5.85E-07 | -1.18E-06 | -2.65E-06 | 1.29E-06 | 1.47E-06 |
| 6 | 7.11E-06 | 6.55E-06 | 3.26E-06 | 9.89E-07 | 4.01E-06 |
| 7 | 5.86E-05 | 5.79E-05 | 5.42E-05 | 4.83E-05 | 4.16E-05 |
| 8 | -3.72E-08 | -8.09E-07 | 5.32E-06 | 1.55E-05 | 2.15E-05 |
| 9 | -4.09E-06 | -2.40E-06 | -3.10E-07 | 1.30E-06 | 1.55E-07 |
| 10 | 1.20E-07 | -2.15E-06 | -2.50E-06 | -4.99E-06 | -4.24E-06 |
| 11 | -6.15E-06 | -4.04E-06 | -2.14E-06 | -3.11E-06 | -1.65E-06 |
| 12 | -3.22E-06 | -1.98E-06 | -2.70E-06 | -2.95E-06 | -4.98E-06 |
| 13 | -2.56E-06 | -3.32E-06 | -3.80E-06 | -2.00E-06 | -5.02E-07 |
| 14 | -6.80E-07 | -1.19E-06 | -4.16E-06 | -2.97E-06 | -3.32E-06 |
| 15 | -4.70E-06 | -4.74E-06 | -2.83E-06 | -2.32E-06 | -1.90E-06 |
| 16 | -2.95E-06 | -4.35E-06 | -2.85E-06 | -3.88E-06 | -4.54E-06 |
| 17 | -3.18E-06 | -4.17E-06 | -5.01E-06 | -5.55E-06 | -6.40E-06 |
| 18 | -2.47E-06 | -2.94E-06 | -2.56E-06 | -3.52E-06 | -2.67E-06 |
| 19 | -3.91E-06 | -1.91E-06 | -4.37E-06 | -2.46E-06 | -2.29E-06 |
| 20 | -2.21E-06 | -2.54E-06 | -1.44E-06 | -2.04E-06 | -1.46E-06 |
| 21 | -6.15E-06 | -4.68E-06 | -3.86E-06 | -2.97E-06 | -2.47E-06 |
| 22 | -1.99E-06 | -2.21E-06 | -2.51E-06 | -4.45E-06 | -6.09E-06 |
| 23 | -2.98E-06 | -2.93E-06 | -3.31E-06 | -2.69E-06 | -2.41E-06 |
| 24 | -1.83E-06 | -1.55E-06 | -1.02E-06 | -2.26E-07 | 4.16E-07 |
| 25 | -5.02E-07 | -6.49E-08 | -1.92E-06 | -3.28E-06 | -5.26E-06 |
| 26 | -3.25E-06 | -2.80E-06 | -5.02E-07 | -1.50E-06 | -3.12E-07 |
| 27 | -1.43E-06 | -3.75E-06 | -2.72E-06 | -1.20E-06 | -2.54E-06 |
| 28 | -3.05E-06 | -2.93E-06 | -3.12E-06 | -1.76E-06 | -1.05E-07 |
| 29 | 1.16E-06 | 5.56E-07 | 2.94E-07 | -1.59E-06 | -1.50E-06 |
| 30 | -2.72E-07 | 2.99E-06 | 1.77E-06 | 1.24E-06 | 1.24E-06 |
| 31 | 5.77E-06 | 4.98E-06 | 8.56E-06 | 2.20E-05 | 2.45E-05 |
| 32 | 3.12E-05 | 3.33E-05 | 3.28E-05 | 2.30E-05 | 1.95E-05 |
| 33 | 8.54E-06 | 6.23E-06 | 4.17E-06 | 1.72E-06 | 1.50E-06 |
| 34 | 6.91E-07 | -5.80E-07 | -1.39E-07 | -2.82E-07 | 8.46E-07 |
| 35 | -2.01E-06 | -1.91E-06 | -4.45E-06 | -4.27E-06 | -5.03E-06 |
| 36 | -2.59E-06 | -2.44E-06 | -1.78E-06 | -2.15E-06 | -1.80E-06 |
| 37 | -2.40E-06 | -2.37E-06 | -1.55E-06 | -7.28E-07 | -5.84E-07 |
| 38 | -3.78E-06 | -4.65E-06 | -5.12E-06 | -4.20E-06 | -4.64E-06 |
| 39 | -2.53E-06 | -1.61E-06 | -2.45E-07 | -2.86E-06 | -1.95E-06 |
| 40 | -3.47E-06 | -3.78E-06 | -5.19E-06 | -4.29E-06 | -4.38E-06 |
| 41 | -4.44E-06 | -4.81E-06 | -4.71E-06 | -4.50E-06 | -1.98E-06 |
| 42 | -2.73E-06 | -2.30E-06 | -2.69E-06 | -2.74E-06 | -4.98E-06 |
| 43 | -5.11E-06 | -5.18E-06 | -4.63E-06 | -5.00E-06 | -5.35E-06 |
| 44 | -4.31E-06 | -4.52E-06 | -4.58E-06 | -2.94E-06 | -4.38E-06 |
| 45 | -3.80E-06 | -3.03E-06 | -3.29E-06 | -3.97E-06 | -2.47E-06 |
| 46 | -2.65E-06 | -4.44E-06 | -3.98E-06 | -3.71E-06 | -4.88E-06 |
| 47 | -3.83E-06 | -1.36E-06 | -2.33E-06 | -2.03E-06 | -1.72E-06 |
| 48 | -2.79E-06 | -4.45E-06 | -1.80E-06 | -3.07E-06 | -2.61E-06 |
| 49 | -2.97E-06 | 1.33E-07 | -3.12E-06 | -2.30E-06 | -3.13E-06 |
| 50 | 1.80E-05 | 1.46E-05 | 1.13E-05 | 5.97E-07 | 1.45E-07 |
| 51 | 4.13E-05 | 4.23E-05 | 4.85E-05 | 5.65E-05 | 5.65E-05 |
| 52 | 1.48E-06 | 2.03E-06 | -1.76E-07 | 1.62E-06 | 1.07E-06 |
| 53 | 1.03E-06 | 6.08E-07 | 1.42E-06 | 1.54E-06 | 2.59E-06 |
| 54 | 8.20E-07 | -5.03E-08 | -4.97E-07 | 1.62E-06 | 2.80E-06 |
| 55 | 1.08E-06 | 1.90E-06 | 1.60E-06 | 7.98E-07 | 1.42E-06 |
| 56 | -6.31E-07 | -2.95E-07 | -6.76E-07 | -1.87E-06 | -1.69E-06 |
| 57 | 1.60E-06 | 6.70E-07 | 1.74E-06 | 3.01E-07 | 1.90E-08 |
| 58 | -3.14E-06 | -2.18E-06 | -1.41E-06 | 2.25E-06 | 4.30E-07 |
| 59 | -1.97E-05 | -2.25E-05 | -2.36E-05 | -2.56E-05 | -2.39E-05 |

## Table 27: Curvatures – Sample 7(Mode 3)

| pt | L5 | L4 | L3 | L2 | L1 |
|---|---|---|---|---|---|
| 1 | -1.95E-06 | -2.78E-06 | -2.63E-06 | -3.18E-06 | -2.84E-06 |
| 2 | 9.74E-07 | 1.38E-06 | 1.20E-06 | 2.50E-06 | 1.93E-06 |
| 3 | -1.22E-07 | -3.25E-07 | 6.08E-08 | 1.30E-07 | 1.36E-06 |
| 4 | -5.38E-07 | -8.18E-09 | 2.43E-07 | -1.35E-07 | -7.47E-07 |
| 5 | 1.10E-06 | 1.55E-06 | 1.61E-06 | 9.43E-07 | 6.03E-07 |
| 6 | 4.21E-06 | 3.27E-06 | 1.90E-06 | 1.48E-06 | 2.30E-06 |
| 7 | -3.91E-07 | -2.33E-07 | -9.09E-08 | 6.28E-07 | 2.36E-08 |
| 8 | -1.12E-06 | -5.63E-07 | 4.16E-07 | 2.75E-07 | 3.68E-07 |
| 9 | -2.41E-07 | -6.61E-07 | -4.74E-07 | -1.68E-07 | -5.18E-07 |
| 10 | 2.69E-07 | 2.65E-07 | -2.71E-07 | 8.58E-08 | 6.14E-07 |
| 11 | -4.42E-07 | -9.03E-07 | -1.12E-06 | -1.47E-06 | -1.27E-06 |
| 12 | -5.78E-07 | -2.02E-07 | -2.53E-07 | -5.05E-07 | -9.42E-07 |
| 13 | -2.13E-07 | -9.25E-08 | 1.67E-07 | -5.64E-08 | -1.73E-07 |
| 14 | -4.17E-07 | -5.49E-07 | -5.64E-07 | -5.59E-07 | -2.82E-07 |
| 15 | -1.07E-07 | 2.74E-08 | 2.73E-09 | 5.14E-07 | 1.86E-07 |
| 16 | -7.22E-08 | -1.34E-07 | 1.71E-07 | -2.26E-07 | 1.92E-08 |
| 17 | -7.22E-07 | -7.85E-07 | -1.31E-06 | -8.78E-07 | -1.06E-06 |
| 18 | -2.99E-07 | -2.52E-07 | 9.12E-08 | -1.49E-07 | 3.31E-07 |
| 19 | 3.66E-07 | 4.29E-07 | 4.03E-08 | 1.26E-07 | -1.93E-07 |
| 20 | 5.30E-07 | 4.84E-08 | 2.35E-07 | 4.53E-08 | 1.61E-07 |
| 21 | 6.98E-07 | 1.44E-06 | 1.69E-06 | 1.11E-06 | 7.44E-07 |
| 22 | 9.66E-07 | 7.94E-07 | 9.85E-07 | 1.78E-06 | 2.05E-06 |
| 23 | 5.42E-07 | 3.95E-07 | -6.70E-09 | 2.06E-07 | 1.70E-07 |
| 24 | 3.24E-07 | 3.20E-07 | 4.87E-07 | 1.34E-07 | 2.03E-07 |
| 25 | -3.00E-07 | -2.38E-07 | -4.23E-07 | -4.12E-08 | -2.69E-07 |
| 26 | -1.67E-07 | -3.79E-07 | -5.21E-08 | -4.55E-07 | -1.91E-07 |
| 27 | 3.01E-08 | 2.38E-07 | -4.50E-07 | -5.72E-07 | -9.34E-07 |
| 28 | -4.82E-07 | -6.64E-07 | -3.91E-07 | -4.38E-07 | 2.88E-07 |
| 29 | -6.09E-07 | -5.01E-07 | -4.76E-07 | 7.18E-08 | -1.10E-07 |
| 30 | -2.95E-07 | -2.78E-07 | 4.49E-08 | -4.88E-07 | -5.76E-07 |
| 31 | -3.63E-07 | -2.32E-07 | -1.24E-07 | 2.33E-07 | -5.61E-08 |
| 32 | -5.26E-08 | -1.58E-07 | -3.18E-07 | -4.57E-07 | -1.64E-07 |
| 33 | -4.03E-07 | -6.56E-07 | -8.21E-07 | -8.15E-07 | -9.97E-07 |
| 34 | -5.94E-07 | -3.30E-07 | -1.80E-07 | -9.05E-08 | -1.26E-07 |
| 35 | 1.78E-08 | 8.61E-08 | 2.74E-07 | 2.37E-07 | 1.45E-07 |
| 36 | 6.34E-08 | -1.52E-07 | -6.12E-07 | -7.70E-07 | -5.93E-07 |
| 37 | 4.93E-07 | 6.23E-07 | 5.54E-07 | 5.25E-07 | 5.56E-07 |
| 38 | 1.74E-07 | 9.55E-08 | 5.10E-07 | 1.36E-07 | 8.30E-08 |
| 39 | 6.92E-07 | 1.09E-06 | 1.07E-06 | 1.73E-06 | 1.28E-06 |
| 40 | 1.02E-06 | 5.78E-07 | 2.55E-07 | -1.50E-07 | 4.44E-07 |
| 41 | 5.75E-07 | 6.71E-07 | 6.42E-07 | 9.57E-07 | 5.12E-07 |
| 42 | 1.85E-07 | 3.16E-07 | 1.73E-07 | -4.26E-07 | -2.16E-07 |
| 43 | -7.54E-07 | -7.50E-07 | -5.78E-07 | -1.32E-09 | 1.65E-08 |
| 44 | -2.81E-07 | -4.41E-07 | -9.21E-08 | -3.41E-07 | 3.87E-08 |
| 45 | -1.37E-07 | -3.11E-07 | -5.10E-07 | -2.97E-07 | -9.64E-07 |
| 46 | -1.34E-07 | -4.83E-07 | -4.65E-07 | -6.95E-07 | -3.27E-07 |
| 47 | -2.23E-07 | 1.69E-07 | 8.21E-08 | 7.02E-07 | 7.08E-07 |
| 48 | -7.51E-07 | -8.20E-07 | -7.61E-07 | -8.45E-07 | -5.57E-07 |
| 49 | -2.44E-07 | 1.73E-07 | 4.08E-08 | -5.70E-07 | -5.13E-07 |
| 50 | -1.01E-06 | -9.94E-07 | -4.23E-07 | 5.04E-08 | -3.21E-07 |
| 51 | -1.36E-07 | -1.30E-07 | -9.60E-08 | -6.67E-07 | -2.80E-07 |
| 52 | 7.65E-07 | 6.78E-07 | 4.94E-08 | 5.31E-07 | -2.43E-07 |
| 53 | -8.73E-07 | -8.47E-07 | -3.41E-07 | -2.04E-07 | 2.96E-07 |
| 54 | 6.85E-07 | 7.37E-07 | 1.42E-06 | 1.77E-06 | 1.18E-06 |
| 55 | 2.86E-06 | 3.20E-06 | 2.27E-06 | 1.97E-06 | 2.16E-06 |
| 56 | 1.54E-06 | 7.97E-07 | 2.91E-07 | -8.67E-07 | -2.43E-07 |
| 57 | -4.71E-07 | -2.10E-07 | -3.37E-07 | 6.31E-07 | 3.63E-08 |
| 58 | -1.04E-09 | 1.70E-07 | 8.85E-07 | 4.06E-07 | 4.22E-07 |
| 59 | -2.50E-06 | -2.77E-06 | -2.83E-06 | -1.63E-06 | -1.11E-06 |

## Table 28: Curvatures – Sample 7(Mode 4)

| pt | L5 | L4 | L3 | L2 | L1 |
|---|---|---|---|---|---|
| 1 | -8.30E-07 | -6.79E-07 | -5.98E-07 | -4.35E-07 | -5.65E-07 |
| 2 | 3.85E-07 | 4.41E-07 | 2.47E-07 | -1.48E-07 | 1.91E-07 |
| 3 | 1.64E-06 | 1.52E-06 | 1.65E-06 | 2.31E-06 | 1.71E-06 |
| 4 | 1.16E-06 | 1.23E-06 | 8.62E-07 | 9.74E-07 | 1.34E-06 |
| 5 | 9.06E-07 | 4.01E-07 | 6.76E-07 | -3.22E-07 | 1.71E-07 |
| 6 | -5.57E-07 | 1.72E-08 | -3.47E-07 | 1.93E-07 | -2.85E-07 |
| 7 | -7.11E-07 | -1.05E-06 | -4.81E-07 | -4.85E-07 | -3.61E-07 |
| 8 | -6.25E-07 | -5.30E-07 | -7.62E-07 | -5.64E-07 | -4.54E-07 |
| 9 | 1.84E-07 | 1.51E-07 | -1.18E-07 | -8.67E-08 | -2.28E-07 |
| 10 | 1.01E-07 | -2.68E-09 | -1.57E-07 | -9.06E-07 | -7.83E-07 |
| 11 | -1.36E-06 | -1.03E-06 | -7.64E-07 | -1.61E-07 | -3.27E-07 |
| 12 | -6.28E-07 | -9.64E-07 | -1.80E-07 | 3.52E-07 | 5.79E-07 |
| 13 | 2.86E-07 | 4.13E-07 | -8.53E-08 | -3.66E-07 | -6.01E-07 |
| 14 | 3.99E-08 | 7.27E-08 | -6.96E-08 | -4.88E-07 | -5.60E-07 |
| 15 | -3.87E-07 | -6.95E-08 | -1.55E-07 | 1.68E-07 | 3.96E-07 |
| 16 | 3.33E-06 | 3.08E-06 | 2.86E-06 | 2.51E-06 | 2.06E-06 |
| 17 | -3.04E-07 | -2.85E-07 | 1.33E-07 | 4.53E-07 | 9.26E-07 |
| 18 | -1.15E-07 | -2.65E-07 | -2.49E-07 | -2.93E-07 | -4.67E-07 |
| 19 | -2.41E-07 | -2.91E-07 | -4.03E-07 | -4.66E-07 | -4.17E-07 |
| 20 | -2.87E-07 | -2.13E-07 | 6.24E-08 | 2.90E-07 | 2.36E-07 |
| 21 | -3.28E-07 | -3.03E-07 | -6.03E-07 | -8.21E-07 | -6.17E-07 |
| 22 | 1.89E-07 | 8.31E-08 | -2.14E-07 | -4.10E-07 | -4.43E-07 |
| 23 | -4.17E-07 | -3.92E-07 | -3.46E-07 | -2.34E-07 | -2.79E-07 |
| 24 | -4.81E-07 | -3.51E-07 | -4.14E-10 | -8.48E-08 | -2.11E-07 |
| 25 | -7.38E-07 | -7.18E-07 | -5.87E-07 | -4.04E-07 | -4.29E-07 |
| 26 | -4.48E-08 | -1.12E-07 | -3.57E-07 | -6.97E-07 | -7.03E-07 |
| 27 | -3.85E-07 | -3.92E-07 | -5.94E-07 | -3.15E-07 | -2.41E-07 |
| 28 | -7.03E-08 | -1.96E-07 | 5.38E-08 | 1.42E-07 | 3.18E-07 |
| 29 | 2.98E-07 | 7.17E-07 | 1.38E-06 | 1.55E-06 | 1.35E-06 |
| 30 | 3.13E-06 | 2.90E-06 | 1.85E-06 | 1.59E-06 | 1.60E-06 |
| 31 | -3.06E-07 | -3.82E-07 | 3.91E-08 | 1.32E-07 | 2.58E-07 |
| 32 | -1.71E-07 | -8.60E-08 | -2.03E-07 | -1.75E-07 | -3.21E-07 |
| 33 | -3.09E-07 | -3.35E-07 | -2.89E-07 | -2.89E-07 | -2.58E-07 |
| 34 | -3.45E-07 | -5.63E-07 | -5.58E-07 | -6.82E-07 | -5.09E-07 |
| 35 | -3.57E-07 | -1.32E-07 | -2.32E-07 | -9.63E-08 | -2.84E-07 |
| 36 | -3.55E-07 | -6.10E-07 | -3.20E-07 | -5.21E-07 | -4.79E-07 |
| 37 | -5.12E-07 | -3.27E-07 | -5.69E-07 | -5.67E-07 | -5.69E-07 |
| 38 | -8.33E-08 | 3.72E-08 | 5.41E-08 | -6.52E-08 | -2.16E-07 |
| 39 | -5.11E-07 | -5.60E-07 | -4.69E-07 | -3.71E-07 | -1.91E-07 |
| 40 | -2.40E-08 | -1.49E-07 | -2.02E-07 | -3.11E-07 | -4.73E-07 |
| 41 | -6.57E-07 | -5.33E-07 | -6.95E-07 | -4.67E-07 | -4.09E-07 |
| 42 | 7.04E-07 | 8.68E-07 | 1.11E-06 | 1.10E-06 | 1.04E-06 |
| 43 | 2.51E-06 | 2.19E-06 | 2.26E-06 | 2.34E-06 | 2.49E-06 |
| 44 | 3.12E-07 | 4.71E-07 | 2.64E-07 | 2.48E-07 | 1.78E-07 |
| 45 | -1.04E-07 | -3.15E-08 | -1.84E-07 | -3.12E-07 | -1.64E-07 |
| 46 | -1.16E-07 | -2.37E-07 | -6.21E-08 | -3.95E-08 | -3.77E-08 |
| 47 | -3.11E-07 | -5.19E-07 | -5.86E-07 | -4.88E-07 | -5.43E-07 |
| 48 | -1.98E-07 | -4.36E-07 | -5.30E-07 | -7.26E-07 | -7.98E-07 |
| 49 | -7.99E-07 | -4.55E-07 | -3.56E-07 | -2.38E-07 | -2.21E-07 |
| 50 | -4.64E-07 | -2.27E-07 | -1.07E-07 | -2.85E-07 | -5.69E-08 |
| 51 | -3.51E-07 | -5.55E-07 | -8.60E-07 | -6.03E-07 | -8.48E-07 |
| 52 | -9.93E-07 | -1.35E-06 | -8.32E-07 | -6.42E-07 | -3.25E-07 |
| 53 | -4.62E-07 | -1.53E-07 | -1.81E-07 | -1.63E-07 | -6.78E-07 |
| 54 | 2.01E-07 | 2.34E-07 | 5.38E-08 | -6.90E-07 | -6.29E-07 |
| 55 | -4.29E-07 | 1.73E-07 | 4.61E-07 | 1.69E-06 | 2.05E-06 |
| 56 | 2.98E-06 | 3.60E-06 | 3.91E-06 | 3.24E-06 | 3.05E-06 |
| 57 | 2.48E-06 | 1.23E-06 | 8.70E-07 | 5.68E-07 | 3.78E-07 |
| 58 | -4.12E-07 | -1.63E-07 | -6.14E-07 | -2.62E-07 | -1.17E-08 |
| 59 | -1.69E-06 | -2.07E-06 | -1.45E-06 | -1.27E-06 | -1.27E-06 |

## Table 29: Curvatures – Sample 8(Mode 1)

| pt | L5 | L4 | L3 | L2 | L1 |
|---|---|---|---|---|---|
| 1 | -8.16E-05 | -6.33E-05 | -6.88E-05 | -5.68E-05 | -6.08E-05 |
| 2 | 1.76E-05 | 1.03E-05 | 1.47E-05 | -5.92E-06 | -1.14E-05 |
| 3 | -1.02E-05 | 6.58E-06 | -1.12E-05 | 4.32E-06 | 6.38E-06 |
| 4 | -1.72E-06 | -1.56E-05 | -1.63E-06 | -6.11E-06 | 8.40E-06 |
| 5 | -3.11E-07 | 3.52E-06 | -9.15E-07 | 3.77E-06 | -7.57E-06 |
| 6 | 1.14E-05 | 7.76E-06 | 4.14E-06 | -1.63E-05 | -2.05E-05 |
| 7 | 4.94E-06 | 2.87E-06 | 6.82E-06 | 2.34E-05 | 1.53E-05 |
| 8 | -6.00E-07 | 4.49E-06 | 5.19E-06 | 6.46E-06 | 1.81E-05 |
| 9 | 2.84E-06 | 3.01E-06 | 1.81E-06 | -5.09E-07 | 4.81E-08 |
| 10 | 2.91E-05 | 1.64E-06 | 2.11E-05 | -2.91E-06 | -1.06E-06 |
| 11 | 8.02E-06 | 5.08E-05 | 7.64E-06 | 2.98E-05 | 4.97E-06 |
| 12 | 6.84E-05 | 8.72E-05 | 1.10E-04 | 1.81E-04 | 2.31E-04 |
| 13 | 1.75E-04 | 1.18E-04 | 1.47E-04 | 5.65E-05 | 2.66E-05 |
| 14 | -2.13E-05 | 1.32E-06 | -2.23E-05 | 2.01E-06 | 4.58E-06 |
| 15 | -3.03E-06 | -5.10E-06 | -8.11E-06 | -1.04E-05 | -1.04E-05 |
| 16 | -7.04E-06 | -6.29E-06 | -8.61E-06 | -8.62E-06 | -8.20E-06 |
| 17 | -7.55E-06 | -8.42E-06 | -5.65E-06 | -3.70E-06 | -3.74E-06 |
| 18 | -7.73E-06 | -5.31E-06 | -8.88E-06 | -1.37E-05 | -1.55E-05 |
| 19 | -5.50E-06 | -5.99E-06 | -5.40E-06 | -4.98E-06 | -6.21E-06 |
| 20 | -6.03E-06 | -7.59E-06 | -5.36E-06 | -4.24E-06 | -2.67E-06 |
| 21 | -9.67E-06 | -1.03E-05 | -9.54E-06 | -1.18E-05 | -1.28E-05 |
| 22 | -7.42E-06 | -7.69E-06 | -8.99E-06 | -9.61E-06 | -9.68E-06 |
| 23 | -9.85E-06 | -8.27E-06 | -7.05E-06 | -1.63E-06 | 5.53E-07 |
| 24 | -1.31E-05 | -1.25E-05 | -1.18E-05 | -1.11E-05 | -1.11E-05 |
| 25 | -5.73E-06 | -5.94E-06 | -9.36E-06 | -1.20E-05 | -1.33E-05 |
| 26 | -5.97E-06 | -8.97E-06 | -5.83E-06 | -6.76E-06 | -5.59E-06 |
| 27 | -1.14E-05 | -1.01E-05 | -1.25E-05 | -1.10E-05 | -1.14E-05 |
| 28 | -1.01E-05 | -1.11E-05 | -8.69E-06 | -8.03E-06 | -3.64E-06 |
| 29 | -8.30E-06 | -7.65E-06 | -8.94E-06 | -7.19E-06 | -8.52E-06 |
| 30 | -9.18E-06 | -8.69E-06 | -8.00E-06 | -1.10E-05 | -1.30E-05 |
| 31 | -1.34E-05 | -1.45E-05 | -1.58E-05 | -1.68E-05 | -1.62E-05 |
| 32 | -1.04E-05 | -9.33E-06 | -9.18E-06 | -8.96E-06 | -9.51E-06 |
| 33 | -1.04E-05 | -9.50E-06 | -8.86E-06 | -9.35E-06 | -1.04E-05 |
| 34 | -9.14E-06 | -9.62E-06 | -1.01E-05 | -6.59E-06 | -8.69E-06 |
| 35 | -7.81E-06 | -8.75E-06 | -9.36E-06 | -1.10E-05 | -7.64E-06 |
| 36 | -9.35E-06 | -9.02E-06 | -1.05E-05 | -1.17E-05 | -1.43E-05 |
| 37 | -9.12E-06 | -7.70E-06 | -4.96E-06 | -7.09E-06 | -7.52E-06 |
| 38 | -7.83E-06 | -8.35E-06 | -9.76E-06 | -6.37E-06 | -5.58E-06 |
| 39 | -9.51E-06 | -1.22E-05 | -1.35E-05 | -1.32E-05 | -8.29E-06 |
| 40 | -5.49E-06 | -2.75E-06 | -4.17E-06 | -5.00E-06 | -9.75E-06 |
| 41 | -8.17E-06 | -8.57E-06 | -2.80E-06 | -7.05E-06 | -6.02E-06 |
| 42 | -8.17E-06 | -6.69E-06 | -7.41E-06 | -3.44E-06 | -6.95E-06 |
| 43 | -5.41E-06 | -6.65E-06 | -5.27E-06 | -6.88E-06 | -3.74E-06 |
| 44 | -6.09E-07 | -1.43E-06 | -6.13E-06 | -5.68E-06 | 1.10E-05 |
| 45 | 8.35E-05 | 7.85E-05 | 5.24E-05 | 3.96E-05 | 1.84E-05 |
| 46 | 1.66E-04 | 1.72E-04 | 2.02E-04 | 1.95E-04 | 1.39E-04 |
| 47 | 1.44E-05 | 1.18E-05 | 1.30E-05 | 3.60E-05 | 1.09E-04 |
| 48 | 8.07E-06 | 1.06E-05 | 1.03E-05 | 8.60E-06 | -2.81E-06 |
| 49 | 6.35E-06 | 6.73E-06 | 4.81E-06 | 1.97E-07 | 1.24E-06 |
| 50 | 8.54E-07 | -1.30E-06 | -1.21E-06 | 4.57E-06 | 3.48E-06 |
| 51 | 3.43E-06 | 3.85E-06 | 3.93E-06 | 5.73E-06 | 5.79E-06 |
| 52 | 8.12E-06 | 6.08E-06 | 4.03E-06 | -2.75E-06 | -7.49E-06 |
| 53 | -1.60E-06 | 4.96E-06 | 1.02E-05 | 8.56E-06 | 9.17E-06 |
| 54 | 3.43E-07 | -4.03E-06 | -7.78E-06 | -3.10E-06 | -1.61E-07 |
| 55 | 2.08E-06 | -1.29E-06 | -6.64E-06 | -7.47E-06 | 2.24E-08 |
| 56 | -1.45E-06 | 1.19E-06 | 2.28E-06 | 4.68E-06 | -7.50E-07 |
| 57 | -2.91E-06 | -1.38E-06 | 6.54E-06 | 4.55E-06 | 5.48E-07 |
| 58 | -1.47E-06 | -3.76E-06 | -1.44E-06 | 1.01E-06 | -1.94E-06 |
| 59 | -9.96E-05 | -1.06E-04 | -1.25E-04 | -1.19E-04 | -1.11E-04 |

## Table 30: Curvatures – Sample 8(Mode 2)

| pt | L5 | L4 | L3 | L2 | L1 |
|---|---|---|---|---|---|
| 1 | -2.01E-05 | -1.82E-05 | -1.95E-05 | -1.82E-05 | -1.81E-05 |
| 2 | -1.34E-06 | -6.34E-07 | 1.73E-06 | -2.11E-06 | -1.86E-06 |
| 3 | 1.25E-06 | 4.39E-06 | 2.96E-06 | 1.99E-06 | 5.59E-09 |
| 4 | -9.93E-07 | -2.70E-06 | -1.45E-06 | -8.88E-07 | 2.07E-06 |
| 5 | 4.91E-06 | 3.47E-06 | 2.17E-06 | 4.63E-06 | 2.51E-06 |
| 6 | 2.57E-05 | 2.66E-05 | 1.58E-05 | 7.47E-06 | 1.78E-06 |
| 7 | 5.36E-05 | 5.37E-05 | 6.47E-05 | 6.51E-05 | 6.98E-05 |
| 8 | -3.43E-06 | -1.14E-06 | -2.00E-06 | 5.06E-06 | 5.85E-06 |
| 9 | 1.89E-06 | -1.36E-06 | 8.76E-08 | -1.67E-06 | -1.16E-06 |
| 10 | -6.11E-06 | -3.89E-06 | -6.73E-06 | -3.09E-06 | -2.38E-06 |
| 11 | -3.03E-06 | -4.70E-06 | -5.37E-07 | -3.19E-06 | -4.03E-06 |
| 12 | -2.39E-06 | -1.29E-06 | -2.90E-06 | -2.55E-06 | -3.30E-06 |
| 13 | -3.61E-06 | -6.82E-06 | -6.02E-06 | -4.38E-06 | -3.09E-06 |
| 14 | -4.08E-06 | -3.26E-06 | -3.83E-06 | -3.81E-06 | -3.96E-06 |
| 15 | -5.31E-06 | -3.80E-06 | -3.50E-06 | -5.28E-06 | -6.04E-06 |
| 16 | -3.07E-06 | -3.10E-06 | -4.51E-06 | -4.95E-06 | -5.90E-06 |
| 17 | -2.91E-06 | -4.05E-06 | -2.53E-06 | -1.43E-07 | 2.19E-06 |
| 18 | -4.57E-06 | -3.51E-06 | -4.46E-06 | -5.18E-06 | -5.10E-06 |
| 19 | -4.36E-06 | -4.16E-06 | -2.89E-06 | -4.51E-06 | -5.53E-06 |
| 20 | -4.27E-06 | -4.72E-06 | -5.42E-06 | -4.32E-06 | -4.00E-06 |
| 21 | -2.78E-06 | -3.20E-06 | -2.48E-06 | -2.47E-06 | -3.37E-06 |
| 22 | -4.70E-06 | -3.39E-06 | -4.54E-06 | -4.66E-06 | -4.15E-06 |
| 23 | -3.58E-06 | -3.69E-06 | -3.93E-06 | -4.43E-06 | -4.66E-06 |
| 24 | -3.01E-06 | -3.14E-06 | -2.37E-06 | -2.13E-06 | -1.91E-06 |
| 25 | -2.04E-06 | -2.55E-06 | -3.19E-06 | -2.18E-06 | -2.16E-06 |
| 26 | -2.36E-06 | -2.30E-06 | -1.98E-06 | -2.52E-06 | -2.44E-06 |
| 27 | -1.84E-06 | -4.99E-07 | -1.95E-06 | -1.55E-06 | -1.63E-06 |
| 28 | 4.60E-07 | -1.28E-06 | 3.11E-07 | -9.17E-07 | -9.48E-08 |
| 29 | -2.59E-06 | -3.16E-07 | -1.36E-06 | -3.68E-07 | -1.98E-06 |
| 30 | -3.64E-08 | -1.89E-06 | -2.76E-07 | -1.79E-06 | -2.94E-07 |
| 31 | 5.47E-06 | 7.45E-06 | 1.09E-05 | 2.15E-05 | 2.15E-05 |
| 32 | 4.62E-05 | 4.49E-05 | 4.24E-05 | 3.30E-05 | 3.26E-05 |
| 33 | 4.52E-06 | 5.21E-06 | 3.60E-06 | 4.34E-06 | 3.70E-06 |
| 34 | 1.24E-06 | -3.77E-07 | -1.81E-07 | -2.81E-06 | -2.49E-06 |
| 35 | -3.53E-06 | -2.95E-06 | -5.45E-06 | -2.95E-06 | -4.16E-06 |
| 36 | -3.98E-06 | -4.90E-06 | -1.97E-06 | -2.66E-06 | -2.70E-07 |
| 37 | -3.72E-06 | -2.45E-06 | -4.45E-06 | -3.74E-06 | -4.98E-06 |
| 38 | -2.55E-06 | -2.92E-06 | -1.40E-06 | -3.24E-06 | -2.55E-06 |
| 39 | -3.26E-06 | -3.67E-06 | -4.85E-06 | -4.35E-06 | -5.05E-06 |
| 40 | -4.43E-06 | -4.52E-06 | -3.25E-06 | -3.04E-06 | -2.29E-06 |
| 41 | -5.44E-06 | -4.78E-06 | -4.97E-06 | -3.74E-06 | -4.11E-06 |
| 42 | -4.41E-06 | -4.50E-06 | -3.85E-06 | -4.07E-06 | -4.26E-06 |
| 43 | -5.34E-06 | -5.57E-06 | -6.30E-06 | -5.45E-06 | -6.08E-06 |
| 44 | -4.34E-06 | -4.83E-06 | -5.83E-06 | -7.41E-06 | -2.40E-06 |
| 45 | -3.06E-06 | -2.47E-06 | -3.49E-06 | -1.39E-06 | -4.85E-06 |
| 46 | -6.11E-06 | -6.04E-06 | -4.00E-06 | -9.49E-06 | -1.02E-05 |
| 47 | -3.61E-06 | -3.34E-06 | -2.93E-06 | 4.07E-07 | -3.25E-06 |
| 48 | -2.46E-06 | -2.76E-06 | -3.30E-06 | -3.48E-06 | 4.45E-07 |
| 49 | -2.55E-06 | -3.09E-06 | -3.26E-06 | -2.17E-06 | -3.55E-06 |
| 50 | 2.11E-05 | 2.32E-05 | 2.03E-05 | 5.77E-06 | -3.64E-08 |
| 51 | 4.76E-05 | 4.58E-05 | 4.82E-05 | 6.09E-05 | 6.72E-05 |
| 52 | 1.52E-06 | 2.03E-06 | 2.52E-06 | 4.18E-06 | 4.49E-06 |
| 53 | 2.44E-06 | 1.96E-06 | 1.81E-06 | 1.28E-06 | 1.07E-06 |
| 54 | -8.79E-07 | -9.85E-09 | -4.98E-07 | 1.16E-06 | 1.46E-06 |
| 55 | 1.13E-06 | -9.68E-07 | 8.01E-07 | -3.89E-07 | -1.44E-07 |
| 56 | 1.16E-06 | 3.70E-06 | 2.28E-06 | 2.35E-06 | -2.77E-07 |
| 57 | 7.36E-07 | -1.06E-06 | 2.24E-08 | -3.04E-06 | -3.07E-07 |
| 58 | -3.23E-06 | -2.76E-06 | -3.66E-06 | 4.11E-07 | -1.43E-07 |
| 59 | -2.51E-05 | -2.53E-05 | -2.53E-05 | -2.59E-05 | -2.41E-05 |

## Table 31: Curvatures – Sample 8(Mode 3)

| pt | L5 | L4 | L3 | L2 | L1 |
|---|---|---|---|---|---|
| 1 | -2.36E-06 | -2.29E-06 | -1.45E-06 | -9.81E-07 | -8.66E-07 |
| 2 | -2.62E-07 | -5.69E-08 | -3.38E-07 | -8.33E-07 | -1.43E-06 |
| 3 | 9.64E-07 | 9.81E-07 | 1.05E-06 | 7.15E-07 | 6.97E-07 |
| 4 | 3.11E-07 | 7.65E-07 | 8.17E-07 | 1.60E-06 | 2.41E-06 |
| 5 | 1.70E-06 | 2.26E-06 | 2.46E-06 | 1.51E-06 | 7.04E-07 |
| 6 | 3.83E-06 | 3.01E-06 | 2.91E-06 | 4.33E-06 | 3.98E-06 |
| 7 | 2.97E-07 | -4.14E-07 | -6.81E-07 | -9.94E-07 | -1.07E-07 |
| 8 | -1.19E-06 | -5.60E-07 | -7.54E-07 | -1.05E-06 | -1.28E-06 |
| 9 | -4.96E-07 | -4.07E-07 | -4.67E-08 | -6.17E-07 | -4.19E-07 |
| 10 | -4.21E-07 | -6.98E-07 | -5.43E-07 | -1.52E-07 | -3.59E-07 |
| 11 | 3.39E-07 | 3.88E-07 | -7.09E-08 | 4.59E-08 | -2.38E-07 |
| 12 | -9.35E-07 | -9.70E-07 | -4.33E-07 | -4.30E-07 | -8.06E-09 |
| 13 | -1.00E-06 | -5.21E-07 | -7.51E-07 | -6.44E-07 | -3.70E-07 |
| 14 | -1.15E-07 | -4.87E-07 | -4.18E-07 | -7.84E-07 | -1.09E-06 |
| 15 | -6.40E-07 | -4.45E-07 | -6.22E-07 | -6.81E-07 | -6.99E-07 |
| 16 | -4.68E-07 | -5.39E-07 | -1.65E-07 | 5.57E-07 | 2.61E-07 |
| 17 | -5.01E-08 | 8.67E-08 | -3.88E-07 | -8.67E-07 | -6.42E-07 |
| 18 | -2.88E-07 | -4.57E-07 | -9.23E-08 | -1.99E-07 | -3.26E-07 |
| 19 | -4.66E-07 | -4.44E-07 | -4.82E-07 | -4.30E-07 | -4.40E-07 |
| 20 | 1.41E-07 | 1.95E-08 | -5.15E-08 | 1.78E-07 | 4.41E-07 |
| 21 | 1.97E-06 | 2.23E-06 | 2.44E-06 | 2.14E-06 | 1.94E-06 |
| 22 | 2.36E-06 | 2.46E-06 | 2.21E-06 | 2.00E-06 | 1.68E-06 |
| 23 | 3.13E-10 | -1.56E-07 | 3.08E-07 | 8.68E-07 | 1.33E-06 |
| 24 | 3.78E-07 | 1.43E-07 | -5.68E-07 | -7.02E-07 | -7.50E-07 |
| 25 | -1.21E-07 | 5.26E-08 | 1.43E-07 | 1.58E-08 | 2.06E-07 |
| 26 | -4.47E-07 | -4.68E-07 | -2.03E-07 | -9.45E-08 | -2.95E-07 |
| 27 | -2.05E-07 | -1.51E-07 | -2.61E-07 | -3.59E-07 | -4.92E-07 |
| 28 | -5.25E-07 | -6.13E-07 | -6.62E-07 | -7.47E-07 | -7.15E-07 |
| 29 | -6.47E-07 | -8.41E-07 | -7.99E-07 | -7.95E-07 | -7.19E-07 |
| 30 | -3.30E-07 | -3.26E-08 | -2.25E-07 | 1.43E-07 | 1.64E-07 |
| 31 | -5.59E-07 | -8.34E-07 | -4.33E-07 | -2.97E-07 | -3.10E-08 |
| 32 | -8.06E-07 | -4.04E-07 | -3.64E-07 | -4.76E-07 | -4.47E-07 |
| 33 | -4.21E-08 | -1.82E-07 | -4.67E-07 | -7.71E-07 | -1.22E-06 |
| 34 | -1.16E-07 | -2.08E-07 | -1.69E-07 | -5.18E-07 | -4.25E-07 |
| 35 | -5.22E-07 | -5.33E-07 | -5.72E-07 | -2.29E-07 | -3.79E-07 |
| 36 | 1.24E-07 | 1.47E-07 | 2.61E-07 | 2.47E-07 | 3.43E-07 |
| 37 | -3.11E-07 | -3.14E-07 | -2.32E-07 | -7.78E-08 | 7.21E-08 |
| 38 | 5.66E-07 | 6.27E-07 | 3.50E-07 | 1.81E-07 | 1.83E-08 |
| 39 | 1.09E-06 | 1.10E-06 | 1.23E-06 | 1.35E-06 | 1.59E-06 |
| 40 | 1.47E-06 | 1.45E-06 | 1.61E-06 | 1.56E-06 | 1.45E-06 |
| 41 | 6.30E-07 | 6.42E-07 | 3.46E-07 | 2.86E-07 | 1.03E-07 |
| 42 | -2.22E-07 | -2.76E-07 | -1.34E-07 | 1.28E-07 | 3.44E-07 |
| 43 | 2.73E-07 | 1.60E-07 | 6.86E-08 | -8.36E-08 | -5.98E-08 |
| 44 | -2.99E-07 | -1.89E-07 | -1.23E-07 | -1.73E-07 | -2.76E-07 |
| 45 | -9.53E-07 | -1.04E-06 | -9.81E-07 | -1.03E-06 | -8.98E-07 |
| 46 | -6.48E-07 | -6.07E-07 | -4.45E-07 | -2.07E-07 | -3.68E-07 |
| 47 | 8.70E-08 | 3.35E-07 | -9.58E-08 | -3.43E-07 | -1.43E-07 |
| 48 | -1.77E-07 | -7.14E-07 | -5.13E-07 | -3.46E-07 | -3.90E-07 |
| 49 | -4.60E-07 | -1.31E-07 | -6.85E-08 | -4.03E-07 | -2.58E-07 |
| 50 | 1.80E-08 | 1.81E-07 | -3.64E-07 | -5.70E-07 | -1.01E-06 |
| 51 | -1.11E-06 | -1.41E-06 | -7.16E-07 | -7.64E-07 | -3.22E-07 |
| 52 | -1.03E-06 | -3.30E-07 | -3.09E-07 | 5.07E-07 | -1.83E-07 |
| 53 | 3.03E-07 | -5.08E-07 | -2.60E-07 | -7.37E-07 | -4.16E-07 |
| 54 | 3.03E-06 | 4.05E-06 | 3.54E-06 | 4.15E-06 | 4.43E-06 |
| 55 | 2.52E-06 | 2.15E-06 | 2.05E-06 | 1.38E-06 | 9.67E-07 |
| 56 | 6.25E-08 | -8.29E-07 | -1.11E-06 | -1.55E-06 | -1.21E-06 |
| 57 | -4.31E-07 | -2.53E-08 | 5.74E-07 | 1.50E-06 | 1.51E-06 |
| 58 | 1.46E-07 | 3.11E-07 | 7.52E-07 | 1.29E-06 | 1.45E-06 |
| 59 | -1.65E-06 | -2.18E-06 | -3.51E-06 | -4.40E-06 | -4.23E-06 |

## Table 32: Curvatures – Sample 8(Mode 4)

| pt | L5 | L4 | L3 | L2 | L1 |
|---|---|---|---|---|---|
| 1 | -1.29E-06 | -1.34E-06 | -1.14E-06 | -1.32E-06 | -1.14E-06 |
| 2 | 5.28E-07 | 6.66E-07 | 1.66E-07 | 7.37E-07 | 2.96E-07 |
| 3 | 5.37E-06 | 5.49E-06 | 4.89E-06 | 3.87E-06 | 3.47E-06 |
| 4 | 1.36E-06 | 1.09E-06 | 2.13E-06 | 2.82E-06 | 3.34E-06 |
| 5 | -9.12E-07 | -9.14E-07 | -1.05E-06 | -1.00E-06 | -7.50E-07 |
| 6 | -6.85E-08 | 1.34E-07 | -3.40E-08 | 1.80E-07 | -5.33E-08 |
| 7 | -7.28E-07 | -9.95E-07 | -1.01E-06 | -1.73E-06 | -1.27E-06 |
| 8 | -4.76E-07 | -3.57E-07 | -4.31E-07 | -6.04E-08 | -5.44E-07 |
| 9 | -8.62E-07 | -9.96E-07 | -9.90E-07 | -1.25E-06 | -6.90E-07 |
| 10 | -9.83E-07 | -8.47E-07 | -1.05E-06 | -7.69E-07 | -1.21E-06 |
| 11 | -7.88E-07 | -4.95E-07 | 1.74E-08 | -1.53E-07 | -2.05E-07 |
| 12 | -5.31E-07 | -6.79E-07 | -8.39E-07 | -3.73E-07 | -6.16E-07 |
| 13 | -5.35E-07 | -5.75E-07 | -4.24E-07 | -5.30E-07 | -1.99E-07 |
| 14 | -5.20E-07 | -5.51E-07 | -9.12E-07 | -1.20E-06 | -1.37E-06 |
| 15 | 1.22E-06 | 1.31E-06 | 1.69E-06 | 1.16E-06 | 1.11E-06 |
| 16 | 5.17E-06 | 4.99E-06 | 4.71E-06 | 5.43E-06 | 5.63E-06 |
| 17 | -2.97E-07 | -9.09E-08 | -5.82E-08 | -7.73E-08 | -9.07E-08 |
| 18 | -5.82E-07 | -7.17E-07 | -5.33E-07 | -6.48E-07 | -8.14E-07 |
| 19 | 8.44E-08 | 1.50E-07 | -1.55E-07 | -2.21E-07 | -1.77E-07 |
| 20 | -6.33E-07 | -9.27E-07 | -9.23E-07 | -9.21E-07 | -6.76E-07 |
| 21 | -1.25E-06 | -9.11E-07 | -6.44E-07 | -4.64E-07 | -4.46E-07 |
| 22 | -4.51E-07 | -6.05E-07 | -6.45E-07 | -6.87E-07 | -7.61E-07 |
| 23 | -5.07E-07 | -5.24E-07 | -6.38E-07 | -6.18E-07 | -6.89E-07 |
| 24 | -6.55E-07 | -6.82E-07 | -5.30E-07 | -6.09E-07 | -6.64E-07 |
| 25 | -5.90E-07 | -5.86E-07 | -8.04E-07 | -9.20E-07 | -9.29E-07 |
| 26 | -8.92E-07 | -9.04E-07 | -6.23E-07 | -3.75E-07 | -1.96E-07 |
| 27 | -1.49E-07 | -1.04E-07 | -1.36E-07 | -2.13E-07 | -3.14E-07 |
| 28 | -4.51E-08 | 9.77E-08 | -2.88E-07 | -6.19E-07 | -7.96E-07 |
| 29 | 1.94E-06 | 2.30E-06 | 2.24E-06 | 1.79E-06 | 1.75E-06 |
| 30 | 4.16E-06 | 3.72E-06 | 3.83E-06 | 4.52E-06 | 4.62E-06 |
| 31 | -7.05E-07 | -7.77E-07 | -4.00E-07 | -1.62E-07 | -3.07E-08 |
| 32 | -2.38E-07 | -1.20E-07 | -2.76E-07 | -5.08E-07 | -6.09E-07 |
| 33 | -6.50E-07 | -7.87E-07 | -8.37E-07 | -6.28E-07 | -6.44E-07 |
| 34 | -5.59E-07 | -6.68E-07 | -3.77E-07 | -3.87E-07 | 1.18E-07 |
| 35 | -2.88E-07 | -1.26E-07 | -6.55E-07 | -7.70E-07 | -1.21E-06 |
| 36 | -8.61E-07 | -8.21E-07 | -4.31E-07 | -7.84E-07 | -8.00E-07 |
| 37 | -9.03E-07 | -8.62E-07 | -1.03E-06 | -7.88E-07 | -8.27E-07 |
| 38 | -6.07E-07 | -8.09E-07 | -8.74E-07 | -7.75E-07 | -6.24E-07 |
| 39 | -8.27E-07 | -6.67E-07 | -3.88E-07 | -1.88E-07 | -2.07E-07 |
| 40 | -3.01E-07 | -2.76E-07 | -4.65E-07 | -6.75E-07 | -8.32E-07 |
| 41 | -3.37E-07 | -4.03E-07 | -4.56E-07 | -6.27E-07 | -4.93E-07 |
| 42 | 8.74E-07 | 1.02E-06 | 1.05E-06 | 7.36E-07 | 5.15E-07 |
| 43 | 5.65E-06 | 5.66E-06 | 5.74E-06 | 6.02E-06 | 6.10E-06 |
| 44 | -3.92E-07 | -5.13E-07 | -5.73E-07 | -3.19E-07 | -1.41E-07 |
| 45 | 2.49E-07 | 1.69E-07 | -6.48E-08 | -4.68E-07 | -7.51E-07 |
| 46 | -1.11E-06 | -9.89E-07 | -5.28E-07 | 1.51E-07 | 2.93E-07 |
| 47 | -8.72E-07 | -1.14E-06 | -1.23E-06 | -1.34E-06 | -1.05E-06 |
| 48 | 1.43E-07 | 2.64E-07 | -1.52E-07 | -5.68E-07 | -7.69E-07 |
| 49 | -1.16E-06 | -1.15E-06 | -1.22E-06 | -1.06E-06 | -9.63E-07 |
| 50 | -1.16E-06 | -1.18E-06 | -7.08E-07 | -7.10E-07 | -7.36E-07 |
| 51 | -8.53E-07 | -5.21E-07 | -5.33E-07 | -7.26E-07 | -9.99E-07 |
| 52 | -1.06E-06 | -1.25E-06 | -1.49E-06 | -1.19E-06 | -1.13E-06 |
| 53 | -8.28E-07 | -1.25E-06 | -1.04E-06 | -1.17E-06 | -6.41E-07 |
| 54 | -4.94E-07 | 1.92E-07 | 1.12E-07 | -5.25E-08 | -6.82E-07 |
| 55 | 2.30E-07 | 1.23E-07 | 9.24E-07 | 1.59E-06 | 1.59E-06 |
| 56 | 8.75E-06 | 8.66E-06 | 7.96E-06 | 7.77E-06 | 7.63E-06 |
| 57 | 4.02E-07 | 3.08E-07 | 2.20E-07 | -4.75E-07 | -4.71E-09 |
| 58 | -2.05E-07 | -4.12E-08 | -1.59E-07 | 2.93E-07 | 2.31E-07 |
| 59 | -3.09E-06 | -3.38E-06 | -2.78E-06 | -2.68E-06 | -1.97E-06 |